The use and development of exploratory multi-omic analysis for complex disease: A COVID-19 proof-of-concept

Bradley Ward

Thesis presented to obtain the degree of Doctor of biomedical sciences and pharmaceutics

Promotor: Prof. Laure Elens (LDRI, UCLouvain)

Co-promotor: Prof. Leïla Belkhir (IREC, UCLouvain)

December 2025

Louvain Drug Research Institute (LDRI) and Institute of experimental and clinical research (IREC)

Université catholique de Louvain (UCLouvain)

Members of the Jury

Promotor

Prof L. Elens

Co-Promotor

Prof L. Belkhir

President

Prof I. Leclercq

Members

Prof. Patrice Cani

Prof. Jean-Luc Balligand

Prof. Jean Cyr Yombi

Prof. Laurent Gatto

Invited members

Prof. Abhishek Garg

Prof. Michel Moutschen

ABBREVIATIONS **6**

ACKNOWLEDGEMENTS **8**

INTRODUCTION **10**

SECTION I 5 YEARS ON COVID-19: A PATHOPHYSIOLOGICAL REVIEW **14**

INTRODUCTION 14
1. VIRAL ENTRY AND REPLICATION MECHANISMS 16
1.1 Viral Structure and Cell Entry Pathways *16*
1.2 Viral Tropism and Replication Kinetics *17*
1.3 Viral Evolution and Variants *18*
2. IMMUNE RESPONSE AND HYPERINFLAMMATION 21
2.1 Innate Immune Activation and Interferons *21*
2.2 Key Immune Cells in COVID-19 Pathogenesis *22*
2.3 The "Cytokine Storm" *26*
2.4 Immunothrombosis: Intersection of Inflammation and Coagulation *31*
2.5 SARS-CoV-2 innate immune evasion *36*
3 POST-ACUTE SEQUELAE OF SARS-COV-2 (PASC, LONG COVID) 42
3.1 Clinical Spectrum and Impact of Long COVID *44*
3.2 Pathophysiological Mechanisms of PASC *51*
4 CURRENT CLINICAL MANAGEMENT OF COVID-19 AND PASC 84
CONCLUSION 86
REFERENCES 88

SECTION II HYGIEIA: HYPOTHESIZING THE GENESIS OF INFECTIOUS DISEASES AND EPIDEMICS THROUGH AN INTEGRATED SYSTEMS BIOLOGY APPROACH **104**

ABSTRACT 105
1. INTRODUCTION 106
1.1. Clinical Problem and Phenotype Definition *106*
1.2. Previous Research and Gaps in Knowledge *108*
2. MATERIALS AND METHODS 117
2.1. Cohort Population, Inclusion Criteria, and Sampling Methodology *117*
2.2. Multi-Omic Analysis *119*
2.3. Network Construction and Multi-Omic Integration *122*
2.4. Clinical Translation *124*
3. CONCLUSIONS 125

REFERENCES 127

SECTION III DEEP PLASMA PROTEOMICS WITH DATA-INDEPENDENT ACQUISITION: CLINICAL STUDY PROTOCOL OPTIMIZATION WITH A COVID-19 COHORT **136**

ABSTRACT 137
GRAPHICAL ABSTRACT 138
■ INTRODUCTION 139
■ METHODS 142
■ STATISTICAL ANALYSIS 149
■ RESULTS 150
Enhanced Protein Detection with Fractionation *150*
Comparative Advantages of DIA over Traditional DDA Approaches *155*
■ DISCUSSION 163
■ CONCLUSIONS 170
■ ASSOCIATED CONTENT 171
■ REFERENCES 173

SECTION V LONGITUDINAL MULTI-OMICS NETWORK ANALYSIS REVEALS COMPLEMENT–COAGULATION REWIRING IN LONG COVID **179**

ABSTRACT 180
INTRODUCTION 181
COVID-19 overview *181*
Post-acute sequelae of COVID-19 (PASC) *182*
Multi-omic studies of PASC *183*
METHODS 186
Patient cohort composition, sample collection, and storage *186*
Wet-lab methodology *187*
Bioinformatic preprocessing pipelines *189*
Analytical methodologies *191*
RESULTS 194
Differential expression and GSEA analysis *194*
Multi-omic network construction and topology *196*
Differential wiring (PASC vs recovered) *198*
Regulation within the complement control layer *200*
Broader coagulation and anticoagulant neighbourhoods *202*
DISCUSSION 204

REFERENCES 212

SECTION VI OVERALL CONCLUSIONS AND HOLISTIC DISCUSSION OF LONG COVID MECHANISMS **217**

HOW PASC RISK IS PLANTED DURING THE ACUTE PHASE OF COVID-19 217
FACTORS PROPAGATING PASC DURING THE CONVALESCENT PHASE OF COVID-19 220
A UNIFYING MODEL 221
FUTURE STEPS: FROM EXPLORATION TO TESTABLE HYPOTHESES 222
LIMITATIONS 223
CLOSING NOTE 226

APPENDIX **229**

SUPPLEMENTARY INFORMATION 1: MULTI-ORGAN INVOLVEMENT OF COVID-19 229
1.1 Pulmonary Pathology and ARDS Development *229*
1.2 Endothelial Dysfunction and Endothelialitis *232*
1.3 Neurological Implications *235*
1.4 Cardiovascular Implications *240*
1.5 Gastrointestinal and Hepatic Effects *245*
References *251*
SUPPLEMENTARY INFORMATION 2: DATA MANAGEMENT PLAN 259
SUPPLEMENTARY INFORMATION 3: ADDITIONAL MULTI-OMIC ANALYTICAL METHODOLOGIES. 261
References *273*
SUPPLEMENTARY INFORMATION 4: SUPPLEMENTARY METHODOLOGY RELATING TO SECTION V 275
References *292*
SUPPLEMENTARY INFORMATION 5: SUPPLEMENTARY RESULTS RELATING TO SECTION V 295

Abbreviations

ACE2 - Angiotensin-Converting Enzyme 2

AD - Alzheimer's Disease

ADH - Antidiuretic Hormone

AKI - Acute Kidney Injury

ALT - Alanine Aminotransferase

AM - Alveolar Macrophages

ANA - Antinuclear Antibodies

Ang II - Angiotensin II

ANG-1 - Angiopoietin 1

ANS - Autonomic Nervous System

anti-TPO - Thyroid Peroxidase Antibodies

ARDS - Acute Respiratory Distress Syndrome

Arg-1 - Arginase-1

AST - Aspartate Aminotransferase

AT2 - Alveolar Type 2 Cell

Aβ - Amyloid Beta Peptide

BBB - Blood-Brain Barrier

BiPS - Binding Immunoglobulin Protein

C/EBPβ - CCAAT/Enhancer-Binding Protein β

CAC - COVID-19–Associated Coagulopathy

CD11a - Integrin Alpha L

CDC - US Centres for Disease Control and Prevention

CFS - Chronic Fatigue Syndrome

CKD - Chronic Kidney Disease

CLR - C-Type Lectin Receptor

CMV - Cytomegalovirus

CNS - Central Nervous System

COPD - Chronic Obstructive Pulmonary Disease

CRP - C-Reactive Protein

CSF - Blood-Cerebrospinal Fluid

CYP - Cytochrome P450

DAd - Delayed Afterdepolarizations

DAD - Diffuse Alveolar Damage

DAT - Deaminotyrosine

DC - Dendritic Cells

DIC - Disseminated Intravascular Coagulation

DLCO - Diffusing Capacity of the Lungs for Carbon Monoxide

EA - EBV Early Antigen

EBV - Epstein–Barr Virus

EHR - Electronic Health Record

ENA - Extractable Nuclear Antigens

EPCR - Endothelial Protein C Receptor

FMS - Fibromyalgia Syndrome

fAAbs – Functional Autoantibodies

GBP - Guanylate Binding Proteins

GBS - Guillain-Barré Syndrome

GI - Gastrointestinal

GM-CSF - Granulocyte-Macrophage Colony-Stimulating Factor

G-MDSC - Granulocytic Myeloid-Derived Suppressor Cells

gp130 - Glycoprotein 130

GPCR - G-Protein-Coupled Receptors

GSDMD - Gasdermin D

HHV - Herpesvirus

HR - Hazard Ratio

HSPC - Hematopoietic Stem/Progenitor Cells

IBD - Inflammatory Bowel Disease

IBS - Irritable Bowel Syndrome

ICAM-1 - Intercellular Adhesion Molecule-1

ICU - Intensive Care Unit

IFITM - Interferon-Induced Transmembrane Proteins

IFN - Interferon

IFNAR - IFN-α/β Receptors

IL - Interleukin

IRF3 - IFN Regulatory Factor 3

ISG - Interferon-Stimulated Gene

IκB - Inhibitor of κB

JAK - Janus Kinase

KCO - Carbon Monoxide Transfer Coefficient

LPS - Lipopolysaccharide

MAIT - Mucosal-Associated Invariant T

MAPK - Mitogen-Activated Protein Kinase

MAVS - Mitochondrial Antiviral-Signalling Protein

MCP-1 - Monocyte Chemoattractant Protein 1

MDM - Monocyte-Derived Macrophages

ME - Myalgic Encephalomyelitis

MHC - Major Histocompatibility Complex

MMN - Multifocal Motor Neuropathy

MMP-9 - Matrix Metalloproteinase-9

MPO - Myeloperoxidase

NET - Neutrophil Extracellular Traps

NICE - British National Institute for Health and Care Excellence

NIH - US National Institutes of Health

NIHSS - NIH Stroke Scale

NINJ1 - Ninjurin-1

NK - Natural Killer

NO - Nitric Oxide

NRP-1 - Neuropilin-1

NSP - Non-Structural Proteins

OR - Odds Ratio

PAIS - Post-Acute Infectious Symptoms

PAI-1 - Plasminogen Activator Inhibitor-1

PASC - Post-Acute Sequelae of SARS-CoV-2 Infection

PBMC - Peripheral Blood Mononuclear Cells

PD-1 - Programmed Cell Death Protein 1

PDC - Plasmacytoid Dendritic Cell

PKR - Protein Kinase R

Plpro - Papain-Like Protease

PNS - Peripheral Nervous System

POTS - Postural Orthostatic Tachycardia Syndrome

PRR - Pattern Recognition Receptors

P-SEL - P-selectin

PTSD - Post-Traumatic Stress Disorder

RAAS - Renin-Angiotensin-Aldosterone System

RHD - Rel Homology Domain

ROS - Reactive Oxygen Species

S protein - Spike protein

SCFA - Short-Chain Fatty Acid

SFN - Small-Fibre Neuropathy

sHLH - Secondary Hemophagocytic Lymphohistiocytosis

SLC6A19 - Sodium-Dependent Neutral Amino Acid Transporter B0AT1

SLE - Systemic Lupus Erythematosus

STAT - Signal Transducers and Activators of Transcription

STING - Stimulator of Interferon Genes

TBK1 - TANK-Binding Kinase 1

TCM - Takotsubo Cardiomyopathy

TF - Tissue Factor

TIM-3 - T-cell Immunoglobulin and Mucin Domain 3

TJ - Tight Junctions

TLR - Toll-Like Receptors

TMPRSS2 - Transmembrane protease serine 2

V/Q - Airflow/Blood Flow

VCA - EBV Viral Capsid Antigen

VE-Cad - VE-Cadherin

VEGF - Vascular Endothelial Growth Factor

VOC - Variant of Concern

vWF - von Willebrand Factor

VZV - Varicella-Zoster Virus

WHO - World Health Organization

Acknowledgements

This thesis was only possible by the combined contributions of a huge number of people. I am deeply grateful to my supervisors, Prof. Laure Elens and Prof. Leïla Belkhir, for conceiving this project and guiding me in its implementation with much needed support and insight.

I also thank the Systems Biology consortium for the essential contributions to the success of this work, Prof. Jean-Luc Balligand, Dr Bertrand Bearzatto, Dr Guido Bommer, Prof. Patrice D. Cani, Dr Julien De Greef, Dr Joseph P. Dewulf, Prof. Laurent Gatto, Prof. Vincent Haufroid, Dr Sébastien Jodogne, Prof. Benoît Kabamba, Dr Sébastien Pyr dit Ruys, Dr Didier Vertommen, and Prof. Jean Cyr Yombi. I am additionally thankful to Prof. Laure Bindels and Maxime Lingurski for their support in the implementation and execution of key aspects of the project.

I would also like to thank the study nurses and coordinators from Cliniques Universitaires Saint-Luc, Céline D'Aoust, Valérie Kin, Anne Bouvier, and Françoise Leunen, for their dedication to patient recruitment, bio-sample collection, follow-ups, and patient medical information collection.

Finally, I wish to express my profound gratitude to all the participants who volunteered for this study. Their willingness to provide bio-samples and return for follow-up visits made this research possible.

Introduction

The COVID-19 pandemic made clear the need for fast, reliable ways to move from samples to insight. This thesis answers that need with three goals. First, wet-lab and bioinformatic pipelines were built at UCLouvain, integrated within Belgium healthcare through Cliniques Universitaires Saint-Luc and Grand Hôpital De Charleroi, allowing for investigations both into **rare, complex diseases** and **rapid responses to new pathogens**. Second, using COVID-19 as a test case, we apply these pipelines to study **post-acute sequelae of SARS-CoV-2 infection** (PASC/long COVID). Third, we use the results to **propose clear, testable hypotheses** that can help researchers **focus resources** where they matter most.

Section I reviews what is known about acute SARS-CoV-2 and outlines leading ideas for PASC onset and continuation. It organises the field around **persistent stimuli**, **immune and inflammatory changes**, **vascular and coagulation pathways**, and **organ-specific effects**, motivating a **multi-omic approach to a multisystem problem**.

Section II features the first article published in regard to this project, describing the programme backbone ("HYGIEIA"). It covers governance, biobanking, pre-analytics, the proposed laboratory methodologies (genomics, transcriptomics, proteomics, metabolomics, metagenomics), and planned bioinformatic workflows. The emphasis is on **standard operating procedures and reusable code** so cohorts can be activated rapidly, and analyses reproduced.

Section III is another published original article detailing part of the wet-lab protocol optimisation using deep plasma proteomics with data-independent acquisition (DIA). We benchmarked unfractionated against fractionated and pooled-fractionated workflows.

Fractionation improved coverage, especially for low-abundance proteins, with a respectable time and cost trade-off for clinical studies. Paired with a streamlined DIA analysis pipeline, this yields a **robust, scalable platform for biomarker discovery and systems analysis beyond COVID-19**. It should be noted that although only the proteomics workflow was published, extensive work was undertaken to ensure **robust and optimised SOPs were created for all omics**.

Section IV contains another original article tackling a gap in the current literature: **respiratory shotgun metagenomics in people who did or did not develop PASC**. Across time, overall diversity differences were limited, but differential abundance and network analyses pointed to **taxa that may be protective against PASC**. ***Dolosigranulum pigrum*** and certain ***Corynebacterium* species** formed a candidate "protective consortium" linked to better outcomes. Exploratory signals also suggested **antibiotic exposure could influence trajectories**, an observation that warrants targeted prospective testing. This article represents **the first PASC longitudinal respiratory microbiome analyses conducted** so far.

Section V features the main multi-omic article of this project, **integrating systemic proteomic, metabolomic, transcriptomic, and genomic data** from the same individuals to **probe post-acute biology at the pathway and network level**. Single-omic, gene-level hits were sparse after correction, but gene-set and network models revealed insight. **Complement and coagulation pathway activity and immunoglobulin features distinguished participants** with persistent symptoms from those who recovered. Network wiring highlighted regulatory molecules and immunoglobulin heavy-chain architecture as

potential control points, and cross-omic links plus drug-target overlays prioritised mechanisms suitable for follow-up studies. This article presents a **refreshed bioinformatic methodology for network analysis** by comparatively analysing network connectivity between patient groups to identify “rewired” nodes.

Section VI discusses the project as a whole and synthesises the previous work into a **microvascular model in which complement, coagulation, platelets, and endothelium remain tightly coupled after COVID-19**, producing low-grade, spatially heterogeneous microthrombosis rather than large single-marker shifts. It identifies risk in the acute phase, shaped by residual organ injury as suggested in our work by a lack of an upper-airway “protective consortium” (notably *Dolosigranulum pigrum* and *Corynebacterium*) whose depletion aligns with later PASC, and shows how, in convalescence, network rewiring (C3-biased complement control, prothrombin/F2–thrombin context, coagulation and complement regulatory dysfunction (heparin cofactor II, alpha-1 antitrypsin, complement factor H-related 5), and altered immunoglobulin connections) propagates this loop. From this model follow two suggestions: PASC therapeutic approaches should **prioritise primary prevention (vaccination, early treatment, and careful antibiotic use)**, and secondly, **research into PASC can be elevated through network and system approaches**; such approaches can thus also be applied to the **exploration of other novel and complex diseases**. The section then sets near-term next steps such as **validating the airway–microbiome axis** and **testing the complement–coagulation–platelet hypothesis**. The section closes with a targeted account of limitations (**blood-centric sampling, causal**

ambiguity, limited power and timepoints, and real-world confounding) alongside remedies for future work.

In short, this thesis delivers both infrastructure and insight. It establishes a deployable **lab-to-analysis pipeline that can be reused across diseases and in future outbreaks**; applies it to COVID-19 to generate **integrative findings on PASC**; and distils those findings into **clear hypotheses to guide the next wave of experiments**. While built in response to SARS-CoV-2, the approach is deliberately general and ready to support future work on rare, complex, or newly emerging diseases.

Section I 5 years on COVID-19: A pathophysiological review

Introduction

Five years on from its identification in late 2019, SARS-CoV-2 has since (as of November 2025) **infected almost 800 million** people globally, **killed over 7 million** people worldwide, and caused a full-scale pandemic resulting in a **$16 trillion economic toll** across the world [1,2]. COVID-19, caused by SARS-CoV-2 infection, manifests as a multi-phase illness, ranging from asymptomatic or mild upper respiratory symptoms to severe pneumonia, acute respiratory distress syndrome (ARDS), and multi-organ failure [3]. Disease severity hinges on viral dynamics and host responses. Patients mounting a strong early immune defence often clear the virus and avoid severe illness, whereas delayed or dysregulated responses can result in unchecked viral replication, hyperinflammation, and even life-threatening consequences [4]. This first section delineates the state-of-the-art understanding of COVID-19 pathophysiology, spanning acute infection and PASC, with an emphasis on mechanisms of disease and organ-specific pathology. To this end, we aim to summarize and clarify the extensive scientific research that has taken place in the previous 5 years, highlighting mechanisms of particular interest or areas of research not yet sufficiently explored.

As a first brief overview of the pathophysiological phases, acute COVID-19 typically involves an incubation period with initial viral replication in the nasopharynx, potentially progressing to systemic involvement. Key acute-phase mechanisms include: Direct **viral cytotoxicity** in infected tissues [5]; **Endothelial damage** and **microvascular injury** [6]; Innate and adaptive **immune dysregulation** leading to hyperinflammatory states (cytokine storms) [7]; **Coagulopathy** with *in-situ* thrombosis [8]; Renin–angiotensin–aldosterone system **(RAAS) perturbations** via angiotensin-converting enzyme 2 (ACE2) [9]; **Monocyte and**

macrophage dysregulation [10]; Neutrophil extracellular traps **(NETs) and immunothrombosis** [11]; **Hyperactivation and exhaustion of T cells** [12]. Following the acute phase, PASC encompass persistent symptoms beyond 4–12 weeks (roughly, its exact definition changes based on the defining body, this is discussed later in chapter 3 of this section). PASC is commonly associated with **persistent immune dysregulation** and **chronic inflammation**, as supported by numerous studies and reviews such as those by the RECOVER initiative. PASC is likely driven by one or a combination of the following proposed mechanisms: **Viral RNA and protein persistence** [13]; **Reprogramming of immune cells** towards pro-activation and NET-forming signatures [14]; SARS-CoV-2 triggered **autoantibody production** [15]; **Endothelial damage** leading to microthrombi formation and abnormal organ function [16]; **Dysautonomia** [17]; **Reactivation of latent viruses** (notably Epstein–Barr Virus (EBV)) [18]; **Altered cellular metabolism** and **impaired mitochondrial function** [19]; Enhanced susceptibility to PASC through **microbiome compositions** [20]. We structure this review by first addressing acute COVID-19 pathophysiology by system (virology, immune response, coagulation, pulmonary, etc.), then examine PASC mechanisms and clinical sequelae. Each section integrates recent findings and seminal works to provide a comprehensive understanding.

1. Viral Entry and Replication Mechanisms

1.1 Viral Structure and Cell Entry Pathways

SARS-CoV-2 is an enveloped positive-sense RNA virus of the Betacoronavirus genus. It shares ~79% genomic identity with SARS-CoV-1 (SARS 2003) and ~50% with MERS-CoV (2012), but exhibits unique features that enhance infectivity [21]. The viral spike (S) protein mediates host cell entry by binding to the ACE2 receptor. SARS-CoV-2 spike protein has 10–20-fold higher affinity for human ACE2 than SARS-CoV-1 spike, partly explaining its efficient human transmission [22]. ACE2 is broadly expressed in numerous tissues, including airway epithelia, lung alveolar type II (AT2) cells, heart, endothelium, kidneys, intestines, and others. Because SARS-CoV-2 is primarily transmitted through the air, initial infection most commonly occurs when infectious respiratory particles are inhaled and deposited on the apical side of multiciliated epithelial cells, which prominently display ACE2 on their distal cilia extensions [23,24].

After ACE2 attachment, the S protein requires priming by host proteases for membrane fusion. Transmembrane protease serine 2 (TMPRSS2), abundantly expressed on respiratory epithelium (especially type II pneumocytes), cleaves the S protein at the S1/S2 site [25]. SARS-CoV-2 uniquely possesses a polybasic (furin) cleavage site at S1/S2 absent in SARS-CoV-1, enabling more effective priming by furin-like proteases [26]. This difference likely contributes to SARS-CoV-2's heightened infectivity. The entry process can be summarized in stages:

- **Attachment**: S protein S1 subunit binds to ACE2 on the host cell surface.
- **Priming**: TMPRSS2 (and other proteases like furin or cathepsins) cleave the S protein at the S1-S2 site, exposing and activating the membrane fusion S2 subunit trimers.

- **Membrane Fusion**: The viral envelope fuses with the host cell membrane, facilitating entry of the viral RNA genome into the cytoplasm.
- **Replication**: Viral RNA is translated; the replication-transcription complex synthesizes new genomes and subgenomic RNAs. Viral proteins (structural and non-structural) are produced using host machinery.
- **Assembly & Release**: New virions assemble in the endoplasmic reticulum and Golgi and are released via exocytosis to infect neighbouring cells.

Targeting entry mechanisms is a therapeutic strategy. Agents blocking ACE2-spike interaction (soluble ACE2 decoys, monoclonal antibodies) or inhibiting TMPRSS2 (camostat) have been explored [27–29]. In addition, emerging evidence indicates ACE2-independent entry routes for SARS-CoV-2, notably in immune cells. Neuropilin-1 (NRP-1) is one such alternative receptor that binds the furin-cleaved S1 fragment, enhancing infectivity of cells with low ACE2 [30]. For example, NRP-1 is highly expressed in olfactory epithelium and may facilitate neuro-invasion via the olfactory nerve. Another candidate is cell-surface binding immunoglobulin protein (BiPS), proposed as a coreceptor on monocytes enabling ACE2-independent viral entry [31]. While ACE2 remains the principal entry route in most tissues, these auxiliary pathways could contribute to tissue tropism and need further study.

1.2 Viral Tropism and Replication Kinetics

Upon initial infection in the upper respiratory tract, SARS-CoV-2 replicates efficiently in nasal and bronchial epithelial cells. High viral loads in the nasopharynx are detectable around symptom onset. As infection progresses, the virus can disseminate to the lower respiratory tract and potentially cause viremia, seeding other organs. One pivotal autopsy

study demonstrated widespread distribution and persistence of SARS-CoV-2 RNA in more than 80 distinct anatomical locations and body fluids, including notable organs such as the lungs, heart, gastrointestinal (GI) tract, endothelium, kidneys, liver, and brain [32]. Within this study, it was also found viral RNA persisted in some tissues up to 230 days after symptom onset. Despite this dissemination, the same study noted minimal inflammation in some organs despite high viral RNA, suggesting that direct viral presence doesn't always correlate with immune response intensity. These findings hint at reservoirs of SARS-CoV-2 that might underlie prolonged symptoms in PASC, even as acute illness resolves.

The efficiency of viral replication and early spread is a key determinant of disease severity. An early robust interferon (IFN) response can curb replication, resulting in mild disease [33]. Conversely, SARS-CoV-2 has evolved mechanisms to evade or delay the innate antiviral response, allowing unchecked replication in initial days. These evasion tactics are discussed below (Section I, chapter 2.5) and can lead to a blunted early IFN response, a feature strongly associated with severe COVID-19. These patients often have inappropriately low type I IFN levels in the acute phase. In this regard, Zhang *et al.* found severe patients had enrichment of loss-of-function mutations in *TLR3*, *IRF7*, and other IFN activating genes, whilst Bastard *et al.* found over 10% of these patients harboured high titres of neutralizing autoantibodies against IFN-α2 and IFN-ω [34,35]. These findings underscore the critical role of early innate immunity in controlling viral replication.

1.3 Viral Evolution and Variants

Although the focus of this review is pathophysiology, it's noteworthy that SARS-CoV-2 has rapidly evolved into multiple variants with differing pathogenic profiles. The SARS-CoV-2

replication rate is estimated at $1.3x10^{-6}$ mutations per nucleotide per replication cycle, consistent with other betacoronaviruses but below the typical range for other RNA viruses like HCV or HIV [36]. However, during the early phase of the pandemic, three highly divergent lineages emerged (variants of concern (VOCs) Alpha, Beta, and Gamma) in different parts of the world independently, likely from continued viral replication during chronic infection [37]. The key mutations in these and other VOCs occur in the S protein, at areas critical for ACE2 binding, such as the receptor-binding domain, or at the N-terminal domain and furin cleavage sites, which alter infectivity and immune evasion.

The Beta variant (B.1.351) actually likely emerged first, sometime before June 2020 in South Africa, but was not detected until October 2020 [38]. Following this, Alpha (B.1.1.7) likely emerged in September 2020 in the United Kingdom, followed by Delta (B.1.617.2) in October 2020 in India and Gamma (P.1) in November 2020 in Brazil [39–41]. These VOCs possessed mutations that either enhanced transmissibility, increased virulence, and/or reduced the efficacy of monoclonal antibodies and vaccines [39,42–47]. Alpha and Delta were particularly transmissible, with the Alpha variant being the major infectious agent during April 2021, before Delta became the dominating virus during the latter half of the year. These variants have all been associated with more severe respiratory disease, resulting in increased hospitalizations and mortality rates when compared to wild-type lineage [38,48,49].

The later emergence of Omicron (B.1.1.529) in South Africa marked the start of a new phase of the pandemic. The first three Omicron lineages, BA.1 (the main lineage), BA.2, and BA.3, all emerged independently in October 2021, these were then followed by BA.4 and BA.5 in December 2021 and January 2022 respectively; these constitute the main

Omicron sub-lineages [50,51]. The numbers of S protein mutations identified within Omicron variants are 3-4-fold higher than those of previous variants, which despite leading to higher transmissibility and less susceptibility to vaccines, often caused milder disease severity [52]. Omicron became the most dominant variant across the globe, and its subvariants have continued its dominance up to the time of writing (November 2025), such as the “Stratus” or “Frankenstein” variant, a recombinant Omicron lineage XFG which has become dominant in parts of Europe since mid-2025. Some of these subvariants show altered cell entry preference, such as BA.1 and BA.2 which shifted from TMPRSS2-dependent fusion toward endosomal entry, potentially affecting which cell types are infected (shifting more towards the upper airway) [53].

This shift was in part due to the need to escape neutralizing antibodies in its host population becoming the dominant selective pressure, a mechanism precedented by studies of HIV-1 evolution in a host [54]. This shift, while enhancing its capacity for antibody evasion, has rendered Omicron more vulnerable to innate restriction factors such as guanylate binding proteins (GBPs) and interferon-induced transmembrane proteins (IFITMs), a trade-off that likely contributes to its lower pathogenicity and milder disease severity [55]. Nonetheless, the core mechanisms of pathogenesis largely persist across variants, with severe disease linked to host factors and immune responses rather than direct cytopathic effect alone.

2. Immune Response and Hyperinflammation

2.1 Innate Immune Activation and Interferons

At the onset of SARS-CoV-2 infection, innate immunity provides the earliest host defence, involving epithelial barriers, signalling molecules, and rapid cellular responses that detect the virus, induce antiviral programmes (including type I/III IFNs), recruit effector cells, and shape the subsequent adaptive immune response. Airway epithelial cells, alveolar macrophages (AMs), and dendritic cells recognize viral components via pattern recognition receptors (PRRs), namely Toll-like receptors (TLRs) and RIG-I-like receptors (RLRs). This then triggers production of type I/III IFNs (mainly IFN-α/β) along with pro-inflammatory cytokines such as tumour necrosis factor (TNF), interleukin (IL)-1, and IL-6. These molecules spread throughout the infected tissue, initiating antiviral defences in neighbouring cells and recruiting and activating additional immune cells. In COVID-19, an early and well-controlled interferon response is generally linked to better viral control, whereas delayed or dysregulated interferon signalling together with sustained inflammatory cytokine production has been associated with severe disease [56].

Specifically, IFNs (named for their ability to interfere with virus replication) bind to IFN-α/β receptors (IFNARs) on neighbouring cells, activating the Janus kinase/signal transducers and activators of transcription (JAK-STAT) signalling pathway, leading to the formation and translocation of the interferon-stimulated gene (ISG) factor 3 complex to the nucleus where it induces the transcription of hundreds of ISGs [57].

The proteins encoded by ISGs function to interfere with virtually every stage of the viral life cycle. For example, protein kinase R (PKR) is activated by viral double-stranded RNA and subsequently phosphorylates the translation initiation factor eIF2α, which shuts down

both viral and host protein synthesis to inhibit viral replication [58]. Mx proteins are another such ISG and work by directly binding viral nucleocapsids, or other viral components, to trap and degrade them, preventing viral replication [59,60]. A third protein of interest is OAS1, which is activated in the cytoplasm by viral dsRNA and synthesizes 2',5'-oligoadenylates that in turn activates RNaseL, an enzyme that cleaves cellular and viral RNAs [61]. Finally, another key ISG, is a ubiquitin homologue that targets at least 158 proteins including signalling components (JAK1 and STAT1), PRRs (RIG-I), and other antiviral effector proteins (MxA, PKR and RNaseL) [62–64]. Unlike the target protein degrading effects of K48-linked ubiquitination, ISG15 instead parallels the activating effects of K63-linked ubiquitination through a ISGylation pathway which stabilizes antiviral regulators and promotes antiviral enzyme activity [65,66].

Thus, type I IFNs serve as a critical first line of defence by rapidly alerting uninfected cells and orchestrating a broad-spectrum antiviral response essential for controlling early viral infections. In mild COVID-19, this process is timely and robust, leading to viral clearance.

2.2 Key Immune Cells in COVID-19 Pathogenesis

Airway epithelial cells are the initial targets for SARS-CoV-2 and so are among the first to produce IFNs upon viral infection. However, as discussed before, the IFN response is notably delayed and insufficient to immediately control viral replication, allowing the virus to spread before a robust antiviral state is established. As the infection progresses, additional immune cells are activated through multiple complementary mechanisms. Below, the most relevant to pathogenesis are discussed.

Plasmacytoid dendritic cells (pDCs) are a rare subset of dendritic cells specialized for antiviral defence. They are often called “professional interferon-producing cells”, which rapidly secrete large quantities of IFN-α/β, upon viral detection, to bridge innate and adaptive immunity by activating natural killer (NK) cells and T cells for virus clearance [67]. Notably, *in vitro* studies indicate pDCs detect SARS-CoV-2 more effectively by sensing infected cells, rather than free virus particles, through intercellular adhesion molecule-1 (ICAM1) and integrin alpha L (CD11a) engagement between pDCs and infected cells [68]. Selective pressures have promoted some variants to limit this sensing, through reduced CD11a induction for Alpha variants, or through perturbation of IFN production in the case of Delta and Omicron [68]. pDCs are typically the most potent producers of type I and III IFNs during viral infections, releasing 10–100 times more than most other cells and making them crucial elements of the immune response [69]. This lack of early pDC-driven IFN is a hallmark of severe COVID-19, and indeed, in patients with severe COVID-19, a pronounced lack of functional pDCs in both blood and lung tissues is evident from the very onset of the disease [70–74]. This “pDC desert” could be hypothesised to result from a combination of excessive recruitment into infected tissues and rapid, chronic activation, causing function impairment, exhaustion and apoptosis due to the hyperinflammatory environment. As a result, the pDCs present in the lungs of severe patients produce little to no IFN, contributing to a deficient antiviral response. On the other hand, some studies caution that if pDCs produce IFN too persistently it might contribute to tissue damage in later stages, so a balanced pDC response is key [75–77]. Overall, SARS-CoV-2’s ability to diminish pDC numbers and interfere with their interferon production impairs a critical antiviral defence, setting the stage for severe disease progression.

AMs are tissue-resident cells that, under normal conditions, quietly maintain lung homeostasis by clearing debris and pathogens while preventing excessive inflammation. During early SARS-CoV-2 infection they engulf viral particles and secrete cytokines to recruit additional immune cells. In patients with severe disease, functional AMs are diminished and the remaining infected AMs upregulate genes for IL1B, CCL4, CCL20, CXCL10 and CXCL11 which serve to recruit massive numbers of blood monocytes (and T cells) to the lung for reinforcements [78]. Normally, these monocytes would then differentiate and polarize into pro-inflammatory (M1) or anti-inflammatory (M2) macrophages depending on the cytokine environment [79]. Usually this process helps balance the immune response, however, SARS-CoV-2 induces a molecular shift in macrophages by promoting the uptake of viral RNA, which triggers proinflammatory cytokine release and drives macrophages toward an M1-like, pathogenic phenotype whilst preventing their reversion to an anti-inflammatory state [80]. In severe cases, this becomes a positive feedback loop of inflammation as the incoming monocytes flood the alveolar space and differentiate into monocyte-derived macrophages (MDMs) with M1-like signatures, secreting abundant IL-6, IL-8, TNF-α and other cytokines [81]. These cytokines majorly contribute to the cytokine storm, whilst the chemokines sustain lung inflammation through monocytes and neutrophils recruitment. Further, MDMs in the lungs of severe COVID-19 patients often express tissue-factor (TF) and contribute to immunothrombosis and fibrosis, linking the inflammatory response to some of the vascular complications of COVID-19 [82,83].

Neutrophils, the most abundant blood leukocytes, are rapid responders that migrate to infection sites, often within minutes of trauma. However, in the lungs and alveolar space, efficient AM pathogen clearance restricts neutrophil recruitment only to periods of significant infection, thereby preventing constant inflammation [84]. When recruited, neutrophils clear pathogens through phagocytosis, inactivating them within phagolysosomes using proteases and reactive oxygen species (ROS), a controlled response that minimizes bystander damage. In contrast, excessive stimulation by pathogen-associated molecular patterns (PAMPs) and damage-associated molecular patterns (DAMPs) triggers neutrophils to unleash their full arsenal without restraint (NETs, granules, oxidants, and proteases) which in severe COVID-19 is linked to lung injury and thrombosis. Specifically, uncontrolled degranulation and NET release damage the alveolar–capillary barrier via enzymes such as elastase and myeloperoxidase (MPO) and cytokines like IL-8 [85–87]. Furthermore, studies have found excessive NETs in the blood of severe COVID-19 patients forming thrombo-inflammatory clusters that contribute to microthrombi and organ injury [88,89]. Importantly, SARS-CoV-2 induces emergency granulopoiesis in severe disease, prematurely releasing immature neutrophils and granulocytic myeloid-derived suppressor cells (G-MDSCs) [90]. These left-shifted neutrophils exhibit enhanced degranulation and ROS production and uncontrolled NET formation, whilst G-MDSCs are defined most notably by suppressing T-cell proliferation and cytokine production, through secretion of molecules like arginase-1 (Arg-1), ROS, and IL-10 [90,91]. The resulting neutrophilia and high neutrophil-to-lymphocyte ratio are negative prognostic indicators [92]. This creates a situation in which neutrophils exacerbate tissue-damaging inflammation while concurrently dampening adaptive immunity.

2.3 The "Cytokine Storm"

In patients where the immune response and IFN production are not sufficiently calibrated, SARS-CoV-2 gains an early foothold that predisposes to life-threatening outcomes. During the initial "stealth" phase, infected cells produce minimal IFN while secreting abundant proinflammatory chemokines, allowing unchecked viral replication before the immune system fully responds [93]. This sets the stage for a cascade of dysregulated immunity.

By the time the host mounts a substantial IFN response, the infection is often widespread. A late "compensatory" surge of IFNs may occur as accumulating viral RNA and cell damage eventually trigger PRRs. Paradoxically, IFNs that are protective when produced early can be detrimental if produced too late or in excess, with elevated systemic IFN levels at later stages of COVID-19 disease correlated with worsening disease outcomes [94]. Prolonged or high-dose IFN exposure can amplify inflammation and impede lung tissue-repair processes [95,96]. This timing mismatch, weak IFN activity during initial viral expansion followed by an uncoordinated surge, leads to an excessive and dysregulated innate response that can spiral towards immunopathology. The innate immune system, now fully alarmed, releases a torrent of cytokines into the lungs and circulation, creating a vicious cycle that recruits additional immune cells which in turn secrete more cytokines and increase the number of target cells for infection [97–99]. The lung tissue becomes a battleground of uncontrolled inflammation, leading to diffuse alveolar damage, pneumonia, and ARDS [56]. In critical cases, the inflammation spills over systemically, causing vasculature dysfunction, coagulopathy, and multi-organ exhaustion and injury. Early in the pandemic, reports described this hyperactivation as a "cytokine storm", an immune hyperactivation resembling secondary hemophagocytic lymphohistiocytosis (sHLH), a severe, life-

threatening syndrome characterised by an excessive inflammatory response. However, later studies have argued COVID-19 hyperinflammation is distinct and less extreme than sHLH, with only rare cases meeting full HLH criteria [100].

A cytokine storm is not unique to COVID-19, and was first coined in 1993 to describe an acute graft-versus-host disease [101]. Historically, *Yersinia pestis*, responsible for three major pandemics encompassing 1500 years (Plague of Justinian, Black Death, and the Third plague pandemic), has been seen to trigger inflammatory cytokine storms in infected individuals [102]. Similarly, it is believed that an exaggerated immune response triggered by the H1N1 virus played a significant role in the high mortality observed during the 1918 influenza pandemic [103]. A study investigating cytokine storms across various diseases found that these storms are characterized by progressive hypercytokinemia, with elevated levels of TNF-α, IL-6, IL-1β, proinflammatory chemokines, activated macrophages, and increased NF-κB [104].

NF-κB is a master transcription factor that orchestrates the expression of numerous inflammatory cytokines and mediators yet is maintained in an inactive state in quiescent cells by inhibitor of κB (IκB) binding to its Rel homology domain (RHD), thereby preventing its nuclear localization. During SARS-CoV-2 infection, however, NF-κB is markedly activated through multiple mechanisms, including TLR-mediated sensing of S protein (TLR2/4) and viral RNA (TLR3/7/8), cytosolic detection via RIG-I/MDA5, and TNF-α-driven amplification [105–107]. Other viral proteins including NSP3, NSP14, ORF3a, ORF6, and Nucleocapsid also show direct or indirect activation of NF-κB [108–112]. NF-κB is also additionally activated through cellular stress and ROS, a scenario especially pertinent in patients with pre-

existing conditions like cardiovascular disease, diabetes, or chronic lung disease where baseline oxidative stress and NF-κB activity are already elevated and thus one of the reasons such conditions are risk factors for severe disease [113,114]. Once within the nucleus, NF-κB drives the transcription of proinflammatory cytokines and chemokines (e.g. IL-1β, IL-6, TNF-α) that further launch their own signalling cascades. Moreover, its interplay with inflammatory pathways such as JAK-STAT and mitogen-activated protein kinase (MAPK) amplifies cytokine production. For example, NF-κB-driven IL-6 expression activates STAT3, further promoting additional proinflammatory mediator transcription, a key event in the progression toward cytokine storm [115]. High levels of NF-κB activity have been directly correlated with the severity of disease in COVID-19 [116]. Concurrently, NF-κB also regulates the expression of genes involved in cell survival, proliferation, and the inhibition of apoptosis. While these functions are beneficial in mounting an effective immune response, their persistent activation can result in pathological cellular survival and prolonged inflammation. In many patients, particularly those with pre-existing conditions or advanced age, the regulatory mechanisms that normally dampen NF-κB activity (such as the re-synthesis of IκB proteins) may be compromised [117]. This imbalance predisposes to the uncontrolled and sustained inflammatory response observed in severe cases.

IL-1β and TNF-α are often among the first cytokines released following NF-κB activation and play pivotal roles in priming and amplifying inflammatory responses. IL-1β is predominantly produced by monocytes and macrophages in a two-step process: NF-κB induced transcription of pro-IL-1β and NLRP3 as a first step, then if cellular stress is detected such as K^+ efflux, this triggers NLRP3 inflammasome assembly which activates

caspase-1 which cleaves pro-IL-1β (as well as pro-IL-18) into its mature, secreted form [118]. Caspase-1 is also responsible for plasma membrane rupture during pyroptosis, via gasdermin D (GSDMD) and Ninjurin-1 (NINJ1), allowing cytokine secretion, but also contributing to pathological inflammation [118]. Once released, IL-1β binds to IL-1 receptor type I (IL-1R1) and culminates in further NF-κB and MAPK pathway activation. In COVID-19, excessive IL-1β signalling triggers endothelial activation and dysfunction, inducing TF expression on both endothelial and immune cells and initiating the extrinsic coagulation cascade with subsequent thrombin generation and fibrin deposition [119]. Concurrent suppression of anticoagulant pathways and increased plasminogen activator inhibitor-1 (PAI-1) production shift the balance toward a prothrombotic state, ultimately driving hypercoagulation and, in severe cases, disseminated intravascular coagulation (DIC), which are associated with increased morbidity and mortality [120]. In a complementary manner, TNF-α, rapidly produced by activated macrophages, T cells, B cells, and dendritic cells, signals through TNF receptors (TNFR1 and TNFR2) to also activate both NF-κB and MAPK pathways [118]. In particular, TNFR1 recruits TRADD and TRAF2, leading to the activation of TAK1 and downstream inflammatory cascades. TNF-α also enhances IL-1β signaling and vice versa, contributing to cytokine cross-talk that fuels the storm [120]. In the pulmonary system, TNF-α drives tissue injury by promoting bronchial constriction, increasing endothelial permeability, and stimulating epithelial cells to release inflammatory mediators such as granulocyte-macrophage colony-stimulating factor (GM-CSF) and IL-8 [121]. TNF-α activation of neutrophils results in degranulation and release of proteases like matrix metalloproteinase-9 (MMP-9), further degrading lung architecture and function.

IL-6 has emerged as another critical cytokine in COVID-19, with studies consistently demonstrating markedly elevated levels in critically ill patients that strongly predict respiratory failure and the need for mechanical ventilation [120]. Following NF-κB activation, monocytes, macrophages, and dendritic cells rapidly produce and secrete IL-6. IL-6 signals to a broad range of cells using membrane-bound or soluble IL-6 receptors. The IL-6/IL-6R complex recruits glycoprotein 130 (gp130), initiating the JAK/STAT3 pathway [120]. Activated STAT3 translocates to the nucleus, to regulate expression of proinflammatory and prothrombotic genes. Through STAT3 activation, IL-6 drives Th17 differentiation, promotes B cell maturation, enhances cytotoxic T cell responses, and increases neutrophil recruitment, while concurrently suppressing regulatory T cells generation, skewing the immune balance toward uncontrolled inflammation [120]. STAT3 also upregulates acute-phase proteins like c-reactive protein (CRP) and fibrinogen in hepatocytes, increasing blood viscosity, enhancing platelet activation and increasing expression of adhesion molecules and TF, further tipping the haemostatic balance toward a prothrombotic state [122]. Such mechanisms link IL-6 to the COVID-19 hypercoagulable state. Moreover, IL-6 trans-signalling in endothelial cells is particularly pathogenic, as it induces the release of IL-8 and monocyte chemoattractant protein 1 (MCP-1/CCL2) that recruit proinflammatory neutrophils and macrophages, and stimulates vascular endothelial growth factor (VEGF) secretion which disrupts tight junction (TJ) proteins to increase endothelial permeability [120].

These immunological processes in severe COVID-19 are highly interconnected, unfolding concurrently as delayed IFN responses enable unchecked viral replication, subsequently

triggering dysregulated cytokine production via pathways such as NF-κB, MAPK, and JAK-STAT. A self-amplifying cycle is created, driving systemic inflammation, coagulopathy, and multi-organ injury. Importantly, this chapter highlights just a fraction of the many molecules and pathways involved in the complex pathophysiology of cytokine storm. This hyperinflammatory state is tightly linked with the next topic, coagulopathy, since inflammation and coagulation activate each other (the so-called thromboinflammatory cycle).

2.4 Immunothrombosis: Intersection of Inflammation and Coagulation

A striking feature of COVID-19 is coagulopathy with microthrombosis in the microvasculature of various organs, particularly the lungs (see Supplementary information 1). Figure 1 represents and discusses a simplified normal interaction of complement and coagulation pathways in healthy individuals, whilst the below text discusses in detail how these pathways are perturbed in COVID-19 infection. Although coagulopathy occurs in various severe infections such as bacterial sepsis, viral haemorrhagic fevers (e.g., Ebola and dengue), and influenza, COVID-19–associated coagulopathy (CAC) has distinct clinical characteristics and mechanisms. Specifically, CAC predominantly exhibits a thrombotic rather than haemorrhagic profile, though bleeding complications may still occur in advanced stages or with anticoagulation therapy [123]. CAC is identifiable through unique laboratory markers: elevated levels of D-dimer and fibrinogen, mild thrombocytopenia, and generally normal clotting times [124]. Elevated D-dimer levels (>0.5–1.0 µg/mL) correlate with poorer outcomes, with rising levels during hospitalization linked to increased mortality. Beyond microvascular thrombosis, CAC also predisposes patients to macrovascular complications such as deep vein thrombosis, pulmonary embolism, and

stroke [125]. This distinct profile likely reflects a multifactorial pathogenesis involving direct viral injury, heightened inflammation, complement activation, platelet hyperreactivity, and NETosis.

Viral infection of the endothelium leads to endotheliitis and a loss of the endothelium's inherent antithrombotic functions [126]. Damage to endothelial cells reduces protective molecules like thrombomodulin and heparin sulphate, which normally inhibit clotting, while simultaneously increasing prothrombotic factors such as von Willebrand factor (vWF) and P-SEL [127,128]. Although autopsy studies consistently demonstrate widespread endothelial inflammation in COVID-19, direct evidence of active viral replication within endothelial cells remains limited and controversial [129–132]. Thus, vascular injury may primarily result from indirect immune-mediated responses or initial viral entry without full replication. Such endothelial dysfunction creates a localized environment that favours thrombosis over bleeding, thereby contributing to the overall hypercoagulable state observed in COVID-19.

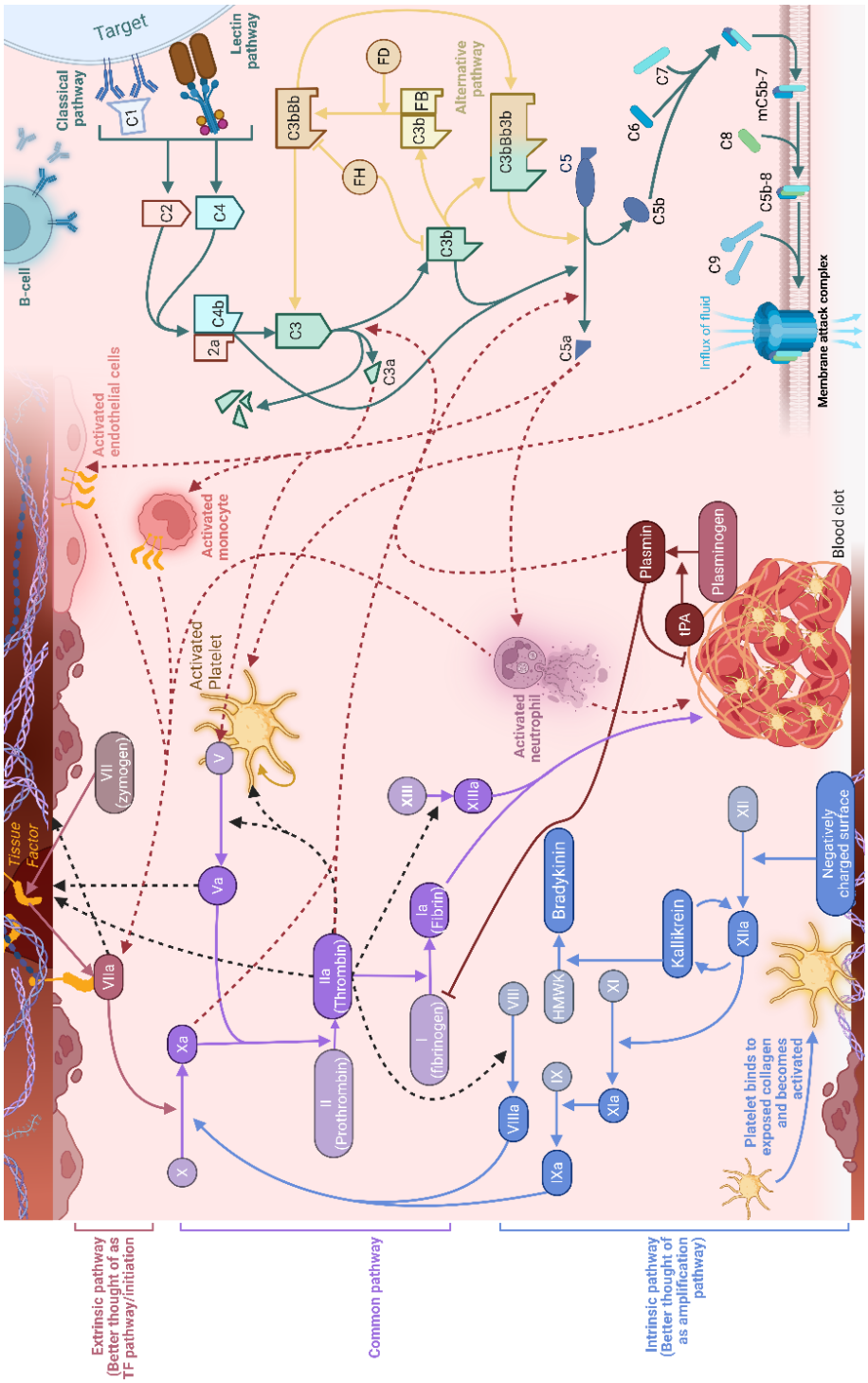

Target
Classical pathway
Lectin pathway
C1
C2
C4
B-cell
C4b
2a
C3
C3a
C3bBb
FD
FB
C3b
Alternative pathway
C3bBb3b
FH
C5
C5a
C6
C7
C8
mC5b-7
C5b-8
C9
C5b
Influx of fluid
Membrane attack complex
Activated endothelial cells
Activated monocyte
Activated Platelet
Activated neutrophil
Plasmin
Plasminogen
tPA
Blood clot
Tissue Factor
VII (zymogen)
VIIa
V
Va
Xa
X
II (Prothrombin)
IIa (Thrombin)
I (fibrinogen)
Ia (Fibrin)
XIII
XIIIa
VIII
VIIIa
IX
IXa
XI
XIa
HMWK
Bradykinin
Kallikrein
XII
XIIa
Negatively charged surface
Platelet binds to exposed collagen and becomes activated
Extrinsic pathway (Better thought of as TF pathway/initiation
Common pathway
Intrinsic pathway (Better thought of as amplification pathway)

Figure 1: Complement and coagulation pathways interactions (simplified).

Coagulation: Vascular injury exposes tissue factor (TF) on subendothelial cells (extrinsic pathway). Factor VII moves to this TF surface and is activated by trace amounts of already activated VII (VIIa), activated factor X (Xa), or thrombin (IIa). TF binds VIIa and the resulting complex activates factor X. In conjunction, factor V is recruited to activated platelets and activated mainly by thrombin. Xa and Va assemble on a phospholipid membrane and convert prothrombin (factor II) to thrombin (factor IIa), which converts fibrinogen (factor I) to fibrin (factor Ia).
In parallel, exposed collagen/vWF capture and activate platelets, providing the negatively charged surface where most thrombin is generated *in vivo* (intrinsic pathway). Highly anionic surfaces (notably platelet polyphosphate, NET DNA/RNA, extracellular RNA from damaged cells, exposed basement membrane, and foreign materials) promote factor XII activation (XIIa). XIIa converts prekallikrein to kallikrein, which feeds back to activate more XII; XIIa also activates factor XI (Xia), which then activates factor IX (IXa). IXa binds to FVIIIa to form intrinsic tenase, which greatly amplifies thrombin and fibrin generation. Further, kallikrein cleaves High-molecular-weight kininogen (HMWK) to bradykinin, increasing vascular permeability and vasodilation.

Complement: The classical (IgM/IgG–C1qrs binding) and lectin (MBL/ficolins–MASP binding) pathways both lead to C2 and C4 cleavage to form the same classical C3 convertase (C4b2a). This then cleaves large amounts of C3 to C3b and C3a (alongside other fragments). Once a large amount of C3b forms on a surface, it binds with C4b2a to form the C5 convertase of the classical and lectin pathways.
In conjunction, the alternative pathway binds C3b to factor B and promotes its cleavage via Factor D, forming C3bBb, the alternative C3 convertase. This is an amplification loop to dump large amounts of C3b onto whichever surface is not protected by complement regulators (factor H, MCP/CD46, etc.). C3bBb then binds another C3b to form the alternative C5 convertase. Factor H (FH) regulates this by serving as a cofactor for C3b cleavage and accelerates the decay of C3bBb. Both C5 convertases cleave C5 into C5a and C5b, which recruits C6, C7, C8, and polymerizes C9 to form a pore (MAC). On host cells at sublytic levels, MAC activates endothelium and platelets, increasing TF, vWF release, permeability, and leukocyte adhesion, making them procoagulant and pro-inflammatory.

Crosstalk: C5a (and, to a lesser extent, C3a) activates monocytes, endothelium, and platelets, driving TF expression (promoting extrinsic pathway activation) and platelet aggregation. NETs bind platelets and provide a scaffold for factor XII activation. Conversely, thrombin, factor Xa, and plasmin can directly cleave C3/C5 to C3a/C5a-like fragments, sustaining complement activity. Endothelium releases tPA, which converts plasminogen to plasmin on fibrin; plasmin clears crosslinked fibrin (and can degrade fibrinogen) while also contributing to complement cleavage.

Created in BioRender. Elens, L. (2025) https://BioRender.com/w1ylbg9

Immunologically, CAC is driven by several interconnected mechanisms. Pro-inflammatory cytokines, particularly IL-6 and TNF-α, stimulate hepatic fibrinogen synthesis and upregulate TF expression on endothelial cells and monocytes [133]. This activity triggers the extrinsic coagulation cascade and subsequent thrombin generation. Elevated IL-6 levels correlate with increased fibrinogen, vWF, factor VIII, and D-dimer, whilst TNF-α and IL-1β suppress natural anticoagulants like thrombomodulin and the endothelial protein C receptor (EPCR) [134–136]. Neutrophils also contribute significantly through the release of NETs which trap platelets and clotting factors to facilitate thrombus formation; their presence in lung tissues and blood of COVID-19 patients strongly correlates with thrombotic events [88,137].

Complement activation also plays a critical role, detectable even in early or mild disease and correlating with disease severity [138]. Mechanistically, SARS-CoV-2 triggers aberrant activation of the lectin and alternative pathways, generating potent anaphylatoxins (e.g., C3a, C5a) that amplify cytokine release and promote leukocyte recruitment, intensifying pulmonary and systemic inflammation [139]. This dysregulated response also promotes the formation of the membrane attack complex (C5b-9), which contributes to the endothelial injury and microvascular thrombosis observed in severe COVID-19 cases [139]. Evidence further suggests that SARS-CoV-2 may directly interact with complement components, leading to the formation of persistent immune complexes and sustained complement activation during infection and potentially up to a year following [140,141]. Additionally, impaired regulation of complement-mediated clearance mechanisms may contribute to autoinflammatory responses and has been implicated in the pathogenesis of PASC [142,143]. It

is worth noting in this regard, a preprint by Farztdinov *et al.* found no evidence of persistent complement activation in PASC patients when adjusting proteomic data for age, BMI, and sex, but it remains the only study reporting such findings and has not yet undergone peer review at the time of this writing (October 2025) [144].

Immunothrombosis significantly contributes to organ damage in severe COVID-19. Autopsy studies have revealed widespread microvascular thrombi in pulmonary alveolar capillaries, which are strongly implicated in the development of ARDS and impaired gas exchange [145]. Similarly, microthrombi in coronary microcirculation have been linked to myocardial injury and dysfunction, often presenting as arrhythmias or heart failure [146]. Renal involvement often involves thrombotic obstruction of small vessels, resulting in acute kidney injury [147]. In the cerebral circulation, immunothrombosis is associated with an increased risk of stroke in critically ill patients [148]. Finally, skin manifestations frequently display complement deposits and NET presence, further underscoring the systemic impact of immunothrombosis [149]. These findings illustrate an interplay of immune responses and coagulation pathways in driving localized thrombosis and multi-organ dysfunction during severe COVID-19.

2.5 SARS-CoV-2 innate immune evasion

SARS-CoV-2 has evolved multiple strategies to evade the innate immune response, particularly by suppressing early type I IFN signalling. Among the 29 viral proteins, 23 are implicated in innate immune interference, often through overlapping functions. These include: interfering with the host's PRRs (13 proteins); concealing viral RNA to avoid detection (9 proteins); antagonizing the JAK-STAT signalling pathway to block IFN

signalling (8 proteins); suppressing translation to prevent synthesis of antiviral proteins (6 proteins); and inhibiting nuclear transport of immune signalling molecules (5 proteins) [150]. An overview of the multiple ways in which these molecules allow for the evasion of the immune system is provided in figure 2, the following text will discuss these proteins in more detail.

Several non-structural proteins (NSPs) play critical roles in immune evasion. NSP1 binds to the host 40S ribosomal subunit, inhibiting translation and antagonizing IFN signalling [151]. It also epigenetically represses antiviral gene expression, through demethylation of histone H3K9 at promoters of key antiviral genes, highlighting a previously unrecognized mechanism of host suppression [152]. NSP3, via its papain-like protease (PLpro) domain, not only processes viral polyproteins but also removes ubiquitin and ISG15 from host proteins, blunting antiviral signalling through IFN regulatory factor 3 (IRF3) and stimulator of interferon genes (STING) pathways [153,154]. NSP13 suppresses IFN activation by targeting TANK-binding kinase 1 (TBK1) (part of the IFN activation pathway) for degradation, whereas NSP15 functions as an endoribonuclease that degrades viral dsRNA intermediates to evade PRR detection [155,156]. NSP8 interferes with IRF3 activation and nuclear translocation to supress IFN I and III; NSP8 also further suppress IFN I through inhibition of MDA5 (a critical cytosolic sensor of viral dsRNA) by impairing TRIM4-mediated MDA5 K63-linked polyubiquitination [157,158]. NSP9 also suppresses IFN and inflammatory signalling by reducing RIG-I expression, NF-κB signalling, and TBK1 activity [159]. Last, NSP14 reduces surface IFNAR expression, weakening downstream IFN signal transduction [160].

Accessory proteins also contribute significantly. ORF6 inhibits nuclear translocation of STAT1/2 and suppresses IRF3 and NF-κB activation [161,162]. ORF7b and ORF8 robustly suppress ISG transcription through distinct pathways by blocking upstream IFN production, and ORF8 additionally disrupts IRF3 function and IFN signalling [163,164]. ORF3a inhibits STAT1 phosphorylation, reduces IFN signalling, and promotes inflammasome activation; ORF3b potently suppresses IFN induction through IRF3 suppression; while ORF3c localizes to mitochondria, promoting mitochondrial antiviral signalling protein (MAVS) cleavage and reducing IFN-β production [111,165,166]. IFN signalling is further blocked by ORF9b disrupting MAVS signalling through TOM70 targeting, and by ORF9c which impairs antigen presentation and inflammatory pathways [167,168]. ORF10 is one of the smallest and least understood SARS-CoV-2 proteins and its role currently remains unclear, however, it may modulate immune responses through its interaction with STING [169]. Finally, the structural M protein disrupts RIG-I/MDA5 signalling, reducing IFN-β promoter activation [170]. In addition to IFN evasion, SARS-CoV-2 modulates other innate immune pathways. The nucleocapsid protein dysregulates the NLRP3 inflammasome, promoting IL-1β and IL-18 secretion and pyroptosis, leading to inflammation rather than viral clearance [171]. NSP6 and ORF3a disrupt autophagy by inhibiting autophagosome maturation and lysosomal fusion, impairing antigen presentation [172,173]. NSP1 and ORF6 also appear to impair NK cell cytotoxicity by downregulating the NKG2D activating ligands (e.g., MIC-A/B) on infected cells, reducing early viral clearance [174,175].

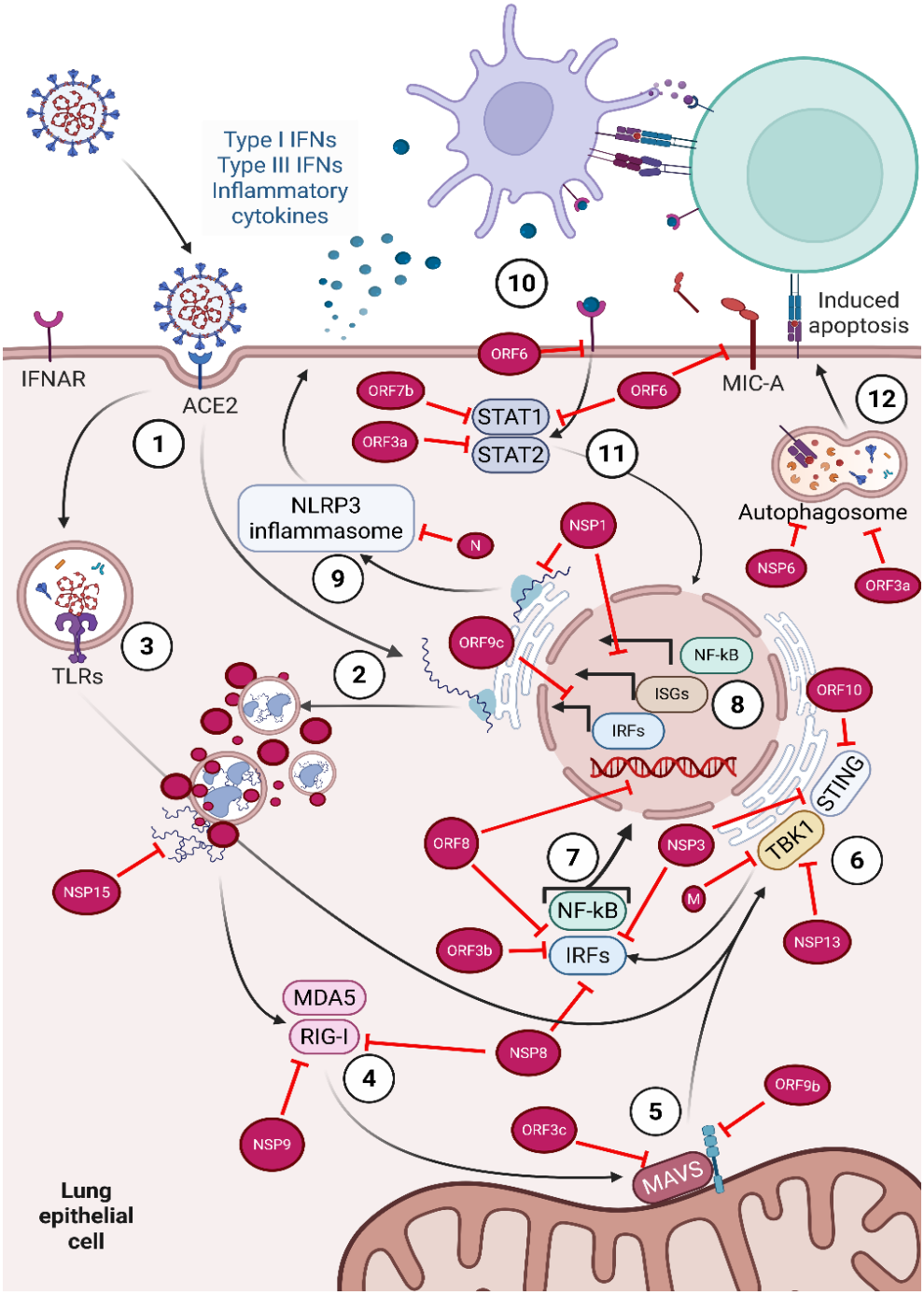

Type I IFNs
Type III IFNs
Inflammatory cytokines
Induced apoptosis
IFNAR
ACE2
MIC-A
ORF6
ORF7b
ORF3a
STAT1
STAT2
NLRP3 inflammasome
N
NSP1
Autophagosome
NSP6
ORF3a
TLRs
ORF9c
NF-kB
ISGs
IRFs
ORF10
STING
TBK1
NSP3
M
NSP13
ORF8
NSP15
ORF3b
MDA5
RIG-I
NSP8
NSP9
ORF3c
ORF9b
MAVS
Lung epithelial cell
1
2
3
4
5
6
7
8
9
10
11
12

Figure 2: Mechanisms of SARS-CoV-2 immune evasion.

1: SARS-CoV-2 attaches to and enters cell through ACE2, releasing its genome into the cell.
2: Viral polymerase is translated using host machinery, followed by viral transcription and translation inside replication organelles, generating dsRNA intermediates and releasing viral proteins. NSP15 degrades viral dsRNA to evade detection and reduce IFN induction.
3: Endosomal TLR3/7 detect viral RNA and activate antiviral response through TBK1.
4: RIG-I and MDA5 recognise cytosolic viral dsRNA ligands and recruit and activate the adapter protein MAVS. NSP9 suppresses RIG-I expression, whilst NSP8 binds to MDA5 and prevents polyubiquitination, reducing antiviral responsiveness.
5: Activated RIG-I and MDA5 translocate to the mitochondria and activate MAVS signalling. ORF3c additionally localises to the mitochondria to promote MAVS cleavage, halting this process. ORF9b also disrupts this signalling by targeting TOM70, a crucial receptor that binds MAVS and recruits downstream signal components.
6: The MAVS pathway goes on to recruit and subsequently activate TBK1; cGAS-STING can also be indirectly triggered via organelle damage. Structural M protein and NSP13 disrupt RIG-I/MDA5 signalling by promoting TBK1 degradation. Additionally, ORF10 binds to STING, blocking TBK1 association and IRF activation, while NSP3 inhibits signalling through STING deubiquitylation.
7: Activated TBK1 phosphorylates IRFs, allowing nuclear entry; NF-κB also enters following activation via TAK1-IKKβ. These molecules upregulate viral response genes. NSP3, NSP8, ORF3b, and ORF8 all disrupt either activation or nuclear translocation of IRF3, impairing its viral response pathway.
8: Viral response genes are upregulated. NSP1, ORF8, and ORF9c all suppress the transcription and/or translation of ISG/NF-κB transcriptional products. ORF9c further impairs antigen presentation to the endoplasmic reticulum, impairing recognition by CD8+ T-cells.
9: As part of the antiviral response, the NLRP3 inflammasome is activated. Nucleocapsid protein dysregulates this process, promoting inflammatory action rather than viral clearance actions in its downstream products.
10: Released IFNs alert cells to initiate antiviral defences. In infected cells, NSP14 reduces surface IFNAR expression, weakening IFN signal transduction. ORF6 also inhibits cell signalling by inducing shedding of NKG2D activating ligands (MIC-A/B) on infected cells, preventing recognition by NK cells.
11: IFNAR activation signalling uses the JAK/STAT pathway to induce ISGs. This is disrupted by ORF6 inhibiting nuclear translocation of STAT1/2, and by ORF7b and ORF3a inhibiting their phosphorylation.
12: Autophagy delivers proteins to lysosomes for antigen processing. NSP6 limits autophagosome growth and ORF3a blocks autophagosome-lysosome fusion, reducing antigen presentation.
Created in BioRender. Huaux, F. (2025) https://BioRender.com/nznylu5

Host factors further influence the IFN response to SARS-CoV-2 infection. Genetic mutations in critical components of the IFN signalling pathways, such as TLR7, IRF7, and IRF9, compromise IFN production [35,176]. Additionally, neutralizing autoantibodies against type I IFNs (not present in mild phenotypes but found in approximately 10% of severe COVID-19 cases) reduce functional IFN-α/ω levels, permitting uncontrolled viral replication and severe inflammation [34].

Notably, SARS-CoV-2 VOCs have evolved their own immune evasion strategies. For instance, the Alpha variant reduces pDC activation by downregulating ICAM-1/CD11a interactions, weakening the IFN response [68]. For the Delta variant, structural changes in the receptor-binding domain reduced binding of neutralizing antibodies from prior infection or vaccination [177]. Lastly, the Omicron subvariants developed a number of strategies: resistance to type I, II, and III IFNs; increased ORF6 and N protein expression to suppress IRF3 and STAT1 signalling; evasion of neutralizing antibodies following S protein mutations; and mutations in proteins like NSP6, NSP13, ORF9b, and ORF7b that enhance suppression of autophagy, IFN signalling, and NK cell activity [178–180,180].

In summary, severe COVID-19 arises from a combination of viral evasion strategies and host predispositions that compromise the initial IFN response, allowing viral spread and excessive inflammation. Delayed or insufficient IFN production allows increased viral replication and triggers a compensatory surge in pro-inflammatory cytokines such as IL-6, TNF, and IL-1β, as discussed in Section I, chapter 2.3. This hyperinflammation exacerbates lung injury, vascular leakage, and coagulopathy, hallmark features of severe COVID-19.

3 Post-Acute Sequelae of SARS-CoV-2 (PASC, Long COVID)

While most patients recover from the acute phase of COVID-19 within a few weeks, a significant subset experience persisting or new symptoms well beyond the acute illness. This condition, known as Post-Acute Sequelae of SARS-CoV-2 (PASC) or colloquially "long COVID", has emerged as a major public health concern in the pandemic's aftermath. There is no universally accepted definition of PASC, but it generally encompasses symptoms lasting more than four to twelve weeks after acute infection, not explained by an alternative diagnosis. The most accepted is the World Health Organizations (WHO), which defines it as "the continuation or development of new symptoms three months after the initial SARS-CoV-2 infection, with these symptoms lasting for at least two months with no other explanation". Other institutions, for example the US Centers for Disease Control and Prevention (CDC) require symptoms to be present for at least three months, whilst the US National Institutes of Health (NIH) place the onset of PASC at 4 weeks after acute COVID-19. Furthermore, the British National Institute for Health and Care Excellence (NICE) divides long COVID into two categories, ongoing symptomatic COVID-19 for symptoms lasting four to twelve weeks, and post-COVID-19 syndrome for symptoms lasting more than twelve weeks. Finally, the most exhaustive study to define PASC was conducted by the RECOVER initiative, which identified 37 symptoms which may persist, recur, or newly emerge four or more weeks following acute COVID-19, and cannot be explained by alternative diagnoses [181].

The scale of the SARS-CoV-2 pandemic has made the presence of these post-acute infectious symptoms (PAISs) more numerous among the general population, however, persistent symptoms following an acute infection are not specific to SARS-CoV-2. Some of

the more well-established such PAISs include Q fever fatigue syndrome following *Coxiella burnetii* infection, post-dengue fatigue, post-Ebola virus syndrome, and myalgic encephalomyelitis/chronic fatigue syndrome often following a viral infection, such as mononucleosis [182–185]. Common symptoms include severe fatigue, post-exertional malaise cognitive symptoms, sleep disturbances, and autonomic complaints. Psychiatric morbidities and chronic fatigue phenotypes were also reported in survivors of the 2003 SARS outbreak at a four-year follow-up [186]. The pathophysiology of these PAISs is not well understood, but the commonality in symptoms, despite disparate infectious triggers, may suggest a common pathology. In Section I, chapter 3.2, the major hypothetical mechanisms of PASC are discussed, but these same mechanisms may also apply to other PAISs.

As this is a historically under-researched area (this is now changing due to the public visibility of PASC), prevalence of these syndromes is limited and varies depending on the study and the infection, complicating interpretations. For example, cohort studies of young adults with infectious mononucleosis found that 30-40% had persistent symptoms several weeks after symptom onset, dropping to 4% at two years [187,188]. For other diseases, the prevalences can be much higher. Longitudinal estimates put the prevalence of persistent post-West Nile virus symptoms at between 40% to 70% of survivors at two-years post infection [189,190].

Reported prevalence of PASC varies depending on population and methodology. The largest study, RECOVER Initiative Real-World Electronic Health Record (EHR) Study, puts the incidence of PASC at 8.5% to 26.4% in adults (depending on definition), based on

around six million U.S. electronic health records of COVID-positive patients [191]. Meanwhile, a global meta-analysis of 41 studies from North America, South America, Europe, and Asia estimated global prevalence higher at 34% and 54% of non-hospitalized and hospitalized patients respective [192]. Risk factors associated with PASC include middle age (between 40-69 years, odds ratio (OR) ~2.4), female sex (OR 1.4), COVID-19 hospitalization (OR 3.8), extended hospitalization (8-30 days OR 1.69, 30+ days OR 3.38), mechanical ventilation (OR 1.44), and certain COVID-19 comorbidities (depression, chronic obstructive pulmonary disease (COPD), obesity) [193]. On the other hand, other COVID-19 comorbidities (substance abuse, cardiomyopathy, psychosis, and dementia) where associated with reduced likelihood of PASC diagnosis, alongside younger age (18-29 years), male sex, and non-Hispanic black ethnicity [193].

3.1 Clinical Spectrum and Impact of Long COVID

Long COVID is a heterogeneous syndrome affecting multiple organ systems. The clinical manifestations span a wide range, commonly including: profound fatigue, often with post-exertional malaise (a hallmark also seen in chronic fatigue syndrome); neurocognitive difficulties ("brain fog," memory lapses, difficulty concentrating); sleep disturbances; headaches; anosmia/dysgeusia; dyspnea and reduced exercise tolerance; cough and chest pain; palpitations and tachycardia; orthostatic intolerance or postural orthostatic tachycardia syndrome (POTS); arthralgias and myalgias; and an array of other symptoms like GI upset, depression/anxiety, and autonomic dysfunction [194]. Patients often describe their condition as relapsing-remitting, with flares triggered by physical or mental activity (hence pacing is advised) [195]. Objective findings can include impaired pulmonary diffusion capacity, autonomic function test abnormalities, memory and attention deficits on

neuropsychological testing, and elevated markers of inflammation [196–199]. However, standard clinical workups are frequently normal, which can make identification, validation, and management challenging [200].

As PASC manifests with such heterogeneous signs and symptoms (the mechanisms of which will be discussed in Section I, chapter 3.2), it can be useful to categorize them by system (please note, the terms "PASC patients" and "COVID-19 survivors" will be used liberally in this section, "PASC patients" refers to people who had COVID-19 and have now been diagnosed with PASC, whilst COVID-19 survivors refers to people who had COVID-19 and recovered, but have not formally been diagnosed with PASC. Such differences appear as certain studies did not discuss PASC prevalence in their populations, or where conducted before PASC was being widely investigated) :

- **Neurologic/Cognitive**: Many PASC patients experience cognitive impairment (short-term memory issues, difficulty with word-finding, mental fatigue). Meta-analyses of objective and subjective studies have placed the prevalence of cognitive issues following acute disease to be just over 20% [201,202]. Odds of cognitive conditions were found to continue to increase over a two-year follow-up and were more likely to be identified if objective testing was used, indicating a potential lack of participant awareness in their cognitive decline. This "brain fog" can be debilitating and akin to chemo-brain or what's seen in post- intensive care unit (ICU) syndrome. Some of the most common symptoms were neuropathic symptoms like paraesthesia (33.3% of PASC patients), as well as sleep disorders (32.9%), musculoskeletal pain (27.8%), dizziness (26.4%), and headaches (21.3%) [203]. Dysnosmia and dysgeusia were also

relatively common at 17.7% and 16.5%, respective. A small number develop more serious sequelae like strokes (hazard ratio (HR) 1.11 compared to any other respiratory infection) or new-onset epilepsy/seizures after COVID-19 (HR 1.14) [204]. For strokes, HRs returned to baseline within 66 days, indicating a potential delayed onset to acute disease, perhaps because of coagulation complications during COVID-19. For epilepsy and seizures however, these outcomes showed persistent HRs over one at the end of the two-year follow-up.

- **Psychiatric**: Meta-analysis review of 165 studies, encompassing just under 10 million patients, identified commonly reported mental-health sequelae such as depression, anxiety, and sleep disorders in 23%, 23%, and 45% of PASC patients, respective [205]. Post-traumatic stress disorder (PTSD) -like symptoms have also been identified in 18% of patients [206]. Survivors of a severe acute disease were more likely to suffer from PTSD and sleep disturbances, whilst those with a mild disease course had higher burden of anxiety following recovery [206].

- **Respiratory**: One of the most common respiratory manifestations experienced by PASC patients is dyspnea, with between 26% and 41% of COVID-19 survivors experiencing the symptoms more than 4 weeks post-infection, depending on if you measure the symptoms based on presence/absence or using the Medical Research Council dyspnea scale [207]. Pooled prevalence of self-reported prevalence decrease significantly over time, from 28% at 1-6 months, to 20% at 7-12 months; further follow-up studies of COVID-19 survivors found this figure to drop further to around

10% at two years post-infection [208,209]. Pulmonary function tests show reduced diffusing capacity of the lungs for carbon monoxide (DLCO < 80%) in 30% to 50% of COVID-19 survivors between three and six months, and imaging reveals ground-glass opacities or fibrotic strings in up to 60% of lungs, especially those who has pneumonia/ARDS [210,211]. This is combined with a decrease in alveolar volume and a relatively normal carbon monoxide transfer coefficient (KCO), results consistent with a loss of alveolar capillary structure. Interestingly, some PASC patients have dyspnoea despite normal imaging and pulmonary functional tests, which might relate to dysregulation of breathing control or pulmonary microvascular injury not captured on routine tests. Beyond dyspnoea, other common persistent respiratory symptoms among PASC patients include inspiratory muscle weakness (40%-50%), exercise intolerance (22%-36%), and chronic cough (17.7%) [212–215].

- **Cardiovascular**: Cardiovascular disease, a leading cause of global mortality, is indicated to be a significant component of PASC, representing the third most common clinical manifestation of the disease [216]. These patients have a 1-year elevated HR of 1.6 to develop new onset cardiovascular diseases of any type, compared to healthy population [217]. Common causes leading to symptom occurrence include thrombotic disorders (HR 3.12 between 2 and 12 months post-COVID), arrhythmias (HR 1.6), or cardiomyopathy and myocarditis (HR 1.7 and 6.11 respective); these can usually be identified, and thus managed, through relevant examinations [218]. However, many PASC patients exhibit cardiovascular symptoms without objective evidence [219]. The most common cardiovascular symptoms seen in PASC patients are chest pain at 22%,

hypertension at 19%, palpitations and at 18% [220]. Additionally, a number of PASC patients appear to meet the criteria for autonomic disorders such as Postural Orthostatic Tachycardia Syndrome (POTS), a neurological condition whereby a person's heart rate increases excessively upon standing. Although meta-analysis review has not yet been done, studies have found that between 17%-79% of PASC patients meet the criteria for POTS with excessive heart rate increase on standing (≥30 bpm) accompanied by symptoms like light-headedness, weakness, and palpitations [221–223].

- **Musculoskeletal**: Both myalgias and arthralgias are commonly reported PASC symptoms. Myalgia prevalence among PASC patients varies greatly between studies, but meta-analysis puts pooled prevalence at around 11% to 19% [224,225]. Individual studies found a decrease in myalgia from 54.6% to 42.2% between 60 days and one year, showing a slight recovery overtime [226]. Arthralgias on the other hand, with pooled prevalence of 13% in all PASC patients, are part of the small number of symptoms that increased overtime following COVID-19, from around 28% to 38% from 60 days to one year [225,226]. Both arthralgias and myalgias appear to more commonly present are widespread (33% and 40% respective), rather than localized (26% and 23% respective) [227]. There is also some evidence that a number of patients develop a fibromyalgia syndrome (FMS)-like picture post-COVID, although often with less severe fatigue than observed with chronic fatigue syndrome (CFS), and less severe pain than observed with FMS [228]. Whilst large-scale data is pending, case reports, case series, and retrospective cohort studies are building mounting evidence

that SARS-CoV-2 infection can trigger new autoimmune rheumatologic conditions such as rheumatoid arthritis, systemic lupus erythematosus, and axial spondylarthritis [229–231].

- **Gastrointestinal**: A large proportion of PASC patients sufferer from GI issues; the main long-term symptoms are dysphagia (22%), nausea/vomiting (19%), abdominal/visceral pain (14%), constipation (11%), and diarrhoea (10%) [232]. Such symptoms are reminiscent of irritable bowel syndrome (IBS), a common chronic GI disorder characterized by abdominal pain, bloating, and altered bowel habits (diarrhoea and/or constipation) without any identifiable structural cause. Investigations between PASC patients and IBS put the prevalence of new cases around 5% to 10% of the patient population (according to Rome IV criteria), above that of the general population at 4-5% [233].

- **Renal**: Acute kidney injury (AKI) occurs in around one third of (unvaccinated) hospitalized COVID-19 patients, and renal replacement therapy was required in 14% of these patients [234]. Following acute disease, there does not appear to be a consensus on weather kidney injuries resole post COVID-19. A three-year follow-up study of 120 COVID-19 survivors with and without AKI or chronic kidney disease (CKD) found that kidney function returned to baseline and did not show permanent kidney damage or further progression of CKD [235]. This is supported by another study of 7500 COVID-19 patients which found no increased risk of CKD following the acute phase of COVID-19 (up to six months), regardless of initial disease severity [236]. However, a

much larger US study of 2.8 million COVID-19 patients, alongside a Canadian study of 457 patients, found COVID-19 significantly increases the risk of CKD, nephritic/nephrotic syndromes, and glomerular disorders [237,238].

- **Metabolic:** Lastly, new-onset diabetes has been observed post-infection; a systemic review found a 59% higher risk of developing incident diabetes in COVID-19 survivors vs healthy controls [239]. From this analysis, severe patients were more than twice as likely to develop new-onset diabetes compared to mild and moderate patients.

It is important to note that individual patients with PASC may have completely different constellations of symptoms. One person might predominantly have fatigue and cognitive issues, while another has tachycardia and shortness of breath. Clustering analyses have identified a few common phenotypes: for example, a "cardio-respiratory cluster" (dominated by chest pain, dyspnea, palpitations), a "musculoskeletal cluster" (arthralgia, myalgia, headache), and a "chronic fatigue-like cluster" (fatigue, memory loss, shortness of breath) [240,241]. Many patients can span multiple clusters. The diversity of PASC suggests that multiple underlying pathophysiological processes are at play.

Beyond symptoms, PASC carries significant functional and economic impact. Many sufferers experience impaired quality of life; some have difficulty returning to work or exercise for months. A Canadian study found 16% of PASC patients experienced a decrease in employment (full-time to part-time to unemployed) compared to just 5% of recovered patients [242]. Cognitive impairment from PASC has raised concerns about

increased dementia risk down the line, though data are not yet available, there has been some concerns of an increased risk of Alzheimer's disease (AD) after COVID-19 [243]. The burden of PASC is such that specialized "long COVID clinics" have been established in many regions to provide multidisciplinary care (including pulmonologists, cardiologists, neurologists, rehabilitation specialists, and mental health professionals).

3.2 Pathophysiological Mechanisms of PASC

Inflammation during acute infection is typically rapid and time-limited, with the intensity and duration shaped by both pathogen control and host regulatory processes. Importantly, return to homeostasis requires an active resolution phase, including clearance of inflammatory cells, reprogramming of myeloid cells, and engagement of pro-resolving mediators that promote tissue repair [244]. If inflammatory stimuli persist, or if resolution pathways are incomplete, inflammatory signalling can remain engaged and progress toward a chronic, non-resolving state. In the context of PASC, several of the mechanisms discussed below can be interpreted as factors that sustain inflammatory cues or impair resolution after the acute phase.

The mechanisms driving PASC are an area of intense research, and although not fully elucidated, several leading hypotheses have emerged, as visualised in figure 3. The major mechanistic drivers of PASC can be organized into four higher-order groups. The "Persistent stimuli" group consists of SARS- CoV-2 reservoirs/remnants, reactivation of latent viruses (like EBV), and gut/lung dysbiosis with microbial-product leak. The "Immune and inflammation" group consists of chronic cytokine signalling/exhaustion, and autoimmunity. The "Vascular coagulation" group with complement dysregulation,

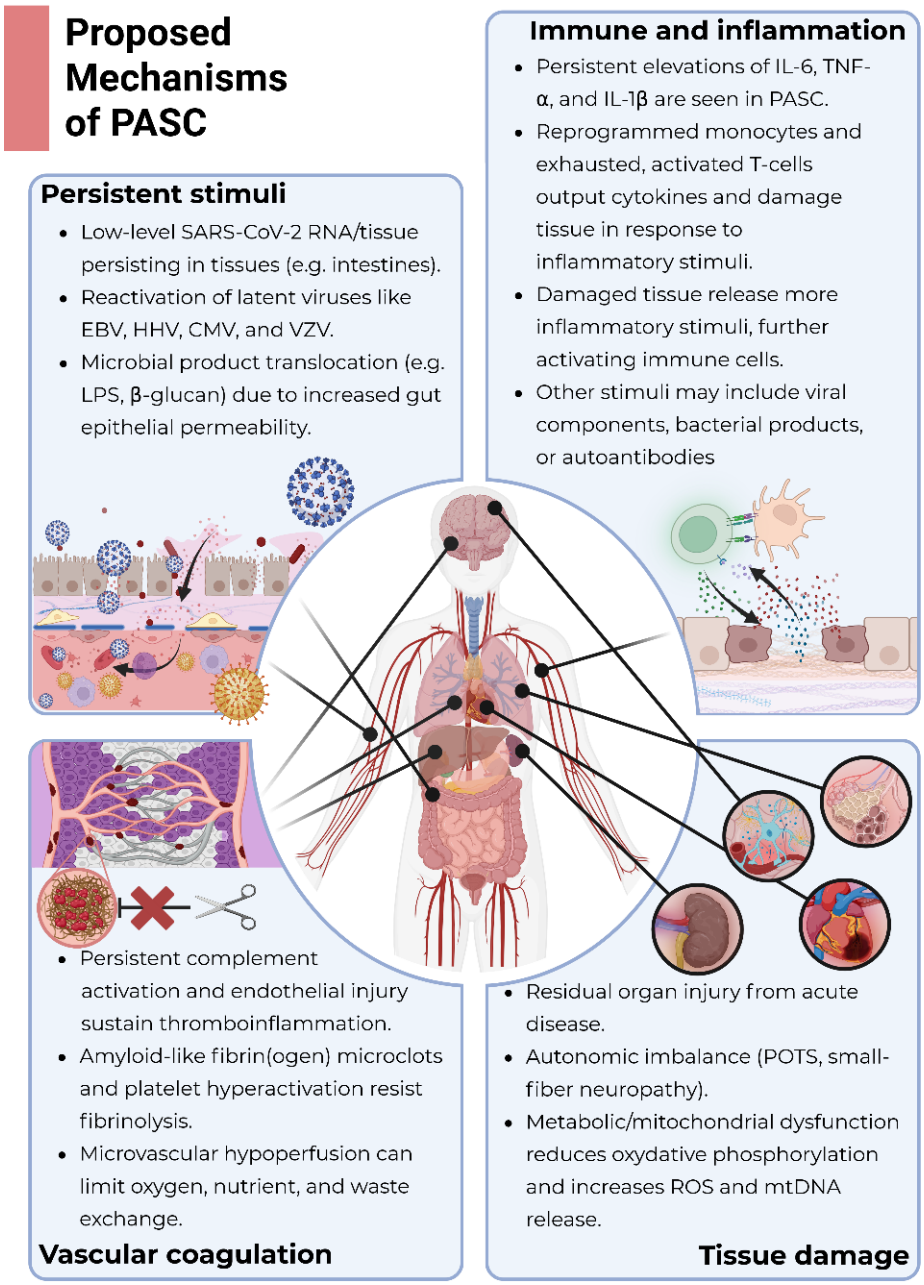


Figure 3: Proposed mechanisms of PASC.
A summary of the main mechanisms implicated in PASC as discussed in Section I, chapter 3.2.
Created in BioRender. Elens, L. (2025) https://BioRender.com/qs7guci

endothelial injury, and micro-thrombi. The “Tissue-specific and non-specific damage and dysregulation” group consisting of residual organ damage, autonomic imbalance, and metabolic/mitochondrial dysfunction. These groups are not mutually exclusive, and it is likely that PASC represents a spectrum where different patients may have different dominant causes (or combinations thereof), leading to the patient phenotype clusters mentioned previously. For example, viral persistence can drive prolonged immune activation; immune dysregulation can injure endothelium and propagate micro-clotting; chronic hypoxia from micro-vascular dysfunction may in turn worsen metabolic and autonomic disturbances. Consequently, individual PASC patients may exhibit signatures from multiple groups simultaneously. To this end, clinical management may pivot towards matching targeted interventions against patient endotypes. Antivirals for the “Persistent stimuli” group, immune-modulators for the “Immune and inflammation” group, anticoagulants or complement blockers for the “Immune and inflammation” groups, and multidisciplinary rehabilitation for the “Tissue-specific and non-specific damage and dysregulation” group. This can lead to extremely heterogenous therapeutic options for PASC patients, in which two patients undergo completely different treatments. Such targeted medicine is being used to successfully treat other heterogenous diseases such as asthma, cancer, and cystic fibrosis, but clinical implementation for PASC has not yet commenced [245,246].

3.2.1 Persistent stimuli

Persistent Viral Reservoirs

SARS-CoV-2 or its viral proteins may persist within the body for months, potentially driving chronic immune activation and sustained inflammation. Although the virus typically clears from the nasopharynx within weeks, multiple studies report viral RNA and protein presence in tissues extending beyond the acute illness phase in both symptomatic and asymptomatic individuals [247–250]. However, the levels of viral particles detected in these tissues are generally very low, and in most cases replication-competent virus are not found but rather fragments and proteins. Despite the growing body of evidence, the association between viral persistence and PASC remains modest, given the conflicting findings of the below studies, and their limited use of controls.

Significant autopsy studies, have consistently identified SARS-CoV-2 RNA and proteins in various tissues including the lungs, heart, GI tract, lymph nodes, kidneys, adrenal glands, and brain [251]. Some viral particles were detected up to 230 days post symptom onset, long after nasal swabs were negative and despite no obvious cytopathic damage in some of those sites. A RECOVER study confirmed and expanded on these findings to include skeletal muscle, pancreas, and reproductive tissues, highlighting low-level but detectable sub-genomic RNA, suggestive (though not conclusive) of residual viral replication [250]. Moreover, other studies detected persistent SARS-CoV-2 proteins in both small- and large-intestinal biopsies from PASC patients up to seven months post-infection [248,252].

Indeed, the most well-supported and accessible tissues for viral persistence are the gut tissues, supported by tissue biopsies and prolonged viral shedding in stool months after

negative respiratory samples [248,253,254]. In autopsy and biopsy studies, viral antigens are most frequently observed in the small-intestinal mucosa (the innermost layer of the small intestines, responsible for nutrient absorption and protection) and mesenteric lymph nodes (lymphoid organs responsible for lymph drainage of the intestinal mucosa). These tissues have high ACE2/NRP-1 expression, allowing for efficient viral entry, and persistence within may be aided by the relative immune privilege these tissues possess. Immune cells themselves may also act as potential reservoirs, with nonclassical-monocytes showing persistent S1 protein up to 15 months post-infection [255]. It should also be noted that several studies have proposed fat as a reservoir due to ACE2 expression and its pro-inflammatory profile (particularly in obesity); however, direct evidence of viral persistence in adipocytes is less established than for gut tissues [256]. Endothelial cells and the central nervous system (CNS) have also been suggested or hypothesized as a reservoir of interest, but evidence is likewise limited [257,258]. Specifically, whilst SARS-CoV-2 demonstrates some neuroinvasive capacity during acute infection (discussed in Supplementary information 1.3), and can thus invade the CNS, very little evidence currently supports CNS persistence following COVID-19 resolution.

Regardless of the exact location of a viral reservoir, and even in the absence of ongoing replication, viral persistence has been of particular interest due to its association with PASC symptoms. The S1 antigen has been detected in 43% of individuals with symptomatic PASC but in just 21% of asymptomatic post-COVID individuals, suggesting a link between the two [259]. Further, examinations of tissues with viral persistence often show low-grade complement deposition, microvascular fibrin, and mild lymphocytic

infiltration, suggesting ongoing endothelial injury [260,261]. In the gut, N protein has been found co-localized with TLR7-high macrophages and zonulin-positive sites of epithelial disruption [248]. Zonulin is a regulator of intestinal permeability, and so its elevation correlates with increased intestinal permeability and systemic immune activation, plausibly linking PASC symptoms such as fatigue or dysautonomia to the persistence of viral proteins.

The mechanisms by which SARS-CoV-2 reservoirs are theorised to contribute to PASC phenotypes generally revolve around immune alteration and activation. Multiple studies converge on a signature of persistent type I and III IFN signalling, activated monocytes ($CD14^+/CD16^+$), exhausted SARS-CoV-2–specific $CD8^+$ T cells, and persistent activation of CD4+ T cells in patients with ongoing antigen presence, in contrast to the immune quiescence seen in fully recovered individuals [255,262]. These monocytes exhibit a pro-inflammatory phenotype, the exhausted $CD8^+$ T cells express inhibitory receptors, like programmed cell death protein 1 (PD-1) and T-cell immunoglobulin and mucin domain 3 (TIM-3), reflecting chronic antigen exposure and impaired viral control, whilst the activated CD4+ T cells may contribute to immune dysregulation and chronic inflammation. This ongoing immune dysregulation, especially combined with immunosuppressive treatments used to mitigate severe acute COVID-19 severity, has been associated with reactivation of latent viruses, including EBV and cytomegalovirus (CMV) [263,264]. These immunological patterns resemble those observed in other post-viral syndromes, such as Ebola or Chikungunya, where persistent viral antigens correlate with prolonged symptoms.

Reactivation of latent viruses

A consistent theme in the literature (as briefly mentioned above) is that SARS-CoV-2 may disrupt the host–virus balance, enabling reactivation of dormant herpesviruses; most prominently EBV, but also human herpesvirus 6 and 7 (HHV-6/7), CMV, and varicella-zoster virus (VZV) [265]. Studies investigating the presence of serological markers such as EBV early antigen (EA-IgG) and viral capsid antigen (VCA-IgM), or using PCR evidence of EBV DNA, report up to 67% EBV reactivation in PASC patients compared to just 10% in fully recovered controls [18,264,266,267]. Reactivated EBV may cause symptoms by itself such as fatigue, cognitive dysfunction, or rash, suggesting that some PASC manifestations could be driven by "long EBV" effects. However, a number of studies have demonstrated no significant EBV reactivation, citing poor correlation between serological markers and active replication [268,269].

HHV-6 has also been linked to PASC in a similar way as EBV, with active virus leading to fatigue, abdominal complaints and thyroid dysfunction. Unfortunately, there has been a lower number of investigations into PASC and HHV-6 reactivation, but Zubchenko *et al.* found that in PASC patients, reactivation of EBV was observed 42.6%, HHV-6 in 25.0%, and EBV plus HHV-6 in 32.4% [270]. Additionally, compared to controls, herpes reactivation PASC patients presented more frequently with slight fever temperature, headache, psycho-neurological disorders, pulmonary abnormalities and myalgia. Finally, although not focusing necessarily on PASC, VZV reactivation (shingles) has been reported to occur more frequently in post-COVID-19 cases, with an estimated increased risk of VZV reactivation of between 15% and 59% [271–274].

It has been hypothesized that chronic SARS-CoV-2 antigenemia may impair antiviral T-cell surveillance, facilitating viral reactivation, which in turn amplifies IFN and IL-6 production [275]. Expanding on this mechanism, the marked depletion or exhaustion of EBV-specific $CD8^+$ T cells and persistent type I IFN signalling (perhaps due to ongoing SARS-CoV-2 antigen presence), alongside impaired NK cell cytotoxicity, create a permissive niche for herpesvirus replication [276]. Meanwhile, herpesvirus proteins like EBV dUTPase can activate TLR2 and C-type lectin receptor (CLR) pathways, heightening systemic IL-6 and TNF-α production, perpetuating a low-grade cytokine storm. These dynamics suggest that PASC may not be driven solely by SARS-CoV-2, but also by the cascade of viral reactivations it can trigger in a dysregulated immune environment.

Gut/lung dysbiosis with microbial-product leak

COVID-19 causes severe and long-lasting gut microbiome disturbances; some of these changes are associated with PASC [277–279]. SARS-CoV-2 antigen persistence in the intestinal mucosa is thought to contribute to chronic enteric dysbiosis and immune activation. Cohort studies following patients three months to one year post-COVID found that PASC patients often have depletion of beneficial short-chain fatty acid (SCFA)–producing microbes *Faecalibacterium prausnitzii, Dorea,* and *Eubacterium,* and expansion of pathobionts *Ruminococcus gnavus, Clostridium Bolteae,* and *Bacteroides vulgatus,* up to a year post-infection [278,280–283].

F. prausnitzii is a dominant gut bacterium known for producing anti-inflammatory butyrate, *Eubacterium* also produce butyrate whilst *Dorea* typically produce acetate and formate; such SCFA-producing microbes play a key role in maintaining epithelial integrity

and regulating anti-inflammatory immune responses [284,285]. These particular SCFA-producing microbes are within the *Firmicutes* phylum and their depletion is linked to inflammatory bowel disease (IBD), irritable bowel syndrome (IBS), and metabolite disorders such as obesity and type 2 diabetes [286]. *R. gnavus* and *C. Bolteae* are also members of the *Firmicutes* phylum, whilst *B. vulgatus* belongs to the *Bacteroidetes* phylum. These pathobiont species produce immune-stimulatory molecules and potential neuroactive metabolites; their enrichment has been associated with IBD, IBS, type 1 diabetes, and Autism spectrum disorders [287,288]. Low levels of SCFAs with relatively higher levels of potentially harmful tryptophan metabolites (indole, indoxyl sulfate, and skatole) indicate a microbial shift away from a beneficial state; this shift, alongside a reduction in α-diversity, is correlated with fatigue, cognitive scores, and PASC inflammatory biomarkers like CRP in PASC patients [278,282].

Immunological studies link these microbial changes to markers of epithelial barrier dysfunction, such aszonulin, lipopolysaccharide (LPS), and β-glucan, as well as to a PASC associated plasma signature enriched for type I/III IFNs and TNF-α [289,290]. In the acute phase, SARS-CoV-2 infected enterocytes downregulate TJ proteins (occludin, claudin-1) [291]. In conjunction, general infection is associated with systemic IL-6 which is associated to overexpression of zonulin [292]. This combination may increase paracellular permeability and allow for Gram-negative microbial product leakage. These barrier defects may persist in some individuals, allowing persistent translocation of these microbial products. Elevated levels of zonulin, beta-D-glycan, and LPS binding protein have been observed in the blood of PASC patients, and were associated with higher levels of inflammatory cytokines [293,294].

Within the blood, LPS and β-glucan can activate TLR4/myeloid differentiation factor 2 (MD-2) receptors on monocytes, driving IL-6/TNF-α production, whilst circulating bacterial CpG DNA can boost pDC IFN-α output; fuelling the chronic low-grade complement and coagulation cascades responsible for PASC symptoms [295,296].

Importantly, gut barrier disruption and microbial translocation provide a mechanistic route by which enteric dysbiosis may have "knock-on" effects beyond the gastrointestinal tract. For example, murine models have found that colonisation of *Clostridium tyrobutyricum*, a butyrate producer, can result in upregulation of tight junction proteins and a decrease in blood-brain barrier (BBB) permeability [297]. Some pathways through which the gut can send signals to the brain include changes in the gut microbiota which alternate circulating levels of pro/anti-inflammatory cytokines; generating neurotransmitters or neuromodulators in the intestinal lumen; and activating sensory vagal fibres [298]. Likewise, the brain can also affect the microbiome through HPA axis activation, anti-inflammatory sympathetic activation, or activation of CNS regulatory areas of satiety to regulate immune cells locally in the gut, affect its permeability, and impact nutrient availability [298]. Through the microbiota–gut–brain axis, circulating microbial products and inflammatory mediators can promote BBB dysfunction and microglial activation, while dysbiosis-associated changes in microbial metabolites (including SCFAs and tryptophan-derived pathways) might contribute to fatigue, cognitive symptoms, and neuropsychiatric features reported in subsets of PASC patients.

Although dysbiosis has been reported across multiple mucosal sites after COVID-19, the gut (particularly the colon) represents the largest microbial reservoir and is therefore a

plausible dominant source of sustained systemic exposure to microbial products when epithelial barrier function is compromised. In contrast, shifts in the nasopharyngeal/upper airway microbiome are more likely to influence local mucosal immunity and respiratory inflammation, and the extent to which NP dysbiosis contributes directly to systemic inflammation remains less clearly established. A small post-COVID airway study suggested a shift of the lung microbiome, with enrichment of *Prevotella* and *Veillonella* several weeks after discharge [299]. More recently, a much larger metagenomic study conducted as part of this thesis (Section IV) has provided initial evidence that the presence of certain protective species in the respiratory microbiome during the acute phase (*Dolosigranulum pigrum and Corynebacterium),* that may reduce the initial innate immune response, preventing immune-mediated lung damage and subsequent pulmonary-injury related PASC.

3.2.2 Immune and inflammation

Chronic cytokine signalling and exhaustion

Regardless of the causation, multiple studies and reviews characterizing PASC point to the presence of persistent, low-grade inflammation as one of the main causes of PASC symptoms. This non-resolving inflammatory state, lasting months-years, is usually distinguished by mild but sustained elevation of inflammatory markers and cytokines in the blood, indicating ongoing immune activation. This persistent immune stimulation can be detected even in those who initially had mild-to-moderate acute illness, underscoring that chronic inflammation in PASC is not simply a byproduct of acute disease severity [300].

Pro-inflammatory cytokines are central to this chronic inflammatory milieu. Levels of circulating IL-6, TNF-α, and IL-1β (dubbed the "macrophage triad") are usually raised in PASC cohorts (see Section I, Chapter 2.3 for more information) [301–303]. Low-grade systemic inflammation is further evidenced by raised levels of certain acute phase and tissue injury markers in some patients (e.g. CRP, ferritin, and D-Dimer, etc), pointing to ongoing inflammatory processes affecting multiple organ systems [304]. These various perturbations can persist for many months after the infectious period, indicating a failure of the immune system to fully reset to baseline activity.

One key factor to this persistent cytokine signalling is aberrant type I/III IFN persistence. Normally, these IFNs are acute antiviral cytokines that taper off after an infection is cleared. However, several PASC cohorts show an increased type I/III IFN signature up to eight months following acute infection, in which plasma IFN-β and IFN-λ1 remain at levels more than two-fold higher than in fully recovered controls [300,305]. This prolonged IFN response suggests continued immune stimulation, possible by the residual viral antigens, reactivated viruses, or microbial products described above. However, as noted, PASC is heterogenous in its presentation: e.g. in fibrotic lung PASC patients, IFN-β was not elevated, whilst TGF-β and IL-1α was [306]. This indicates that certain PASC cytokine signatures may be correlated to certain PASC phenotypes.

Another important mechanism is monocyte and macrophage reprogramming leading to "trained immunity", a phenomenon whereby innate immune cells acquire immunological memory. Analysis of patients 4-12 months following COVID-19 infection show epigenetic changes in both classical and nonclassical monocytes towards a proinflammatory state,

with enhanced cytokine release in response to TLR agonists and INF- α [307]. Classical monocytes usually differentiate into macrophages within a few days, and thus the presence of monocyte epigenetic changes months-years following COVID-19 suggests these changes originate upstream in hematopoietic stem/progenitor cells (HSPCs), which give rise to monocytes and can survive for years [307]. Evidence suggests the epigenetic changes of HSPCs are likely driven by excessive IL-6R signalling during the acute disease phase, potentially through STAT3-dependent chromatin structural changes [307]. The resulting monocytes derived from these cells months later are hyper-responsive and biased towards cytokine production, allowing for continuous, low-level secretion of IL-6, IL-1β, TNF-α and other mediators, effectively sustaining a cycle of inflammation.

In respiratory PASC, these proinflammatory monocyte-derived macrophages are believed to be the primary drivers of lung inflammation and fibrosis through TGF-β and IFN-γ signalling. Following lung injury, AT2 cells, lung epithelial stem-like cells, begin to regenerate the epithelium by entering a transitional state, ultimately becoming alveolar type I (AT1) cells, large and thin cells responsible for gas exchange. However, the mechanism of PASC lung fibrosis suggests that inflammatory monocytes infiltrate the lung tissue, whereupon even minimal priming via IFN-γ causes excessive secretion of TGF-β [308]. TGF-β keeps AT2 cells in a transitional state, preventing AT1 maturation, resulting in an accumulation of transitional cells within the lungs that begin to express pro-fibrotic and cellular senescence signals, as well as additional TGF-β [309]. The disruption of alveolar architecture and reduced gas exchange due to fibrotic lungs may then result in persistent pulmonary PASC symptoms such as dyspnoea, cough, and reduced exercise tolerance.

The other main monocyte-derived cell, dendritic cells (DCs) also play a role in dysregulated cytokine signalling. DCs are the body's primary source of IFN-α, and the lack of pDCs in the peripheral blood is a hallmark of severe COVID-19 [72,74]. Recovery for these patients can be incomplete, with some convalescent patients (especially those with severe illness) having persistent pDC deficiencies for at least 7 months post-infection [310]. Additionally, likewise to macrophages, elevated levels of activated pDCs have also been observed in PASC patients alongside cell markers indicating increased migration into inflammatory sites and exhaustion [307,310]. Taken together, this evidence suggests a reduction of pDC levels in peripheral blood likely due to migration of these cells into inflamed tissues. Additionally, exhausted or reduced pDCs may produce less antiviral type I IFN in response to stimuli, potentially allowing intermittent viral reactivations or poor regulation of inflammation, however, as high type I IFN is common in PASC, this is either unlikely, or pDCs are not the main IFN source in PASC.

Concurrently, there is evidence of T cell dysregulation and exhaustion in PASC. The persistent antigenic stimulation (from viral remnants or ongoing inflammation) can push T cells into a chronic activated state followed by functional exhaustion. PASC patients have been found to lack naïve T cells and instead harbour increased proportions of differentiated and activated T cells, as if the immune system is continuously fighting an infection [300,311]. These patients also exhibited exhausted SARS-CoV-2-specific CD8+ T cells expressing high levels of inhibitory receptors PD-1 and CTLA4, consistent with chronic stimulation [312,313]. PASC patient CD4+ T cells were also enriched for phenotypes associated with homing to inflamed tissue such as CXCR4, CXCR5 and CCR6 [313]. Such findings imply

that the adaptive immune system in PASC remains abnormally active, but uncoordinated and ineffective, leading to T cell "burnout" or immune exhaustion; functionally, this means the T cells are present but less capable of clearing threats. This dysfunction is highlighted in the recent finding that CD8+ T cells from PASC patients spontaneously secreted IFN-γ without any exogenous stimulus, a phenomenon not seen in healthy controls; this secretion appeared to be dependent on major histocompatibility complex (MHC) class I–dependent antigen presentation by CD14+ cells [314]. IFN-γ secretion was correlated with PASC symptoms, with significant symptom resolution over 31 months post-COVID-19 as IFN-γ release decreased over time or following vaccination.

A combination of the above mechanisms, and more, likely maintain the chronic cytokine signalling and immune dysfunction in PASC. Phetsouphanh *et al.* identified IFN-β, PTX3, IFN-γ, IFN-λ2/3 and IL-6, as a set of analytes, that in combination, could distinguish PASC with ~80% accuracy [300]. To delve into speculation (that is to say, the following text does not infer causality or imply these processes are happening in PASC but is included to help the reader appreciate just how far reaching cytokinetic activity is within the body), such cytokines may not act just as potential biomarkers but may directly mediate PASC symptomatology. IL-6 and IL-1β can cross the blood–brain barrier and influence memory processes, modulate regional activity and connectivity, modulate sleep-related processes, and cause general neuroinflammation [315–317]. These activities might result in cognitive dysfunction, "brain fog", fatigue, sleep disruption, and mood disturbances frequently reported in PASC patients. Lung function could also be affected. IL-6 is associated with decreased lung function, whilst IL-1β may contribute to interfere with alveolar

regeneration [318,319]. In the periphery, IL-1β and TNF-α can activate endothelial cells to sustain inflammation [319]. Elevated levels of TNF-α have additionally been correlated with reduced peak VO_2 and exercise capacity in PASC patients, potentially contributing to the general exercise intolerance observed in PASC [320,321]. Finally, as mentioned above, long-lived HSPCs could result in prolonged production of hyper-responsive monocytes that continuously secrete cytokines, resulting in a high IL-6 and IL-1β proinflammatory environment that is self-perpetuating through the TLR4/RAGE-loop positive reinforcement[307,322]. The presence of these cytokines may drive much of the pathophysiology discussed throughout this chapter, generating the multi-organ inflammation that persists throughout the body.

Although the above text in speculative in nature in terms of its contribution to PASC, it is of importance to understanding the wide-reaching implications of dysregulated cytokine and inflammatory systems as they appear central to PASC.

Autoimmunity

In addition to the PASC associated immune dysregulation and chronic inflammation, multiple studies have also found elevated levels of preexisting or *de novo* autoantibodies such as against ACE2, β2-adrenoceptor, muscarinic M2 receptor, angiotensin II AT1 receptor and the angiotensin 1–7 MAS receptor [323,324]. High levels of other more general autoantibodies have also been found in a number of PASC patients, including those that target tissues, organ systems, and immune-related proteins and components [325]. High levels these autoantibodies were additionally found to be inversely correlated with protective SARS-CoV-2 antibodies, suggesting patients with autoantibodies may have

more breakthrough infections [324]. The situation is complicated however, as a major comprehensive study by Klein *et al.* did not find such autoantibodies to be a major component of PASC [312]**.** In contrast, a number of other studies on the topic have found specific autoantibodies to correlate with PASC symptoms [323,326–328]. Beyond association studies, functional autoantibodies targeting GPCRs (including β2-adrenergic and muscarinic receptors) (GPCR-fAAbs) have been demonstrated in established bioassays in subsets of PASC patients [323]. For such subsets of PASC patients, treatment with Rovunaptabin to neutralise GPCR-fAAbs has been shown to significantly reduce patient fatigue symptoms and improve quality of life [329]. On a broader epidemiological scale, large cohort studies of almost four million participants have shown that SARS-CoV-2 infection of any severity significantly increases the risk of developing rheumatic autoimmune diseases such as rheumatoid arthritis, systemic lupus erythematosus, and systemic sclerosis [330].

Multiple, non-mutually exclusive mechanisms may explain how SARS-CoV-2 infection triggers these self-reactive antibodies. Molecular mimicry is one well-recognized mechanism: viral antigens from SARS-CoV-2 can share sequence or structural homology with human proteins, leading the host's antibodies to cross-react with self-antigens. Bioinformatics analyses have identified hundreds to thousands of potential shared peptides between SARS-CoV-2 and human proteins which may pose as mimicry targets [331]. In addition, bystander activation can happen during intense acute COVID-19, whereby a highly inflammatory environment leads to a breakdown of self-tolerance, allowing autoreactive T and B cells (which would normally be anergic or deleted) to become activated and produce antibodies against self-antigens released during tissue damage.

These mechanisms create an environment that favours loss of tolerance and the expansion of autoantibody-producing B cells long after the acute infection has resolved.

A striking finding in COVID-19 immunology was the discovery of neutralizing autoantibodies against IFNs. Meta-analysis showed anti-IFN was detected in around 10% of severe COVID-19 cases and was associated with increased risk of severity and mechanical ventilation (Odd ratio 7.75 and 4.19 respective) [332]. These antibodies impair innate antiviral immunity and may allow for unchecked viral replication early in infection.

Given their pathogenic role in acute disease, attention has turned to whether anti-IFN autoantibodies persist and contribute to the chronic symptoms of PASC. The presence of anti-IFNs in this context is hypothesized to impair the body's antiviral defence, contributing to viral persistence, immune dysregulation, and chronic symptoms in PASC. However, whilst anti-IFNs appear to be of interest during the acute disease, multiple studies show the proportion of PASC patients with anti-IFNs is very low (<2%), and likely not significantly higher than in people who recover fully from COVID-19 [333–335].

Other studies have investigated broader autoantibody profiles, including antinuclear antibodies (ANA) and extractable nuclear antigens (ENA), which are often found in systemic autoimmune diseases such as lupus. Son *et al.* reported that ANA and ENA were detectable in 79% of COVID-19 patients three months post infection, in 78% at six months, and in 41% at twelve months [326]. Levels of these antibodies were associated with elevated inflammatory markers and partially predictive of PASC symptoms such as fatigue and dyspnoea. However, the cohort was relatively small (~100 patients).

In a similar vein, Visvabharathy *et al.* showed that autoantibodies associated with systemic lupus erythematosus (SLE) and other systemic autoimmune diseases were more elevated in neuro-PASC patients than in convalescent controls [336]. These levels were also associated with poorer cognitive performance and higher symptom severity, particularly with respect to depression.

Organ-specific autoimmunity, such as in relation to the thyroid, and autoantibodies targeting neurotransmitter receptors have also been explored in relation PASC, but are unlikely to contribute meaningfully [337,338].

Taken together, the current body of evidence suggests that SARS-CoV-2 can act as an immunological trigger in genetically susceptible individuals. Importantly, such susceptibility may include a preclinical phase of autoreactivity that can be present for years before overt autoimmune disease. In SLE, autoantibodies frequently precede diagnosis, supporting the concept that infection may amplify or unmask underlying loss of tolerance rather than initiating autoimmunity *de novo* [339]. However, the presence of autoantibodies in individuals does not necessarily correlate with PASC development, although certain subsets may contribute to symptom onset. Similar infection-associated contributions have been described in other autoimmune diseases, with recent mechanistic work implicating EBV in the development of pathogenic autoreactive B cell states in SLE [340]. Unfortunately, most of the studies investigating autoantibodies and PASC appear to suffer from limited statistical power, with most investigations to date having relatively small cohorts, often involving fewer than 100 COVID-19 patients and frequently fewer than 50. Moreover, few studies include pre-infection samples, making it difficult to

determine whether detected autoantibodies are a consequence of SARS-CoV-2 infection or merely incidental findings. Finally, many autoantibodies detected in PASC patients, such as ANA, anti-TPO, or GPCR-targeted IgG, can also be found in low levels in the general population or in individuals with other post-infectious syndromes. Pending larger scale studies or meta-analyses with clear functional validation or longitudinal association with symptoms, it is difficult to discuss the effect to which autoantibodies drive PASC symptoms.

3.2.3 Vascular coagulation

Complement dysregulation, endothelial injury, and micro-thrombi

Complement dysregulation, endothelial injury, and micro-thrombi formation collectively establish a self-sustaining loop of vascular dysfunction central to the pathology of PASC. Persistent complement activation, viral antigens, and inflammatory cytokines collectively injure endothelial cells. This activation results in the expression of adhesion molecules (e.g. ICAM-1, VCAM-1, selectins), inflammatory mediators, and procoagulant factors, whilst reducing the expression of anticoagulant factors [257]. These conditions foster micro-thrombi formation that obstructs capillary networks, limiting oxygen and nutrient delivery, particularly affecting the lungs, brain, and muscles, thus contributing to hallmark PASC symptoms such as dyspnoea, fatigue, chest pain, and cognitive impairment ("brain fog") due to chronic hypoperfusion and inflammation.

Persistent thrombo-inflammation is tightly interconnected with cytokine release. For instance, IL-6 signalling in endothelial cells promotes the release of IL-8 and MCP-1, which recruit neutrophils and macrophages, and stimulate VEGF production, disrupting TJ

proteins which increases endothelial permeability [120]. This cytokine-rich systemic environment results in immune cell migration, heightened inflammation, and sustained tissue damage [322].

Several studies have validated complement dysregulation in PASC. Markers indicative of classical (C1s-C1INH complex), alternative (Ba, iC3b), and terminal (C5a, TCC) complement pathway activation are significantly elevated in PASC patients [341]. Notably, a specific combination of complement activation fragments (iC3b, TCC, Ba, and C5a) was predictive of PASC with reasonable accuracy (AUC 0.785). These data indicate that complement remains in an activated state in PASC, driving inflammation, microthrombosis, and complement-mediated tissue damage which would additionally activate the complement system. Further supporting this, elevated complement activity and signs of increased attack complex formation (C5bC6-C7) have been observed at six and twelve months post-infection, alongside signs of complement-mediated haemolysis (low hemopexin and increased heme levels), contributing to ongoing endothelial damage and reduced oxygen-carrying capacity [143].

Elevated levels of vWF, platelet activation, angiopoietin 1 (ANG-1), P-SEL, and VE-cadherin (VE-Cad) have all also been associated with PASC, important endothelial dysfunction and vascular transformation biomarkers [143,342,343]. Elevated VE-Cad levels in PASC indicates a breakdown in endothelial junctions and increased permeability [343]. Concurrently, elevated ANG-1 suggests an ongoing wound-repair process due to sustained vascular injury. Increased soluble P-SEL levels further underscore platelet and endothelial activation, and

drive inflammation and thrombosis; soluble (s)P-SEL was particularly significantly correlated with PASC [343–345].

Endothelial dysfunction, recognized as a central contributor to PASC, has been documented in two separate meta-analyses to be observed in PASC patients for up to a year post-infection, with increasing impairment correlating with PASC symptoms severity [346,347]. Endothelial cells play roles in haemostasis, immune reaction and angiogenesis; the barriers they form contribute to organ protection (BBB), gas exchange (blood-air barrier), nutrient absorption (intestinal-blood barrier), and waste removal (glomerular filtration barrier) [348]. Endothelial injury results in the following: increased permeability across barriers, allowing immune cells, inflammatory molecules, and even small blood clots to enter tissues; shedding of glycocalyx, a protective layer on the surface of endothelial cells, which makes the endothelium more vulnerable to damage; and the extension of phosphatidylserine-rich filopods, finger like projections that signal stress and promote clotting [349]. The combined effect is general barrier damage, disrupting blood vessel integrity and driving chronic inflammation, clotting, and tissue damage. During the convalescence period, a subset of patients is unable to fully restore endothelial function, contributing to PASC. For example, reduced pulmonary function (DLCO < 80%) has commonly been observed in COVID-19 survivors [210,211]. Investigations into endothelial damage in these patients observed that elevations in circulating epithelial and endothelial pulmonary markers are increased in patients with reduced DLCO, and in particular, soluble ICAM-1 and ANG-2 were especially correlated with extremely low DLCO (under <50% predicted) compared to those with normal lung function [350]. This implies ongoing

pulmonary capillary endothelial disruption in long COVID, contributing to limited oxygen diffusion and breathlessness. Another example refers to the gut microbial product leak discussed above, whereby microbial changes are correlated with markers of epithelial barrier dysfunction, and increased barrier permeability allows metabolite leakage, fuelling further PASC inflammation.

In addition to endothelial damage, endothelial activation also results in the release of inflammatory molecules, which in conjunction to pre-existing inflammatory cytokines, activated immune cells, persistent antigens, and complement dysregulation discussed previously, creates a hypercoagulable environment, priming patients for micro-thrombi formation. Multiple studies have observed plasma from PASC patients to contain large insoluble amyloid microclots that are resistant to normal fibrinolysis [351–355]. Further, it appears presence of SARS-CoV-2 S1 spike protein can directly induce these abnormal clots, suggesting a direct link between chronic thrombosis and viral persistence [351,356]. These blood clots can block microcapillaries and thereby inhibit oxygen exchange, leading to symptoms such as tissue hypoxia and fatigue.

If oxygen is restored too rapidly to these hypoxic tissues, such as through shear stress during movement or increased circulation, ischemia-reperfusion may occur [357]. The rapid influx of oxygen generates a burst of ROS which increases oxidative stress in these tissues. This oxidative stress produces inflammatory cytokines, and vice versa, producing a prothrombotic cycle. This process is most visibly observed as a set of chilblain-like lesions, or “COVID toes”, whereby extremities get cold, followed by a period of rewarming, commonly resulting in a rash on or around the toes [358].

Taken together, PASC appears as a vascular disorder leading to diffuse micro-thrombi and chronic tissue hypoperfusion. This thrombo-inflammatory loop presents as PASC symptoms such as fatigue, dyspnoea, and cognitive dysfunction, and explains why objective deficits (reduced DLCO, impaired 6-minute-walk distance, etc) tightly track endothelial and coagulation biomarkers.

3.2.4 Tissue-specific and non-specific damage and dysregulation

Residual organ damage

In many patients, PASC may simply reflect the residual organ damage from severe acute COVID-19, the specifics of which are discussed in Supplementary information 1. Very simplistically, patients who developed ARDS may have chronic pulmonary fibrosis and reduced lung capacity, those who had acute kidney injury might have chronic kidney disease, and those who had cardiac involvement might have residual reduced ejection fraction or scar tissue. There a few ways in which SARS-CoV-2 can damage organs: direct viral invasion and cell damage; endothelial inflammation and secondary damage; microthrombosis resulting in ischemia and hypoxia; viral-mediated release of toxic cytokines. Meta-analysis has revealed hospitalized and ICU COVID-19 patients had more than double the risk of developing PASC [359]. This increased risk may in part be due to severe disease resulting in severe organ damage that does not fully resolve in a seemingly large proportion of these patients, perhaps due to, or exacerbated by, ongoing inflammation and endothelial damage as discussed above. This would also partly explain the trend for PASC to diminish over years, as these patients slowly recover proper organ function.

However, even during COVID-19 in low-risk individuals, 70% of patients had damage to at least one organ (heart, lungs, liver, kidneys, pancreas, or spleen), and 29% had multi-organ damage [360]. At a one year follow-up by the same research group, 59% of participants had single-organ damage, and 27% presented with multi-organ damage [361].

Many PASC patients experience cognitive impairment. Studies indicate a prevalence of over 20%, and evidence shows that the odds of such impairments continue to rise even two years after the initial infection [201,202]. Serious maladies that increase post COVID-19 are stroke and new-onset epilepsy/seizures [204]. While stroke risk appears to return to baseline over time, the risk of seizures and epilepsy remains elevated even at the two-year mark. Together these observations imply potential ongoing or progressive neuronal damage or altered brain excitability. Further supporting this, investigations have found that the presence of white and grey matter abnormalities are strongly associated with persistent neurological PASC [362]. Widespread neuroinflammation due to these abnormalities has been proposed as a central mediator of symptoms including fever, headache, fatigue, brain fog, and pain. Additionally, lasting structural changes within the brain such as reduced cortical thickness, brain volume loss, and white matter disruption (known precursors of neurodegenerative diseases), in combination with persistent neuroinflammation may potentially contribute to the increased dementia risk observed following COVID-19 [243].

Looking at other organ systems also reveal ongoing impairments. There is reduced lung function and signs of pulmonary fibrosis or scarring in roughly half of COVID -19 survivors between three and six months, consistent with a loss of alveolar capillary structure [210,211].

For the heart, at one year follow-up, Puntmann *et al.* revealed ongoing cardiac impairment in 58% of PASC patients, whilst Zhang *et al.* and Xie *et al.* additionally found increased of cardiovascular diseases and disorders [217,218,363]. For the kidneys, AKI and renal replacement is often seen in severe COVID-19 patients, and following disease, the risk of CKD, nephritic/nephrotic syndromes, and glomerular disorders is significantly increased [234,237,238]. Further, severe COVID-19 survivors are at a substantially increased risk of developing incident diabetes, potentially due to ongoing pancreatic damage [239].

These persistent dysfunctions following COVID-19 can contribute to the development of PASC symptoms through chronic hypoxia, systemic inflammation, and metabolic dysregulation. Lung fibrosis and impaired gas exchange may reduce oxygen delivery to tissues, promoting fatigue and cognitive symptoms. Cardiac dysfunction can lead to exercise intolerance, chest pain, and autonomic symptoms, while renal injury and pancreatic damage can lead to fluid-electrolyte imbalances and glucose dysregulation, respectively, contributing to fatigue, cognitive impairment, and generalized malaise. These interconnected ongoing organ impairments create a physiological environment conducive to sustained multisystem symptoms characteristic of PASC.

Autonomic imbalance

Autonomic imbalance refers to a disruption in the normal functioning and coordination between the two branches of the autonomic nervous system (ANS): the sympathetic ("fight or flight") and parasympathetic ("rest and digest") systems. Normally, these systems work in balance to regulate involuntary functions like heart rate, blood pressure, digestion, and temperature control. When this balance is disrupted, such as due to

inflammation, nerve injury, or viral effects as seen in COVID-19, one branch may become overactive or underactive, leading to symptoms like rapid heartbeat, fatigue, dizziness, poor temperature regulation, and GI issues. This dysregulation is a recognized contributor to PASC.

POTS is a disorder of the ANS characterized by an excessive increase in heart rate when moving from lying down to standing, without a significant drop in blood pressure. Studies have found that between 17%-79% of PASC patients meet the criteria for POTS and are accompanied by symptoms like light-headedness, weakness, and palpitations [221–223]. The high incidence of POTS and orthostatic symptoms suggests that SARS-CoV-2 (or immune responses to it) may damage autonomic nerve fibres or central autonomic circuits.

Small PASC cohorts report small-fibre neuropathy (SFN) and, less often, multifocal motor neuropathy (MMN), likely from SARS-CoV-2–driven immune dysregulation [364]. In POTS-PASC, widespread autonomic dysfunction is observed, including elevated sympathetic activity, SFN, and dermal synuclein deposition [365]. SFN predominates because small (poorly myelinated) autonomic fibres are vulnerable; their loss explains orthostatic intolerance, tachycardia, and thermoregulatory instability. About 25% with SFN progress to large-fibre neuropathy affecting vibration/touch, though this is not yet shown post-COVID [366]. Other studies investigating PASC patients further identify blunted parasympathetic responses, providing evidence of impaired cardiac autonomic control [367,368].

Other mechanisms of autonomic dysfunction include lingering inflammation in the brain (microglia activation), which could disrupt autonomic regulation and contribute to

symptoms like tachycardia and thermodysregulation. Another angle is dysfunction of the vagal nerve, which might be affected by either direct viral involvement (vagus has sensory fibres in lung/gut where virus replicates) or by inflammation. Finally, various studies and case-series have presented other causes such as: phosphorylated α-synuclein aggregates in cutaneous autonomic nerves, a driver of autonomic failure in classic synucleinopathies; and humoral autoimmunity against β-adrenergic, muscarinic and other vasoregulatory GPCRs [369,370].

Metabolic/mitochondrial dysfunction

There is growing recognition that PASC shares features with other post-critical illness syndromes and chronic fatigue conditions where cellular metabolic shifts occur, such as myalgic encephalomyelitis (ME)/CFS. Such metabolic shifts could explain exercise intolerances, for example, some PASC cohorts report disproportionate exhaustion after minimal activity, and cardiopulmonary exercise testing demonstrates reduced oxygen utilization and early transition to anaerobic metabolism [371]. A core aspect of this metabolic and energy dysfunction involves the mitochondria, the primary organelles responsible for cellular energy production. As major sources of ROS such as hydrogen peroxide and superoxide, they are extremely vulnerable to oxidative stress.

Multiple lines of evidence now support the presence of mitochondrial dysfunction in PASC. Large-scale studies now converge on mitochondrial and broader metabolic dysfunction as a unifying mechanism that may account for some of the diverse clinical manifestations observed across patients [372,373]. Peripheral blood mononuclear cells (PBMCs) from PASC patients show consistent abnormalities in mitochondrial respiration,

bioenergetic capacity, and expression of mitochondria-related genes [374–376]. Further mitochondrial dysfunction has also been observed in muscle tissues and the brain of PASC patients [377,378]. These abnormalities are consistent with widespread, compromised mitochondrial energy production and may underlie the hallmark symptoms of fatigue, exercise intolerance and/or muscle weakness. One such hallmark, chronic fatigue, has been directly linked to deficits in mitochondrial ATP production in PASC patients [379]. The reduction in mitochondrial-derived ATP leads to energy shortfalls that may also impact muscle function, cognitive processes, and overall physical capacity, significantly affecting quality of life.

Mitochondrial dysfunction is tightly interconnected with oxidative stress, and indeed, elevated levels of circulating biomarkers associated with oxidative stress and mitochondrial damage have been reported [380–382]. These biomarkers, such as F2-isoprostanes, malondialdehyde, and reduced levels of antioxidants like coenzyme Q10, can both contribute to, and be a result, of oxidative stress, forming a bidirectional harmful feedback loop. Increased mtDNA quantities, which can mark mitochondrial stress and damage, are correlated with fatigue and dyspnoea scores in PASC patients, directly linking mitochondrial dysfunction to PASC symptom severity [383].

Whole-genome sequencing from a cohort of patients with severe PASC identified ten pathogenic or likely pathogenic variants in genes implicated in mitochondrial function, including *ACOT9, SDHAF3, ALG14, PTCD3, ANTKMT, ATP2A1, FA2H, RARS2, LAMA2*, and *PDF* [384]. This suggests an underlying genetic predisposition to mitochondrial vulnerability; however, the rarity of these alleles (> 0.0005%) compared to the regularity of PASC likely

indicates that this is not a major mechanism through which mitochondrial dysfunction arises in PASC.

Epigenetic reprogramming of mtDNA may also play a role in PASC. Alongside a similar mechanism as HSPC trained immunity, mitochondrial DNA expression may be robustly altered because of severe disease. Epigenetic signatures such as methylation, hydroxymethylation and miRNAs can alter mitochondrial gene expression, resulting in higher ROS production, disruption in the replication process, and disruption of important gene families such as COX, OXPHOS, ND, and DNMT [385]. Although this mechanism has not yet been observed in PASC, it has associated with a variety of metabolic, cardiovascular, and neurodegenerative disorders [385].

Other mechanisms involve mitochondrial injury because of sustained inflammatory and cytokine-rich environment observed in PASC patients. These cytokines upregulate glycolytic enzymes and pyruvate dehydrogenase kinases, which shift cell metabolism in two ways: increasing the burn rate of glucose in the cytosol (glycolysis); and inhibiting conversion of pyruvate to acetyl-CoA, starving the Krebs cycle of substrate and reducing ATP production within the mitochondria [386–388]. This shift results in increased lactate production as pyruvate is increasingly reduced to lactate to regenerate NAD^+ and sustain glycolytic flux; lactate is then exported into the surrounding tissue which largely contributes to the pH drop observed in inflamed tissues [389]. Lactate can be considered pro- or anti-inflammatory depending on context by exerting pleiotropic effects on the inflammatory process by targeting post-translational modifications, GPCRs, and/or activating transcription factors like NF-κB and HIF-1 to modulate signalling pathways [389].

Pro-inflammatory cytokines can also promote mitochondrial ROS production by altering electron transport chain function and damage mitochondrial DNA [390,391]. This shift in energy production strategies, alongside mitochondrial injury, reduces ATP output and induces mitochondrial atrophy, leading to a holistic reduction in energy production capacities which may lead to fatigue and exercise intolerance.

SARS-CoV-2 can also directly interact with the mitochondria, exploiting mitochondrial dynamics for virus proliferation and causing long-lasting structural damage [392,393]. Specifically, SARS-CoV-2 has been observed to form double-membrane vesicles derived from mitochondrial membranes as a part of cell defence system evasion, interfering with normal mitochondrial function and contributing to organelle degradation [393].

Viral proteins also interfere with mitochondrial antiviral-signalling protein (MAVS), a critical component of the innate immune response which can trigger the release of IFNs. ORF3c can localize to mitochondria where it interacts with MAVS and PGAM5, inducing MAVS cleavage via caspase-3 [166]. Similarly, ORF10 binds to NIX to translocate to the mitochondria, whereupon it forms a tri-molecular complex with LC3B (NIX–ORF10–LC3B), this tethers the mitochondria to an autophagosome, triggering mitophagy to degrade the mitochondria and its resident signalling proteins such as MAVS [394]. These viral proteins suppress IFN signalling to evade the immune system at the expense of mitochondrial survival, greatly affecting energy production.

There is also concern about autoimmune responses. As previously discussed, the immune system's response to SARS-CoV-2 might include the development of autoantibodies that

mistakenly target mitochondrial proteins, leading to continuous immune-mediated damage to mitochondria.

Integrating these mechanistic insights, a unifying model emerges. Mitochondrial injury, whether due to inflammatory, viral, autoimmune, or genetic factors, initiates a shift from oxidative phosphorylation to aerobic glycolysis. This transition leads to inefficient energy production, accumulation of ROS, and sustained inflammation. In turn, these effects reinforce mitochondrial impairment, creating a vicious cycle that underlies many of the persistent symptoms of PASC.

3.2.5 Conclusions of the interactions of PASC mechanisms

It is likely that multiple mechanisms coexist in many PASC patients. For instance, a person might have persistent viral antigen in the gut driving immune activation, plus autoantibodies that cause POTS, plus deconditioning from a long ICU stay. A unifying feature in many hypotheses is the immune system: whether due to lingering virus, autoimmunity, or reactivation of EBV, an aberrant immune activation seems central to PASC. This is supported by the finding that immunomodulatory drugs (like corticosteroids, antihistamines, or intravenous immunoglobulin (IVIG)) have anecdotal efficacy in some PASC cases, implying symptoms are immune-mediated rather than from fixed damage. Another consistent theme is microvascular dysfunction: from brain fog to kidney issues, inadequate tissue perfusion due to endothelial damage or micro clots could tie many PASC symptoms together.

Large consortia such as the NIH RECOVER Initiative are now conducting detailed studies which include imaging, tissue biopsy, and molecular profiling, to pinpoint PASC

mechanisms. **Preliminary results confirm that no single cause explains all cases**, but **subgroups** can be identified. For example, one subgroup might show **evidence of viral persistence** (spike antigenemia, high SARS-CoV-2-specific T-cell activation), another might show an **autoimmune signature** (ANA+, rheumatoid factor, etc.), and another might primarily have **dysautonomia** with small fibre neuropathy on skin biopsy. These phenotypes could guide personalized therapies in the future.

In conclusion, PASC likely results from a **combination of persistent immunological stimulation, residual organ injury, and dysregulated homeostasis after acute SARS-CoV-2 infection**. Viral remnants can keep the immune system in a simmering activated state; the immune system may in turn misfire and attack self (autoimmunity) or fail to properly reset (as seen by chronic inflammation and immune exhaustion markers). Coagulation pathways remain overactive in some, causing micro clots that impede recovery. The ANS can be knocked off balance. Figuratively, the “COVID pebble” thrown in the pond creates ripples that continue long after the initial splash. Understanding which ripples dominate in each patient is key to developing effective interventions for PASC.

4 Current clinical management of COVID-19 and PASC

The COVID-19 pandemic has seen an evolution in clinical management, from the uncertain early days of 2020 to the more evidence-based standard of care in 2025. Although clinical practices of COVID-19 and PASC have been discussed whenever relevant within this thesis, this summary has been written as a reference to the reader to the current therapeutic approaches more generally. The below chapter is a summarisation of recommendations based primarily on the "Clinical management of COVID-19: living guideline" and the "Therapeutics and COVID-19: living guideline" documents produced by the World Health Organisation, for more detailed information, it is recommended to read this document in its entirety [395,396].

4.1 Management and therapeutic care of acute COVID-19

The first step of care involves screening through laboratory diagnosis and triaging patients WHO COVID-19 disease severity classifications of mild, moderate, or severe [396]. Asymptomatic individuals are then asked to be isolated for 5 days, whilst symptomatic individuals, who are much more likely to spread the disease, are advised to isolate for 10 days (periods may be shortened according to rapid antigen testing) [396]. Following this, the management of COVID-19 is dependent on the severity of the disease.

For symptomatic patients with risk factors who are not hospitalised, patients should be provided with pulse oximetry monitoring for early detection and intervention of severe disease [396]. These patients should otherwise isolate at home. Mild and moderate patients with a moderate risk of hospitalisation can be prescribed nirmatrelvir and ritonavir [395]. Nirmatrelvir and ritonavir also recommended for mild and moderate patients with a high risk of hospitalisation, and are deemed to be a superior choice compared to the

prescription of remdesivir or molnupiravir due to its greater reduction in hospitalization, ease of administration, and reduced undesirable effects [395].

For severe and critical patients, blood cultures should be taken upon admission, and patients should be placed immediately on standard oxygen therapy (SOT) [396]. Severe and critical patients with acute hypoxemic respiratory failure (AHRF), but not needing intubation, should be placed on high-flow nasal oxygen (HFNO), continuous positive airway pressure (CPAP), or non-invasive ventilation (NIV) as preferred by the clinician [396]. Severe and critical patients are generally prescribed prophylactic dosing of heparins, consistent with the current standard of care for hospitalized patients to control thromboembolic events [395]. Therapeutic care recommendations now involve a combined administration of systemic corticosteroids (dexamethasone), IL-6 blockers (tocilizumab/sarilumab), and Janus-kinase inhibitors (baricitinib) [395]. The typical regimen is dexamethasone 6 mg daily (or equivalent) for up to 10 days and help reduce the excessive inflammatory response; tocilizumab/sarilumab and baricitinib help further dampen this response [395]. Remdesivir, the only antiviral approved for hospitalized patients, is further recommended for severe patients due to its important reduction in mortalities in this patient population, but not for critical patients as it has little to no mortality impact in these cases [395].

During the first wave, hydroxychloroquine was used as an antiviral and immunomodulatory agent in the majority of patients, as reported by the Antwerp University Hospital in Belgium, but this practice was subsequently abandoned in favour of the more effective systemic corticosteroids that now form the cornerstone of COVID-19

treatments [397]. Other therapies that were proposed and later dropped after trials showed little benefit to their interventions include ivermectin, azithromycin, and convalescent plasma [395]. These changes represent the evolution of the clinical approach as evidence drives and refines therapies and supportive care.

4.2 Management and therapeutic care of acute COVID-19

For PASC patients, care revolves around education and support for the self-management of symptoms [396]. For example, anti-inflammatory drugs for arthralgia symptoms, breathing control and pacing for breathing impairment, assistive products and environmental modifications for cognitive impairment, physical exercise for fatigue and orthostatic intolerance, etc [396]. There is currently a lack of evidence for any pharmacological interventions to treat the condition itself, highlighting the need for research into the pathophysiology of this condition in order to improve patient care, or at least better prevent PASC development.

Conclusion

Five years of concerted global investigations have reframed COVID-19 from a purely pulmonary infection into a prototypical **systems disease** in which direct viral cytotoxicity, delayed or blunted type I IFN signalling, endothelial injury and a feed-forward loop of immunothrombosis converge to drive acute illness severity. Autopsy and clinical studies consistently demonstrate that unchecked early viral replication, coupled with evasion of innate sensing, precipitates a surge of pro-inflammatory cytokines and complement activation that shreds vascular integrity, and seeds diffuse micro- and macro-vascular thrombosis across lung, heart, brain, kidney and gut vasculature. This mechanistic triad

explains the distinctive coagulopathy, vascular leak and multi-organ involvement that differentiate severe COVID-19 from other viral pneumonias.

The same pathways set the stage for PASC. Longitudinal cohorts reveal that between 8% and 54% of survivors, particularly middle-aged women and those with severe disease, experience persistent or relapsing symptoms beyond three months. Mounting evidence implicate diverse interconnected mechanisms centred around immune function and regulation as drivers of these sequelae. Together they appear to sustain a low-grade thrombo-inflammatory milieu that manifests clinically as PASC.

Looking forward, the field must pivot **from descriptive cataloguing to integrative, multi-omic and longitudinal analyses** that can disentangle **causal pathways**, identify **predictive biomarkers** and **stratify patients** for targeted intervention. Early combination antiviral–immunomodulatory therapy, judicious anticoagulation, complement or NET-directed inhibitors, microbiome restoration and personalised rehabilitation represent rational therapeutic avenues that warrant rigorous trial evaluation. By illuminating the intertwined virological, immunological and vascular threads laid out in this review, we move closer to precision prevention and treatment strategies that can blunt acute mortality and mitigate the long tail of PASC.

References

1. Cutler DM, Summers LH. The COVID-19 Pandemic and the $16 Trillion Virus. *JAMA*. 2020;324(15):1495-1496. doi:10.1001/jama.2020.19759
2. World Health Organization. World Health Organization 2023 data.who.int. February 28, 2025. Accessed February 28, 2025. https://data.who.int/dashboards/covid19
3. Mehta OP, Bhandari P, Raut A, Kacimi SEO, Huy NT. Coronavirus Disease (COVID-19): Comprehensive Review of Clinical Presentation. *Front Public Health*. 2021;8:582932. doi:10.3389/fpubh.2020.582932
4. Zhu Y, Sharma L, Chang D. Pathophysiology and clinical management of coronavirus disease (COVID-19): a mini-review. *Front Immunol*. 2023;14:1116131. doi:10.3389/fimmu.2023.1116131
5. Gonzalez-Garcia P, Fiorillo Moreno O, Zarate Peñata E, et al. From Cell to Symptoms: The Role of SARS-CoV-2 Cytopathic Effects in the Pathogenesis of COVID-19 and Long COVID. *IJMS*. 2023;24(9):8290. doi:10.3390/ijms24098290
6. Bernard I, Limonta D, Mahal L, Hobman T. Endothelium Infection and Dysregulation by SARS-CoV-2: Evidence and Caveats in COVID-19. *Viruses*. 2020;13(1):29. doi:10.3390/v13010029
7. Montazersaheb S, Hosseiniyan Khatibi SM, Hejazi MS, et al. COVID-19 infection: an overview on cytokine storm and related interventions. *Virol J*. 2022;19(1):92. doi:10.1186/s12985-022-01814-1
8. Yousefi P, Soltani S, Siri G, et al. Coagulopathy and thromboembolic events a pathogenic mechanism of COVID-19 associated with mortality: An updated review. *Clinical Laboratory Analysis*. 2023;37(11-12):e24941. doi:10.1002/jcla.24941
9. Rysz S, Al-Saadi J, Sjöström A, et al. COVID-19 pathophysiology may be driven by an imbalance in the renin-angiotensin-aldosterone system. *Nat Commun*. 2021;12(1):2417. doi:10.1038/s41467-021-22713-z
10. Meidaninikjeh S, Sabouni N, Marzouni HZ, Bengar S, Khalili A, Jafari R. Monocytes and macrophages in COVID-19: Friends and foes. *Life Sciences*. 2021;269:119010. doi:10.1016/j.lfs.2020.119010
11. Middleton EA, He XY, Denorme F, et al. Neutrophil extracellular traps contribute to immunothrombosis in COVID-19 acute respiratory distress syndrome. *Blood*. 2020;136(10):1169-1179. doi:10.1182/blood.2020007008
12. Alahdal M, Elkord E. Exhaustion and over-activation of immune cells in COVID-19: Challenges and therapeutic opportunities. *Clinical Immunology*. 2022;245:109177. doi:10.1016/j.clim.2022.109177
13. Sherif ZA, Gomez CR, Connors TJ, Henrich TJ, Reeves WB, RECOVER Mechanistic Pathway Task Force. Pathogenic mechanisms of post-acute sequelae of SARS-CoV-2 infection (PASC). *eLife*. 2023;12:e86002. doi:10.7554/eLife.86002
14. Mohandas S, Jagannathan P, Henrich TJ, et al. Immune mechanisms underlying COVID-19 pathology and post-acute sequelae of SARS-CoV-2 infection (PASC). *eLife*. 2023;12:e86014. doi:10.7554/eLife.86014
15. Wang EY, Mao T, Klein J, et al. Diverse functional autoantibodies in patients with COVID-19. *Nature*. 2021;595(7866):283-288. doi:10.1038/s41586-021-03631-y
16. Wu X, Xiang M, Jing H, Wang C, Novakovic VA, Shi J. Damage to endothelial barriers and its contribution to long COVID. *Angiogenesis*. 2024;27(1):5-22. doi:10.1007/s10456-023-09878-5
17. Chadda KR, Blakey EE, Huang CLH, Jeevaratnam K. Long COVID-19 and Postural Orthostatic Tachycardia Syndrome- Is Dysautonomia to Be Blamed? *Front Cardiovasc Med*. 2022;9:860198. doi:10.3389/fcvm.2022.860198
18. Gold JE, Okyay RA, Licht WE, Hurley DJ. Investigation of Long COVID Prevalence and Its Relationship to Epstein-Barr Virus Reactivation. *Pathogens*. 2021;10(6):763. doi:10.3390/pathogens10060763
19. Scherer PE, Kirwan JP, Rosen CJ. Post-acute sequelae of COVID-19: A metabolic perspective. *eLife*. 2022;11:e78200. doi:10.7554/eLife.78200
20. Su Q, Lau RI, Liu Q, et al. The gut microbiome associates with phenotypic manifestations of post-acute COVID-19 syndrome. *Cell Host & Microbe*. 2024;32(5):651-660.e4. doi:10.1016/j.chom.2024.04.005
21. Goyal R, Gautam RK, Chopra H, et al. Comparative highlights on MERS-CoV, SARS-CoV-1, SARS-CoV-2, and NEO-CoV. *EXCLI J*. 2022;21:1245-1272. doi:10.17179/excli2022-5355
22. Shum MHH, Lee Y, Tam L, et al. Binding affinity between coronavirus spike protein and human ACE2 receptor. *Computational and Structural Biotechnology Journal*. 2024;23:759-770. doi:10.1016/j.csbj.2024.01.009
23. Ahn JH, Kim J, Hong SP, et al. Nasal ciliated cells are primary targets for SARS-CoV-2 replication in the early stage of COVID-19. *J Clin Invest*. 2021;131(13):e148517, 148517. doi:10.1172/JCI148517
24. Gallagher T, McCray PB. The first few days of a SARS-CoV-2 infection viewed at single-cell resolution. *PLoS Biol*. 2021;19(4):e3001217. doi:10.1371/journal.pbio.3001217
25. Hoffmann M, Kleine-Weber H, Schroeder S, et al. SARS-CoV-2 Cell Entry Depends on ACE2 and TMPRSS2 and Is Blocked by a Clinically Proven Protease Inhibitor. *Cell*. 2020;181(2):271-280.e8. doi:10.1016/j.cell.2020.02.052
26. Örd M, Faustova I, Loog M. The sequence at Spike S1/S2 site enables cleavage by furin and phospho-regulation in SARS-CoV2 but not in SARS-CoV1 or MERS-CoV. *Sci Rep*. 2020;10(1):16944. doi:10.1038/s41598-020-74101-0
27. Chen Y, Zhang YN, Yan R, et al. ACE2-targeting monoclonal antibody as potent and broad-spectrum coronavirus blocker. *Sig Transduct Target Ther*. 2021;6(1):315. doi:10.1038/s41392-021-00740-y
28. Krishnamurthy S, Lockey RF, Kolliputi N. Soluble ACE2 as a potential therapy for COVID-19. *American Journal of Physiology-Cell Physiology*. 2021;320(3):C279-C281. doi:10.1152/ajpcell.00478.2020
29. Hernández-Mitre MP, Morpeth SC, Venkatesh B, et al. TMPRSS2 inhibitors for the treatment of COVID-19 in adults: a systematic review and meta-analysis of randomized clinical trials of nafamostat and camostat mesylate. *Clinical Microbiology and Infection*. 2024;30(6):743-754. doi:10.1016/j.cmi.2024.01.029

30. Cantuti-Castelvetri L, Ojha R, Pedro LD, et al. Neuropilin-1 facilitates SARS-CoV-2 cell entry and infectivity. *Science*. 2020;370(6518):856-860. doi:10.1126/science.abd2985
31. Han B, Lv Y, Moser D, et al. ACE2-independent SARS-CoV-2 virus entry through cell surface GRP78 on monocytes – evidence from a translational clinical and experimental approach. *eBioMedicine*. 2023;98:104869. doi:10.1016/j.ebiom.2023.104869
32. Stein SR, Ramelli SC, Grazioli A, et al. SARS-CoV-2 infection and persistence in the human body and brain at autopsy. *Nature*. 2022;612(7941):758-763. doi:10.1038/s41586-022-05542-y
33. Setaro AC, Gaglia MM. All hands on deck: SARS-CoV-2 proteins that block early anti-viral interferon responses. *Current Research in Virological Science*. 2021;2:100015. doi:10.1016/j.crviro.2021.100015
34. Bastard P, Rosen LB, Zhang Q, et al. Autoantibodies against type I IFNs in patients with life-threatening COVID-19. *Science*. 2020;370(6515):eabd4585. doi:10.1126/science.abd4585
35. Zhang Q, Bastard P, Liu Z, et al. Inborn errors of type I IFN immunity in patients with life-threatening COVID-19. *Science*. 2020;370(6515):eabd4570. doi:10.1126/science.abd4570
36. Amicone M, Borges V, Alves MJ, et al. Mutation rate of SARS-CoV-2 and emergence of mutators during experimental evolution. *Evolution, Medicine, and Public Health*. 2022;10(1):142-155. doi:10.1093/emph/eoac010
37. Markov PV, Ghafari M, Beer M, et al. The evolution of SARS-CoV-2. *Nat Rev Microbiol*. 2023;21(6):361-379. doi:10.1038/s41579-023-00878-2
38. Tegally H, Wilkinson E, Giovanetti M, et al. Detection of a SARS-CoV-2 variant of concern in South Africa. *Nature*. 2021;592(7854):438-443. doi:10.1038/s41586-021-03402-9
39. Faria NR, Mellan TA, Whittaker C, et al. Genomics and epidemiology of the P.1 SARS-CoV-2 lineage in Manaus, Brazil. *Science*. 2021;372(6544):815-821. doi:10.1126/science.abh2644
40. Hill V, Du Plessis L, Peacock TP, et al. The origins and molecular evolution of SARS-CoV-2 lineage B.1.1.7 in the UK. *Virus Evolution*. 2022;8(2):veac080. doi:10.1093/ve/veac080
41. McCrone JT, Hill V, Bajaj S, et al. Context-specific emergence and growth of the SARS-CoV-2 Delta variant. *Nature*. 2022;610(7930):154-160. doi:10.1038/s41586-022-05200-3
42. Jangra S, Ye C, Rathnasinghe R, et al. SARS-CoV-2 spike E484K mutation reduces antibody neutralisation. *The Lancet Microbe*. 2021;2(7):e283-e284. doi:10.1016/S2666-5247(21)00068-9
43. Liu Y, Rocklöv J. The reproductive number of the Delta variant of SARS-CoV-2 is far higher compared to the ancestral SARS-CoV-2 virus. *Journal of Travel Medicine*. 2021;28(7):taab124. doi:10.1093/jtm/taab124
44. Meng B, Kemp SA, Papa G, et al. Recurrent emergence of SARS-CoV-2 spike deletion H69/V70 and its role in the Alpha variant B.1.1.7. *Cell Reports*. 2021;35(13):109292. doi:10.1016/j.celrep.2021.109292
45. Wang P, Nair MS, Liu L, et al. Antibody resistance of SARS-CoV-2 variants B.1.351 and B.1.1.7. *Nature*. 2021;593(7857):130-135. doi:10.1038/s41586-021-03398-2
46. Tian F, Tong B, Sun L, et al. N501Y mutation of spike protein in SARS-CoV-2 strengthens its binding to receptor ACE2. *eLife*. 2021;10:e69091. doi:10.7554/eLife.69091
47. Wibmer CK, Ayres F, Hermanus T, et al. SARS-CoV-2 501Y.V2 escapes neutralization by South African COVID-19 donor plasma. *Nat Med*. 2021;27(4):622-625. doi:10.1038/s41591-021-01285-x
48. Funk T, Pharris A, Spiteri G, et al. Characteristics of SARS-CoV-2 variants of concern B.1.1.7, B.1.351 or P.1: data from seven EU/EEA countries, weeks 38/2020 to 10/2021. *Eurosurveillance*. 2021;26(16). doi:10.2807/1560-7917.ES.2021.26.16.2100348
49. Harrigan SP, Velásquez García HA, Abdia Y, et al. The Clinical Severity of COVID-19 Variants of Concern: Retrospective Population-Based Analysis. *JMIR Public Health Surveill*. 2024;10:e45513. doi:10.2196/45513
50. Tegally H, Moir M, Everatt J, et al. Emergence of SARS-CoV-2 Omicron lineages BA.4 and BA.5 in South Africa. *Nat Med*. 2022;28(9):1785-1790. doi:10.1038/s41591-022-01911-2
51. Viana R, Moyo S, Amoako DG, et al. Rapid epidemic expansion of the SARS-CoV-2 Omicron variant in southern Africa. *Nature*. 2022;603(7902):679-686. doi:10.1038/s41586-022-04411-y
52. He X, Hong W, Pan X, Lu G, Wei X. SARS-CoV-2 Omicron variant: Characteristics and prevention. *MedComm*. 2021;2(4):838-845. doi:10.1002/mco2.110
53. Willett BJ, Grove J, MacLean OA, et al. SARS-CoV-2 Omicron is an immune escape variant with an altered cell entry pathway. *Nat Microbiol*. 2022;7(8):1161-1179. doi:10.1038/s41564-022-01143-7
54. Foster TL, Wilson H, Iyer SS, et al. Resistance of Transmitted Founder HIV-1 to IFITM-Mediated Restriction. *Cell Host & Microbe*. 2016;20(4):429-442. doi:10.1016/j.chom.2016.08.006
55. Mesner D, Reuschl AK, Whelan MVX, et al. SARS-CoV-2 evolution influences GBP and IFITM sensitivity. *Proc Natl Acad Sci USA*. 2023;120(5):e2212577120. doi:10.1073/pnas.2212577120
56. Domingo P, Mur I, Pomar V, Corominas H, Casademont J, de Benito N. The four horsemen of a viral Apocalypse: The pathogenesis of SARS-CoV-2 infection (COVID-19). *EBioMedicine*. 2020;58:102887. doi:10.1016/j.ebiom.2020.102887
57. Schneider WM, Chevillotte MD, Rice CM. Interferon-stimulated genes: a complex web of host defenses. *Annu Rev Immunol*. 2014;32:513-545. doi:10.1146/annurev-immunol-032713-120231
58. Sadler AJ, Williams BRG. Interferon-inducible antiviral effectors. *Nat Rev Immunol*. 2008;8(7):559-568. doi:10.1038/nri2314
59. Kochs G, Haller O. Interferon-induced human MxA GTPase blocks nuclear import of Thogoto virus nucleocapsids. *Proc Natl Acad Sci USA*. 1999;96(5):2082-2086. doi:10.1073/pnas.96.5.2082

60. Accola MA, Huang B, Al Masri A, McNiven MA. The Antiviral Dynamin Family Member, MxA, Tubulates Lipids and Localizes to the Smooth Endoplasmic Reticulum. *Journal of Biological Chemistry*. 2002;277(24):21829-21835. doi:10.1074/jbc.M201641200
61. Donovan J, Dufner M, Korennykh A. Structural basis for cytosolic double-stranded RNA surveillance by human oligoadenylate synthetase 1. *Proc Natl Acad Sci USA*. 2013;110(5):1652-1657. doi:10.1073/pnas.1218528110
62. Giannakopoulos NV, Luo JK, Papov V, et al. Proteomic identification of proteins conjugated to ISG15 in mouse and human cells. *Biochemical and Biophysical Research Communications*. 2005;336(2):496-506. doi:10.1016/j.bbrc.2005.08.132
63. Zhao C, Denison C, Huibregtse JM, Gygi S, Krug RM. Human ISG15 conjugation targets both IFN-induced and constitutively expressed proteins functioning in diverse cellular pathways. *Proc Natl Acad Sci USA*. 2005;102(29):10200-10205. doi:10.1073/pnas.0504754102
64. Takeuchi T, Yokosawa H. Detection and Analysis of Protein ISGylation. In: Kannicht C, ed. *Post-Translational Modifi Cations of Proteins*. Vol 446. Methods in Molecular Biology™. Humana Press; 2008:139-149. doi:10.1007/978-1-60327-084-7_10
65. Desai SD, Haas AL, Wood LM, et al. Elevated Expression of ISG15 in Tumor Cells Interferes with the Ubiquitin/26S Proteasome Pathway. *Cancer Research*. 2006;66(2):921-928. doi:10.1158/0008-5472.CAN-05-1123
66. Perng YC, Lenschow DJ. ISG15 in antiviral immunity and beyond. *Nat Rev Microbiol*. 2018;16(7):423-439. doi:10.1038/s41579-018-0020-5
67. McKenna K, Beignon AS, Bhardwaj N. Plasmacytoid Dendritic Cells: Linking Innate and Adaptive Immunity. *J Virol*. 2005;79(1):17-27. doi:10.1128/JVI.79.1.17-27.2005
68. Cai C, Pham TNQ, Adam D, Brochiero E, Cohen ÉA. Sensing of SARS-CoV-2-infected cells by plasmacytoid dendritic cells is modulated via an interplay between CD54/ICAM-1 and CD11a/LFA-1 αL integrin. *J Virol*. 2025;99(2):e0123524. doi:10.1128/jvi.01235-24
69. Fitzgeraldbocarsly P, Dai J, Singh S. Plasmacytoid dendritic cells and type I IFN: 50 years of convergent history. *Cytokine & Growth Factor Reviews*. 2008;19(1):3-19. doi:10.1016/j.cytogfr.2007.10.006
70. Bénard A, Jacobsen A, Brunner M, et al. Interleukin-3 is a predictive marker for severity and outcome during SARS-CoV-2 infections. *Nat Commun*. 2021;12(1):1112. doi:10.1038/s41467-021-21310-4
71. Kreutmair S, Unger S, Núñez NG, et al. Distinct immunological signatures discriminate severe COVID-19 from non-SARS-CoV-2-driven critical pneumonia. *Immunity*. 2021;54(7):1578-1593.e5. doi:10.1016/j.immuni.2021.05.002
72. Severa M, Diotti RA, Etna MP, et al. Differential plasmacytoid dendritic cell phenotype and type I Interferon response in asymptomatic and severe COVID-19 infection. Diamond MS, ed. *PLoS Pathog*. 2021;17(9):e1009878. doi:10.1371/journal.ppat.1009878
73. Van Der Sluis RM, Cham LB, Gris-Oliver A, et al. TLR2 and TLR7 mediate distinct immunopathological and antiviral plasmacytoid dendritic cell responses to SARS-CoV-2 infection. *The EMBO Journal*. 2022;41(10):e109622. doi:10.15252/embj.2021109622
74. Van der Sluis RM, Holm CK, Jakobsen MR. Plasmacytoid dendritic cells during COVID-19: Ally or adversary? *Cell Rep*. 2022;40(4):111148. doi:10.1016/j.celrep.2022.111148
75. Carvalho T, Krammer F, Iwasaki A. The first 12 months of COVID-19: a timeline of immunological insights. *Nat Rev Immunol*. 2021;21(4):245-256. doi:10.1038/s41577-021-00522-1
76. Sposito B, Broggi A, Pandolfi L, et al. The interferon landscape along the respiratory tract impacts the severity of COVID-19. *Cell*. 2021;184(19):4953-4968.e16. doi:10.1016/j.cell.2021.08.016
77. Wack A. Monocyte and dendritic cell defects in COVID-19. *Nat Cell Biol*. 2021;23(5):445-447. doi:10.1038/s41556-021-00685-y
78. Grant RA, Morales-Nebreda L, Markov NS, et al. Circuits between infected macrophages and T cells in SARS-CoV-2 pneumonia. *Nature*. 2021;590(7847):635-641. doi:10.1038/s41586-020-03148-w
79. Chaintreuil P, Kerreneur E, Bourgoin M, et al. The generation, activation, and polarization of monocyte-derived macrophages in human malignancies. *Front Immunol*. 2023;14:1178337. doi:10.3389/fimmu.2023.1178337
80. Simón-Fuentes M, Ríos I, Herrero C, et al. MAFB shapes human monocyte–derived macrophage response to SARS-CoV-2 and controls severe COVID-19 biomarker expression. *JCI Insight*. 2023;8(24):e172862. doi:10.1172/jci.insight.172862
81. Knoll R, Schultze JL, Schulte-Schrepping J. Monocytes and Macrophages in COVID-19. *Front Immunol*. 2021;12:720109. doi:10.3389/fimmu.2021.720109
82. Meisel SR, Xu XP, Edgington TS, et al. Differentiation of adherent human monocytes into macrophages markedly enhances tissue factor protein expression and procoagulant activity. *Atherosclerosis*. 2002;161(1):35-43. doi:10.1016/S0021-9150(01)00616-5
83. Sachetto ATA, Mackman N. Tissue Factor and COVID-19: An Update. *CDT*. 2022;23(17):1573-1577. doi:10.2174/1389450123666220926144432
84. Neupane AS, Willson M, Chojnacki AK, et al. Patrolling Alveolar Macrophages Conceal Bacteria from the Immune System to Maintain Homeostasis. *Cell*. 2020;183(1):110-125.e11. doi:10.1016/j.cell.2020.08.020
85. Castanheira FVS, Kubes P. Neutrophils and NETs in modulating acute and chronic inflammation. *Blood*. 2019;133(20):2178-2185. doi:10.1182/blood-2018-11-844530
86. Peñaloza HF, Lee JS, Ray P. Neutrophils and lymphopenia, an unknown axis in severe COVID-19 disease. Morrison TE, ed. *PLoS Pathog*. 2021;17(9):e1009850. doi:10.1371/journal.ppat.1009850

87. Yang SC, Tsai YF, Pan YL, Hwang TL. Understanding the role of neutrophils in acute respiratory distress syndrome. *Biomedical Journal*. 2021;44(4):439-446. doi:10.1016/j.bj.2020.09.001
88. Zuo Y, Yalavarthi S, Shi H, et al. Neutrophil extracellular traps in COVID-19. *JCI Insight*. Published online April 24, 2020. doi:10.1172/jci.insight.138999
89. Ackermann M, Anders HJ, Bilyy R, et al. Patients with COVID-19: in the dark-NETs of neutrophils. *Cell Death Differ*. 2021;28(11):3125-3139. doi:10.1038/s41418-021-00805-z
90. Schulte-Schrepping J, Reusch N, Paclik D, et al. Severe COVID-19 Is Marked by a Dysregulated Myeloid Cell Compartment. *Cell*. 2020;182(6):1419-1440.e23. doi:10.1016/j.cell.2020.08.001
91. Youn JI, Gabrilovich DI. The biology of myeloid-derived suppressor cells: the blessing and the curse of morphological and functional heterogeneity. *Eur J Immunol*. 2010;40(11):2969-2975. doi:10.1002/eji.201040895
92. Liu Y, Du X, Chen J, et al. Neutrophil-to-lymphocyte ratio as an independent risk factor for mortality in hospitalized patients with COVID-19. *Journal of Infection*. 2020;81(1):e6-e12. doi:10.1016/j.jinf.2020.04.002
93. Blanco-Melo D, Nilsson-Payant BE, Liu WC, et al. Imbalanced Host Response to SARS-CoV-2 Drives Development of COVID-19. *Cell*. 2020;181(5):1036-1045.e9. doi:10.1016/j.cell.2020.04.026
94. Da Silva RP, Gonçalves JIB, Zanin RF, Schuch FB, De Souza APD. Circulating Type I Interferon Levels and COVID-19 Severity: A Systematic Review and Meta-Analysis. *Front Immunol*. 2021;12:657363. doi:10.3389/fimmu.2021.657363
95. Park A, Iwasaki A. Type I and Type III Interferons – Induction, Signaling, Evasion, and Application to Combat COVID-19. *Cell Host & Microbe*. 2020;27(6):870-878. doi:10.1016/j.chom.2020.05.008
96. Schultze JL, Aschenbrenner AC. COVID-19 and the human innate immune system. *Cell*. 2021;184(7):1671-1692. doi:10.1016/j.cell.2021.02.029
97. Acharya D, Liu G, Gack MU. Dysregulation of type I interferon responses in COVID-19. *Nat Rev Immunol*. 2020;20(7):397-398. doi:10.1038/s41577-020-0346-x
98. Brewer RC, Robinson WH, Lanz TV. SARS-CoV-2 infection of monocytes: balancing acts of antibodies and inflammasomes. *Sig Transduct Target Ther*. 2022;7(1):250. doi:10.1038/s41392-022-01112-w
99. Zanza C, Romenskaya T, Manetti A, et al. Cytokine Storm in COVID-19: Immunopathogenesis and Therapy. *Medicina*. 2022;58(2):144. doi:10.3390/medicina58020144
100. Liu JM, Chi J. Is COVID-19-associated cytokine storm distinct from non-COVID-19 secondary hemophagocytic lymphohistiocytosis? *Exp Biol Med (Maywood)*. 2022;247(4):330-337. doi:10.1177/15353702211068840
101. Ferrara JL, Abhyankar S, Gilliland DG. Cytokine storm of graft-versus-host disease: a critical effector role for interleukin-1. *Transplant Proc*. 1993;25(1 Pt 2):1216-1217.
102. Pechous RD, Sivaraman V, Price PA, Stasulli NM, Goldman WE. Early host cell targets of Yersinia pestis during primary pneumonic plague. *PLoS Pathog*. 2013;9(10):e1003679. doi:10.1371/journal.ppat.1003679
103. Kash JC, Tumpey TM, Proll SC, et al. Genomic analysis of increased host immune and cell death responses induced by 1918 influenza virus. *Nature*. 2006;443(7111):578-581. doi:10.1038/nature05181
104. Morris G, Bortolasci CC, Puri BK, et al. The cytokine storms of COVID-19, H1N1 influenza, CRS and MAS compared. Can one sized treatment fit all? *Cytokine*. 2021;144:155593. doi:10.1016/j.cyto.2021.155593
105. Khan S, Shafiei MS, Longoria C, Schoggins JW, Savani RC, Zaki H. SARS-CoV-2 spike protein induces inflammation via TLR2-dependent activation of the NF-κB pathway. *eLife*. 2021;10:e68563. doi:10.7554/eLife.68563
106. Milani D, Caruso L, Zauli E, et al. p53/NF-kB Balance in SARS-CoV-2 Infection: From OMICs, Genomics and Pharmacogenomics Insights to Tailored Therapeutic Perspectives (COVIDomics). *Front Pharmacol*. 2022;13:871583. doi:10.3389/fphar.2022.871583
107. Niu C, Liang T, Chen Y, et al. SARS-CoV-2 spike protein induces the cytokine release syndrome by stimulating T cells to produce more IL-2. *Front Immunol*. 2024;15:1444643. doi:10.3389/fimmu.2024.1444643
108. Negron S, Kessinger C, Lin Z. Expressing a truncated SARS-COV-2 spike protein in mouse heart induces cardiac hypertrophy. *European Heart Journal*. 2021;42(Supplement_1):ehab724.3287. doi:10.1093/eurheartj/ehab724.3287
109. Gori Savellini G, Anichini G, Gandolfo C, Cusi MG. Nucleopore Traffic Is Hindered by SARS-CoV-2 ORF6 Protein to Efficiently Suppress IFN-β and IL-6 Secretion. *Viruses*. 2022;14(6):1273. doi:10.3390/v14061273
110. Li TW, Kenney AD, Park JG, et al. SARS-CoV-2 Nsp14 protein associates with IMPDH2 and activates NF-κB signaling. *Front Immunol*. 2022;13:1007089. doi:10.3389/fimmu.2022.1007089
111. Rashid F, Xie Z, Suleman M, Shah A, Khan S, Luo S. Roles and functions of SARS-CoV-2 proteins in host immune evasion. *Front Immunol*. 2022;13:940756. doi:10.3389/fimmu.2022.940756
112. Xie S, Song Z, Chen R, et al. The SARS-unique domain (SUD) of SARS-CoV-2 nsp3 protein inhibits the antiviral immune responses through the NF-κB pathway. *Journal of Medical Virology*. 2024;96(10):e70007. doi:10.1002/jmv.70007
113. Dhiman M, Thakur S, Upadhyay S, Kaur A, Mantha AK. Oxidative Stress and Inflammation in Cardiovascular Diseases: Two Sides of the Same Coin. In: Rani V, Yadav UCS, eds. *Free Radicals in Human Health and Disease*. Springer India; 2015:259-278. doi:10.1007/978-81-322-2035-0_17
114. Newsholme P, Cruzat VF, Keane KN, Carlessi R, De Bittencourt PIH. Molecular mechanisms of ROS production and oxidative stress in diabetes. *Biochemical Journal*. 2016;473(24):4527-4550. doi:10.1042/BCJ20160503C
115. Nan J, Wang Y, Yang J, Stark GR. IRF9 and unphosphorylated STAT2 cooperate with NF-κB to drive IL6 expression. *Proc Natl Acad Sci USA*. 2018;115(15):3906-3911. doi:10.1073/pnas.1714102115
116. Prezioso C, Limongi D, Checconi P, et al. Role of miR-9 in Modulating NF-κB Signaling and Cytokine Expression in COVID-19 Patients. *IJMS*. 2024;25(16):8930. doi:10.3390/ijms25168930
117. Yan J, McCombe PA, Pender MP, Greer JM. Reduced IκB-α Protein Levels in Peripheral Blood Cells of Patients with Multiple Sclerosis—A Possible Cause of Constitutive NF-κB Activation. *JCM*. 2020;9(8):2534. doi:10.3390/jcm9082534

118. Paik S, Kim JK, Silwal P, Sasakawa C, Jo EK. An update on the regulatory mechanisms of NLRP3 inflammasome activation. *Cell Mol Immunol*. 2021;18(5):1141-1160. doi:10.1038/s41423-021-00670-3
119. Subramaniam S, Kothari H, Bosmann M. Tissue factor in COVID-19-associated coagulopathy. *Thrombosis Research*. 2022;220:35-47. doi:10.1016/j.thromres.2022.09.025
120. Kang S, Kishimoto T. Interplay between interleukin-6 signaling and the vascular endothelium in cytokine storms. *Exp Mol Med*. 2021;53(7):1116-1123. doi:10.1038/s12276-021-00649-0
121. Thomson EM, Williams A, Yauk CL, Vincent R. Overexpression of Tumor Necrosis Factor-α in the Lungs Alters Immune Response, Matrix Remodeling, and Repair and Maintenance Pathways. *The American Journal of Pathology*. 2012;180(4):1413-1430. doi:10.1016/j.ajpath.2011.12.020
122. Zhou Z, Xu MJ, Gao B. Hepatocytes: a key cell type for innate immunity. *Cell Mol Immunol*. 2016;13(3):301-315. doi:10.1038/cmi.2015.97
123. Thomas MR, Scully M. Clinical features of thrombosis and bleeding in COVID-19. *Blood*. 2022;140(3):184-195. doi:10.1182/blood.2021012247
124. Gerber GF, Chaturvedi S. How to recognize and manage COVID-19-associated coagulopathy. *Hematology Am Soc Hematol Educ Program*. 2021;2021(1):614-620. doi:10.1182/hematology.2021000297
125. Manolis AS, Manolis TA, Manolis AA, Papatheou D, Melita H. COVID-19 Infection: Viral Macro- and Micro-Vascular Coagulopathy and Thromboembolism/Prophylactic and Therapeutic Management. *J Cardiovasc Pharmacol Ther*. 2021;26(1):12-24. doi:10.1177/1074248420958973
126. Flaumenhaft R, Enjyoji K, Schmaier AA. Vasculopathy in COVID-19. *Blood*. 2022;140(3):222-235. doi:10.1182/blood.2021012250
127. Zhang J, Tecson KM, McCullough PA. Endothelial dysfunction contributes to COVID-19-associated vascular inflammation and coagulopathy. *Rev Cardiovasc Med*. 2020;21(3):315. doi:10.31083/j.rcm.2020.03.126
128. Plášek J, Gumulec J, Máca J, et al. COVID-19 associated coagulopathy: Mechanisms and host-directed treatment. *The American Journal of the Medical Sciences*. 2022;363(6):465-475. doi:10.1016/j.amjms.2021.10.012
129. Bhatnagar J, Gary J, Reagan-Steiner S, et al. Evidence of Severe Acute Respiratory Syndrome Coronavirus 2 Replication and Tropism in the Lungs, Airways, and Vascular Endothelium of Patients With Fatal Coronavirus Disease 2019: An Autopsy Case Series. *The Journal of Infectious Diseases*. 2021;223(5):752-764. doi:10.1093/infdis/jiab039
130. Bryce C, Grimes Z, Pujadas E, et al. Pathophysiology of SARS-CoV-2: the Mount Sinai COVID-19 autopsy experience. *Modern Pathology*. 2021;34(8):1456-1467. doi:10.1038/s41379-021-00793-y
131. Bgatova N, Savchenko S, Lamanov A, et al. Intracellular organelles remodeling in myocardial endotheliocytes in COVID-19: an autopsy-based study. *Ultrastructural Pathology*. 2024;48(1):66-74. doi:10.1080/01913123.2023.2286977
132. Bussani R, Porcari A, Pinamonti M, et al. Lung damage in SARS - CoV -2 patients: An autopsy study in the era of vaccination. *Eur J Clin Investigation*. 2025;55(1):e14325. doi:10.1111/eci.14325
133. Esmon CT. Possible involvement of cytokines in diffuse intravascular coagulation and thrombosis. *Best Practice & Research Clinical Haematology*. 1999;12(3):343-359. doi:10.1053/beha.1999.0029
134. Nan B, Lin P, Lumsden AB, Yao Q, Chen C. Effects of TNF-α and curcumin on the expression of thrombomodulin and endothelial protein C receptor in human endothelial cells. *Thrombosis Research*. 2005;115(5):417-426. doi:10.1016/j.thromres.2004.10.010
135. Menschikowski M, Hagelgans A, Eisenhofer G, Siegert G. Regulation of endothelial protein C receptor shedding by cytokines is mediated through differential activation of MAP kinase signaling pathways. *Experimental Cell Research*. 2009;315(15):2673-2682. doi:10.1016/j.yexcr.2009.05.015
136. McConnell MJ, Kawaguchi N, Kondo R, et al. Liver injury in COVID-19 and IL-6 trans-signaling-induced endotheliopathy. *Journal of Hepatology*. 2021;75(3):647-658. doi:10.1016/j.jhep.2021.04.050
137. Obermayer A, Jakob LM, Haslbauer JD, Matter MS, Tzankov A, Stoiber W. Neutrophil Extracellular Traps in Fatal COVID-19-Associated Lung Injury. Pichler R, ed. *Disease Markers*. 2021;2021:1-10. doi:10.1155/2021/5566826
138. Meroni PL, Croci S, Lonati PA, et al. Complement activation predicts negative outcomes in COVID-19: The experience from Northen Italian patients. *Autoimmunity Reviews*. 2023;22(1):103232. doi:10.1016/j.autrev.2022.103232
139. Skendros P, Mitsios A, Chrysanthopoulou A, et al. Complement and tissue factor–enriched neutrophil extracellular traps are key drivers in COVID-19 immunothrombosis. *Journal of Clinical Investigation*. 2020;130(11):6151-6157. doi:10.1172/JCI141374
140. Barratt-Due A, Pettersen K, Børresdatter-Dahl T, et al. Escalated complement activation during hospitalization is associated with higher risk of 60-day mortality in SARS-CoV-2-infected patients. *J Intern Med*. 2024;296(1):80-92. doi:10.1111/joim.13783
141. Gebetsberger L, Malekshahi Z, Teutsch A, et al. SARS-CoV-2 hijacks host CD55, CD59 and factor H to impair antibody-dependent complement-mediated lysis. *Emerging Microbes & Infections*. 2024;13(1):2417868. doi:10.1080/22221751.2024.2417868
142. Baillie K, Davies HE, Keat SBK, et al. Complement dysregulation is a predictive and therapeutically amenable feature of long COVID. *Infectious Diseases (except HIV/AIDS)*. Preprint posted online October 28, 2023. doi:10.1101/2023.10.26.23297597
143. Cervia-Hasler C, Brüningk SC, Hoch T, et al. Persistent complement dysregulation with signs of thromboinflammation in active Long Covid. *Science*. 2024;383(6680):eadg7942. doi:10.1126/science.adg7942
144. Farztdinov V, Zühlke B, Sotzny F, et al. Role of the complement system in Long COVID. *Respiratory Medicine*. Preprint posted online March 18, 2024. doi:10.1101/2024.03.14.24304224

145. Ackermann M, Verleden SE, Kuehnel M, et al. Pulmonary Vascular Endothelialitis, Thrombosis, and Angiogenesis in Covid-19. *N Engl J Med*. 2020;383(2):120-128. doi:10.1056/NEJMoa2015432
146. Pellegrini D, Kawakami R, Guagliumi G, et al. Microthrombi as a Major Cause of Cardiac Injury in COVID-19: A Pathologic Study. *Circulation*. 2021;143(10):1031-1042. doi:10.1161/CIRCULATIONAHA.120.051828
147. Henry BM, Sinkovits G, Szergyuk I, et al. Complement Levels at Admission Reflecting Progression to Severe Acute Kidney Injury (AKI) in Coronavirus Disease 2019 (COVID-19): A Multicenter Prospective Cohort Study. *Front Med*. 2022;9:796109. doi:10.3389/fmed.2022.796109
148. Meaney JFM, O'Donnell JS, Bridgewood C, Harbison J, McGonagle D. Perspective: The Case for Acute Large Vessel Ischemic Stroke in COVID-19 Originating Within Thrombosed Pulmonary Venules. *Stroke*. 2022;53(7):2411-2419. doi:10.1161/STROKEAHA.121.038056
149. Giavedoni P, Podlipnik S, Pericàs JM, et al. Skin Manifestations in COVID-19: Prevalence and Relationship with Disease Severity. *JCM*. 2020;9(10):3261. doi:10.3390/jcm9103261
150. Minkoff JM, tenOever B. Innate immune evasion strategies of SARS-CoV-2. *Nat Rev Microbiol*. Published online January 11, 2023. doi:10.1038/s41579-022-00839-1
151. Schubert K, Karousis ED, Jomaa A, et al. SARS-CoV-2 Nsp1 binds the ribosomal mRNA channel to inhibit translation. *Nat Struct Mol Biol*. 2020;27(10):959-966. doi:10.1038/s41594-020-0511-8
152. Anastasakis DG, Benhalevy D, Çuburu N, Altan-Bonnet N, Hafner M. Epigenetic repression of antiviral genes by SARS-CoV-2 NSP1. Liu HM, ed. *PLoS ONE*. 2024;19(1):e0297262. doi:10.1371/journal.pone.0297262
153. Shin D, Mukherjee R, Grewe D, et al. Papain-like protease regulates SARS-CoV-2 viral spread and innate immunity. *Nature*. 2020;587(7835):657-662. doi:10.1038/s41586-020-2601-5
154. Cao D, Duan L, Huang B, Xiong Y, Zhang G, Huang H. The SARS-CoV-2 papain-like protease suppresses type I interferon responses by deubiquitinating STING. *Sci Signal*. 2023;16(783):eadd0082. doi:10.1126/scisignal.add0082
155. Vazquez C, Swanson SE, Negatu SG, et al. SARS-CoV-2 viral proteins NSP1 and NSP13 inhibit interferon activation through distinct mechanisms. Jin DY, ed. *PLoS ONE*. 2021;16(6):e0253089. doi:10.1371/journal.pone.0253089
156. Otter CJ, Bracci N, Parenti NA, et al. SARS-CoV-2 nsp15 endoribonuclease antagonizes dsRNA-induced antiviral signaling. *Proc Natl Acad Sci USA*. 2024;121(15):e2320194121. doi:10.1073/pnas.2320194121
157. Deng J, Zheng S, Xiao Y, et al. SARS-CoV-2 NSP8 suppresses type I and III IFN responses by modulating the RIG-I/MDA5, TRIF, and STING signaling pathways. *Journal of Medical Virology*. 2023;95(4):e28680. doi:10.1002/jmv.28680
158. Zhang X, Yang Z, Pan T, et al. SARS-CoV-2 Nsp8 suppresses MDA5 antiviral immune responses by impairing TRIM4-mediated K63-linked polyubiquitination. Gallagher T, ed. *PLoS Pathog*. 2023;19(11):e1011792. doi:10.1371/journal.ppat.1011792
159. Lundrigan E, Toudic C, Pennock E, Pezacki JP. SARS-CoV-2 Protein Nsp9 Is Involved in Viral Evasion through Interactions with Innate Immune Pathways. *ACS Omega*. 2024;9(24):26428-26438. doi:10.1021/acsomega.4c02631
160. Maddaloni L, Santinelli L, Bugani G, et al. Differential expression of Type I interferon and inflammatory genes in SARS-CoV-2-infected patients treated with monoclonal antibodies. *Immunity Inflam & Disease*. 2023;11(10):e968. doi:10.1002/iid3.968
161. Miorin L, Kehrer T, Sanchez-Aparicio MT, et al. SARS-CoV-2 Orf6 hijacks Nup98 to block STAT nuclear import and antagonize interferon signaling. *Proc Natl Acad Sci USA*. 2020;117(45):28344-28354. doi:10.1073/pnas.2016650117
162. Lu Y, Michel HA, Wang PH, Smith GL. Manipulation of innate immune signaling pathways by SARS-CoV-2 non-structural proteins. *Front Microbiol*. 2022;13:1027015. doi:10.3389/fmicb.2022.1027015
163. Rashid F, Dzakah EE, Wang H, Tang S. The ORF8 protein of SARS-CoV-2 induced endoplasmic reticulum stress and mediated immune evasion by antagonizing production of interferon beta. *Virus Research*. 2021;296:198350. doi:10.1016/j.virusres.2021.198350
164. Shemesh M, Aktepe TE, Deerain JM, et al. SARS-CoV-2 suppresses IFNβ production mediated by NSP1, 5, 6, 15, ORF6 and ORF7b but does not suppress the effects of added interferon. Pekosz A, ed. *PLoS Pathog*. 2021;17(8):e1009800. doi:10.1371/journal.ppat.1009800
165. Wang R, Yang X, Chang M, et al. ORF3a Protein of Severe Acute Respiratory Syndrome Coronavirus 2 Inhibits Interferon-Activated Janus Kinase/Signal Transducer and Activator of Transcription Signaling via Elevating Suppressor of Cytokine Signaling 1. *Front Microbiol*. 2021;12:752597. doi:10.3389/fmicb.2021.752597
166. Stewart H, Lu Y, O'Keefe S, et al. The SARS-CoV-2 protein ORF3c is a mitochondrial modulator of innate immunity. *iScience*. 2023;26(11):108080. doi:10.1016/j.isci.2023.108080
167. Dominguez Andres A, Feng Y, Campos AR, et al. SARS-CoV-2 ORF9c Is a Membrane-Associated Protein that Suppresses Antiviral Responses in Cells. *Bioinformatics*. Preprint posted online August 19, 2020. doi:10.1101/2020.08.18.256776
168. Ayinde KS, Pinheiro GMS, Ramos CHI. Binding of SARS-CoV-2 protein ORF9b to mitochondrial translocase TOM70 prevents its interaction with chaperone HSP90. *Biochimie*. 2022;200:99-106. doi:10.1016/j.biochi.2022.05.016
169. Han L, Zheng Y, Deng J, et al. SARS-CoV-2 ORF10 antagonizes STING-dependent interferon activation and autophagy. *Journal of Medical Virology*. 2022;94(11):5174-5188. doi:10.1002/jmv.27965
170. Zheng Y, Zhuang MW, Han L, et al. Severe acute respiratory syndrome coronavirus 2 (SARS-CoV-2) membrane (M) protein inhibits type I and III interferon production by targeting RIG-I/MDA-5 signaling. *Sig Transduct Target Ther*. 2020;5(1):299. doi:10.1038/s41392-020-00438-7
171. Pan P, Shen M, Yu Z, et al. SARS-CoV-2 N protein promotes NLRP3 inflammasome activation to induce hyperinflammation. *Nat Commun*. 2021;12(1):4664. doi:10.1038/s41467-021-25015-6

172. Zhang Y, Sun H, Pei R, et al. The SARS-CoV-2 protein ORF3a inhibits fusion of autophagosomes with lysosomes. *Cell Discov*. 2021;7(1):31. doi:10.1038/s41421-021-00268-z
173. Zhang C, Jiang Q, Liu Z, et al. SARS-CoV-2 NSP6 reduces autophagosome size and affects viral replication via sigma-1 receptor. Gallagher T, ed. *J Virol*. 2024;98(11):e00754-24. doi:10.1128/jvi.00754-24
174. Lee MJ, Leong MW, Rustagi A, et al. SARS-CoV-2 escapes direct NK cell killing through Nsp1-mediated downregulation of ligands for NKG2D. *Cell Reports*. 2022;41(13):111892. doi:10.1016/j.celrep.2022.111892
175. Hartmann JA, Cardoso MR, Talarico MCR, et al. Evasion of NKG2D-mediated cytotoxic immunity by sarbecoviruses. *Cell*. 2024;187(10):2393-2410.e14. doi:10.1016/j.cell.2024.03.026
176. Van Der Made CI, Simons A, Schuurs-Hoeijmakers J, et al. Presence of Genetic Variants Among Young Men With Severe COVID-19. *JAMA*. 2020;324(7):663. doi:10.1001/jama.2020.13719
177. Baral P, Bhattarai N, Hossen ML, et al. Mutation-induced changes in the receptor-binding interface of the SARS-CoV-2 Delta variant B.1.617.2 and implications for immune evasion. *Biochemical and Biophysical Research Communications*. 2021;574:14-19. doi:10.1016/j.bbrc.2021.08.036
178. Hossain A, Akter S, Rashid AA, Khair S, Alam ASMRU. Unique mutations in SARS-CoV-2 Omicron subvariants' non-spike proteins: Potential impacts on viral pathogenesis and host immune evasion. *Microbial Pathogenesis*. 2022;170:105699. doi:10.1016/j.micpath.2022.105699
179. Nchioua R, Schundner A, Klute S, et al. Reduced replication but increased interferon resistance of SARS-CoV-2 Omicron BA.1. *Life Sci Alliance*. 2023;6(6):e202201745. doi:10.26508/lsa.202201745
180. Reuschl AK, Thorne LG, Whelan MVX, et al. Evolution of enhanced innate immune suppression by SARS-CoV-2 Omicron subvariants. *Nat Microbiol*. 2024;9(2):451-463. doi:10.1038/s41564-023-01588-4
181. Thaweethai T, Jolley SE, Karlson EW, et al. Development of a Definition of Postacute Sequelae of SARS-CoV-2 Infection. *JAMA*. 2023;329(22):1934. doi:10.1001/jama.2023.8823
182. Morroy G, Keijmel SP, Delsing CE, et al. Fatigue following Acute Q-Fever: A Systematic Literature Review. Samuel JE, ed. *PLoS ONE*. 2016;11(5):e0155884. doi:10.1371/journal.pone.0155884
183. Hung TM, Wills B, Clapham HE, Yacoub S, Turner HC. The Uncertainty Surrounding the Burden of Post-acute Consequences of Dengue Infection. *Trends in Parasitology*. 2019;35(9):673-676. doi:10.1016/j.pt.2019.06.004
184. Carod-Artal FJ. Post-Ebolavirus disease syndrome: what do we know? *Expert Review of Anti-infective Therapy*. 2015;13(10):1185-1187. doi:10.1586/14787210.2015.1079128
185. Pricoco R, Meidel P, Hofberger T, et al. One-year follow-up of young people with ME/CFS following infectious mononucleosis by Epstein-Barr virus. *Front Pediatr*. 2024;11:1266738. doi:10.3389/fped.2023.1266738
186. Lam MHB. Mental Morbidities and Chronic Fatigue in Severe Acute Respiratory Syndrome Survivors: Long-term Follow-up. *Arch Intern Med*. 2009;169(22):2142. doi:10.1001/archinternmed.2009.384
187. Katz BZ, Shiraishi Y, Mears CJ, Binns HJ, Taylor R. Chronic Fatigue Syndrome After Infectious Mononucleosis in Adolescents. *Pediatrics*. 2009;124(1):189-193. doi:10.1542/peds.2008-1879
188. Buchwald DS, Rea TD, Katon WJ, Russo JE, Ashley RL. Acute infectious mononucleosis: characteristics of patients who report failure to recover. *The American Journal of Medicine*. 2000;109(7):531-537. doi:10.1016/S0002-9343(00)00560-X
189. Sejvar JJ, Curns AT, Welburg Leonie, et al. Neurocognitive and functional outcomes in persons recovering from West Nile virus illness. *Journal of Neuropsychology*. 2008;2(2):477-499. doi:10.1348/174866407X218312
190. Murray KO, Garcia MN, Rahbar MH, et al. Survival Analysis, Long-Term Outcomes, and Percentage of Recovery up to 8 Years Post-Infection among the Houston West Nile Virus Cohort. Baldanti F, ed. *PLoS ONE*. 2014;9(7):e102953. doi:10.1371/journal.pone.0102953
191. Mandel H, Yoo Y, Allen A, et al. Long COVID incidence in adults and children between 2020 and 2023: a real-world data study from the RECOVER Initiative. *In Review*. Preprint posted online April 26, 2024. doi:10.21203/rs.3.rs-4124710/v1
192. Chen C, Haupert SR, Zimmermann L, Shi X, Fritsche LG, Mukherjee B. Global Prevalence of Post-Coronavirus Disease 2019 (COVID-19) Condition or Long COVID: A Meta-Analysis and Systematic Review. *The Journal of Infectious Diseases*. 2022;226(9):1593-1607. doi:10.1093/infdis/jiac136
193. Hill EL, Mehta HB, Sharma S, et al. Risk factors associated with post-acute sequelae of SARS-CoV-2: an N3C and NIH RECOVER study. *BMC Public Health*. 2023;23(1):2103. doi:10.1186/s12889-023-16916-w
194. Wang L, Foer D, MacPhaul E, Lo YC, Bates DW, Zhou L. PASCLex: A comprehensive post-acute sequelae of COVID-19 (PASC) symptom lexicon derived from electronic health record clinical notes. *Journal of Biomedical Informatics*. 2022;125:103951. doi:10.1016/j.jbi.2021.103951
195. Parker M, Sawant HB, Flannery T, et al. Effect of using a structured pacing protocol on post-exertional symptom exacerbation and health status in a longitudinal cohort with the post-COVID-19 syndrome. *J Med Virol*. 2023;95(1):e28373. doi:10.1002/jmv.28373
196. Eldokla AM, Ali ST. Autonomic function testing in long-COVID syndrome patients with orthostatic intolerance. *Autonomic Neuroscience*. 2022;241:102997. doi:10.1016/j.autneu.2022.102997
197. Arbula S, Pisanu E, Bellavita G, et al. Insights into attention and memory difficulties in post-COVID syndrome using standardized neuropsychological tests and experimental cognitive tasks. *Sci Rep*. 2024;14(1):4405. doi:10.1038/s41598-024-54613-9
198. Yelin D, Ghantous N, Awwad M, et al. Pulmonary diffusing capacity among individuals recovering from mild to moderate COVID-19: a cross-sectional study. *Sci Rep*. 2024;14(1):26767. doi:10.1038/s41598-024-74404-6

199. Brambilla M, Fumoso F, Conti M, et al. Low-Grade Inflammation in Long COVID Syndrome Sustains a Persistent Platelet Activation Associated With Lung Impairment. *JACC: Basic to Translational Science*. 2025;10(1):20-39. doi:10.1016/j.jacbts.2024.09.007
200. Erlandson KM, Geng LN, Selvaggi CA, et al. Differentiation of Prior SARS-CoV-2 Infection and Postacute Sequelae by Standard Clinical Laboratory Measurements in the RECOVER Cohort. *Ann Intern Med*. 2024;177(9):1209-1221. doi:10.7326/M24-0737
201. Ceban F, Ling S, Lui LMW, et al. Fatigue and cognitive impairment in Post-COVID-19 Syndrome: A systematic review and meta-analysis. *Brain Behav Immun*. 2022;101:93-135. doi:10.1016/j.bbi.2021.12.020
202. van der Feltz-Cornelis C, Turk F, Sweetman J, et al. Prevalence of mental health conditions and brain fog in people with long COVID: A systematic review and meta-analysis. *Gen Hosp Psychiatry*. 2024;88:10-22. doi:10.1016/j.genhosppsych.2024.02.009
203. Pinzon RT, Wijaya VO, Jody AA, Nunsio PN, Buana RB. Persistent neurological manifestations in long COVID-19 syndrome: A systematic review and meta-analysis. *Journal of Infection and Public Health*. 2022;15(8):856-869. doi:10.1016/j.jiph.2022.06.013
204. Taquet M, Sillett R, Zhu L, et al. Neurological and psychiatric risk trajectories after SARS-CoV-2 infection: an analysis of 2-year retrospective cohort studies including 1 284 437 patients. *The Lancet Psychiatry*. 2022;9(10):815-827. doi:10.1016/S2215-0366(22)00260-7
205. Seighali N, Abdollahi A, Shafiee A, et al. The global prevalence of depression, anxiety, and sleep disorder among patients coping with Post COVID-19 syndrome (long COVID): a systematic review and meta-analysis. *BMC Psychiatry*. 2024;24(1):105. doi:10.1186/s12888-023-05481-6
206. Zeng N, Zhao YM, Yan W, et al. A systematic review and meta-analysis of long term physical and mental sequelae of COVID-19 pandemic: call for research priority and action. *Mol Psychiatry*. 2023;28(1):423-433. doi:10.1038/s41380-022-01614-7
207. Zheng B, Daines L, Han Q, et al. Prevalence, risk factors and treatments for post-COVID-19 breathlessness: a systematic review and meta-analysis. *Eur Respir Rev*. 2022;31(166):220071. doi:10.1183/16000617.0071-2022
208. Rahmati M, Udeh R, Yon DK, et al. A systematic review and meta-analysis of long-term sequelae of COVID-19 2-year after SARS-CoV-2 infection: A call to action for neurological, physical, and psychological sciences. *Journal of Medical Virology*. 2023;95(6):e28852. doi:10.1002/jmv.28852
209. Fernandez-de-las-Peñas C, Notarte KI, Macasaet R, et al. Persistence of post-COVID symptoms in the general population two years after SARS-CoV-2 infection: A systematic review and meta-analysis. *Journal of Infection*. 2024;88(2):77-88. doi:10.1016/j.jinf.2023.12.004
210. Cabo-Gambin R, Benítez ID, Carmona P, et al. Three to Six Months Evolution of Pulmonary Function and Radiological Features in Critical COVID-19 Patients: A Prospective Cohort. *Archivos de Bronconeumología*. 2022;58:59-62. doi:10.1016/j.arbres.2021.07.005
211. Cornelissen MEB, Leliveld A, Baalbaki N, et al. Pulmonary function 3–6 months after acute COVID-19: A systematic review and multicentre cohort study. *Heliyon*. 2024;10(6):e27964. doi:10.1016/j.heliyon.2024.e27964
212. Kingery JR, Safford MM, Martin P, et al. Health Status, Persistent Symptoms, and Effort Intolerance One Year After Acute COVID-19 Infection. *J GEN INTERN MED*. 2022;37(5):1218-1225. doi:10.1007/s11606-021-07379-z
213. Wang HI, Doran T, Crooks MG, et al. Prevalence, risk factors and characterisation of individuals with long COVID using Electronic Health Records in over 1.5 million COVID cases in England. *Journal of Infection*. 2024;89(4):106235. doi:10.1016/j.jinf.2024.106235
214. Salem AM, Al Khathlan N, Alogily M, et al. Respiratory muscle weakness, reduced exercise capacity, and impaired lung functions in long-term post-COVID-19 patients. *ELECTRON J GEN MED*. 2025;22(3):em646. doi:10.29333/ejgm/16228
215. Verduri A, Tonelli R, Donatelli P, et al. Respiratory Muscle Dysfunction and Associated Risk Factors Following COVID-19-Related Hospitalisation. *Life*. 2025;15(2):194. doi:10.3390/life15020194
216. Gyöngyösi M, Alcaide P, Asselbergs FW, et al. Long COVID and the cardiovascular system—elucidating causes and cellular mechanisms in order to develop targeted diagnostic and therapeutic strategies: a joint Scientific Statement of the ESC Working Groups on Cellular Biology of the Heart and Myocardial and Pericardial Diseases. *Cardiovascular Research*. 2023;119(2):336-356. doi:10.1093/cvr/cvac115
217. Xie Y, Xu E, Bowe B, Al-Aly Z. Long-term cardiovascular outcomes of COVID-19. *Nat Med*. 2022;28(3):583-590. doi:10.1038/s41591-022-01689-3
218. Zhang T, Li Z, Mei Q, et al. Cardiovascular outcomes in long COVID-19: a systematic review and meta-analysis. *Front Cardiovasc Med*. 2025;12:1450470. doi:10.3389/fcvm.2025.1450470
219. Gluckman TJ, Bhave NM, Allen LA, et al. 2022 ACC Expert Consensus Decision Pathway on Cardiovascular Sequelae of COVID-19 in Adults: Myocarditis and Other Myocardial Involvement, Post-Acute Sequelae of SARS-CoV-2 Infection, and Return to Play. *Journal of the American College of Cardiology*. 2022;79(17):1717-1756. doi:10.1016/j.jacc.2022.02.003
220. Huang LW, Li HM, He B, Wang XB, Zhang QZ, Peng WX. Prevalence of cardiovascular symptoms in post-acute COVID-19 syndrome: a meta-analysis. *BMC Med*. 2025;23(1):70. doi:10.1186/s12916-025-03908-3
221. Jamal SM, Landers DB, Hollenberg SM, et al. Prospective Evaluation of Autonomic Dysfunction in Post-Acute Sequela of COVID-19. *Journal of the American College of Cardiology*. 2022;79(23):2325-2330. doi:10.1016/j.jacc.2022.03.357
222. Seeley MC, Gallagher C, Wilson G, Page A, Lau DH. Autonomic dysfunction is prevalent in PASC of Covid-19 [PASC]. *European Journal of Cardiovascular Nursing*. 2024;23(Supplement_1):zvae098.097. doi:10.1093/eurjcn/zvae098.097

223. Seeley MC, Gallagher C, Ong E, et al. High Incidence of Autonomic Dysfunction and Postural Orthostatic Tachycardia Syndrome in Patients with Long COVID: Implications for Management and Health Care Planning. *The American Journal of Medicine*. 2025;138(2):354-361.e1. doi:10.1016/j.amjmed.2023.06.010
224. Favas TT, Dev P, Chaurasia RN, et al. Neurological manifestations of COVID-19: a systematic review and meta-analysis of proportions. *Neurol Sci*. 2020;41(12):3437-3470. doi:10.1007/s10072-020-04801-y
225. Hoshijima H, Mihara T, Seki H, Hyuga S, Kuratani N, Shiga T. Incidence of long-term post-acute sequelae of SARS-CoV-2 infection related to pain and other symptoms: A systematic review and meta-analysis. *PLoS One*. 2023;18(11):e0250909. doi:10.1371/journal.pone.0250909
226. Tran VT, Porcher R, Pane I, Ravaud P. Course of post COVID-19 disease symptoms over time in the ComPaRe long COVID prospective e-cohort. *Nat Commun*. 2022;13(1):1812. doi:10.1038/s41467-022-29513-z
227. Karaarslan F, Demircioğlu Güneri F, Kardeş S. Postdischarge rheumatic and musculoskeletal symptoms following hospitalization for COVID-19: prospective follow-up by phone interviews. *Rheumatol Int*. 2021;41(7):1263-1271. doi:10.1007/s00296-021-04882-8
228. Haider S, Janowski AJ, Lesnak JB, et al. A comparison of pain, fatigue, and function between post–COVID-19 condition, fibromyalgia, and chronic fatigue syndrome: a survey study. *Pain*. 2023;164(2):385-401. doi:10.1097/j.pain.0000000000002711
229. Gracia-Ramos AE, Saavedra-Salinas MÁ. Can the SARS-CoV-2 infection trigger systemic lupus erythematosus? A case-based review. *Rheumatol Int*. 2021;41(4):799-809. doi:10.1007/s00296-021-04794-7
230. Wong JRY, Zhu L, Shah S, Gadikoppula S. A Case of Axial Spondyloarthritis Triggered by SARS-CoV-2 Infection. *Cureus*. Published online March 5, 2022. doi:10.7759/cureus.22860
231. Karkabayeva A, Mirakhmedova K, Khusinova S, Mamasaidov A, Baimukhamedov C. COVID-19 is a trigger of autoimmune rheumatic diseases: a hypothesis tested over time. *Rheumatol Int*. 2024;45(1):11. doi:10.1007/s00296-024-05766-3
232. Sherif ZA, Deverapalli M, Challa SR, et al. Potential long-term neurological and gastrointestinal effects of COVID-19: A review of adult cohorts. *World J Methodol*. 2023;13(4):323-336. doi:10.5662/wjm.v13.i4.323
233. Silva JTC, Fonseca Neto OCLD. Post-COVID-19 irritable bowel syndrome: an integrative review. *Rev Col Bras Cir*. 2023;50:e20233618. doi:10.1590/0100-6991e-20233618-en
234. Hirsch JS, Ng JH, Ross DW, et al. Acute kidney injury in patients hospitalized with COVID-19. *Kidney International*. 2020;98(1):209-218. doi:10.1016/j.kint.2020.05.006
235. Filev R, Lyubomirova M, Bogov B, et al. Post-Acute Sequelae of SARS-CoV-2 Infection (PASC) for Patients-3-Year Follow-Up of Patients with Chronic Kidney Disease. *Biomedicines*. 2024;12(6):1259. doi:10.3390/biomedicines12061259
236. Kemeç Z, Akgül F. Are Patients with Covid-19 at Risk of Long-Term Chronic Kidney Disease? *Nigerian Journal of Clinical Practice*. 2023;26(3):341-346. doi:10.4103/njcp.njcp_382_22
237. Roumelioti ME, Mir H, Argyropoulos C. COVID-19 Infection Is a Risk Factor for CKD and Glomerulonephritis: TH-PO902. *Journal of the American Society of Nephrology*. 2022;33(11S):306-306. doi:10.1681/ASN.20223311S1306d
238. Thompson JR, Atiquzzaman M, Shao S, Djurdjev O, Levin A, Birks PC. Long-Term Effect of COVID-19 Infection on Kidney Function Among COVID-19 Patients Followed in a Post-COVID-19 Recovery Clinic in British Columbia, Canada: TH-PO901. *Journal of the American Society of Nephrology*. 2022;33(11S):306-306. doi:10.1681/ASN.20223311S1306c
239. Banerjee M, Pal R, Dutta S. Risk of incident diabetes post-COVID-19: A systematic review and meta-analysis. *Primary Care Diabetes*. 2022;16(4):591-593. doi:10.1016/j.pcd.2022.05.009
240. Kenny G, McCann K, O'Brien C, et al. Identification of Distinct Long COVID Clinical Phenotypes Through Cluster Analysis of Self-Reported Symptoms. *Open Forum Infectious Diseases*. 2022;9(4):ofac060. doi:10.1093/ofid/ofac060
241. Gentilotti E, Górska A, Tami A, et al. Clinical phenotypes and quality of life to define post-COVID-19 syndrome: a cluster analysis of the multinational, prospective ORCHESTRA cohort. *eClinicalMedicine*. 2023;62:102107. doi:10.1016/j.eclinm.2023.102107
242. Jaber F, Hoang MA, Feldman DE, Saunders S, Mazer B. Factors associated with changes in employment in individuals with long COVID. *WORK: A Journal of Prevention, Assessment & Rehabilitation*. Published online January 22, 2025:10519815241300409. doi:10.1177/10519815241300409
243. Golzari-Sorkheh M, Weaver DF, Reed MA. COVID-19 as a Risk Factor for Alzheimer's Disease. *JAD*. 2023;91(1):1-23. doi:10.3233/JAD-220800
244. Nathan C, Ding A. Nonresolving Inflammation. *Cell*. 2010;140(6):871-882. doi:10.1016/j.cell.2010.02.029
245. Snyderman R, Spellmeyer D. PRecision Medicine: Beyond Genomics to Targeted Therapies. *Per Med*. 2016;13(2):97-100. doi:10.2217/pme.15.48
246. Chung KF. Precision medicine in asthma: linking phenotypes to targeted treatments. *Current Opinion in Pulmonary Medicine*. 2018;24(1):4-10. doi:10.1097/mcp.0000000000000434
247. Craddock V, Mahajan A, Krishnamachary B, Spikes L, Chalise P, Dhillon NK. Persistent Presence of Spike protein and Viral RNA in the Circulation of Individuals with Post-Acute Sequelae of COVID-19. *Cold Spring Harbor Laboratory*. Preprint posted online August 9, 2022. doi:10.1101/2022.08.07.22278520
248. Zollner A, Koch R, Jukic A, et al. Postacute COVID-19 is Characterized by Gut Viral Antigen Persistence in Inflammatory Bowel Diseases. *Gastroenterology*. 2022;163(2):495-506.e8. doi:10.1053/j.gastro.2022.04.037
249. Peluso MJ, Swank ZN, Goldberg SA, et al. Plasma-based antigen persistence in the post-acute phase of SARS-CoV-2 infection. *Cold Spring Harbor Laboratory*. Preprint posted online October 25, 2023. doi:10.1101/2023.10.24.23297114

250. El-Baky NA, Amara AA, Uversky VN, Redwan EM. Intrinsic factors behind long COVID: III. Persistence of SARS-CoV-2 and its components. *J of Cellular Biochemistry*. 2024;125(1). doi:10.1002/jcb.30514
251. Chertow D, Stein S, Ramelli S, et al. SARS-CoV-2 infection and persistence throughout the human body and brain. *Springer Science and Business Media LLC*. Preprint posted online December 20, 2021. doi:10.21203/rs.3.rs-1139035/v1
252. Meringer H, Tokuyama M, Tankelevich M, et al. DOP19 Myeloid and lymphoid cell abnormalities persist in the intestinal mucosa of patients who recover from COVID-19 infection. *Journal of Crohn's and Colitis*. 2022;16(Supplement_1):i068-i069. doi:10.1093/ecco-jcc/jjab232.058
253. Joukar F, Yaghubi Kalurazi T, Khoshsorour M, et al. Persistence of SARS-CoV-2 RNA in the nasopharyngeal, blood, urine, and stool samples of patients with COVID-19: a hospital-based longitudinal study. *Virol J*. 2021;18(1). doi:10.1186/s12985-021-01599-9
254. Rubin R. SARS-CoV-2 RNA Can Persist in Stool Months After Respiratory Tract Clears Virus. *JAMA*. 2022;327(22):2175. doi:10.1001/jama.2022.7892
255. Patterson BK, Francisco EB, Yogendra R, et al. Persistence of SARS CoV-2 S1 Protein in CD16+ Monocytes in Post-Acute Sequelae of COVID-19 (PASC) up to 15 Months Post-Infection. *Front Immunol*. 2022;12. doi:10.3389/fimmu.2021.746021
256. Proal AD, VanElzakker MB, Aleman S, et al. SARS-CoV-2 reservoir in post-acute sequelae of COVID-19 (PASC). *Nat Immunol*. 2023;24(10):1616-1627. doi:10.1038/s41590-023-01601-2
257. Ahamed J, Laurence J. Long COVID endotheliopathy: hypothesized mechanisms and potential therapeutic approaches. *J Clin Invest*. 2022;132(15):e161167. doi:10.1172/JCI161167
258. Leng A, Shah M, Ahmad SA, et al. Pathogenesis Underlying Neurological Manifestations of Long COVID Syndrome and Potential Therapeutics. *Cells*. 2023;12(5):816. doi:10.3390/cells12050816
259. Swank Z, Borberg E, Chen Y, et al. Measurement of circulating viral antigens post-SARS-CoV-2 infection in a multicohort study. *Clinical Microbiology and Infection*. 2024;30(12):1599-1605. doi:10.1016/j.cmi.2024.09.001
260. Magro C, Mulvey JJ, Berlin D, et al. Complement associated microvascular injury and thrombosis in the pathogenesis of severe COVID-19 infection: A report of five cases. *Translational Research*. 2020;220:1-13. doi:10.1016/j.trsl.2020.04.007
261. Islam MS, Wang Z, Abdel-Mohsen M, Chen X, Montaner LJ. Tissue injury and leukocyte changes in post-acute sequelae of SARS-CoV-2: review of 2833 post-acute patient outcomes per immune dysregulation and microbial translocation in long COVID. *Journal of Leukocyte Biology*. 2023;113(3):236-254. doi:10.1093/jleuko/qiac001
262. Opsteen S, Files JK, Fram T, Erdmann N. The role of immune activation and antigen persistence in acute and long COVID. *Journal of Investigative Medicine*. 2023;71(5):545-562. doi:10.1177/10815589231158041
263. Chorya HP, Naik AK. COVID-19 Infection and the Risk of CMV Reactivation: A Systematic Review of Case Reports and Case Series. *Apollo Medicine*. Published online November 6, 2024. doi:10.1177/09760016241290598
264. Maguire C, Chen J, Rouphael N, et al. Chronic Viral Reactivation and Associated Host Immune Response and Clinical Outcomes in Acute COVID-19 and Post-Acute Sequelae of COVID-19. *Cold Spring Harbor Laboratory*. Preprint posted online November 16, 2024. doi:10.1101/2024.11.14.622799
265. Banko A, Miljanovic D, Cirkovic A. Systematic review with meta-analysis of active herpesvirus infections in patients with COVID-19: Old players on the new field. *International Journal of Infectious Diseases*. 2023;130:108-125. doi:10.1016/j.ijid.2023.01.036
266. Peluso MJ, Deveau TM, Munter SE, et al. Chronic viral coinfections differentially affect the likelihood of developing long COVID. *Journal of Clinical Investigation*. 2023;133(3). doi:10.1172/jci163669
267. Rohrhofer J, Graninger M, Lettenmaier L, et al. Association between Epstein-Barr-Virus reactivation and development of Long-COVID fatigue. *Allergy*. 2023;78(1):297-299. doi:10.1111/all.15471
268. Gärtner BC, Kortmann K, Schäfer M, et al. No Correlation in Epstein-Barr Virus Reactivation Between Serological Parameters and Viral Load. *J Clin Microbiol*. 2000;38(6):2458-2458. doi:10.1128/jcm.38.6.2458-2458.2000
269. Hoeggerl AD, Nunhofer V, Lauth W, et al. Epstein-Barr virus reactivation is not causative for post-COVID-19-syndrome in individuals with asymptomatic or mild SARS-CoV-2 disease course. *BMC Infect Dis*. 2023;23(1). doi:10.1186/s12879-023-08820-w
270. Zubchenko S, Kril I, Nadizhko O, Matsyura O, Chopyak V. Herpesvirus infections and post-COVID-19 manifestations: a pilot observational study. *Rheumatol Int*. 2022;42(9):1523-1530. doi:10.1007/s00296-022-05146-9
271. Barda N, Dagan N, Ben-Shlomo Y, et al. Safety of the BNT162b2 mRNA Covid-19 Vaccine in a Nationwide Setting. *N Engl J Med*. 2021;385(12):1078-1090. doi:10.1056/nejmoa2110475
272. Bhavsar A, Lonnet G, Wang C, et al. Increased Risk of Herpes Zoster in Adults ≥50 Years Old Diagnosed With COVID-19 in the United States. *Open Forum Infectious Diseases*. 2022;9(5). doi:10.1093/ofid/ofac118
273. Chen Y, Ho C, Liu T, et al. Long-term risk of herpes zoster following COVID-19: A retrospective cohort study of 2 442 686 patients. *Journal of Medical Virology*. 2023;95(4). doi:10.1002/jmv.28745
274. Correcher-Martínez E, López-Lacort M, Muñoz-Quiles C, Díez-Domingo J, Orrico-Sánchez A. Risk of herpes zoster in adults with SARS-CoV-2 infection in Spain: A population-based, retrospective cohort study. *International Journal of Infectious Diseases*. 2024;143:107037. doi:10.1016/j.ijid.2024.107037
275. Lupi L, Vitiello A, Parolin C, Calistri A, Garzino-Demo A. The Potential Role of Viral Persistence in the Post-Acute Sequelae of SARS-CoV-2 Infection (PASC). *Pathogens*. 2024;13(5):388. doi:10.3390/pathogens13050388

276. Macedo C, Webber SA, Donnenberg AD, et al. EBV-Specific CD8+ T Cells from Asymptomatic Pediatric Thoracic Transplant Patients Carrying Chronic High EBV Loads Display Contrasting Features: Activated Phenotype and Exhausted Function. *The Journal of Immunology*. 2011;186(10):5854-5862. doi:10.4049/jimmunol.1001024
277. Zhou Y, Zhang J, Zhang D, Ma WL, Wang X. Linking the gut microbiota to persistent symptoms in survivors of COVID-19 after discharge. *J Microbiol*. 2021;59(10):941-948. doi:10.1007/s12275-021-1206-5
278. Liu Q, Mak JWY, Su Q, et al. Gut microbiota dynamics in a prospective cohort of patients with post-acute COVID-19 syndrome. *Gut*. 2022;71(3):544-552. doi:10.1136/gutjnl-2021-325989
279. Ancona G, Alagna L, Alteri C, et al. Gut and airway microbiota dysbiosis and their role in COVID-19 and long-COVID. *Front Immunol*. 2023;14. doi:10.3389/fimmu.2023.1080043
280. Zhou Y, Zhang J, Zhang D, Ma WL, Wang X. Linking the gut microbiota to persistent symptoms in survivors of COVID-19 after discharge. *J Microbiol*. 2021;59(10):941-948. doi:10.1007/s12275-021-1206-5
281. Liu Q, Su Q, Zhang F, et al. Multi-kingdom gut microbiota analyses define COVID-19 severity and post-acute COVID-19 syndrome. *Nat Commun*. 2022;13(1). doi:10.1038/s41467-022-34535-8
282. Zhang D, Zhou Y, Ma Y, et al. Gut Microbiota Dysbiosis Correlates With Long COVID-19 at One-Year After Discharge. *J Korean Med Sci*. 2023;38(15). doi:10.3346/jkms.2023.38.e120
283. Olbjørn C, Hagen M, Moen AEF, et al. Longitudinal Fecal Microbiota Profiles in A Cohort of Non-Hospitalized Adolescents and Young Adults with COVID-19: Associations with SARS-CoV-2 Status and Long-Term Fatigue. *Pathogens*. 2024;13(11):953. doi:10.3390/pathogens13110953
284. Palmnäs-Bédard MS, Costabile G, Vetrani C, et al. The human gut microbiota and glucose metabolism: a scoping review of key bacteria and the potential role of SCFAs. *The American Journal of Clinical Nutrition*. 2022;116(4):862-874. doi:10.1093/ajcn/nqac217
285. Singh V, Lee G, Son H, et al. Butyrate producers, "The Sentinel of Gut": Their intestinal significance with and beyond butyrate, and prospective use as microbial therapeutics. *Front Microbiol*. 2023;13. doi:10.3389/fmicb.2022.1103836
286. Montandon S, Jornayvaz F. Effects of Antidiabetic Drugs on Gut Microbiota Composition. *Genes*. 2017;8(10):250. doi:10.3390/genes8100250
287. Lloyd-Price J, Arze C, Ananthakrishnan AN, et al. Multi-omics of the gut microbial ecosystem in inflammatory bowel diseases. *Nature*. 2019;569(7758):655-662. doi:10.1038/s41586-019-1237-9
288. De Sales-Millán A, Aguirre-Garrido JF, González-Cervantes RM, Velázquez-Aragón JA. Microbiome–Gut–Mucosal–Immune–Brain Axis and Autism Spectrum Disorder (ASD): A Novel Proposal of the Role of the Gut Microbiome in ASD Aetiology. *Behavioral Sciences*. 2023;13(7):548. doi:10.3390/bs13070548
289. Żak-Gołąb A, Kocełak P, Aptekorz M, et al. Gut Microbiota, Microinflammation, Metabolic Profile, and Zonulin Concentration in Obese and Normal Weight Subjects. *International Journal of Endocrinology*. 2013;2013:1-9. doi:10.1155/2013/674106
290. Chancharoenthana W, Kamolratanakul S, Schultz MJ, Leelahavanichkul A. The leaky gut and the gut microbiome in sepsis - targets in research and treatment. *Clin Sci (Lond)*. 2023;137(8):645-662. doi:10.1042/CS20220777
291. Volcic M, Nchioua R, Pastorio C, et al. Attenuated replication and damaging effects of SARS-CoV-2 Omicron variants in an intestinal epithelial barrier model. *Journal of Medical Virology*. 2024;96(7). doi:10.1002/jmv.29783
292. Llorens S, Nava E, Muñoz-López M, Sánchez-Larsen Á, Segura T. Neurological Symptoms of COVID-19: The Zonulin Hypothesis. *Front Immunol*. 2021;12. doi:10.3389/fimmu.2021.665300
293. Teixeira PC, Dorneles GP, Santana Filho PC, et al. Increased LPS levels coexist with systemic inflammation and result in monocyte activation in severe COVID-19 patients. *International Immunopharmacology*. 2021;100:108125. doi:10.1016/j.intimp.2021.108125
294. Giron LB, Peluso MJ, Ding J, et al. Markers of fungal translocation are elevated during post-acute sequelae of SARS-CoV-2 and induce NF-κB signaling. *JCI Insight*. 2022;7(18). doi:10.1172/jci.insight.164813
295. Takauji R, Iho S, Takatsuka H, et al. CpG-DNA-induced IFN-alpha production involves p38 MAPK-dependent STAT1 phosphorylation in human plasmacytoid dendritic cell precursors. *J Leukoc Biol*. 2002;72(5):1011-1019.
296. Dalmo RA, Bøgwald J. ß-glucans as conductors of immune symphonies. *Fish & Shellfish Immunology*. 2008;25(4):384-396. doi:10.1016/j.fsi.2008.04.008
297. Braniste V, Al-Asmakh M, Kowal C, et al. The gut microbiota influences blood-brain barrier permeability in mice. *Sci Transl Med*. 2014;6(263). doi:10.1126/scitranslmed.3009759
298. Petra AI, Panagiotidou S, Hatziagelaki E, Stewart JM, Conti P, Theoharides TC. Gut-Microbiota-Brain Axis and Its Effect on Neuropsychiatric Disorders With Suspected Immune Dysregulation. *Clin Ther*. 2015;37(5):984-995. doi:10.1016/j.clinthera.2015.04.002
299. Haran JP, Bradley E, Zeamer AL, et al. Inflammation-type dysbiosis of the oral microbiome associates with the duration of COVID-19 symptoms and long COVID. *JCI Insight*. 2021;6(20). doi:10.1172/jci.insight.152346
300. Phetsouphanh C, Darley DR, Wilson DB, et al. Immunological dysfunction persists for 8 months following initial mild-to-moderate SARS-CoV-2 infection. *Nat Immunol*. 2022;23(2):210-216. doi:10.1038/s41590-021-01113-x
301. Schultheiß C, Willscher E, Paschold L, et al. The IL-1β, IL-6, and TNF cytokine triad is associated with post-acute sequelae of COVID-19. *Cell Reports Medicine*. 2022;3(6):100663. doi:10.1016/j.xcrm.2022.100663
302. Yin JX, Agbana YL, Sun ZS, et al. Increased interleukin-6 is associated with long COVID-19: a systematic review and meta-analysis. *Infect Dis Poverty*. 2023;12(1):43. doi:10.1186/s40249-023-01086-z
303. Almulla AF, Thipakorn Y, Zhou B, Vojdani A, Maes M. Immune activation and immune-associated neurotoxicity in Long-COVID: A systematic review and meta-analysis of 103 studies comprising 58 cytokines/chemokines/growth factors. *Brain, Behavior, and Immunity*. 2024;122:75-94. doi:10.1016/j.bbi.2024.07.036

304. Pasini E, Corsetti G, Romano C, et al. Serum Metabolic Profile in Patients With Long-Covid (PASC) Syndrome: Clinical Implications. *Front Med*. 2021;8:714426. doi:10.3389/fmed.2021.714426
305. Santa Cruz A, Mendes-Frias A, Azarias-da-Silva M, et al. Post-acute sequelae of COVID-19 is characterized by diminished peripheral CD8+β7 integrin+ T cells and anti-SARS-CoV-2 IgA response. *Nat Commun*. 2023;14(1):1772. doi:10.1038/s41467-023-37368-1
306. Colarusso C, Maglio A, Terlizzi M, et al. Post-COVID-19 Patients Who Develop Lung Fibrotic-like Changes Have Lower Circulating Levels of IFN-β but Higher Levels of IL-1α and TGF-β. *Biomedicines*. 2021;9(12):1931. doi:10.3390/biomedicines9121931
307. Cheong JG, Ravishankar A, Sharma S, et al. Epigenetic memory of coronavirus infection in innate immune cells and their progenitors. *Cell*. 2023;186(18):3882-3902.e24. doi:10.1016/j.cell.2023.07.019
308. Li C, Qian W, Wei X, et al. Comparative single-cell analysis reveals IFN-γ as a driver of respiratory sequelae after acute COVID-19. *Sci Transl Med*. 2024;16(756):eadn0136. doi:10.1126/scitranslmed.adn0136
309. Yao C, Parimon T, Espindola MS, et al. Maladaptive TGF-β Signals to the Alveolar Epithelium Drive Fibrosis after COVID-19 Infection. *Am J Respir Crit Care Med*. 2023;208(2):201-204. doi:10.1164/rccm.202302-0264LE
310. Pérez-Gómez A, Vitallé J, Gasca-Capote C, et al. Dendritic cell deficiencies persist seven months after SARS-CoV-2 infection. *Cell Mol Immunol*. 2021;18(9):2128-2139. doi:10.1038/s41423-021-00728-2
311. LaVergne SM, Dutt TS, McFann K, et al. Persistent CD8+ T cell proliferation and activation in COVID-19 adult survivors with post-acute sequelae: a longitudinal, observational cohort study of persistent symptoms and T cell markers. *Front Immunol*. 2024;14:1303971. doi:10.3389/fimmu.2023.1303971
312. Klein J, Wood J, Jaycox JR, et al. Distinguishing features of long COVID identified through immune profiling. *Nature*. 2023;623(7985):139-148. doi:10.1038/s41586-023-06651-y
313. Yin K, Peluso MJ, Luo X, et al. Long COVID manifests with T cell dysregulation, inflammation and an uncoordinated adaptive immune response to SARS-CoV-2. *Nat Immunol*. 2024;25(2):218-225. doi:10.1038/s41590-023-01724-6
314. Krishna BA, Lim EY, Metaxaki M, et al. Spontaneous, persistent, T cell–dependent IFN-γ release in patients who progress to Long Covid. *Sci Adv*. 2024;10(8):eadi9379. doi:10.1126/sciadv.adi9379
315. Kappelmann N, Dantzer R, Khandaker GM. Interleukin-6 as potential mediator of long-term neuropsychiatric symptoms of COVID-19. *Psychoneuroendocrinology*. 2021;131:105295. doi:10.1016/j.psyneuen.2021.105295
316. Visvabharathy L, Hanson BA, Orban ZS, et al. Neuro-PASC is characterized by enhanced CD4+ and diminished CD8+ T cell responses to SARS-CoV-2 Nucleocapsid protein. *Front Immunol*. 2023;14:1155770. doi:10.3389/fimmu.2023.1155770
317. Klein R, Vanderheiden A, Hill J, et al. Vaccination prevents IL-1β-mediated cognitive deficits after COVID-19. *In Review*. Preprint posted online September 15, 2023. doi:10.21203/rs.3.rs-3353171/v1
318. Littlefield KM, Watson RO, Schneider JM, et al. SARS-CoV-2-specific T cells associate with reduced lung function and inflammation in pulmonary post-acute sequalae of SARS-CoV-2. *Immunology*. Preprint posted online February 15, 2022. doi:10.1101/2022.02.14.480317
319. Narasimhan H, Cheon IS, Qian W, et al. Proximal immune-epithelial progenitor interactions drive chronic tissue sequelae post COVID-19. *Immunology*. Preprint posted online September 14, 2023. doi:10.1101/2023.09.13.557622
320. Reid MB, Li YP. Tumor necrosis factor-α and muscle wasting: a cellular perspective. *Respir Res*. 2001;2(5):269. doi:10.1186/rr67
321. Durstenfeld MS, Peluso MJ, Kaveti P, et al. Abstract 10570: Inflammation During Early Post-Acute Covid-19 is Associated With Reduced Exercise Capacity and Long Covid Symptoms After 1 Year. *Circulation*. 2022;146(Suppl_1). doi:10.1161/circ.146.suppl_1.10570
322. Holms R. Long COVID (PASC) Is Maintained by a Self-Sustaining Pro-Inflammatory TLR4/RAGE-Loop of S100A8/A9 > TLR4/RAGE Signalling, Inducing Chronic Expression of IL-1b, IL-6 and TNFa: Anti-Inflammatory Ezrin Peptides as Potential Therapy. *Immuno*. 2022;2(3):512-533. doi:10.3390/immuno2030033
323. Wallukat G, Hohberger B, Wenzel K, et al. Functional autoantibodies against G-protein coupled receptors in patients with persistent Long-COVID-19 symptoms. *Journal of Translational Autoimmunity*. 2021;4:100100. doi:10.1016/j.jtauto.2021.100100
324. Su Y, Yuan D, Chen DG, et al. Multiple early factors anticipate post-acute COVID-19 sequelae. *Cell*. 2022;185(5):881-895.e20. doi:10.1016/j.cell.2022.01.014
325. Wang EY, Mao T, Klein J, et al. Diverse functional autoantibodies in patients with COVID-19. *Nature*. 2021;595(7866):283-288. doi:10.1038/s41586-021-03631-y
326. Son K, Jamil R, Chowdhury A, et al. Circulating anti-nuclear autoantibodies in COVID-19 survivors predict long-COVID symptoms. *Eur Respir J*. Published online September 22, 2022:2200970. doi:10.1183/13993003.00970-2022
327. Chen HJ, Appelman B, Willemen H, et al. Transfer of IgG from Long COVID patients induces symptomology in mice. *Immunology*. Preprint posted online May 31, 2024. doi:10.1101/2024.05.30.596590
328. Santos Guedes De Sa K, Silva J, Bayarri-Olmos R, et al. A causal link between autoantibodies and neurological symptoms in long COVID. *Allergy and Immunology*. Preprint posted online June 19, 2024. doi:10.1101/2024.06.18.24309100
329. Hohberger B, Ganslmayer M, Harrer T, et al. Safety, tolerability and clinical effects of rovunaptabin, also known as BC007 on fatigue and quality of life in patients with Post-COVID syndrome (reCOVer): a prospective, exploratory, placebo-controlled, double-blind, randomised phase IIa clinical trial (RCT). *eClinicalMedicine*. 2025;86:103358. doi:10.1016/j.eclinm.2025.103358

330. Chang R, Yen-Ting Chen T, Wang SI, Hung YM, Chen HY, Wei CCJ. Risk of autoimmune diseases in patients with COVID-19: a retrospective cohort study. *eClinicalMedicine*. 2023;56:101783. doi:10.1016/j.eclinm.2022.101783
331. Arévalo-Cortés A, Rodriguez-Pinto D, Aguilar-Ayala L. Evidence for Molecular Mimicry between SARS-CoV-2 and Human Antigens: Implications for Autoimmunity in COVID-19. Mageed R, ed. *Autoimmune Diseases*. 2024;2024(1):8359683. doi:10.1155/2024/8359683
332. Araújo FC, Amaral ACD, Silva HJ, et al. Autoantibodies as potential prognostic factors for clinical outcomes related to COVID-19: a systematic review of inception prospective cohort studies with GRADE recommendations. *Braz J Med Biol Res*. 2025;58:e13965. doi:10.1590/1414-431x2024e13965
333. Hansen KS, Jørgensen SE, Skouboe MK, et al. Examination of autoantibodies to type I interferon in patients suffering from long COVID. *Journal of Medical Virology*. 2023;95(9):e29089. doi:10.1002/jmv.29089
334. Peluso MJ, Mitchell A, Wang CY, et al. Low Prevalence of Interferon α Autoantibodies in People Experiencing Symptoms of Post–Coronavirus Disease 2019 (COVID-19) Conditions, or Long COVID. *The Journal of Infectious Diseases*. 2023;227(2):246-250. doi:10.1093/infdis/jiac372
335. Cockx M, Geukens N, Michiels B, et al. Long-term follow-up of anti-IFN-α2 autoantibody levels in hospitalized individuals with COVID-19. *Clinical Immunology Communications*. 2024;6:26-30. doi:10.1016/j.clicom.2024.11.001
336. Visvabharathy L, Dalil N, Leonor L, et al. Mild Primary or Breakthrough SARS-CoV-2 Infection Promotes Autoantibody Production in Individuals with and without Neuro-PASC. *ImmunoHorizons*. 2024;8(8):577-585. doi:10.4049/immunohorizons.2400033
337. Matula Z, Király V, Bekő G, et al. High prevalence of long COVID in anti-TPO positive euthyroid individuals with strongly elevated SARS-CoV-2-specific T cell responses and moderately raised anti-spike IgG levels 23 months post-infection. *Front Immunol*. 2024;15:1448659. doi:10.3389/fimmu.2024.1448659
338. Achleitner M, Steenblock C, Dänhardt J, et al. Clinical improvement of Long-COVID is associated with reduction in autoantibodies, lipids, and inflammation following therapeutic apheresis. *Mol Psychiatry*. 2023;28(7):2872-2877. doi:10.1038/s41380-023-02084-1
339. Arbuckle MR, McClain MT, Rubertone MV, et al. Development of Autoantibodies before the Clinical Onset of Systemic Lupus Erythematosus. *N Engl J Med*. 2003;349(16):1526-1533. doi:10.1056/NEJMoa021933
340. Younis S, Moutusy SI, Rasouli S, et al. Epstein-Barr virus reprograms autoreactive B cells as antigen-presenting cells in systemic lupus erythematosus. *Sci Transl Med*. 2025;17(824):eady0210. doi:10.1126/scitranslmed.ady0210
341. Baillie K, Davies HE, Keat SBK, et al. Complement dysregulation is a prevalent and therapeutically amenable feature of long COVID. *Med*. 2024;5(3):239-253.e5. doi:10.1016/j.medj.2024.01.011
342. Fogarty H, Townsend L, Morrin H, et al. Persistent endotheliopathy in the pathogenesis of long COVID syndrome. *Journal of Thrombosis and Haemostasis*. 2021;19(10):2546-2553. doi:10.1111/jth.15490
343. Patel MA, Knauer MJ, Nicholson M, et al. Elevated vascular transformation blood biomarkers in Long-COVID indicate angiogenesis as a key pathophysiological mechanism. *Mol Med*. 2022;28(1):122. doi:10.1186/s10020-022-00548-8
344. Espín E, Yang C, Shannon CP, Assadian S, He D, Tebbutt SJ. Cellular and molecular biomarkers of long COVID: a scoping review. *eBioMedicine*. 2023;91:104552. doi:10.1016/j.ebiom.2023.104552
345. Di Ciaula A, Liberale L, Portincasa P, et al. Neutrophil degranulation, endothelial and metabolic dysfunction in unvaccinated long COVID patients. *Eur J Clin Investigation*. 2024;54(4):e14155. doi:10.1111/eci.14155
346. Ambrosino P, Sanduzzi Zamparelli S, Mosella M, et al. Clinical assessment of endothelial function in convalescent COVID-19 patients: a meta-analysis with meta-regressions. *Annals of Medicine*. 2022;54(1):3233-3248. doi:10.1080/07853890.2022.2136403
347. Theofilis P, Lampsas S, Oikonomou E, et al. Endothelial dysfunction in convalescent COVID-19 patients: Systematic review and meta-analysis. *Arch Cardiovasc Dis*. 2022;115(12):675-677. doi:10.1016/j.acvd.2022.09.001
348. Wettschureck N, Strilic B, Offermanns S. Passing the Vascular Barrier: Endothelial Signaling Processes Controlling Extravasation. *Physiological Reviews*. 2019;99(3):1467-1525. doi:10.1152/physrev.00037.2018
349. Xu S wen, Ilyas I, Weng J ping. Endothelial dysfunction in COVID-19: an overview of evidence, biomarkers, mechanisms and potential therapies. *Acta Pharmacol Sin*. 2023;44(4):695-709. doi:10.1038/s41401-022-00998-0
350. Sibila O, Perea L, Albacar N, et al. Elevated plasma levels of epithelial and endothelial cell markers in COVID-19 survivors with reduced lung diffusing capacity six months after hospital discharge. *Respir Res*. 2022;23(1):37. doi:10.1186/s12931-022-01955-5
351. Grobbelaar LM, Venter C, Vlok M, et al. SARS-CoV-2 spike protein S1 induces fibrin(ogen) resistant to fibrinolysis: implications for microclot formation in COVID-19. *Bioscience Reports*. 2021;41(8):BSR20210611. doi:10.1042/BSR20210611
352. Pretorius E, Vlok M, Venter C, et al. Persistent clotting protein pathology in Long COVID/Post-Acute Sequelae of COVID-19 (PASC) is accompanied by increased levels of antiplasmin. *Cardiovasc Diabetol*. 2021;20(1):172. doi:10.1186/s12933-021-01359-7
353. Pretorius E, Venter C, Laubscher GJ, et al. Prevalence of symptoms, comorbidities, fibrin amyloid microclots and platelet pathology in individuals with Long COVID/Post-Acute Sequelae of COVID-19 (PASC). *Cardiovasc Diabetol*. 2022;21(1):148. doi:10.1186/s12933-022-01579-5
354. Kell DB, Laubscher GJ, Pretorius E. A central role for amyloid fibrin microclots in long COVID/PASC: origins and therapeutic implications. *Biochemical Journal*. 2022;479(4):537-559. doi:10.1042/BCJ20220016
355. Kruger A, Vlok M, Turner S, et al. Proteomics of fibrin amyloid microclots in long COVID/post-acute sequelae of COVID-19 (PASC) shows many entrapped pro-inflammatory molecules that may also contribute to a failed fibrinolytic system. *Cardiovasc Diabetol*. 2022;21(1):190. doi:10.1186/s12933-022-01623-4

356. Zhang S, Liu Y, Wang X, et al. SARS-CoV-2 binds platelet ACE2 to enhance thrombosis in COVID-19. *J Hematol Oncol*. 2020;13(1):120. doi:10.1186/s13045-020-00954-7
357. Kell DB, Pretorius E. The potential role of ischaemia–reperfusion injury in chronic, relapsing diseases such as rheumatoid arthritis, Long COVID, and ME/CFS: evidence, mechanisms, and therapeutic implications. *Biochemical Journal*. 2022;479(16):1653-1708. doi:10.1042/BCJ20220154
358. Mehta P, Bunker CB, Ciurtin C, et al. Chilblain-like acral lesions in long COVID-19: management and implications for understanding microangiopathy. *The Lancet Infectious Diseases*. 2021;21(7):912. doi:10.1016/S1473-3099(21)00133-X
359. Tsampasian V, Elghazaly H, Chattopadhyay R, et al. Risk Factors Associated With Post−COVID-19 Condition: A Systematic Review and Meta-analysis. *JAMA Intern Med*. 2023;183(6):566. doi:10.1001/jamainternmed.2023.0750
360. Dennis A, Wamil M, Alberts J, et al. Multiorgan impairment in low-risk individuals with post-COVID-19 syndrome: a prospective, community-based study. *BMJ Open*. 2021;11(3):e048391. doi:10.1136/bmjopen-2020-048391
361. Dennis A, Cuthbertson DJ, Wootton D, et al. Multi-organ impairment and long COVID: a 1-year prospective, longitudinal cohort study. *J R Soc Med*. 2023;116(3):97-112. doi:10.1177/01410768231154703
362. Clouston S, Huang C, Ying J, et al. Neuroinflammatory imaging markers in white matter: insights into the cerebral consequences of post-acute sequelae of COVID-19 (PASC). *In Review*. Preprint posted online January 19, 2024. doi:10.21203/rs.3.rs-3760289/v1
363. Puntmann VO, Carerj ML, Wieters I, et al. Outcomes of Cardiovascular Magnetic Resonance Imaging in Patients Recently Recovered From Coronavirus Disease 2019 (COVID-19). *JAMA Cardiol*. 2020;5(11):1265. doi:10.1001/jamacardio.2020.3557
364. Oaklander AL, Mills AJ, Kelley M, et al. Peripheral Neuropathy Evaluations of Patients With Prolonged Long COVID. *Neurol Neuroimmunol Neuroinflamm*. 2022;9(3):e1146. doi:10.1212/NXI.0000000000001146
365. Larsen NW, Machnik JV, Seliger JM, et al. Long-COVID Postural Tachycardia Syndrome: A deep phenotyping study. *Neurology*. Preprint posted online April 29, 2025. doi:10.1101/2025.04.28.25326587
366. Flossdorf P, Haupt WF, Brunn A, et al. Long-Time Course of Idiopathic Small Fiber Neuropathy. *Eur Neurol*. 2018;79(3-4):161-165. doi:10.1159/000487717
367. Da Silva ALG, Vieira LDP, Dias LS, et al. Impact of long COVID on the heart rate variability at rest and during deep breathing maneuver. *Sci Rep*. 2023;13(1):22695. doi:10.1038/s41598-023-50276-0
368. Zanin A, Amah G, Chakroun S, et al. Parasympathetic autonomic dysfunction is more often evidenced than sympathetic autonomic dysfunction in fluctuating and polymorphic symptoms of “long-COVID” patients. *Sci Rep*. 2023;13(1):8251. doi:10.1038/s41598-023-35086-8
369. Miglis MG, Seliger J, Shaik R, Gibbons CH. A case series of cutaneous phosphorylated α-synuclein in Long-COVID POTS. *Clin Auton Res*. 2022;32(3):209-212. doi:10.1007/s10286-022-00867-0
370. Han E, Müller-Zlabinger K, Hasimbegovic E, et al. Circulating Autoantibodies Against Vasoactive Biomarkers Related to Orthostatic Intolerance in Long COVID Patients Compared to No-Long-COVID Populations: A Case-Control Study. *Biomolecules*. 2025;15(2):300. doi:10.3390/biom15020300
371. Barker-Davies RM, Ladlow P, Chamley R, Nicol E, Holdsworth DA. Reduced athletic performance post-COVID-19 is associated with reduced anaerobic threshold. *BMJ Case Rep*. 2023;16(2):e250191. doi:10.1136/bcr-2022-250191
372. Hanson BA, Visvabharathy L, Orban ZS, et al. Plasma proteomics show altered inflammatory and mitochondrial proteins in patients with neurologic symptoms of post-acute sequelae of SARS-CoV-2 infection. *Brain Behav Immun*. 2023;114:462-474. doi:10.1016/j.bbi.2023.08.022
373. Wang K, Khoramjoo M, Srinivasan K, et al. Sequential multi-omics analysis identifies clinical phenotypes and predictive biomarkers for long COVID. *Cell Reports Medicine*. 2023;4(11):101254. doi:10.1016/j.xcrm.2023.101254
374. Nikesjö F, Sayyab S, Karlsson L, et al. Defining post-acute COVID-19 syndrome (PACS) by an epigenetic biosignature in peripheral blood mononuclear cells. *Clin Epigenet*. 2022;14(1):172. doi:10.1186/s13148-022-01398-1
375. Peppercorn K, Edgar CD, Kleffmann T, Tate WP. A pilot study on the immune cell proteome of long COVID patients shows changes to physiological pathways similar to those in myalgic encephalomyelitis/chronic fatigue syndrome. *Sci Rep*. 2023;13(1):22068. doi:10.1038/s41598-023-49402-9
376. Silva BSDA, Pereira T, Minuzzi LG, et al. Mild to moderate post-COVID-19 alters markers of lymphocyte activation, exhaustion, and immunometabolic responses that can be partially associated by physical activity level— an observational sub-analysis fit- COVID study. *Front Immunol*. 2023;14:1212745. doi:10.3389/fimmu.2023.1212745
377. Ernst T, Ryan MC, Liang HJ, et al. Neuronal and Glial Metabolite Abnormalities in Participants With Persistent Neuropsychiatric Symptoms After COVID-19: A Brain Proton Magnetic Resonance Spectroscopy Study. *The Journal of Infectious Diseases*. 2023;228(11):1559-1570. doi:10.1093/infdis/jiad309
378. Ranisavljev M, Todorovic N, Ostojic J, Ostojic S. Reduced tissue creatine levels in patients with long COVID-19: A cross-sectional study. *Journal of Postgraduate Medicine*. 2023;69(3):162-163. doi:10.4103/jpgm.jpgm_65_23
379. Saito S, Shahbaz S, Luo X, et al. Metabolomic and immune alterations in long COVID patients with chronic fatigue syndrome. *Front Immunol*. 2024;15:1341843. doi:10.3389/fimmu.2024.1341843
380. Vollbracht C, Kraft K. Oxidative Stress and Hyper-Inflammation as Major Drivers of Severe COVID-19 and Long COVID: Implications for the Benefit of High-Dose Intravenous Vitamin C. *Front Pharmacol*. 2022;13:899198. doi:10.3389/fphar.2022.899198
381. Mikuteit M, Baskal S, Klawitter S, et al. Amino acids, post-translational modifications, nitric oxide, and oxidative stress in serum and urine of long COVID and ex COVID human subjects. *Amino Acids*. 2023;55(9):1173-1188. doi:10.1007/s00726-023-03305-1

382. Noonong K, Chatatikun M, Surinkaew S, et al. Mitochondrial oxidative stress, mitochondrial ROS storms in long COVID pathogenesis. *Front Immunol*. 2023;14:1275001. doi:10.3389/fimmu.2023.1275001
383. Szögi T, Borsos BN, Masic D, et al. Novel biomarkers of mitochondrial dysfunction in Long COVID patients. *GeroScience*. 2024;47(2):2245-2261. doi:10.1007/s11357-024-01398-4
384. Hansen KS, Jørgensen SE, Cömert C, et al. Genetic Landscape and Mitochondrial Metabolic Dysregulation in Patients Suffering From Severe Long COVID. *J Med Virol*. 2025;97(3):e70275. doi:10.1002/jmv.70275
385. Kumar A, Choudhary A, Munshi A. Epigenetic reprogramming of mtDNA and its etiology in mitochondrial diseases. *J Physiol Biochem*. 2024;80(4):727-741. doi:10.1007/s13105-024-01032-z
386. Ando M, Uehara I, Kogure K, et al. Interleukin 6 Enhances Glycolysis through Expression of the Glycolytic Enzymes Hexokinase 2 and 6-Phosphofructo-2-kinase/Fructose-2,6-bisphosphatase-3. *J Nippon Med Sch*. 2010;77(2):97-105. doi:10.1272/jnms.77.97
387. Park H, Jeoung NH. Inflammation increases pyruvate dehydrogenase kinase 4 (PDK4) expression via the Jun N-Terminal Kinase (JNK) pathway in C2C12 cells. *Biochemical and Biophysical Research Communications*. 2016;469(4):1049-1054. doi:10.1016/j.bbrc.2015.12.113
388. Swanson KV, Deng M, Ting JPY. The NLRP3 inflammasome: molecular activation and regulation to therapeutics. *Nat Rev Immunol*. 2019;19(8):477-489. doi:10.1038/s41577-019-0165-0
389. Manosalva C, Quiroga J, Hidalgo AI, et al. Role of Lactate in Inflammatory Processes: Friend or Foe. *Front Immunol*. 2022;12:808799. doi:10.3389/fimmu.2021.808799
390. Kim J, Xu M, Xo R, et al. Mitochondrial DNA damage is involved in apoptosis caused by pro-inflammatory cytokines in human OA chondrocytes. *Osteoarthritis and Cartilage*. 2010;18(3):424-432. doi:10.1016/j.joca.2009.09.008
391. Li X, Fang P, Mai J, Choi ET, Wang H, Yang X feng. Targeting mitochondrial reactive oxygen species as novel therapy for inflammatory diseases and cancers. *J Hematol Oncol*. 2013;6(1):19. doi:10.1186/1756-8722-6-19
392. Elesela S, Lukacs NW. Role of Mitochondria in Viral Infections. *Life*. 2021;11(3):232. doi:10.3390/life11030232
393. Valdés-Aguayo JJ, Garza-Veloz I, Badillo-Almaráz JI, et al. Mitochondria and Mitochondrial DNA: Key Elements in the Pathogenesis and Exacerbation of the Inflammatory State Caused by COVID-19. *Medicina*. 2021;57(9):928. doi:10.3390/medicina57090928
394. Li X, Hou P, Ma W, et al. SARS-CoV-2 ORF10 suppresses the antiviral innate immune response by degrading MAVS through mitophagy. *Cell Mol Immunol*. 2022;19(1):67-78. doi:10.1038/s41423-021-00807-4
395. World Health Organization. *Therapeutics and COVID-19: Living Guideline, August 2025*. World Health Organization; 2025. doi:10.2471/B09540
396. World Health Organization. *Clinical Management of COVID-19: Living Guideline, June 2025*. World Health Organization; 2025. doi:10.2471/B09467
397. De Paepe A, Vlieghe E, Brusselaers N, et al. COVID-19 in three waves in a tertiary referral hospital in Belgium: a comparison of patient characteristics, management, and outcome. *Virol J*. 2024;21(1):119. doi:10.1186/s12985-024-02360-8

Citation: Ward *et al.* HYGIEIA: HYpothesizing the Genesis of Infectious Diseases and Epidemics through an Integrated Systems Biology Approach. *Viruses* **2022**, *14*, 1373. https://doi.org/10.3390/v14071373

Section II HYGIEIA: HYpothesizing the Genesis of Infectious diseases and Epidemics through an Integrated systems biology Approach

Bradley Ward [1,2,†], Jean Cyr Yombi [3,†], Jean-Luc Balligand [4], Patrice D. Cani [5], Jean-François Collet [6], Julien de Greef [2,3], Joseph P. Dewulf [2,7,8], Laurent Gatto [9], Vincent Haufroid [2,7], Sébastien Jodogne [10], Benoît Kabamba [7,11], Sébastien Pyr dit Ruys [1], Didier Vertommen [12], Laure Elens [1,2,*,‡] and Leïla Belkhir [2,3,*,‡]

1 Integrated Pharmacometrics, Pharmacogenomics and Pharmacokinetics Group (PMGK), Louvain Drug Research Institute (LDRI), UCLouvain, Université Catholique de Louvain, Brussels, 1200, Belgium; bradley.ward@uclouvain.be (B.W.); sebastien.pyrditruys@uclouvain.be (S.P.d.R.)
2 Louvain Center for Toxicology and Applied Pharmacology (LTAP), Institut de Recherche Expérimentale et Clinique (IREC), UCLouvain, Université Catholique de Louvain, Brussels, 1200, Belgium; julien.degreef@saintluc.uclouvain.be (J.d.G.); joseph.dewulf@saintluc.uclouvain.be (J.P.D.); vincent.haufroid@saintluc.uclouvain.be (V.H.)
3 Department of Internal Medicine, Cliniques Universitaires Saint-Luc, UCLouvain, Université Catholique de Louvain, Brussels, 1200, Belgium; jean.yombi@uclouvain.be
4 WELBIO (Walloon Excellence in Life Sciences and Biotechnology), Pole of Pharmacology and Therapeutics (FATH), Institut de Recherche Experimentale et Clinique (IREC), Cliniques Universitaires Saint-Luc, UCLouvain, Université Catholique de Louvain, Brussels, 1200, Belgium; jean-luc.balligand@uclouvain.be
5 WELBIO (Walloon Excellence in Life Sciences and Biotechnology), Metabolism and Nutrition Research Group, Louvain Drug Research Institute (LDRI), UCLouvain, Université Catholique de Louvain, Brussels, 1200, Belgium; patrice.cani@uclouvain.be
6 WELBIO (Walloon Excellence in Life Sciences and Biotechnology), de Duve Institute, UCLouvain, Université Catholique de Louvain, Brussels, 1200, Belgium; jean-francois.collet@uclouvain.be
7 Department of Laboratory Medicine, Cliniques Universitaires Saint-Luc, UCLouvain, Université Catholique de Louvain, Brussels, 1200, Belgium; benoit.kabamba@saintluc.uclouvain.be
8 Department of Biochemistry, de Duve Institute, UCLouvain, Université Catholique de Louvain, Brussels, 1200, Belgium
9 Computational Biology and Bioinformatics Unit (CBIO), de Duve Institute, UCLouvain, Université Catholique de Louvain, Brussels, 1200, Belgium; laurent.gatto@uclouvain.be
10 Computer Science and Engineering Department (INGI), Institute of Information and Communication Technologies, Electronics and Applied Mathematics (ICTEAM), UCLouvain, Université Catholique de Louvain, Louvain-la-Neuve, 1348, Belgium; sebastien.jodogne@uclouvain.be
11 Pôle de Microbiologie, Institut de Recherche Expérimentale et Clinique, UCLouvain, Université Catholique de Louvain, Brussels, 1200, Belgium
12 de Duve Institute, and MASSPROT Platform, UCLouvain, Université Catholique de Louvain, Brussels, 1200, Belgium; didier.vertommen@uclouvain.be
* Correspondence: laure.elens@uclouvain.be (L.E.); leila.belkhir@saintluc.uclouvain.be (L.B.)
†‡ These authors contributed equally to this work.



Abstract

More than two years on, the COVID-19 pandemic continues to wreak havoc around the world and has battle-tested the pandemic-situation responses of all major global governments. Two key areas of investigation that are still unclear are: the molecular mechanisms that lead to heterogenic patient outcomes, and the causes of Post COVID condition (AKA Long-COVID). In this paper, we introduce the HYGIEIA project, designed to respond to the enormous challenges of the COVID-19 pandemic through a multi-omic approach supported by network medicine. It is hoped that in addition to investigating COVID-19, the logistics deployed within this project will be applicable to other infectious agents, pandemic-type situations, and also other complex, non-infectious diseases. Here, we first look at previous research into COVID-19 in the context of the proteome, metabolome, transcriptome, microbiome, host genome, and viral genome. We then discuss a proposed methodology for a large-scale multi-omic longitudinal study to investigate the aforementioned biological strata through high-throughput sequencing (HTS) and mass-spectrometry (MS) technologies. Lastly, we discuss how a network medicine approach can be used to analyze the data and make meaningful discoveries, with the final aim being the translation of these discoveries into the clinics to improve patient care.

Keywords: COVID-19; post COVID condition; proteomics; metabolomics; genomics; metagenomics; transcriptomics; network medicine

1. Introduction

1.1. Clinical Problem and Phenotype Definition

COVID-19 is a multisystemic disease that is characterized by a complex heterogenous clinical pattern—the so called "infectious phenotype". In the time since its initial outbreak in Wuhan at the end of 2019, the pathogen responsible for this disease, SARS-CoV-2, has spread to every country on Earth, infecting over 500 million people, and leading to the death of over 6 million people [1]. COVID-19 symptoms can range from asymptomatic/mild in about 80% of cases, to severe illness in around 5% of cases, potentially resulting in death (exact percentages depending on infectious variant and underlying immunity) [2]. Although vaccinations and improved patient care have greatly reduced the burden of this disease, fatality rates still remain extremely high with a global average of 138 deaths per 100,000 population; for reference, influenza, which is often compared to COVID-19, accounts for between 4.1 and 9.3 deaths per 100,000 [3,4].

1.1.1. Susceptibility to SARS-CoV-2 and Clinical Presentations

Once SARS-CoV-2 infection is established, viral replication begins within the nasopharyngeal mucosa before spreading towards the lower respiratory tract. The trimeric spike (S) protein, which covers the surface of SARS-CoV-2, binds to the host cell receptor angiotensin-converting enzyme 2 (ACE-2) and mediates viral cell entry [5]. Through this mechanism, SARS-CoV-2 is capable of infecting host tissues within the lungs, where ACE-2 is highly expressed, as well as other tissues which express ACE-2 such as the heart, kidneys, liver, and brain [6,7].

Among symptomatic patients, the lungs are the organs most affected by the disease, causing respiratory failure which may progress to acute respiratory distress syndrome (ARDS) requiring mechanical ventilation. This is frequently accompanied by an overwhelming inflammatory reaction (cytokine storm) [8,9]. Risk factors of clinical severity and fatality have been identified and include older age and/or

comorbidities, of which diabetes, obesity, hypertension, cardiovascular, and chronic kidney diseases are the most frequent [10]. Intriguingly, phenotype variability goes beyond severity: clinical data have promptly demonstrated that COVID-19 is a multisystem disease and can present with thrombo-embolic, kidney or neurological symptoms [11–13].

1.1.2. Post COVID Condition

Most COVID-19 patients with mild to moderate disease progressions will usually recover after two to three weeks, but those patients presenting with severe disease usually take at least six weeks to recover. Around 54% and 34% of hospitalized and non-hospitalized patients respectively, will then continue to persist with COVID-19-related symptoms, most commonly including fatigue and muscle weakness, dyspnea, joint and chest pain, and neurocognitive impairment [14,15]. Interestingly, a literature report from the Belgian Health Care Knowledge Center showed an increasing trend of the incidence of displaying post COVID symptoms depending on study follow-up, with a median incidence of 17% (non-hospitalized patients) and 50.9% (hospitalized patients) at 1–3 months, increasing to 25% (non-hospitalized patients) and 62% (hospitalized patients) at 6 months+ follow up [16].

Several studies put the incidence of displaying persistent post COVID symptoms between 30% and 90% at 6 months past initial disease onset [17]. The pathogenesis of post COVID condition is still unclear, but it has been observed to more likely affect patients that suffered severe COVID-19 or those that required hospital admission [18]. A higher incidence is also seen in patients that presented with more than five symptoms during the acute phase of the disease, female patients, obese patients, and those patients with diabetes [19].

Recently, a multi-omic study with a focus on single-cell-omics by Su et al. [20] investigated post COVID conditions at between 2- and 3-months post COVID-19 diagnosis. They reported 61% of patients to have at least one symptom and also

reported four main risk factors to develop post COVID symptoms: type 2 diabetes, reactivated EBV, auto-antibodies, and SARS-CoV-2 blood viral load. These risk factors have the potential to be used to predict patient risk to developing post COVID condition if measured at diagnosis. For example, around half of the patients exhibited auto antibodies at follow-up, also had them at diagnosis, yet the vast majority of these patients did not have any documented autoimmune conditions, suggesting the presence of a pre-existing subclinical condition in these patients. In addition to these risk factors, the study was also able to group patients into four distinct immune endpoints: type 1, type 2, intermediate, and naïve. These endpoints were characterized by unique immune system responses, COVID-19 disease severity, and risk of developing post COVID condition. However, one major drawback to this study was the lack of a genomic aspect, and so any links between host genomics and presence of auto-antibodies or patient immune endpoint groupings cannot be inferred.

In another study looking to identify predictors of post COVID condition, by Cervia et al. [21], a specific immunoglobulin signature during COVID-19 infection was identified in patients who later went on to develop post COVID condition. Using this signature in combination with certain clinical factors, the team were thus able to develop a post COVID prediction model for hospitalized patients.

These studies add to mounting research suggesting post COVID condition is a result of a mix of viral and host factors, such as the host microbiome or residual inflammation [22,23], and highlight the necessity of large scale multi-omic investigations that are able to consider host and viral factors in the context of the genomics, transcriptomics, proteomics, metabolomics, and metagenomics.

1.2. Previous Research and Gaps in Knowledge

The high morbidity and mortality rates of SARS-CoV-2 since the beginning of the pandemic have gradually fallen through a combination of vaccines, milder viral

strains, and the rapid translation of research to clinical settings. Currently, most governments are relying on their vaccination programs to reduce the strain on their healthcare systems. Yet, with the continued emergence of new variants of concern presenting with antibody-escaping features, hospitalizations and reinfection risks continue to increase whilst vaccine efficacy decreases over time (especially against symptomatic infections), prompting governments to recommend "booster shots" in an effort to reinforce their populations immunity [24,25]. In consequence, there is an urgent need to identify and thoroughly map disease pathways at all levels: from the genome and metagenome, to the transcriptome, proteome, and metabolome, in order to elucidate SARS-CoV-2 specific therapeutic targets and biomarkers. Despite the global research effort into COVID-19 pathogenesis, most research tends to focus on single-omic datasets, such as the genome or proteome; even the few articles that have adopted a multi-omic design tend to only investigate two [26–28] or three [29–31] omic-levels. This has led to many gaps in our knowledge of COVID-19 pathogenic pathways, whereby parts of a pathway have been identified, but upstream and downstream consequences are still unknown. This project thus aims to fill these gaps using an unbiased approach to discover novel therapeutic targets and vaccination strategies as well as predictive/prognostic biomarkers.

1.2.1. Viral Genome

Owing to its proofreading gene, *nsp14*, SARS-CoV-2 is characterized by a stable genome [32]. Nevertheless, as SARS-CoV-2 continues to circulate around the world, mutations and variants have emerged. Regarding some notable current and previous variants of concern (as of 01/06/22): Alpha (B.1.1.7), Beta (B.1.351), Gamma (P.1), and Delta (B.1.617.2) have all shown increased transmissibility and severity [33–37], whilst for the Omicron variants (BA.1 and BA.2), transmissibility is also increased, but severity appears to be reduced, especially among populations with a high level of immunity [38–42]. The most recently added variants, two more

Omicron variants, BA.4 and BA.5, first detected in South Africa in January and February 2022 respectively, have since become the dominant variants there, while the Portuguese National Institute of Health estimated that BA.5 accounted for around 37% of positive cases in Portugal as of 8 May 2022, and the ECDC suggests it will likely become the dominant variant in Europe within the next few months [43]. The observed growth advantage of these lineages is likely due to improved immune evasion compared to previous omicron variants, resulting in increased transmissibility, but no observed impact on severity [44,45]. This appears to be in line with the virulence-transmissibility evolutionary trade-off theory whereby it is expected that the emergence of new dominating viral variants will favor increased transmissibility over virulence.

Initial research into viral variant pathogenicity seems to suggest they induce distinct humoral responses and transcriptional profiles [46,47]. However, more research is required in order to identify variant-specific molecules for therapeutic and sanitary countermeasures.

1.2.2. Nasopharyngeal Microbiome

For COVID-19 patients, pathogenic respiratory co-infections have been found frequently in a number of studies, with between 7–14% of hospitalized patients presenting with bacterial co-infections [48,49]. For those patients admitted to the ICU, this number has been seen to rise up to 41% of patients presenting with secondary co-infections, although other studies have also noted lower numbers of 13.9% for ICU patients [50,51]. However, most studies only include targeted diagnosis and the majority tends to focus on bacteria, excluding co-infections of viruses, archaea, and fungal species which make up a sizeable proportion of the microbiome diversity.

Conversely, metagenomic high throughput sequencing (mHTS) has the ability to unbiasedly detect all microorganisms in a sample, providing extra information on

the composition of the microbiome. Using such methods, the diversity of the respiratory microbiome in COVID-19 patients has been observed to decrease by 38% compared to healthy individuals, with a decrease in commensal bacteria and an increase of opportunistic pathogens [52]. Due to a lack of multi-omic studies investigating both host -omics and the microbiome, the consequences of this dysbiosis on COVID-19 progression and severity is yet to be fully characterized. It could be that opportunistic pathogens further exacerbate lung damage, or, it may be due to a reduction in commensal species involved in priming the innate immune system, weakening the patient's immune response [53].

Further, recent evidence has found the microbiome to strongly influence the metabolome around the body and has been associated with cardiovascular disease, drug response, and asthma [54–56]. Specifically, to COVID-19, it has been seen that respiratory microbiome changes due to SARS-CoV-2 are associated with transcriptomic differences in several metabolic pathways [57]. This perhaps reflects metabolomic differences associated with COVID-19 pathogenesis and severity, but as no multi-omic studies have been conducted to investigate this link between the metabolome and microbiome, this currently remains speculation.

1.2.3. Host Transcriptome

In COVID-19 patients, suppression of interferon (IFN) response has emerged as a major clinical determinant, with a complete loss of response associated with the most severe cases; a key differentiator from severe acute respiratory syndrome (SARS) and Middle East respiratory syndrome (MERS) [58–60]. The non-structural proteins NSP 1, 8, 9, and 16, have been indicated as partially responsible for this phenomenon via global suppression of mRNA splicing and translation, and via interfering with membrane trafficking of proteins [61]. Further, enhanced nuclear factor kappa-B (NF-κB) signaling, through a number of SARS-CoV-2 upregulated pathways, has been shown to lead to excessive inflammation, with inhibition of such

molecular processes resulting in alleviation of severe symptoms [62–64]. However, more research is required to better understand these aforementioned pathways in the context of COVID-19 pathogenesis, particularly AGE-RAGE signaling which is associated with COVID-19 comorbidities and consequences like diabetes, inflammatory disease, and acute respiratory distress syndrome (ARDS) [63,65–67]. Also, of interest is the olfactory transduction pathway which is significantly activated during COVID-19 disease; dysfunction of this pathway (resulting in the loss of smell symptom) has been associated with faster recovery, perhaps due to the ultra-rapid antiviral response observed in olfactory receptor neurons [63,68–70]. This link begs further study, and may partially explain why older patients who tend to poses fewer such neurons, have a suppressed earlier antiviral response and higher disease severity in general.

Additional explanations for the increased severity seen in older populations come in the form of age-induced differences in gene expression. Both TMPRSS2 and ACE2, receptors recognized by the SARS-CoV-2 spike protein, show an increased expression with age in mammals, which may be partially responsible for the increased disease severity seen in these patients [71]. Further to this, a study by Mercatelli et al. [72], identified significant overlaps between SARS-CoV-2 interacting proteins and host age-related proteins, with viral infection affecting aging molecular mechanisms centered around eight proteins. Of these proteins, EEF2, NPM1, HMGA1, APEX1, and CHEK1, were found to have an age-dependent modulation in the lung tissues of males, whilst APEX1 was shown to have an age-dependent modulation in females. Such findings suggest a potential mechanism by which age-/sex-dependent severity of COVID-19 may manifest.

Other dysregulated genes include *ACO3*, *ATL3*, *S100A8*, *S100A9*, *IL-1B*, *IL-6*, *IL-8*, *TXNIP*, *ARRDC3*, *ACE-2*, and the *MHC-II* family of genes, and remain of interest due to their roles in cytokine storm development, inflammation, antigen

presentation, viral replication, and immune evasion; 416 genes in total were seen to be deregulated specifically due to SARS-CoV-2 in a transcriptomic analysis [73–78]. This gene dysregulation is likely linked to adherent ncRNA dysregulation also seen in SARS-CoV-2 infections [79–81]. Viral transcript interaction with human ncRNA, as well as viral ncRNA, can enhance viral evasion of the immune system, enhance replication, promote transcript stability, and/or produce alternative transcripts to enhance virulence [82,83]. Specifically, *ORF-6*, *-7a*, and *-7b* contain complementary sequences to a number of ncRNAs involved in the innate/acquired immune response, antibody production, vaccine response, disease severity, and metabolic pathway activation [84–88]. The association of these viral transcripts to human ncRNAs has mainly been demonstrated *in silico* and remain to be studied *in vivo*/*in vitro*.

For further analysis of mRNA and ncRNA, multi-omic studies featuring transcriptomic and proteomic natures will be essential due to the lack of correlation between the two-omic levels, as observed in numerous studies [89–95].

1.2.4. Host Proteomics and Metabolomics

The dysregulation seen within the genome, transcriptome, and microbiome, is also reflected in the proteome and metabolome. This dysregulation can lead to the identification of circulating biomarkers which play critical roles in clinical decision making. Indeed, a number of studies have investigated protein/metabolite biomarkers in relation to COVID-19, identified those that are differentially expressed, and presented molecular signatures that can either differentiate severity or predict progression [96]. However, although these molecular signatures tend to relate to similar pathways, such as platelet degranulation, complement, or coagulation, the specific protein/metabolite patterns in each study are almost never in agreement. This is perhaps related to the tendency of these studies to use lower patient numbers (ranging between 8 and 69) or to use targeted identification

techniques [97–105]. Unbiased, shotgun mass spectrometry techniques with larger patient numbers could potentially overcome this discordance, and result in much more applicable biomarker patterns. Additionally, a multi-omic exploration of such a cohort would be able to identify biomarkers across all strata, further strengthening the credibility of such observed molecular patterns.

1.2.5. Host Genomics

Numerous genome studies have been launched by a variety of institutions. From these studies, several genes/loci have been identified to impact the etiology of COVID-19; of note is the 3p21.31 locus, *OAS 1/2/3* located at 12q24.13, and the ABO loci which were highlighted early on in the COVID-19 pandemic [106]. Both 3p21.31 and 12q24.13 carry haplotypes of Neanderthals origin, which tend to be more difficult in terms of disentangling the causal genetic variants due to their size (often spanning tens of thousands of bases) [107,108].

The protective *OAS 1/2/3* alleles on 12q24.13, which confer around a 23% reduction in the risk of becoming critically ill from COVID-19 [109]. These genes encode enzymes catalyzing short polyadenylate synthesis, this subsequently activates ribonuclease L which degrades intracellular double-stranded RNA and triggers other antiviral mechanisms [110]. A medallion randomization study found higher levels of circulating OAS 1 levels were associated with the observed reduced risk, whilst other transcriptome-wide evidence suggested a stronger association with OAS 3 levels [111,112]. However, a recent study pinpoints to a SNP at rs10774671, located in a splice acceptor site at exon 7 of *OAS 1* [109]. Polymorphisms at this site determines the length of the protein encoded by *OAS 1*, with the protective allele (G) resulting in a longer and more active enzyme, increasing ribonuclease L activation and antiviral countermeasures.

Moving onto the locus 3p21.31, a major common risk factor is rs10490770. Carriers of the risk allele (C) are at increased risk of all-cause mortality and

development of COVID-19 complications such as severe respiratory failure, venous thromboembolism, and hepatic injury [113]. An age dependent impact was also observed, with a more pronounced effect of the risk allele observed in individuals under 60 years of age. Importantly, this risk allele is commonly seen among European (allele frequency = 14.4%) and South Asian (allele frequency = 47.1%) populations, as well as in Admixed Americans, African, and East Asian populations to a lesser extent (allele frequency = 9.5%, 2.4%, and 0.4% respectively). Although specific causal links for 3p21.31 are not yet established, evidence points to variants of *SLC6A20* (which interacts with ACE2) and *CXCR6* (involved in T-cell recruitment) to explain the increased susceptibility and severity [114].

For the ABO locus, blood group O has been correlated with reduced susceptibility, perhaps attributed to anti-A IgG protection [106,115,116]. Other highlighted genetic risk factors include *INFAR2*, *DPP9*, *TYK2*, *ACE2*, and the *HLA* gene family [111,117,118]. These genes are all involved in immune signaling, antigen presentation, and/or cell entry receptors [119–121].

One of the largest genome sequencing studies, which investigated over 7000 critical COVID-19 cases and almost 50,000 controls was able to identify 16 new COVID-19 associated variants [122]. Five of these variants have direct roles in interferon signaling, this includes a probable destabilizing amino acid substitution in *IFNA10,* as well as another variant resulting in a reduction of a subunit of its receptor, *IFNAR2*. The results of the study provide robust evidence that reduced interferon signaling increases patient susceptibility to developing critical COVID-19. In addition to this, the study also identified variants of genes controlling levels of coagulation factor VIII to be associated with critical illness, which may explain some of the clotting abnormalities seen in severe COVID-19.

For most variants and genes associated with COVID susceptibility/severity, questions remain surrounding their causal links with the disease, and how changes within the genome reflect disease pathogenesis within the patient.

1.2.6. Network Integration

Classical reductionism continues to be challenged amid mounting evidence of the importance of looking instead at the numerous interactions between biological components. Previously, such a narrow approach was demanded due to the limitations in data collection and analysis. Now however, multi-omic data can be integrated via computational networks and analyzed to better explain classification, improve predictions, or understand complex molecular pathways that would remain hidden for single-omic studies [123–125]. Song et al. [126] has demonstrated the benefits of such an approach in a study that identified two FDA-approved drugs suitable for repurposing to treat cardiovascular calcification, a pathology that has been under investigation for over 80 years. Previous attempts of this approach in the context of COVID-19 has resulted in improved therapeutic options, novel biomarkers, and enhanced pathophysiological knowledge, yet most studies featured low patient numbers and only included limited biological strata [28–30,104]. Below we present the largest, most detailed multi-omic analysis of a COVID-19 patient cohort to date, featuring data from all levels (host and viral genome, transcriptome, metagenome, proteome, and metabolome). Such an effort holds the promise of revealing novel components, crucial interactions, and emergent properties of this disease which would otherwise remain hidden.

2. Materials and Methods

2.1. Cohort Population, Inclusion Criteria, and Sampling Methodology

The general scheme of the clinical study and sample collection is depicted in figure 1. Patient recruitment is currently ongoing with a planned 225 total patients and 50 total controls expected to be recruited from Cliniques Universitaires Saint-Luc (CUSL), Brussels, Belgium. In addition, patients are also being recruited from other hospitals in the Brussels and Wallonie region of Belgium in a multi-centric effort, and so total cohort size could potentially exceed this. The patient population will be split into three groups comprised of 75 individuals each: mild/moderate, severe, and critical. The control population will be split into two groups: 25 respiratory failure patients and 25 healthy individuals.

Patients will be >18 years old and provide informed consent. COVID-19 status will be determined via a SARS-CoV-2 RT-PCR test performed on nasopharyngeal (NP) swabs. Patient grouping will be based on CDC disease severity guidelines [127]. Respiratory failure controls should have a diagnosis of hypoxemic respiratory failure from an infectious origin (excluding SARS-CoV-2), and should not have tested SARS-CoV-2 positive within 6 months. Healthy controls should present without respiratory failure (i.e., SpO2 > 93%), and should not have tested SARS-CoV-2 positive within 6 months. Biological samples will consist of whole EDTA blood, Tempus™ Blood RNA Tube, heparinized plasma, and NP swabs, taken in the first instance at the time of patient inclusion during the acute phase, and at the second instance around three months later. Later time points may be added for patients beyond three months, however, the principle focus of this project is the investigation of patients displaying post COVID condition at three months after diagnosis. All samples will be stored at −80 °C until patient recruitment is finished and the multi-omic analysis begins.

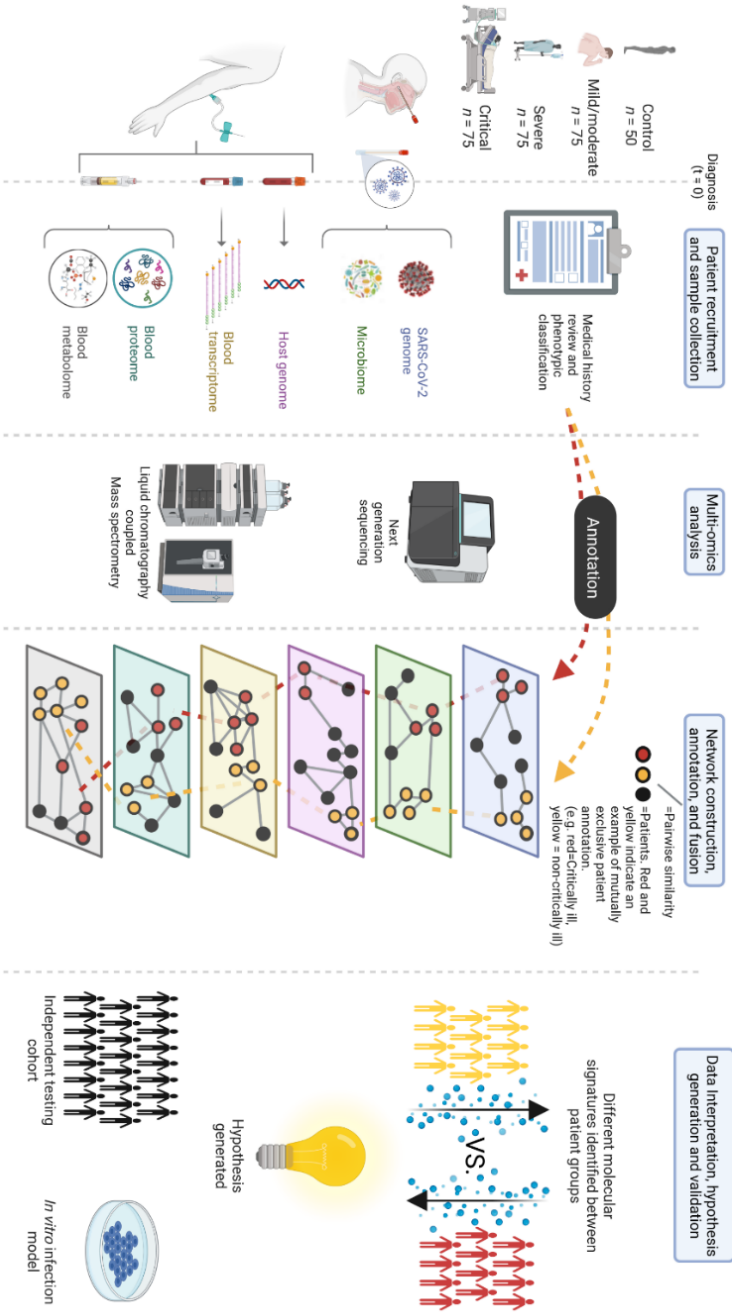


Figure 1. General scheme of the study, from patient recruitment at diagnosis, to -omics analysis, network fusion, data interpretation, and finally hypothesis generation and validation (through cohorts or infection models). (Created with BioRender.com©).

Sample Size Considerations

In this project, we guarantee complete -omics exploration of 225 patients with ideally, 75 each critically, severely and mildly/moderately ill patients and 50 controls. These realistic figures are based on sample inventory done while preparing this project and the ongoing patient recruitment rate at CUSL.

To compare this cohort size to similar multi-omic approaches used in the context of e.g., Alzheimer [128], cancer [129], or cardiovascular disease [130–132], we can see these studies tend to be characterized by smaller (n = 25, n = 63, n = 157) or slightly larger patient cohort sizes (n = 276, n = 364). In addition to this, COVID-19 multi-omic studies also tend to be characterized by both smaller cohort sizes (n = 14, n = 20, n = 102, n = 209), as well as the exploration of a reduced number of -omic strata in comparison to this proposed study [20,28–30]. Further, focusing specifically on post COVID condition, there is again a tendency for studies to either investigate smaller cohort sizes or cohorts of similar size (n = 103, n = 106, n = 121, n = 134, n = 143, n = 165, n = 215 [18,21–23,133–135]). Taken together, it is likely that the size and detail of this study will achieve not just similar, but also more significant results in comparison to these aforementioned studies.

2.2. Multi-Omic Analysis

All analyses will be conducted on patient samples collected at the point of diagnosis, as well as on patient samples collected during follow-ups.

2.2.1. Viral Genotyping

Viral RNA will be extracted from the NP swab sample using the QIAamp Viral RNA Kits (Qiagen, Hilden, Germany). qPCR will be used to assess SARS-CoV-2 viral load, and if viral load is sufficient for sequencing, library preparation will then be performed using the Illumina COVIDSeq Kit (Illumina, San Diego, USA), and sequencing will be carried out on an Illumina NextSeq 1000 system.

2.2.2. Shotgun mHTS

Both DNA and RNA of bacteria, fungi, and viruses will be extracted from the NP swab sample using the AllPrep DNA/RNA kit (Qiagen, Hilden, Germany), and the RNA will then undergo reverse transcription via the QuantiTect Reverse Transcription Kit (Qiagen, Hilden, Germany). Both DNA and cDNA libraries will be prepared using the Illumina DNA prep kit (Illumina, San Diego, USA), and sequencing will be carried out on an Illumina NextSeq 1000 system.

2.2.3. Host Genomics

DNA will be extracted from whole EDTA blood via the QIAamp DNA blood kit (Qiagen, Hilden, Germany), library preparation will be performed using the Illumina Truseq DNA Exome kit (Illumina, San Diego, USA), and sequencing will be carried out on an Illumina NovaSeq 6000 system.

2.2.4. Whole Transcriptomic Shotgun RNAseq

RNA will be extracted from whole blood (Tempus™ Blood RNA Tube (Thermo Fisher Scientific, Waltham, USA) via the Tempus™ Spin RNA Isolation kit (Thermo Fisher Scientific, Waltham, USA), followed by in-column DNase treatment using the RNA Clean & Concentrator™ kit (Zymo Research, Irvine, USA). Library preparation will be performed using the Illumina Stranded Total RNA Prep (Illumina, San Diego, USA) and sequencing will be carried out on an Illumina NovaSeq 6000 system.

2.2.5. Classical Shotgun Bottom-Up Proteomic Profiling

Plasma samples will first undergo protein depletion using the TOP 14 Abundant Protein Depletion kit (Thermo Fisher Scientific, Waltham, USA), using a ratio of 500 μL depletion resin to 18 μL plasma. Once depleted, samples will then be heated to 95 °C for 5 min, cooled, and 300 μL of the sample will be added to a separate LoBind Eppendorf (Thermo Fisher Scientific, Waltham, USA). DTT will then be added to a final concentration of 5 mM and incubated at 56 °C for 1 h at 1000

RPM agitation (Thermomixer C). Following this, chloroacetamide will be added to a final concentration of 50 mM and incubated in the dark at room temperature for 30 min. After incubation, 100% TCA will be added to a final concentration of 15% and the sample will be vigorously vortexed (10 s) and spun down, followed by a 30-min incubation on ice. After, the tube will be centrifuged at 4000× *g* for 5 min, supernatant discarded, and three washes performed as follows: 500 µL 100% acetone added (chilled to −20 °C), sonicated at 37 kHz (pulsed) for 2 min, centrifuged at 4000× *g* for 5 min, and supernatant discarded. After three repetitions, the tube will air dry for 10 min under a fume hood to ensure all acetone is removed, and the pellet reconstituted in 75 µL TEAB 50 mM by two repetitions of sonicating for 2 min and briefly vortexing (10 s). Finally, trypsin will be added in a 1:50 protease:protein ratio and incubated overnight at 37 °C with 750RPM agitation.

Once incubated, the sample will then be split into fractions using the Pierce high pH reversed-phase peptide fractionation kit (Thermo Fisher Scientific, Waltham, USA). Fractions will then be freeze-dried and resuspended in 20 µL 3.5% ACN/0.1% TFA and finally a total of 1.2 µg peptide in 8 µL of buffer will be analyzed by reverse phase chromatography coupled to mass spectrometry on an Orbitrap Exploris 240 system coupled with an Ultimate 3000 RSnano LC system.

2.2.6. Non-Targeted Metabolomic Profiling

A volume of plasma will be added to a LoBind Eppendorf followed by 3 volumes of 100% acetonitrile (MS grade). Samples will then be vortexed vigorously for 10 s and spun-down, then incubated at −20 °C overnight. Following this, samples are then centrifuged at 10,000× *g* at 4 °C for 10 min, and the upper-phase will be transferred to a new LoBind tube and mixed gently to homogenize. Then the homogenate will be divided into four equal parts, transferred to new Eppendorf tubes and dried down on a heating block at 30 °C coupled with a nitrogen flush system. Two tubes will then be resuspended in 50% ACN/0.1% formic acid for

Reverse-phase based UPLC and two tubes will be resuspended in 95% ACN/0.1% formic acid and 10 mM ammonium formate for HILIC based UPLC. Samples will then be centrifuged at 10,000× *g* at 4 °C for 5 min, after which, the supernatant will be transferred to vials ready for injection.

Once samples are ready, they will then be analyzed on a Synapt-XS Q-ToF mass spectrometer (Waters) calibrated in resolution mode, coupled with an Acquity Premier UPLC system. Reverse-phase and HILIC samples will be analyzed on the UPLC-Q-ToF system coupled with an Acquity Premier HSS T3 2.1 × 100 mm, 1.8 μm column (Waters *p*/*n* 186009468) and an Acquity Premier BEH Amide 2.1 × 100 mm, 1.7 μm column (Waters *p*/*n* 186009505), respectively. For both methods, one vial will be analyzed in positive electrospray mode, and the other will be analyzed in negative ionization mode.

2.3. Network Construction and Multi-Omic Integration

As data are generated, network-based statistical methods (such as the nearest neighbor algorithm) will be used to construct individual networks for each -omic data described above. A visual for the proposed networks can be seen in figure 2. Nodes will represent patients, and the edges connecting them will be based on pairwise similarities of the -omic data. This will result in patients clustering based on -omic measurements, signaling matching molecular signatures. These clusters will then be annotated with defined phenotypes and outcomes, for example, patients who did or did not develop critical illness. Differential analysis of these clusters would then identify molecules/microbes/proteins/genes presenting different patterns between groups. The final step of multi-omic integration would consist of fusing all the individual networks together. The networks will be fused by similarity network fusion (SNF) [136], and a feature ranking scheme [137] will sort the features according to their network contribution for a specified patient outcome, generating a ranking list of the most important features/pathways that can be investigated. Such

an approach will not only be used to discover differences between patient groups (i.e., mild/moderate vs. severe), but will also be used to find multi-omic differences between the acute and post-COVID phases of patients, shining a new light on potential causes or biomarkers of the post COVID sequelae.

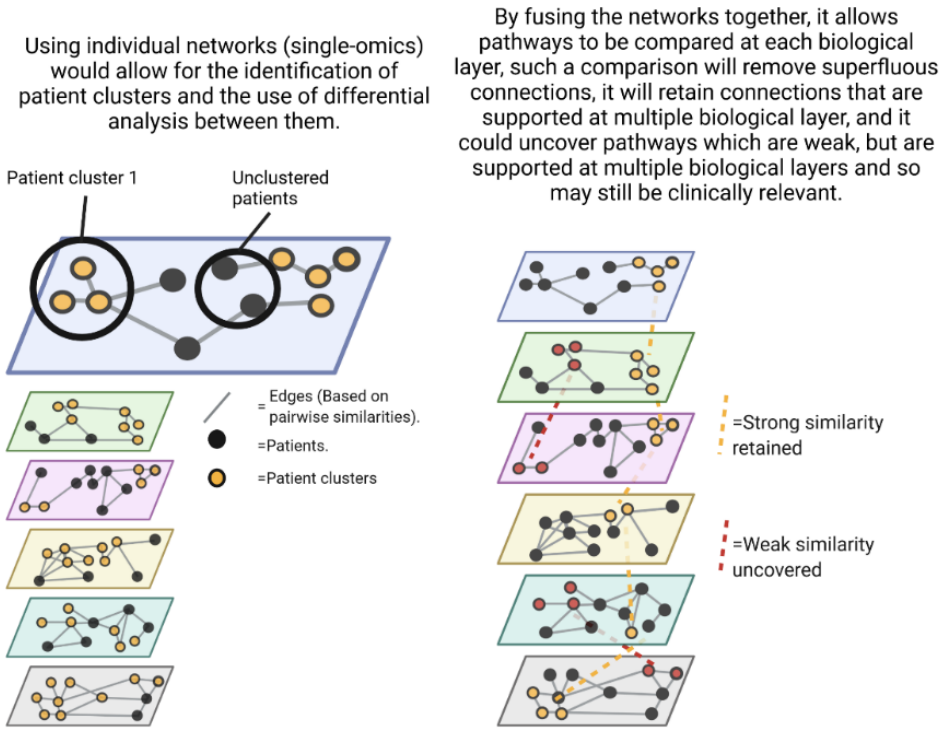


Figure 2. A highlight of the advantages that network analysis of multi-omic data provides, allowing us to not only remove false positives from our analysis, but simultaneously uncover false negatives that would otherwise remain unnoticed. (Created with BioRender.com©).

2.4. Clinical Translation

As a continuation of the project, as connections are revealed through the network construction, annotation, and fusion steps, results will be examined and interpreted in the light of available clinical and fundamental literature, and will enable the generation of novel scientific hypotheses. These will be validated through either an independent testing cohort using targeted assays or through in-house *in vitro* infection models.

3. Conclusions

In this article we highlight the progresses made in the area of COIVD-19 research in the context of a multi-omic overview of the disease, discussing transcriptomics, proteomics, metabolomics, metagenomics, and host and viral genomics. We identify current gaps in the disease knowledge such as the pathogenesis of post COVID-19 condition, the link between COVID-19 induced respiratory microbiome changes and transcriptomic differences, and interactions between viral transcripts and host ncRNA, to list a few. We also identify the need for more detailed multi-omic studies in the sphere of COVID-19 research.

To bridge these gaps, we have proposed a large scale, explorative, multi-omic study of a Belgium cohort featuring 225 COVID-19 patients (split evenly between critical, severe, and mild/moderate phenotypes) and 50 control patients (25 healthy controls and 25 non-COVID-19 respiratory disease patients). We plan to investigate these patients during the acute and post-COVID phase at 6 levels of biological strata: the viral genome, the respiratory microbiome, the host genome, the blood transcriptome, the blood proteome, and the blood metabolome, using gold standard HTS and mass spectrometry technologies. The data generated will then be analyzed through a network medicine approach and new hypotheses will be generated and later validated in follow up experiments.

The aim of such a project is to thoroughly explore the multi-omic state of each patient during and after SARS-CoV-2 infection, in order to identify previously unknown characteristics, biomarkers, or consequences of COVID-19 disease, with the ultimate aim of improving patient care. Additionally, we aim to allow the protocols, bioinformatics, and logistics developed during this project to be rapidly redeployed when another pandemic-type situation arises, improving novel-disease research efficiency and allowing for rapid clinical translation.

Author Contributions: Conceptualization, J.C.Y., J.-L.B., L.G., J.d.G., L.B. and L.E.; methodology, B.W., J.C.Y., J.d.G., J.-L.B., P.D.C., J.-F.C., J.P.D., L.G., V.H., S.J., B.M.K., S.P.d.R., D.V., L.E. and L.B. investigation, B.W., J.C.Y., J.d.G., J.-L.B., P.D.C., J.-F.C., J.D.W., L.G., V.H., S.J., B.M.K., S.P.d.R., D.V., L.E. and L.B.; resources, J.C.Y., J.-L.B., L.G., J.d.G., V.H., B.M.K., J.-F.C., L.B. and L.E.; writing—original draft preparation, B.W., L.E. and L.B.; writing—review and editing, J.C.Y., J.d.G., J.-L.B., P.D.C., J.-F.C., J.D.W., L.G., V.H., S.J., B.M.K., S.P.d.R. and D.V.; supervision, J.C.Y., J.-L.B., L.G., J.d.G., L.B. and L.E.; project administration, J.-L.B. and J.C.Y.; funding acquisition, J.C.Y., J.-L.B., L.G., J.d.G., L.B. and L.E. All authors have read and agreed to the published version of the manuscript.

Funding: This research is funded by the Sofina COVID Solidarity Fund, managed by the King Baudouin Foundation, impulsed by the Fondation Saint Luc (grant number 2021-I4201010-221801) and FNRS Crédit Urgent de Recherche (CUR: HC01020F). PDC is research director at FRS-FNRS (Fonds de la Recherche Scientifique) and P.D.C., J.-F.C., and J.-L.B. are the recipients of grants from FNRS (Projet de Recherche FRFS-WELBIO: WELBIO-CR-2022 A–02; WELBIO-CR-2022 A-01).

Institutional Review Board Statement: The study is conducted in accordance with the Declaration of Helsinki, and approved by the Institutional Review Board (or Ethics Committee) of Cliniques Universitaires Saint Luc (comité éthique hospital-facultaire) (protocol code 2021/30DEC/543, date of approval: 30 December 2021).

Informed Consent Statement: Informed consent was obtained from all subjects involved in the study.

Acknowledgments: The investigators would like to thank all the patients currently involved or who will be involved to take part in this clinical study. Thanks also goes out to the clinical medical research coordinators at Cliniques Universitaires Saint Luc for their help in patient recruitment and collecting biological samples.

Conflicts of Interest: PDC is co-founder A-Mansia SA and coinventor on patents dealing with gut microbes and health. The funders had no role in the design of the study; in the collection, analyses, or interpretation of data; in the writing of the manuscript, or in the decision to publish the results.

References

1. WHO Coronavirus (COVID-19) Dashboard. Available online: https://covid19.who.int/(accessed on 9 May 2022).
2. Sakurai, A.; Sasaki, T.; Kato, S.; Hayashi, M.; Tsuzuki, S.; Ishihara, T.; Iwata, M.; Morise, Z.; Doi, Y. Natural History of Asymptomatic SARS-CoV-2 Infection. *New England Journal of Medicine* **2020**, *383*, 885–886, doi: 10.1056/NEJMc2013020.
3. Mortality Analyses - Johns Hopkins Coronavirus Resource Center. Available online: https://coronavirus.jhu.edu/data/mortality (accessed on 6 May 2022).
4. Jeganathan, N.; Grewal, S.; Sathananthan, M. Comparison of Deaths from COVID-19 and Seasonal Influenza in the USA. *Lung* **2021**, *199*, 559–561.
5. Huang, Y.; Yang, C.; Xu, X. feng; Xu, W.; Liu, S. Structural and Functional Properties of SARS-CoV-2 Spike Protein: Potential Antivirus Drug Development for COVID-19. *Acta Pharmacologica Sinica* **2020**, *41*, 1141–1149.
6. Zou, X.; Chen, K.; Zou, J.; Han, P.; Hao, J.; Han, Z. Single-Cell RNA-Seq Data Analysis on the Receptor ACE2 Expression Reveals the Potential Risk of Different Human Organs Vulnerable to 2019-NCoV Infection. *Frontiers of Medicine* **2020**, *14*, 185–192, doi:10.1007/s11684-020-0754-0.
7. Chen, R.; Wang, K.; Yu, J.; Howard, D.; French, L.; Chen, Z.; Wen, C.; Xu, Z. The Spatial and Cell-Type Distribution of SARS-CoV-2 Receptor ACE2 in the Human and Mouse Brains. *Frontiers in Neurology* **2021**, *11*, 1860, doi:10.3389/fneur.2020.573095.
8. Jenner, A.L.; Aogo, R.A.; Alfonso, S.; Crowe, V.; Deng, X.; Smith, A.P.; Morel, P.A.; Davis, C.L.; Smith, A.M.; Craig, M. COVID-19 Virtual Patient Cohort Suggests Immune Mechanisms Driving Disease Outcomes. *PLOS Pathogens* **2021**, *17*, e1009753, doi:10.1371/JOURNAL.PPAT.1009753.
9. Huang, C.; Soleimani, J.; Herasevich, S.; Pinevich, Y.; Pennington, K.M.; Dong, Y.; Pickering, B.W.; Barwise, A.K. Clinical Characteristics, Treatment, and Outcomes of Critically Ill Patients With COVID-19: A Scoping Review. *Mayo Clin Proc* **2021**, *96*, 183–202, doi:10.1016/J.MAYOCP.2020.10.022.
10. Ackermann, M.; Verleden, S.E.; Kuehnel, M.; Haverich, A.; Welte, T.; Laenger, F.; Vanstapel, A.; Werlein, C.; Stark, H.; Tzankov, A.; et al. Pulmonary Vascular Endothelialitis, Thrombosis, and Angiogenesis in Covid-19. *New England Journal of Medicine* **2020**, *383*, 120–128, doi:10.1056/NEJMOA2015432.
11. Paterson, R.W.; Brown, R.L.; Benjamin, L.; Nortley, R.; Wiethoff, S.; et al. The Emerging Spectrum of COVID-19 Neurology: Clinical, Radiological and Laboratory Findings. *Brain* **2020**, *143*, 3104–3120, doi:10.1093/BRAIN/AWAA240.
12. Kunutsor, S.K.; Laukkanen, J.A. Renal Complications in COVID-19: A Systematic Review and Meta-Analysis. *Ann Med* **2020**, *52*, 345–353, doi:10.1080/07853890.2020.1790643.
13. Khan, A.; Gui, J.; Ahmad, W.; Haq, I.; Shahid, M.; Khan, A.A.; Shah, A.; Khan, A.; Ali, L.; Anwar, Z.; et al. The SARS-CoV-2 B.1.618 Variant Slightly Alters the Spike RBD-ACE2 Binding Affinity and Is an Antibody Escaping Variant: A Computational Structural Perspective. RSC Advances **2021**, doi:10.1039/d1ra04694b.
14. Jimeno-Almazán, A.; Pallarés, J.G.; Buendía-Romero, Á.; Martínez-Cava, A.; Franco-López, F.; Sánchez-Alcaraz Martínez, B.J.; Bernal-Morel, E.; Courel-Ibáñez, J. Post-Covid-19 Syndrome and the Potential Benefits of Exercise. *International Journal of Environmental Research and Public Health* **2021**, *18*.
15. Chen, C.; Haupert, S.R.; Zimmermann, L.; Shi, X.; Fritsche, L.G.; Mukherjee, B. Global Prevalence of Post COVID-19 Condition or Long COVID: A Meta-Analysis and Systematic Review. *The Journal of Infectious Diseases* **2022**, doi:10.1093/infdis/jiac136.
16. Castanares-Zapatero, D.; Kohn, L.; Dauvrin, M.; Detollenaere, J.; Maertens de Noordhout, C.; Primus, C.; Cleemput, I.; Van der Heede, K. Long COVID : Pathophysiology – Epidemiology and Patient Needs. *KCE Reports* **2021**, doi:D/2021/10.273/31.
17. Naeije, R.; Caravita, S. Phenotyping Long COVID. *European Respiratory Journal* **2021**, *58*.
18. Tosato, M.; Carfì, A.; Martis, I.; Pais, C.; Ciciarello, F.; Rota, E.; Tritto, M.; Salerno, A.; Zazzara, M.B.; Martone, A.M.; et al. Prevalence and Predictors of Persistence of COVID-19 Symptoms in Older Adults: A Single-Center Study. *J Am Med Dir Assoc* **2021**, *22*, 1840–1844, doi:10.1016/j.jamda.2021.07.003.
19. Feldman, E.L.; Savelieff, M.G.; Hayek, S.S.; Pennathur, S.; Kretzler, M.; Pop-Busui, R. Covid-19 and Diabetes: A Collision and Collusion of Two Diseases. *Diabetes* **2020**, *69*, 2549–2565, doi:10.2337/dbi20-0032.
20. Su, Y.; Yuan, D.; Chen, D.G.; Ng, R.H.; Wang, K.; Choi, J.; Li, S.; Hong, S.; Zhang, R.; Xie, J.; et al. Multiple Early Factors Anticipate Post-Acute COVID-19 Sequelae. *Cell* **2022**, *185*, 881-895.e20, doi:10.1016/j.cell.2022.01.014.
21. Cervia, C.; Zurbuchen, Y.; Taeschler, P.; Ballouz, T.; Menges, D.; Hasler, S.; Adamo, S.; Raeber, M.E.; Bächli, E.; Rudiger, A.; et al. Immunoglobulin Signature Predicts Risk of Post-Acute COVID-19 Syndrome. *Nature Communications* **2022**, *13*, doi:10.1038/s41467-021-27797-1.

22. Liu, Q.; Mak, J.W.Y.; Su, Q.; Yeoh, Y.K.; Lui, G.C.Y.; Ng, S.S.S.; Zhang, F.; Li, A.Y.L.; Lu, W.; Hui, D.S.C.; et al. Gut Microbiota Dynamics in a Prospective Cohort of Patients with Post-Acute COVID-19 Syndrome. *Gut* **2022**, *71*, 544–552, doi:10.1136/gutjnl-2021-325989.
23. Peluso, M.J.; Lu, S.; Tang, A.F.; Durstenfeld, M.S.; Ho, H.E.; Goldberg, S.A.; Forman, C.A.; Munter, S.E.; Hoh, R.; Tai, V.; et al. Markers of Immune Activation and Inflammation in Individuals With Postacute Sequelae of Severe Acute Respiratory Syndrome Coronavirus 2 Infection. *Journal of Infectious Diseases* **2021**, *224*, 1839–1848, doi:10.1093/infdis/jiab490.
24. Khan, A.; Khan, T.; Ali, S.; Aftab, S.; Wang, Y.; Qiankun, W.; Khan, M.; Suleman, M.; Ali, S.; Heng, W.; et al. SARS-CoV-2 New Variants: Characteristic Features and Impact on the Efficacy of Different Vaccines. *Biomedicine & Pharmacotherapy* **2021**, *143*, 112176, doi:10.1016/J.BIOPHA.2021.112176.
25. Su, Y.; Chen, D.; Yuan, D.; Lausted, C.; Choi, J.; Dai, C.L.; Voillet, V.; Duvvuri, V.R.; Scherler, K.; Troisch, P.; et al. Multi-Omics Resolves a Sharp Disease-State Shift between Mild and Moderate COVID-19. *Cell* **2020**, *183*, 1479-1495.e20, doi:10.1016/J.CELL.2020.10.037.
26. Shi, R.; Feng, Z.; Zhang, X. Integrative Multi-Omics Landscape of Non-Structural Protein 3 of Severe Acute Respiratory Syndrome Coronaviruses. *Genomics, Proteomics & Bioinformatics* **2021**, doi:10.1016/J.GPB.2021.09.007.
27. Zhang, T.; Abdelrahman, Z.; Liu, Q.; Wang, X.; Chen, Z. Comparisons of the Immunological Landscape of COVID-19 Patients Based on Sex and Disease Severity by Multi-Omics Analysis. *Chemico-Biological Interactions* **2022**, *352*, 109777, doi:10.1016/J.CBI.2021.109777.
28. Maras, J.S.; Sharma, S.; Bhat, A.; Rooge, S.; aggrawal, R.; Gupta, E.; Sarin, S.K. Multi-Omics Analysis of Respiratory Specimen Characterizes Baseline Molecular Determinants Associated with SARS-CoV-2 Outcome. *iScience* **2021**, *24*, 102823, doi:10.1016/J.ISCI.2021.102823.
29. Overmyer, K.A.; Shishkova, E.; Miller, I.J.; Balnis, J.; Bernstein, M.N.; Peters-Clarke, T.M.; Meyer, J.G.; Quan, Q.; Muehlbauer, L.K.; Trujillo, E.A.; et al. Large-Scale Multi-Omic Analysis of COVID-19 Severity. *Cell Systems* **2021**, *12*, 23, doi:10.1016/J.CELS.2020.10.003.
30. Bernardes, J.P.; Mishra, N.; Tran, F.; Bahmer, T.; Best, L.; Blase, J.I.; Bordoni, D.; Franzenburg, J.; Geisen, U.; Josephs-Spaulding, J.; et al. Longitudinal Multi-Omics Analyses Identify Responses of Megakaryocytes, Erythroid Cells, and Plasmablasts as Hallmarks of Severe COVID-19. *Immunity* **2020**, *53*, 1296-1314.e9, doi:10.1016/J.IMMUNI.2020.11.017.
31. Romano, M.; Ruggiero, A.; Squeglia, F.; Maga, G.; Berisio, R. A Structural View of SARS-CoV-2 RNA Replication Machinery: RNA Synthesis, Proofreading and Final Capping. *Cells* **2020**, *9*, doi:10.3390/CELLS9051267.
32. Sheikh, A.; McMenamin, J.; Taylor, B.; Robertson, C. SARS-CoV-2 Delta VOC in Scotland: Demographics, Risk of Hospital Admission, and Vaccine Effectiveness. *The Lancet* **2021**, *397*, 2461–2462, doi:10.1016/S0140-6736(21)01358-1.
33. Faria, N.R.; Mellan, T.A.; Whittaker, C.; Claro, I.M.; Candido, D.D.S.; Mishra, S.; Crispim, M.A.E.; Sales, F.C.S.; Hawryluk, I.; McCrone, J.T.; et al. Genomics and Epidemiology of the P.1 SARS-CoV-2 Lineage in Manaus, Brazil. *Science* **2021**, *372*, doi:10.1126/SCIENCE.ABH2644.
34. Funk, T.; Pharris, A.; Spiteri, G.; Bundle, N.; Melidou, A.; Carr, M.; Gonzalez, G.; Garcia-Leon, A.; Crispie, F.; O'Connor, L.; et al. Characteristics of SARS-CoV-2 Variants of Concern B.1.1.7, B.1.351 or P.1: Data from Seven EU/EEA Countries, Weeks 38/2020 to 10/2021. *Eurosurveillance* **2021**, *26*, 2100348, doi:10.2807/1560-7917.ES.2021.26.16.2100348.
35. Tegally, H.; Wilkinson, E.; Giovanetti, M.; Iranzadeh, A.; Fonseca, V.; Giandhari, J.; Doolabh, D.; Pillay, S.; San, E.J.; Msomi, N.; et al. Detection of a SARS-CoV-2 Variant of Concern in South Africa. *Nature 2021 592:7854* **2021**, *592*, 438–443, doi:10.1038/s41586-021-03402-9.
36. Pearson, C.A. Estimates of Severity and Transmissibility of Novel South Africa SARS-CoV-2 Variant 501Y.V2. 1.
37. Wolter, N.; Jassat, W.; Walaza, S.; Welch, R.; Moultrie, H.; Groome, M.; Amoako, D.G.; Everatt, J.; Bhiman, J.N.; Scheepers, C.; et al. Early Assessment of the Clinical Severity of the SARS-CoV-2 Omicron Variant in South Africa. *medRxiv* **2021** , doi:10.1101/2021.12.21.21268116.
38. Fonager, J.; Bennedbæk, M.; Bager, P.; Wohlfahrt, J.; Ellegaard, K.M.; Ingham, A.C.; Edslev, S.M.; Stegger, M.; Sieber, R.N.; Lassauniere, R.; et al. Molecular Epidemiology of the SARS-CoV-2 Variant Omicron BA.2 Sub-Lineage in Denmark, 29 November 2021 to 2 January 2022. *Eurosurveillance* **2022**, *27*, 2200181, doi:10.2807/1560-7917.ES.2022.27.10.2200181.
39. Lewnard, J.A.; Hong, V.X.; Patel, M.M.; Kahn, R.; Lipsitch, M.; Tartof, S.Y. Clinical Outcomes among Patients Infected with Omicron (B.1.1.529) SARS-CoV-2 Variant in Southern California. *medRxiv* **2022**, doi:10.1101/2022.01.11.22269045.

40. Christensen, P.A.; Olsen, R.J.; Long, S.W.; Snehal, R.; Davis, J.J.; Saavedra, M.O.; Reppond, K.; Shyer, M.N.; Cambric, J.; Gadd, R.; et al. Early Signals of Significantly Increased Vaccine Breakthrough, Decreased Hospitalization Rates, and Less Severe Disease in Patients with COVID-19 Caused by the Omicron Variant of SARS-CoV-2 in Houston, Texas. *medRxiv* **2022**, doi:10.1101/2021.12.30.21268560.
41. Sheikh, A.; Kerr, S.; Woolhouse, M.; McMenamin, J.; Robertson, C. Severity of Omicron Variant of Concern and Vaccine Effectiveness against Symptomatic Disease: National Cohort with Nested Test Negative Design Study in Scotland. *Lancet Infect Dis* **2021**, doi:10.1016/S1473-3099(22)00141-4.
42. Lyngse, F.P.; Mortensen, L.H.; Denwood, M.J.; Christiansen, L.E.; Møller, C.H.; Skov, R.L.; Spiess, K.; Fomsgaard, A.; Lassaunière, M.M.; Rasmussen, M.; et al. SARS-CoV-2 Omicron VOC Transmission in Danish Households. *medRxiv* **2021**, doi:10.1101/2021.12.27.21268278.
43. Epidemiological Update: SARS-CoV-2 Omicron Sub-Lineages BA.4 and BA.5. Available online: https://www.ecdc.europa.eu/en/news-events/epidemiological-update-sars-cov-2-omicron-sub-lineages-ba4-and-ba5 (accessed on 1 June 2022).
44. Khan, K.; Karim, F.; Ganga, Y.; Bernstein, M.; Jule, Z.; Reedoy, K.; Cele, S.; Lustig, G.; Amoako, D.; Wolter, N.; et al. Omicron Sub-Lineages BA.4/BA.5 Escape BA.1 Infection Elicited Neutralizing Immunity. *medRxiv* **2022**, doi:10.1101/2022.04.29.22274477.
45. Cao, Y.; Yisimayi, A.; Jian, F.; Song, W.; Xiao, T.; Wang, L.; Du, S.; Wang, J.; Li, Q.; Chen, X.; et al. BA.2.12.1, BA.4 and BA.5 Escape Antibodies Elicited by Omicron Infection. *bioRxiv* **2022**, doi:10.1101/2022.04.30.489997.
46. O'Donnell, K.L.; Pinski, A.N.; Clancy, C.S.; Gourdine, T.; Shifflett, K.; Fletcher, P.; Messaoudi, I.; Marzi, A. Pathogenic and Transcriptomic Differences of Emerging SARS-CoV-2 Variants in the Syrian Golden Hamster Model. *EBioMedicine* **2021**, *73*, doi:10.1016/J.EBIOM.2021.103675.
47. Mohammad, T.; Choudhury, A.; Habib, I.; Asrani, P.; Mathur, Y.; Umair, M.; Anjum, F.; Shafie, A.; Yadav, D.K.; Hassan, M.I. Genomic Variations in the Structural Proteins of SARS-CoV-2 and Their Deleterious Impact on Pathogenesis: A Comparative Genomics Approach. *Frontiers in Cellular and Infection Microbiology* **2021**, *11*, 951, doi:10.3389/FCIMB.2021.765039.
48. Zhang, G.; Hu, C.; Luo, L.; Fang, F.; Chen, Y.; Li, J.; Peng, Z.; Pan, H. Clinical Features and Short-Term Outcomes of 221 Patients with COVID-19 in Wuhan, China. *Journal of Clinical Virology* **2020**, *127*, 104364, doi:10.1016/J.JCV.2020.104364.
49. Bassetti, M.; Kollef, M.H.; Timsit, J.F. Bacterial and Fungal Superinfections in Critically Ill Patients with COVID-19. *Intensive Care Medicine* **2020**, *46*, 2071–2074, doi:10.1007/S00134-020-06219-8/FIGURES/1.
50. Lehmann, C.J.; Pho, M.T.; Pitrak, D.; Ridgway, J.P.; Pettit, N.N. Community-Acquired Coinfection in Coronavirus Disease 2019: A Retrospective Observational Experience. *Clinical Infectious Diseases* **2021**, *72*, 1450–1452, doi:10.1093/CID/CIAA902.
51. Fu, Y.; Yang, Q.; Xu, M.; Kong, H.; Chen, H.; Fu, Y.; Yao, Y.; Zhou, H.; Zhou, J. Secondary Bacterial Infections in Critical Ill Patients With Coronavirus Disease 2019. *Open Forum Infectious Diseases* **2020**, *7*, doi:10.1093/OFID/OFAA220.
52. Hoque, M.N.; Rahman, M.S.; Ahmed, R.; Hossain, M.S.; Islam, M.S.; Islam, T.; Hossain, M.A.; Siddiki, A.Z. Diversity and Genomic Determinants of the Microbiomes Associated with COVID-19 and Non-COVID Respiratory Diseases. *Gene Reports* **2021**, *23*, 101200, doi:10.1016/J.GENREP.2021.101200.
53. Sencio, V.; Machado, M.G.; Trottein, F. The Lung–Gut Axis during Viral Respiratory Infections: The Impact of Gut Dysbiosis on Secondary Disease Outcomes. *Mucosal Immunology* **2021**, *14*, 296, doi:10.1038/S41385-020-00361-8.
54. Rekdal, V.M.; Bess, E.N.; Bisanz, J.E.; Turnbaugh, P.J.; Balskus, E.P. Discovery and Inhibition of an Interspecies Gut Bacterial Pathway for Levodopa Metabolism. *Science* **2019**, *364*, doi:10.1126/SCIENCE.AAU6323.
55. Lee-Sarwar, K.A.; Lasky-Su, J.; Kelly, R.S.; Litonjua, A.A.; Weiss, S.T. Gut Microbial-Derived Metabolomics of Asthma. *Metabolites* **2020**, *10*, doi:10.3390/METABO10030097.
56. Tang, W.H.W.; Wang, Z.; Levison, B.S.; Koeth, R.A.; Britt, E.B.; Fu, X.; Wu, Y.; Hazen, S.L. Intestinal Microbial Metabolism of Phosphatidylcholine and Cardiovascular Risk. *N Engl J Med* **2013**, *368*, 1575, doi:10.1056/NEJMOA1109400.
57. Hoque, M.N.; Sarkar, Md.M.H.; Rahman, M.S.; Akter, S.; Banu, T.A.; Goswami, B.; Jahan, I.; Hossain, M.S.; Shamsuzzaman, A.K.M.; Nafisa, T.; et al. SARS-CoV-2 Infection Reduces Human Nasopharyngeal Commensal Microbiome with Inclusion of Pathobionts. *Scientific Reports* **2021**, *11*, 24042, doi:10.1038/S41598-021-03245-4.
58. Hadjadj, J.; Yatim, N.; Barnabei, L.; Corneau, A.; Boussier, J.; Smith, N.; Péré, H.; Charbit, B.; Bondet, V.; Chenevier-Gobeaux, C.; et al. Impaired Type I Interferon Activity and Inflammatory Responses in Severe COVID-19 Patients. *Science (1979)* **2020**, *369*, 718–724, doi:10.1126/SCIENCE.ABC6027.
59. Zhang, X.; Tan, Y.; Ling, Y.; Lu, G.; Liu, F.; Yi, Z.; Jia, X.; Wu, M.; Shi, B.; Xu, S.; et al. Viral and Host Factors Related to the Clinical Outcome of COVID-19. *Nature* **2020**, *583*, 437–440, doi:10.1038/s41586-020-2355-0.

60. Lokugamage, K.G.; Hage, A.; de Vries, M.; Valero-Jimenez, A.M.; Schindewolf, C.; Dittmann, M.; Rajsbaum, R.; Menachery, V.D. Type I Interferon Susceptibility Distinguishes SARS-CoV-2 from SARS-CoV. *Journal of Virology* **2020**, *94*, doi:10.1128/JVI.01410-20.
61. Banerjee, A.K.; Blanco, M.R.; Bruce, E.A.; Honson, D.D.; Chen, L.M.; Chow, A.; Bhat, P.; Ollikainen, N.; Quinodoz, S.A.; Loney, C.; et al. SARS-CoV-2 Disrupts Splicing, Translation, and Protein Trafficking to Suppress Host Defenses. *Cell* **2020**, *183*, 1325-1339.e21, doi:10.1016/J.CELL.2020.10.004.
62. Obitsu, S.; Ahmed, N.; Nishitsuji, H.; Hasegawa, A.; Nakahama, K. ichi; Morita, I.; Nishigaki, K.; Hayashi, T.; Masuda, T.; Kannagi, M. Potential Enhancement of Osteoclastogenesis by Severe Acute Respiratory Syndrome Coronavirus 3a/X1 Protein. *Archives of Virology* **2009**, *154*, 1457–1464, doi:10.1007/S00705-009-0472-Z.
63. Krishnamoorthy, P.; Raj, A.S.; Roy, S.; Kumar, N.S.; Kumar, H. Comparative Transcriptome Analysis of SARS-CoV, MERS-CoV, and SARS-CoV-2 to Identify Potential Pathways for Drug Repurposing. *Computers in Biology and Medicine* **2021**, *128*, 104123, doi:10.1016/J.COMPBIOMED.2020.104123.
64. Paul, S.; Bravo Vázquez, L.A.; Reyes-Pérez, P.R.; Estrada-Meza, C.; Aponte Alburquerque, R.A.; Pathak, S.; Banerjee, A.; Bandyopadhyay, A.; Chakraborty, S.; Srivastava, A. The Role of MicroRNAs in Solving COVID-19 Puzzle from Infection to Therapeutics: A Mini-Review. *Virus Research* **2022**, *308*, 198631, doi:10.1016/J.VIRUSRES.2021.198631.
65. Reynaert, N.L.; Gopal, P.; Rutten, E.P.A.; Wouters, E.F.M.; Schalkwijk, C.G. Advanced Glycation End Products and Their Receptor in Age-Related, Non-Communicable Chronic Inflammatory Diseases; Overview of Clinical Evidence and Potential Contributions to Disease. *International Journal of Biochemistry and Cell Biology* **2016**, *81*, 403–418, doi:10.1016/J.BIOCEL.2016.06.016.
66. Prasad, K. AGE-RAGE Stress in the Pathophysiology of Pulmonary Hypertension and Its Treatment. *International Journal of Angiology* **2019**, *28*, 71–79, doi:10.1055/S-0039-1687818.
67. Kosmopoulos, M.; Drekolias, D.; Zavras, P.D.; Piperi, C.; Papavassiliou, A.G. Impact of Advanced Glycation End Products (AGEs) Signaling in Coronary Artery Disease. *Biochimica et Biophysica Acta - Molecular Basis of Disease* **2019**, *1865*, 611–619, doi:10.1016/J.BBADIS.2019.01.006.
68. Sepahi, A.; Kraus, A.; Casadei, E.; Johnston, C.A.; Galindo-Villegas, J.; Kelly, C.; García-Moreno, D.; Muñoz, P.; Mulero, V.; Huertas, M.; et al. Olfactory Sensory Neurons Mediate Ultrarapid Antiviral Immune Responses in a TrkA-Dependent Manner. *Proc Natl Acad Sci U S A* **2019**, *116*, 12428–12436, doi:10.1073/PNAS.1900083116.
69. Lechien, J.R.; Chiesa-Estomba, C.M.; de Siati, D.R.; Horoi, M.; le Bon, S.D.; Rodriguez, A.; Dequanter, D.; Blecic, S.; el Afia, F.; Distinguin, L.; et al. Olfactory and Gustatory Dysfunctions as a Clinical Presentation of Mild-to-Moderate Forms of the Coronavirus Disease (COVID-19): A Multicenter European Study. *European Archives of Oto-Rhino-Laryngology* **2020**, *277*, 2251–2261, doi:10.1007/S00405-020-05965-1.
70. Yan, C.H.; Faraji, F.; Prajapati, D.P.; Ostrander, B.T.; DeConde, A.S. Self-Reported Olfactory Loss Associates with Outpatient Clinical Course in COVID-19. *International Forum of Allergy and Rhinology* **2020**, *10*, 821–831, doi:10.1002/ALR.22592.
71. Bilinska, K.; Jakubowska, P.; von Bartheld, C.S.; Butowt, R. Expression of the SARS-CoV-2 Entry Proteins, ACE2 and TMPRSS2, in Cells of the Olfactory Epithelium: Identification of Cell Types and Trends with Age. *ACS Chemical Neuroscience* **2020**, *11*, 1555–1562, doi:10.1021/acschemneuro.0c00210.
72. Mercatelli, D.; Pedace, E.; Veltri, P.; Giorgi, F.M.; Guzzi, P.H. Exploiting the Molecular Basis of Age and Gender Differences in Outcomes of SARS-CoV-2 Infections. *Computational and Structural Biotechnology Journal* **2021**, *19*, 4092–4100, doi:10.1016/j.csbj.2021.07.002.
73. Bell, L.C.K.; Meydan, C.; Kim, J.; Foox, J.; Butler, D.; Mason, C.E.; Shapira, S.D.; Noursadeghi, M.; Pollara, G. Transcriptional Response Modules Characterize IL-1β and IL-6 Activity in COVID-19. *iScience* **2021**, *24*, doi:10.1016/J.ISCI.2020.101896.
74. Silvin, A.; Chapuis, N.; Dunsmore, G.; Goubet, A.G.; Dubuisson, A.; Derosa, L.; Almire, C.; Hénon, C.; Kosmider, O.; Droin, N.; et al. Elevated Calprotectin and Abnormal Myeloid Cell Subsets Discriminate Severe from Mild COVID-19. *Cell* **2020**, *182*, 1401-1418.e18, doi:10.1016/j.cell.2020.08.002.
75. Gasparello, J.; Finotti, A.; Gambari, R. Tackling the COVID-19 "Cytokine Storm" with MicroRNA Mimics Directly Targeting the 3'UTR of pro-Inflammatory MRNAs. *Medical Hypotheses* **2021**, *146*, doi:10.1016/J.MEHY.2020.110415.
76. Thair, S.A.; He, Y.D.; Hasin-Brumshtein, Y.; Sakaram, S.; Pandya, R.; Toh, J.; Rawling, D.; Remmel, M.; Coyle, S.; Dalekos, G.N.; et al. Transcriptomic Similarities and Differences in Host Response between SARS-CoV-2 and Other Viral Infections. *iScience* **2021**, *24*, 101947, doi:10.1016/J.ISCI.2020.101947.
77. Wyler, E.; Mösbauer, K.; Franke, V.; Diag, A.; Gottula, L.T.; Arsiè, R.; Klironomos, F.; Koppstein, D.; Hönzke, K.; Ayoub, S.; et al. Transcriptomic Profiling of SARS-CoV-2 Infected Human Cell Lines Identifies HSP90 as Target for COVID-19 Therapy. *iScience* **2021**, *24*, 102151, doi:10.1016/J.ISCI.2021.102151.

78. Ziegler, C.G.K.; Miao, V.N.; Owings, A.H.; Navia, A.W.; Tang, Y.; Bromley, J.D.; Lotfy, P.; Sloan, M.; Laird, H.; Williams, H.B.; et al. Impaired Local Intrinsic Immunity to SARS-CoV-2 Infection in Severe COVID-19. *Cell* **2021**, *184*, 4713-4733.e22, doi:10.1016/J.CELL.2021.07.023.
79. Vishnubalaji, R.; Shaath, H.; Alajez, N.M. Protein Coding and Long Noncoding RNA (LncRNA) Transcriptional Landscape in SARS-CoV-2 Infected Bronchial Epithelial Cells Highlight a Role for Interferon and Inflammatory Response. *Genes 2020, Vol. 11, Page 760* **2020**, *11*, 760, doi:10.3390/GENES11070760.
80. Cheng, J.; Zhou, X.; Feng, W.; Jia, M.; Zhang, X.; An, T.; Luan, M.; Pan, Y.; Zhang, S.; Zhou, Z.; et al. Risk Stratification by Long Non-Coding RNAs Profiling in COVID-19 Patients. *Journal of Cellular and Molecular Medicine* **2021**, *25*, 4753–4764, doi:10.1111/JCMM.16444.
81. Turjya, R.R.; Khan, M.A.A.K.; Mir Md Khademul Islam, A.B. Perversely Expressed Long Noncoding RNAs Can Alter Host Response and Viral Proliferation in SARS-CoV-2 Infection. *Future Virology* **2020**, *15*, 577–593, doi:10.2217/FVL-2020-0188.
82. Damas, N.D.; Fossat, N.; Scheel, T.K.H. Non-Coding RNA Review Functional Interplay between RNA Viruses and Non-Coding RNA in Mammals. *Noncoding RNA* **2019**, doi:10.3390/ncrna5010007.
83. Henao-Mejia, J.; He, X.; Wang, P. The Opening of Pandora's Box: An Emerging Role of Long Noncoding RNA in Viral Infections. *Frontiers in Immunology* **2019**, *1*, 3138, doi:10.3389/fimmu.2018.03138.
84. Gupta, R.; Leimanis, M.L.; Adams, M.; Bachmann, A.S.; Uhl, K.L.; Bupp, C.P.; Hartog, N.L.; Kort, E.J.; Olivero, R.; Comstock, S.S.; et al. Balancing Precision versus Cohort Transcriptomic Analysis of Acute and Recovery Phase of Viral Bronchiolitis. *American Journal of Physiology - Lung Cellular and Molecular Physiology* **2021**, *320*, L1147–L1157, doi:10.1152/AJPLUNG.00440.2020.
85. Rhead, B.; Brorson, I.S.; Berge, T.; Adams, C.; Quach, H.; Moen, S.M.; Berg-Hansen, P.; Celius, E.G.; Sangurdekar, D.P.; Bronson, P.G.; et al. Increased DNA Methylation of SLFN12 in CD4 + and CD8 + T Cells from Multiple Sclerosis Patients. *PLoS ONE* **2018**, *13*, doi:10.1371/JOURNAL.PONE.0206511.
86. Wang, X.; Sun, H.; Hu, Z.; Mei, P.; Wu, Y.; Zhu, M. NUTM2A-AS1 Silencing Alleviates LPS-Induced Apoptosis and Inflammation in Dental Pulp Cells through Targeting Let-7c-5p/HMGB1 Axis. *International Immunopharmacology* **2021**, *96*, doi:10.1016/J.INTIMP.2021.107497.
87. de Lima, D.S.; Cardozo, L.E.; Maracaja-Coutinho, V.; Suhrbier, A.; Mane, K.; Jeffries, D.; Silveira, E.L.V.; Amaral, P.P.; Rappuoli, R.; de Silva, T.I.; et al. Long Noncoding RNAs Are Involved in Multiple Immunological Pathways in Response to Vaccination. *Proc Natl Acad Sci U S A* **2019**, *116*, 17121–17126, doi:10.1073/PNAS.1822046116.
88. Talotta, R.; Bahrami, S.; Laska, M.J. Sequence Complementarity between Human Noncoding RNAs and SARS-CoV-2 Genes: What Are the Implications for Human Health? *Biochimica et Biophysica Acta (BBA) - Molecular Basis of Disease* **2022**, *1868*, 166291, doi:10.1016/J.BBADIS.2021.166291.
89. Liang, C.; Cheng, S.; Zhang, Y.; Sun, Y.; Fernie, A.R.; Kang, K.; Panagiotou, G.; Lo, C.; Lim, B.L. Transcriptomic, Proteomic and Metabolic Changes in Arabidopsis Thaliana Leaves after the Onset of Illumination. *BMC Plant Biology* **2016**, *16*, doi:10.1186/S12870-016-0726-3.
90. Dong, Y.; Deng, M.; Zhao, Z.; Fan, G. Quantitative Proteomic and Transcriptomic Study on Autotetraploid Paulownia and Its Diploid Parent Reveal Key Metabolic Processes Associated with Paulownia Autotetraploidization. *Frontiers in Plant Science* **2016**, *7*, 892, doi:10.3389/FPLS.2016.00892.
91. Manzoni, C.; Kia, D.A.; Vandrovcova, J.; Hardy, J.; Wood, N.W.; Lewis, P.A.; Ferrari, R. Genome, Transcriptome and Proteome: The Rise of Omics Data and Their Integration in Biomedical Sciences. *Briefings in Bioinformatics* **2018**, *19*, 286–302, doi:10.1093/BIB/BBW114.
92. Bathke, J.; Konzer, A.; Remes, B.; McIntosh, M.; Klug, G. Comparative Analyses of the Variation of the Transcriptome and Proteome of Rhodobacter Sphaeroides throughout Growth. *BMC Genomics* **2019**, *20*, 1–13, doi:10.1186/S12864-019-5749-3.
93. Lemée, J.M.; Clavreul, A.; Aubry, M.; Com, E.; de Tayrac, M.; Mosser, J.; Menei, P. Integration of Transcriptome and Proteome Profiles in Glioblastoma: Looking for the Missing Link. *BMC Molecular Biology* **2018**, *19*, doi:10.1186/S12867-018-0115-6.
94. Bai, Y.; Wang, S.; Zhong, H.; Yang, Q.; Zhang, F.; Zhuang, Z.; Yuan, J.; Nie, X.; Wang, S. Integrative Analyses Reveal Transcriptome-Proteome Correlation in Biological Pathways and Secondary Metabolism Clusters in A. Flavus in Response to Temperature. *Scientific Reports* **2015**, *5*, 1–13, doi:10.1038/srep14582.
95. Gunawardana, Y.; Niranjan, M. Bridging the Gap between Transcriptome and Proteome Measurements Identifies Post-Translationally Regulated Genes. *Bioinformatics* **2013**, *29*, 3060–3066, doi:10.1093/BIOINFORMATICS/BTT537.
96. Mcardle, A.; Washington, K.E.; Orgel, C.; Binek, A.; Manalo, D.-M.; Rivas, A.; Ayres, M.; Pandey, R.; Phebus, C.; Raedschelders, K.; et al. Discovery Proteomics for COVID-19: Where We Are Now. **2021**, doi:10.1021/acs.jproteome.1c00475.

97. Park, J.; Kim, H.; Kim, S.Y.; Kim, Y.; Lee, J.S.; Dan, K.; Seong, M.W.; Han, D. In-Depth Blood Proteome Profiling Analysis Revealed Distinct Functional Characteristics of Plasma Proteins between Severe and Non-Severe COVID-19 Patients. *Scientific Reports* **2020**, *10*, 1–10, doi:10.1038/s41598-020-80120-8.
98. Zhong, W.; Altay, O.; Arif, M.; Edfors, F.; Doganay, L.; Mardinoglu, A.; Uhlen, M.; Fagerberg, L. Next Generation Plasma Proteome Profiling of COVID-19 Patients with Mild to Moderate Symptoms. *eBioMedicine* **2021**, *74*, 103723, doi:10.1016/J.EBIOM.2021.103723.
99. D'Alessandro, A.; Thomas, T.; Dzieciatkowska, M.; Hill, R.C.; Francis, R.O.; Hudson, K.E.; Zimring, J.C.; Hod, E.A.; Spitalnik, S.L.; Hansen, K.C. Serum Proteomics in COVID-19 Patients: Altered Coagulation and Complement Status as a Function of IL-6 Level. *Journal of Proteome Research* **2020**, *19*, 4417–4427, doi:10.1021/ACS.JPROTEOME.0C00365.
100. Liu, T.; Zhang, J.; Yang, Y.; Ma, H.; Li, Z.; Zhang, J.; Cheng, J.; Zhang, X.; Zhao, Y.; Xia, Z.; et al. The Role of Interleukin-6 in Monitoring Severe Case of Coronavirus Disease 2019. *EMBO Molecular Medicine* **2020**, *12*, e12421, doi:10.15252/EMMM.202012421.
101. Wendt, R.; Kalbitz, S.; Lübbert, C.; Kellner, N.; Macholz, M.; Schroth, S.; Ermisch, J.; Latosisnka, A.; Arnold, B.; Mischak, H.; et al. Urinary Peptides Significantly Associate with COVID-19 Severity: Pilot Proof-of-Principle Data and Design of a Multicentric Diagnostic Study. *PROTEOMICS* **2020**, *20*, 2000202, doi:10.1002/PMIC.202000202.
102. Haljasmägi, L.; Salumets, A.; Rumm, A.P.; Jürgenson, M.; Krassohhina, E.; Remm, A.; Sein, H.; Kareinen, L.; Vapalahti, O.; Sironen, T.; et al. Longitudinal Proteomic Profiling Reveals Increased Early Inflammation and Sustained Apoptosis Proteins in Severe COVID-19. *Scientific Reports* **2020**, *10*, 1–12, doi:10.1038/s41598-020-77525-w.
103. Fraser, D.D.; Cepinskas, G.; Patterson, E.K.; Slessarev, M.; Martin, C.; Daley, M.; Patel, M.A.; Miller, M.R.; O'Gorman, D.B.; Gill, S.E.; et al. Novel Outcome Biomarkers Identified With Targeted Proteomic Analyses of Plasma From Critically Ill Coronavirus Disease 2019 Patients. *Critical Care Explorations* **2020**, *2*, e0189, doi:10.1097/CCE.0000000000000189.
104. Shen, B.; Yi, X.; Sun, Y.; Bi, X.; Du, J.; Zhang, C.; Quan, S.; Zhang, F.; Sun, R.; Qian, L.; et al. Proteomic and Metabolomic Characterization of COVID-19 Patient Sera. *Cell* **2020**, *182*, 59-72.e15, doi:10.1016/J.CELL.2020.05.032.
105. Shu, T.; Ning, W.; Wu, D.; Xu, J.; Han, Q.; Huang, M.; Zou, X.; Yang, Q.; Yuan, Y.; Bie, Y.; et al. Plasma Proteomics Identify Biomarkers and Pathogenesis of COVID-19. *Immunity* **2020**, *53*, 1108-1122.e5, doi:10.1016/J.IMMUNI.2020.10.008.
106. The Severe Covid-19 GWAS Group. Genomewide Association Study of Severe Covid-19 with Respiratory Failure. *New England Journal of Medicine* **2020**, *383*, 1522–1534, doi:10.1056/NEJMOA2020283.
107. Zeberg, H.; Pääbo, S. A Genomic Region Associated with Protection against Severe COVID-19 Is Inherited from Neandertals. *Proc Natl Acad Sci U S A* **2021**, *118*, doi:10.1073/pnas.2026309118.
108. Zeberg, H.; Pääbo, S. The Major Genetic Risk Factor for Severe COVID-19 Is Inherited from Neanderthals. *Nature* **2020**, *587*, 610–612, doi:10.1038/s41586-020-2818-3.
109. Huffman, J.E.; Butler-Laporte, G.; Khan, A.; Pairo-Castineira, E.; Drivas, T.G.; Peloso, G.M.; Nakanishi, T.; Ganna, A.; Verma, A.; Baillie, J.K.; et al. Multi-Ancestry Fine Mapping Implicates OAS1 Splicing in Risk of Severe COVID-19. *Nature Genetics* **2022**, *54*, 125–127, doi:10.1038/s41588-021-00996-8.
110. Choi, U.Y. ung; Kang, J.S.; Hwang, Y.S. ahng; Kim, Y.J. Oligoadenylate Synthase-like (OASL) Proteins: Dual Functions and Associations with Diseases. *Exp Mol Med* 2015, *47*, e144.
111. Pairo-Castineira, E.; Clohisey, S.; Klaric, L.; Bretherick, A.D.; Rawlik, K.; Pasko, D.; Walker, S.; Parkinson, N.; Fourman, M.H.; Russell, C.D.; et al. Genetic Mechanisms of Critical Illness in COVID-19. *Nature* **2021**, *591*, 92–98, doi:10.1038/S41586-020-03065-Y.
112. Zhou, S.; Butler-Laporte, G.; Nakanishi, T.; Morrison, D.R.; Afilalo, J.; Afilalo, M.; Laurent, L.; Pietzner, M.; Kerrison, N.; Zhao, K.; et al. A Neanderthal OAS1 Isoform Protects Individuals of European Ancestry against COVID-19 Susceptibility and Severity. *Nature Medicine* **2021**, *27*, 659–667, doi:10.1038/s41591-021-01281-1.
113. Nakanishi, T.; Pigazzini, S.; Degenhardt, F.; Cordioli, M.; Butler-Laporte, G.; Maya-Miles, D.; Bujanda, L.; Bouysran, Y.; Niemi, M.E.K.; Palom, A.; et al. Age-Dependent Impact of the Major Common Genetic Risk Factor for COVID-19 on Severity and Mortality. *Journal of Clinical Investigation* **2021**, *131*, doi:10.1172/JCI152386.
114. Vuille-Dit-Bille, R.N.; Camargo, S.M.; Emmenegger, L.; Sasse, T.; Kummer, E.; Jando, J.; Hamie, Q.M.; Meier, C.F.; Hunziker, S.; Forras-Kaufmann, Z.; et al. Human Intestine Luminal ACE2 and Amino Acid Transporter Expression Increased by ACE-Inhibitors. *Amino Acids* **2015**, *47*, 693–705, doi:10.1007/S00726-014-1889-6.
115. Mapping the Human Genetic Architecture of COVID-19. *Nature* **2021**, doi:10.1038/S41586-021-03767-X.
116. Gérard, C.; Maggipinto, G.; Minon, J.M. COVID-19 and ABO Blood Group: Another Viewpoint. *British Journal of Haematology* **2020**, *190*, e93–e94, doi:10.1111/BJH.16884.

117. Wang, L.; Balmat, T.J.; Antonia, A.L.; Constantine, F.J.; Henao, R.; Burke, T.W.; Ingham, A.; McClain, M.T.; Tsalik, E.L.; Ko, E.R.; et al. An Atlas Connecting Shared Genetic Architecture of Human Diseases and Molecular Phenotypes Provides Insight into COVID-19 Susceptibility. *Genome Medicine* **2021**, *13*, 1–19, doi:10.1186/S13073-021-00904-Z.
118. Horowitz, J.E.; Kosmicki, J.A.; Damask, A.; Sharma, D.; Roberts, G.H.L.; Justice, A.E.; Banerjee, N.; Coignet, M. v.; Yadav, A.; Leader, J.B.; et al. Genome-Wide Analysis in 756,646 Individuals Provides First Genetic Evidence That ACE2 Expression Influences COVID-19 Risk and Yields Genetic Risk Scores Predictive of Severe Disease. *medRxiv* **2021**, doi:10.1101/2020.12.14.20248176.
119. Geiss-Friedlander, R.; Parmentier, N.; Möller, U.; Urlaub, H.; van den Eynde, B.J.; Melchoir, F. The Cytoplasmic Peptidase DPP9 Is Rate-Limiting for Degradation of Proline-Containing Peptides. *Journal of Biological Chemistry* **2009**, *284*, 27211–27219, doi:10.1074/JBC.M109.041871.
120. Nguyen, A.; David, J.K.; Maden, S.K.; Wood, M.A.; Weeder, B.R.; Nellore, A.; Thompson, R.F. Human Leukocyte Antigen Susceptibility Map for Severe Acute Respiratory Syndrome Coronavirus 2. *Journal of Virology* **2020**, *94*, doi:10.1128/JVI.00510-20.
121. Shang, J.; Wan, Y.; Luo, C.; Ye, G.; Geng, Q.; Auerbach, A.; Li, F. Cell Entry Mechanisms of SARS-CoV-2. *Proc Natl Acad Sci U S A* **2020**, *117*, 11727–11734, doi:10.1073/PNAS.2003138117.
122. Kousathanas, A.; Pairo-Castineira, E.; Rawlik, K.; Stuckey, A.; Odhams, C.A.; Walker, S.; Russell, C.D.; Malinauskas, T.; Wu, Y.; Millar, J.; et al. Whole Genome Sequencing Reveals Host Factors Underlying Critical Covid-19. *Nature* **2022**, 1–10, doi:10.1038/s41586-022-04576-6.
123. Murodzhon, A.; Alberto, A.; Montemanni, R.; Francesco, B.; Ivo, K. OmicsNet: Integration of Multi-Omics Data Using Path Analysis in Multilayer Networks. *bioRxiv* **2020**, doi:10.1101/238766.
124. Sharifi-Noghabi, H.; Zolotareva, O.; Collins, C.C.; Ester, M. MOLI: Multi-Omics Late Integration with Deep Neural Networks for Drug Response Prediction. *Bioinformatics* **2019**, *35*, i501–i509, doi:10.1093/BIOINFORMATICS/BTZ318.
125. Rappoport, N.; Safra, R.; Shamir, R. MONET: Multi-Omic Module Discovery by Omic Selection. *PLOS Computational Biology* **2020**, *16*, e1008182, doi:10.1371/JOURNAL.PCBI.1008182.
126. Song, J.S.; Wang, R.S.; Leopold, J.A.; Loscalzo, J. Network Determinants of Cardiovascular Calcification and Repositioned Drug Treatments. *The FASEB Journal* **2020**, *34*, 11087–11100, doi:10.1096/FJ.202001062R.
127. Coronavirus Disease 2019 (COVID-19) Treatment Guidelines. Available online: https://www.covid19treatmentguidelines.nih.gov/(accessed on 9 May 2022).
128. Wang, M.; Li, A.; Sekiya, M.; Beckmann, N.D.; Quan, X.; Schrode, N.; Fernando, M.B.; Yu, A.; Zhu, L.; Cao, J.; et al. Transformative Network Modeling of Multi-Omics Data Reveals Detailed Circuits, Key Regulators, and Potential Therapeutics for Alzheimer's Disease. *Neuron* **2021**, *109*, 257-272.e14, doi:10.1016/j.neuron.2020.11.002.
129. Barupal, D.K.; Gao, B.; Budczies, J.; Phinney, B.S.; Perroud, B.; Denkert, C.; Fiehn, O. Prioritization of Metabolic Genes as Novel Therapeutic Targets in Estrogen-Receptor Negative Breast Tumors Using Multi-Omics Data and Text Mining. *Oncotarget* **2019**, *10*, 3894–3909, doi:10.18632/oncotarget.26995.
130. Mirzakhani, H.; Litonjua, A.A.; McElrath, T.F.; O'Connor, G.; Lee-Parritz, A.; Iverson, R.; MacOnes, G.; Strunk, R.C.; Bacharier, L.B.; Zeiger, R.; et al. Early Pregnancy Vitamin D Status and Risk of Preeclampsia. *Journal of Clinical Investigation* **2016**, *126*, 4702–4715, doi:10.1172/JCI89031.
131. Schlotter, F.; Halu, A.; Goto, S.; Blaser, M.C.; Body, S.C.; Lee, L.H.; Higashi, H.; Delaughter, D.M.; Hutcheson, J.D.; Vyas, P.; et al. Spatiotemporal Multi-Omics Mapping Generates a Molecular Atlas of the Aortic Valve and Reveals Networks Driving Disease. *Circulation* **2018**, *138*, 377–393, doi:10.1161/CIRCULATIONAHA.117.032291.
132. Sharma, A.; Halu, A.; Decano, J.L.; Padi, M.; Liu, Y.Y.; Prasad, R.B.; Fadista, J.; Santolini, M.; Menche, J.; Weiss, S.T.; et al. Controllability in an Islet Specific Regulatory Network Identifies the Transcriptional Factor NFATC4, Which Regulates Type 2 Diabetes Associated Genes. *npj Systems Biology and Applications* **2018**, *4*, 1–11, doi:10.1038/s41540-018-0057-0.
133. Lerum, T.V.; Aaløkken, T.M.; Brønstad, E.; Aarli, B.; Ikdahl, E.; Lund, K.M.A.; Durheim, M.T.; Rodriguez, J.R.; Meltzer, C.; Tonby, K.; et al. Dyspnoea, Lung Function and CT Findings 3 Months after Hospital Admission for COVID-19. *European Respiratory Journal* **2021**, *57*, doi:10.1183/13993003.03448-2020.
134. Froidure, A.; Mahsouli, A.; Liistro, G.; de Greef, J.; Belkhir, L.; Gérard, L.; Bertrand, A.; Koenig, S.; Pothen, L.; Yildiz, H.; et al. Integrative Respiratory Follow-up of Severe COVID-19 Reveals Common Functional and Lung Imaging Sequelae. *Respiratory Medicine* **2021**, *181*, 106383, doi:10.1016/j.rmed.2021.106383.
135. Carfì, A.; Bernabei, R.; Landi, F. Persistent Symptoms in Patients after Acute COVID-19. *JAMA - Journal of the American Medical Association* **2020**, *324*, 603–605.

136. Wang, B.; Mezlini, A.M.; Demir, F.; Fiume, M.; Tu, Z.; Brudno, M.; Haibe-Kains, B.; Goldenberg, A. Similarity Network Fusion for Aggregating Data Types on a Genomic Scale. *Nat Methods* **2014**, *11*, 333–337, doi:10.1038/NMETH.2810.
137. Chierici, M.; Bussola, N.; Marcolini, A.; Francescatto, M.; Zandonà, A.; Trastulla, L.; Agostinelli, C.; Jurman, G.; Furlanello, C. Integrative Network Fusion: A Multi-Omics Approach in Molecular Profiling. *Frontiers in Oncology* **2020**, *10*, 1065, doi:10.3389/fonc.2020.01065.

Citation: Ward *et al.* Deep Plasma Proteomics with Data-Independent Acquisition: Clinical Study Protocol Optimization with a COVID-19 Cohort. *Journal of Proteome Research* **2024**, 23(9), 3806-3822. https://doi.org/10.1021/acs.jproteome.4c00104

Section III Deep Plasma Proteomics with Data-Independent Acquisition: Clinical Study Protocol Optimization with a COVID-19 Cohort

Bradley Ward[1, 2, †], Sébastien Pyr dit Ruys[1, 2, †], Jean-Luc Balligand[3], Leïla Belkhir[2, 4], Patrice D. Cani[5, 6, 7], Jean-François Collet[8], Julien De Greef[2, 4], Joseph P. Dewulf[2, 9, 10], Laurent Gatto[11], Vincent Haufroid[2, 9], Sébastien Jodogne[12], Benoît Kabamba[7, 13], Maxime Lingurski[1], Jean Cyr Yombi[4], Didier Vertommen[14, *, ‡], Laure Elens[1, 2, *, ‡]

Corresponding Author

Laure Elens: Integrated Pharmacometrics, Pharmacogenomics and Pharmacokinetics Group (PMGK), Louvain Drug Research Institute (LDRI), UCLouvain, Université Catholique de Louvain, 1200 Brussels, Belgium; Laure.Elens@UCLouvain.be

Didier Vertommen: De Duve Institute, and MASSPROT Platform, UCLouvain, Université Catholique de Louvain, 1200 Brussels, Belgium ; didier.vertommen@uclouvain.be

Present Addresses

1. Integrated Pharmacometrics, Pharmacogenomics and Pharmacokinetics Group (PMGK), Louvain Drug Research Institute (LDRI), UCLouvain, Université Catholique de Louvain, 1200 Brussels, Belgium
2. Louvain Center for Toxicology and Applied Pharmacology (LTAP), Institut de Recherche Expérimentale et Clinique (IREC), UCLouvain, Université Catholique de Louvain, 1200 Brussels, Belgium
3. WELBIO (Walloon Excellence in Life Sciences and Biotechnology), Pole of Pharmacology and Therapeutics (FATH), Institut de Recherche Experimentale et Clinique (IREC), Cliniques Universitaires Saint-Luc, UCLouvain, Université Catholique de Louvain, 1200 Brussels, Belgium
4. Department of Internal Medicine, Cliniques Universitaires Saint-Luc, UCLouvain, Université Catholique de Louvain, 1200 Brussels, Belgium
5. Metabolism and Nutrition Research Group, Louvain Drug Research Institute (LDRI), UCLouvain, Université Catholique de Louvain, 1200 Brussels, Belgium
6. WELBIO (Walloon Excellence in Life Sciences and Biotechnology), WELBIO department, WEL Research Institute, avenue Pasteur, 6, 1300, Wavre, Belgium
7. Institute of Experimental and Clinical Research (IREC), UCLouvain, Université catholique de Louvain, Brussels, Belgium
8. WELBIO (Walloon Excellence in Life Sciences and Biotechnology), de Duve Institute, UCLouvain, Université Catholique de Louvain, 1200 Brussels, Belgium
9. Department of Laboratory Medicine, Cliniques Universitaires Saint-Luc, UCLouvain, Université Catholique de Louvain, 1200 Brussels, Belgium
10. Department of Biochemistry, de Duve Institute, UCLouvain, Université Catholique de Louvain, 1200 Brussels, Belgium
11. Computational Biology and Bioinformatics Unit (CBIO), de Duve Institute, UCLouvain, Université Catholique de Louvain, 1200 Brussels, Belgium
12. Computer Science and Engineering Department (INGI), Institute of Information and Communication Technologies, Electronics and AppliedMathematics (ICTEAM), UCLouvain, Université Catholique de Louvain, 1348 Louvain-la-Neuve, Belgium
13. Pôle de Microbiologie, Institut de Recherche Expérimentale et Clinique, UCLouvain, Université Catholique de Louvain, 1200 Brussels, Belgium
14. De Duve Institute, and MASSPROT Platform, UCLouvain, Université Catholique de Louvain, 1200 Brussels, Belgium

†These authors contributed equally to this work.

‡ These authors contributed equally to this work.



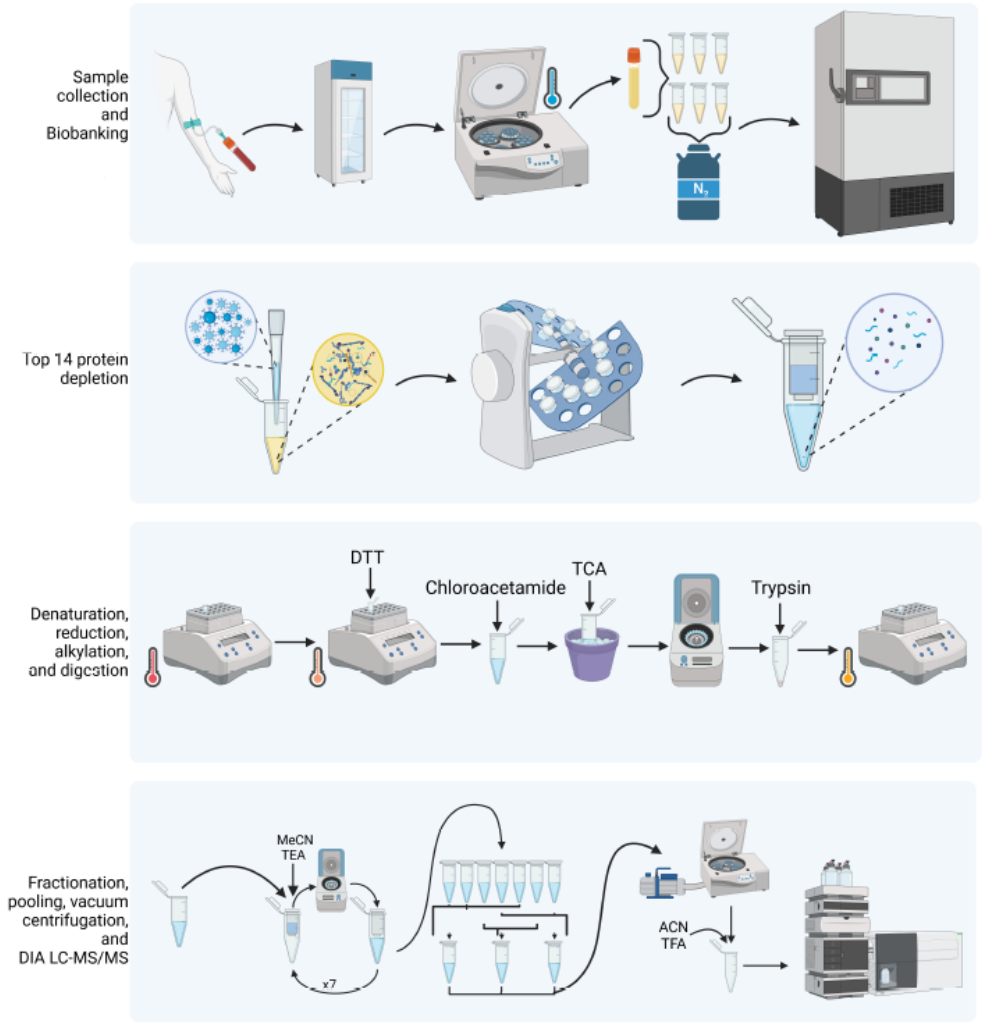
ABSTRACT

Plasma proteomics is a precious tool in human disease research Plasma proteomic is a precious tool in human disease research, but requires extensive sample preparation in order to perform in-depth analysis and biomarker discovery using traditional Data-Dependent Acquisition (DDA). Here, we highlight the efficacy of combining moderate plasma prefractionation and Data-Independent Acquisition (DIA) to significantly improve proteome coverage and depth, while remaining cost-efficient.

Using human plasma collected from a 20-patient COVID-19 cohort, our method utilises commonly available solutions for depletion, sample preparation, and fractionation, followed by 3 LC-MS/MS injections for a 360-minutes total DIA run time. We detect 1,321 proteins on average per patient, and 2,031 unique proteins across the cohort. Differential analysis further demonstrates the applicability of this method for plasma proteomic research and clinical biomarker identification, identifying hundreds of differentially abundant proteins at biological concentrations as low as 47ng/L in human plasma. Data are available via ProteomeXchange with identifier PXD047901.

In summary, this study introduces a streamlined, cost-effective approach to deep plasma proteome analysis, expanding its utility beyond classical research environments and enabling larger-scale multi-omics investigations in clinical settings. Our comparative analysis revealed that fractionation, whether the samples were pooled or separate post-fractionation, significantly improved the number of proteins quantified. This underscores the value of fractionation in enhancing the depth of plasma proteome analysis, thereby offering a more comprehensive landscape for biomarker discovery in diseases such as COVID-19.

GRAPHICAL ABSTRACT



KEYWORDS: *plasma proteomics, fractionation, data-independent acquisition, COVID-19, DIA-NN, biomarkers, deep proteome analysis, clinical proteomics*

INTRODUCTION

Human plasma proteomics is a rapidly evolving field aimed at identifying and understanding the functions of proteins in human blood. Plasma contains a wide array of substances, including hormones, metabolites, and proteins produced by various organs and tissues within the body, providing a comprehensive snapshot of an individual's overall health [1,2]. Over 4,500 canonical proteins have been detected in human plasma, representing approximately 20% of the currently detectable human proteome [3]. Plasma's ease of collection and significant biological relevance make it a valuable resource for disease research. For example, extensive research into the effects of coronavirus disease 2019 (COVID-19 has leveraged plasma proteomics to identify biomarkers such as S100A9 [4,5], ITIH2 [6], TNF- α [7], and cytokines [8]. These studies have partially elucidated disease pathophysiology by discovering dysregulated proteins and pathways, thereby identifying potential drug targets and treatments.

Studying the human plasma proteome, however, presents several challenges. Firstly, plasma is an incredibly heterogeneous sample, containing lipids, metabolites, and other small molecules which must be removed to prevent interference with protein detection and quantification. Secondly, the protein content of plasma is complex, varies between individuals, and is dynamic, with protein concentrations spanning 12-13 orders of magnitude [9]. This is outside the dynamic range of modern analytical instruments, complicating the detection and quantification of low-abundant proteins [10]. Thirdly, many proteins undergo post-translational modifications, generating numerous proteoforms that require specialized techniques and equipment to identify [11]. Lastly, analysing the large datasets generated by these studies requires sophisticated bioinformatics and biostatistical tools, as well as expertise to interpret and validate the data, requiring a multidisciplinary approach [12]. Despite these challenges, advances in

technology and methodology are providing new opportunities to explore the plasma proteome.

Depleting high abundant proteins can enhance the detection of low-abundance ones, but this process may also inadvertently deplete many low-abundant proteins, as high-abundant proteins (such as albumin, immunoglobulins, fibrinogen and apolipoprotein) often have carrier functions [13,14]. Despite this off-target protein depletion, it remains a critical strategy for any proteomic study seeking to delve deeply into the human proteome. As depletion does not completely remove high abundant proteins, high sensitivity techniques (such as Data-Independent Acquisition (DIA)) may still identify them, making this less of an issue. However, because depletion may distort the relative quantification between samples, studies utilising depletion methodologies should back-up quantitative results with targeted methods, such as ELISA, ensuring accuracy and reliability of the relative quantification.

Beyond depletion strategies, fractionation techniques further enhance proteomic analysis by dividing samples into fractions of lower complexity, helping to better identify low-abundant proteins. Fractionation usually occurs after digestion at the peptide level for bottom-up proteomics. Generally, more fractions lead to more proteins identified, with one study showing increases of 90%, 48%, and 32% unique proteins identified at 5 vs 20, 12 vs 24, and 20 vs 40 fractions, respectively [15]. However, drawbacks include minor sample loss and increased analytical time, which can greatly increase costs.

Traditionally, untargeted mass spectrometry proteomics relied on data-dependent acquisition (DDA), but its selectivity and reproducibility have limitations due to its stochastic nature. Consequently, DIA techniques have grown in popularity. Many DIA techniques have been introduced [16–20], but the general results are that all precursor product ions are analysed in a systematic and unbiased manner. This allows DIA to achieve reproducibility rates of up to

99% and 98% at the peptide and protein levels, respectively, compared to around 80% for DDA methods [21]. However, DIA usually results in highly complex MS2 spectra which are challenging to interpret and quantify, requiring specialised software and computational resources.

A multitude of software have been developed to aid in DIA bioinformatics, the most popular being Skyline [22], OpenSWATH [23], EncylopeDIA [24], Spectronaut [25], DIA-Umpire [26], and DIA-NN [27]. DIA-NN, in particular, employs deep neural networks to better distinguish real signals against analytical noise, coupled with new quantification and signal strategies [27,28]. These methodologies enhance detection sensitivity and specificity, as validated in multiple benchmarking studies where DIA-NN has outperformed other DIA analytical strategies in terms of numbers of identified proteins, while minimising missing values within the data [27,29].

Within this paper, we present a simplified sample preparation protocol consisting of depletion followed by fractionation and subsequent pooling of fractions, resulting in 3 LC-MS/MS injections per sample (360 minutes total run time). Coupled with the recent developments in DIA-based proteomics and DIA analytical software, we are able to achieve an average of 1,231 proteins identified per sample and 1,603 unique proteins in a 20-patient preliminary cohort (described below), at a much lower cost-per-sample than highly fractionated DDA methodologies, using widely available commercial kits and solutions (48.77 € ex. VAT, Belgium. Price excludes common laboratory reagents and plastics, machine running costs, and technician hours, which can vary greatly between labs and countries).

METHODS

Proof-of-Concept Sample Cohort

The cohort included in this study comprises a 20 patient sub-cohort from the HYGIEIA study [30]. Patients were enrolled from August 2020 to December 2023. The protocol has received ethical approbation from the local ethical committee (2021/30DEC/543) and has been registered on clinicaltrial.gov (NCT05557539). During recruitment, a subset of 20 patients were selected for a validation cohort and split into five balanced groups (n=4): healthy controls, respiratory infection controls, moderate COVID-19 WHO score <=2, severe COVID-19 WHO score 3-5, and critical COVID-19 WHO score >=6 [31]. Each group was comprised of two males and two females, average age of the cohort was 47 years old at hospitalisation, average BMI was 26kg/m^2. 16 patients were of Caucasian ethnicity, with the remaining four patients having North African, Caribbean, Arab, and unknown ethnicities (self-reported by patient).

Patient Sample Storage

Patient samples were collected during the acute phase of the infection and/or within one day of patient consent to study inclusion. Plasma samples were collected in 4mL Lithium heparin gel prepared S-Monovette tubes (Sarstedt, Nümbrecht, Germany) and kept at 4° C for a maximum of 4 hours until plasma was separated via centrifugation (2600g for 10 minutes at 4° C) (Sigma 3-16KL, Sigma Laboratory Centrifuges, Osterode am Harz, Germany), then aliquoted, snap frozen in liquid nitrogen, and stored at -80° C until later processing.

Protein and Peptide Quantitation

In the following methodology, where appropriate, protein quantitation was performed using the Bio-Rad Protein assay kit II (Bio-Rad Laboratories, Hercules, United State) and peptide quantitation was performed using the Pierce ™ Quantitative Peptide Assays & Standards (Thermo Fisher Scientific, Waltham, United States).

Protein Depletion

Protein depletion was performed according to manufacturer instructions. Briefly, the High Select™ Top14 Abundant Protein Depletion Resin (Thermo Fisher Scientific, Waltham, United States) is gently homogenised by inverting the tube several times. Then 600µl of resin is deposed into a 2mL Protein LoBind® Eppendorf tube (Eppendorf, Hamburg, Germany) and allowed to equilibrate to room temperature (RT) (15° C – 25° C). 22µl of plasma sample are then added and gently mixed via inversion before adding the tube on a rotator (Loopster digital, IKA, Staufen, Germany) at 12 RPM for 10 minutes at room temperature (RT, 18-25° C). It should be noted, the ratio of resin to plasma used allowed for significant depletion of high abundant proteins, without total depletion, to prevent loss of associated carrier proteins.

The plasma-resin mixture is then transferred to a Pierce™ Micro-Spin Column (Thermo Fisher Scientific, Waltham, United States) placed in a 2mL Protein LoBind® Eppendorf tube and centrifuged at 1000g for 2 minutes at RT (Microcentrifuge 5415, Eppendorf, Hamburg, Germany).

Digestion

The flow through is first incubated at 95° C for 5 minutes (ThermoMixer C, Eppendorf, Hamburg, Germany), then the sample is allowed to cool for 5 minutes at RT. 33µl of 50mM DL-Dithiothreitol (5mM final concentration) (Sigma-Aldrich, St. Louis, United States) are then added to the sample and incubated at 56° C for 1 hour at 1000 RPM (ThermoMixer C, Eppendorf, Hamburg, Germany). 37µl of 500mM chloroacetamide (50mM final concentration) (Sigma-Aldrich, St. Louis, United States) are added and the mixture is vortexed briefly (max power, 3 seconds, Vortex-Genie 2, Scientific Industries, Bohemia, United States) and spun down (3 seconds, Mini Centrifuge, ExtraGene, Davis, United States), then incubated at RT for 30 minutes in the dark. Then 65.5µl 100% trichloroacetic acid (15% final concentration) (Sigma-Aldrich, St. Louis, United States) are added, the sample is then vortexed briefly and, again, spun down, and finally, incubated on ice for 30 minutes.

After incubation, the sample is centrifuged for 4000g for 7.5 minutes, then washed 3 times by removing supernatant, adding 500µl -20° C acetone (Carl Roth, Karlsruhe, Germany) sonicating at 37kHz pulsed for 2 minutes (Elmasonic P, Elma, Singen am Hoentwiel, Germany), then centrifuging at 4000g for 5 minutes. After repeating 3 times, the supernatant is again removed, and the sample is allowed to air-dry for 10 minutes at RT. Next, 75µl triethylammonium bicarbonate (TEAB) 50mM (Thermo Fisher Scientific, Waltham, United States) are added to the tube, followed by two rounds of sonication at 37kHz pulsed for 2 minutes each. The sample is subsequently vortexed and spun-down, then 2.5µg sequencing grade modified trypsin (V5117, Promega, Madison, United States) are added (50:1 protein:protease) and the sample is incubated overnight at 37° C at 750 RPM (ThermoMixer C).

Fractionation

Following incubation, 8.3µl 1% trifluoroacetic acid (Biosolve, Dieuze, France) are added to the sample (0.1% final concentration), then 80µg total peptide are directly deposed on a Pierce™ High pH Reversed-Phase Peptide Fractionation column (Thermo Fisher Scientific, Waltham, United States) and centrifuged at 3000g for 2 minutes. The flow through is then discarded, and the column washed with 300µl MS grade water at 3000g for 2 minutes. Fractions are collected from column in 1.5mL Protein LoBind Eppendorf tubes (Eppendorf, Hamburg, Germany) by adding 300µl of the appropriate elution solution to the column and centrifuging at 3000g for 2 minutes. Elution solutions contain 0.1% triethylamine with either 7.5%, 10%, 12.5%, 15%, 17.5%, 20%, or 50% acetonitrile for collecting fractions 1 through 7 respectively.

Following fractionation, pooling of the fractions are carried out with 100µl each of fraction 1, 2, and 5 as pooled fraction 1, 150µl each of fraction 3 and 6 as pooled fraction 2, and 150µl each of fraction 4 and 7 as pooled fraction 3. Pooling fractions in such a way helps ensure chemically dissimilar peptides are pooled

together. The pooled fractions are then incubated on dry ice for 5 minutes, then open tubes are placed into a vacuum concentrator (SpeedVac SRF110, Thermo Fisher Scientific, Waltham, United States) at 4° C until pooled fractions have fully evaporated. 20µL MS resuspension buffer (3.5% ACN, 0.1% TFA) are subsequently used to resuspend each tube, and 3 sonication cycles at 37kHz pulsed for 2 minutes are repeated. Finally, each resuspended sample is briefly vortexed and spun down. A summary of the different fractionation strategies used in this paper can be seen in figure 1.

DIA LC-MS/MS Injection

1 µg of peptides dissolved in solvent A ((MS resuspension buffer) 0.1% TFA in 3.5% ACN) was directly loaded onto a reversed-phase pre-column (Acclaim PepMap 100, Thermo Fisher Scientific, Waltham, United States) and eluted in backflush mode. Peptide separation was achieved using a reversed-phase analytical EasySpray column (Acclaim PepMap RSLC C18, 0.075mm × 250mm, Thermo Fisher Scientific, Waltham, United States) with a 120 minute linear gradient of 4%–32% solvent B (0.1% TFA in 80% ACN) for 100 minutes, 32%–50% solvent B for 5 minutes, 50%–90% for 5 minutes and holding at 95% for the last 9 minutes at a constant flow rate of 300nL/min on an Ultimate 3000 RSLC nanoHPLC system (Thermo Fisher Scientific, Waltham, United States). The peptides were analyzed by an Orbitrap Exploris 240 mass spectrometer (Thermo Fisher Scientific, Waltham, United States) with enabled advanced peak determination (APD). The peptides were subjected to an EasySpray ionization source, followed by MS/MS in the Exploris 240 coupled online to the HPLC. Intact peptides were detected in the Orbitrap at a full width at half-maximum resolution of 30,000 (FWHM) and MS/MS spectra were acquired in the Orbitrap after stepped higher energy collisional dissociation (HCD) fragmentation at 22%, 26% and 30% of maximum. A data-independent procedure of MS/MS scans was applied for the precursor ions within a m/z range of 500-740 and an m/z isolation

window of 4 at a resolution of 60,000 (FWHM). MS1 spectra were obtained with an automatic gain control (AGC) target of 1.2×10^6 ions and a maximum injection time of 55ms. MS2 spectra were acquired with an AGC target of 1.5×10^5 ions and a maximum injection time set to auto. For MS2 scans, the m/z scan range was set at 145 to 1450. Run time for each injection was 120 minutes.

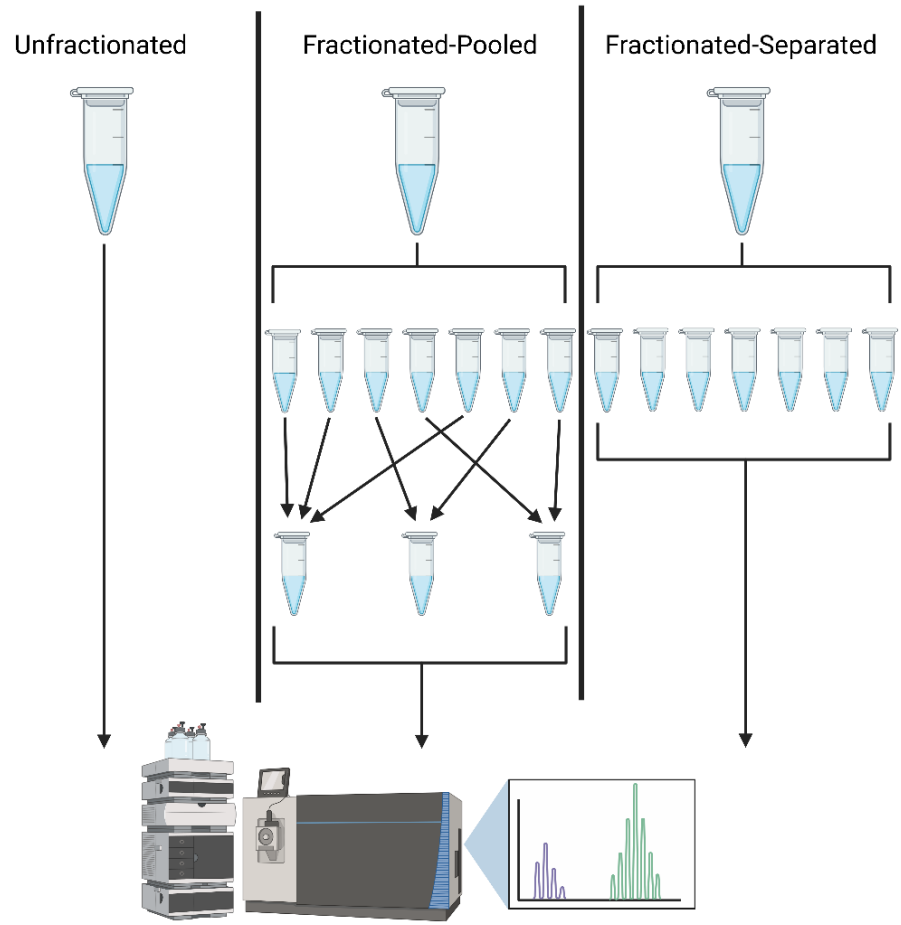


Figure 1. Schema of the fractionation strategies used in the paper. Following protein depletion, denaturation, reduction, alkylation, and digestion, unfractionated samples are directly analyzed. For fractionated samples, the samples are separated into 7 fractions using a high pH reversed-phase column. Fractionated-pooled fractions are then combined into 3 pooled fractions, which are then analyzed, while fractionated-separated fractions are directly analyzed. Created with BioRender.com.

DDA LC-MS/MS Injection

Peptides were injected and separated as described above. The peptides were analyzed by an Exploris240 Orbitrap mass spectrometer (Thermo Fisher Scientific, Waltham, United States). The peptides were subjected to nanospray ion source followed by MS/MS in Exploris240 coupled online to the nano-LC. Intact peptides were detected in the Orbitrap at an FWHM resolution of 60,000. Peptides were selected for MS/MS using HCD setting at 30%; ion fragments were detected in the Orbitrap at an FWHM resolution of 15,000. A data-dependent procedure that alternated between one MS scan followed by MS/MS scans was applied for 3 seconds for ions above a threshold ion count of $1.0e^4$ in the MS survey scan with 40.0 seconds dynamic exclusion. The electrospray voltage applied was 2.1kV. MS1 spectra were obtained with an AGC target of $4e^5$ ions and a maximum injection time of 50ms, MS2 spectra were acquired with an AGC target of $5e^4$ ions and a maximum injection time set to dynamic. For MS scans, the m/z scan range was 375 to 1800. Run time for each injection was 120 minutes.

Bioinformatic Analysis

DIA-NN 1.8.1 was first used to generate an *in-silico* predicted spectral library from the UniProtKB human reference proteome (accession UP000005640) featuring only review (Swiss-Prot) canonical proteins [32,31].

Following HPLC-MS/MS acquisition, Thermo .raw spectra files for all fractions and all patients were imported into DIA-NN 1.8.1 [27] using the Thermo MS File Reader (Thermo Fisher Scientific, Waltham, United States). The *in-silico* library was used as the spectral library, and to further aid peak detection, match-between-runs mode was enabled. In addition to default options, the following options were used: FASTA digest for library-free search/library generation; Deep learning-based spectra, RTs and IMs prediction; Maximum number of variable modifications = 1, Modifications = N-term M excision, C carbamidomethylation, Ox(M); Unrelated runs; MBR; Neural network classifier = Double-pass mode;

Quantification strategy = Any LC (high accuracy); Precursor false discovery rate (%) = 1.0. Quantification was performed at the MS2 level. After processing, the corresponding report file was then loaded into R for processing (v4.3.1) [33]. The complete script can be found in Supporting Material S1, but in brief, runs were separated into pooled fraction 1, pooled fraction 2, and pooled fraction 3 to be processed separately via QFeatures(v3.17) [34], log transformed, and normalised. The 3 fraction assays were then combined and protein intensities were aggregated into protein groups via the robust summary methodology [35] The process for non-fractionated samples was similar, except that runs did not have to be separated and then recombined.

For DDA samples, the resulting MS/MS data was processed using Sequest HT search engine within Proteome Discoverer 2.5 SP1 (Thermo Fisher Scientific, Waltham, United States) against the same Uniprot database used for the DIA predicted library, trypsin was specified as cleavage enzyme allowing up to 2 missed cleavages, 2 modifications per peptide and up to 5 charges. Mass error was set to 10 parts per million (ppm) for precursor ions and 0.02 Da for fragment ions. Oxidation on Met (+15.995 Da), pyro-Glu formation from Gln or Glu (-17.027 Da or -18.011 Da respectively) were considered as variable modifications. C carbamidomethylation was considered as a fixed modification. Quantification was performed at the MS1 level. False discovery rate (FDR) was assessed using Percolator and thresholds for protein, peptide and modification site were specified at 1%. Label free quantification was performed by Proteome Discoverer 2.5 using the area under the curve (AUC) for each peptide.

During data analysis, predicted protein concentrations in plasma were obtained from the human protein atlas [36,37]. For COVID-19 biomarkers and COVID-19 associated proteins, the OncoMX COVID-19 biomarker database and OpenTargets platform (targets associated with COVID-19) were used respectively [38,39]. PCA plots were generated using a 0% missing protein cut-off.

The mass spectrometry proteomics data have been deposited to the ProteomeXchange Consortium via the PRIDE partner repository with the dataset identifier PXD047901 [40].

STATISTICAL ANALYSIS

Statistical analysis of the data was carried out using R(v4.3.1) [33]. Two sample proportion tests and t test were used to evaluate the significance of the data when appropriate, such as when comparing the differences in the mean number of identified proteins in fractionated and non-fractionated samples. The types of test used are referenced within the text when needed alongside the adjusted p-values. For t tests comparing DDA to DIA, or non-fractionated to fractionated, the assumption is that DIA, or fractionation, produces superior results and so one-sided t tests are used in these cases. Significance levels of protein abundances was calculated using t tests. All code used to generate statistics can be found in Supporting Material S1.

RESULTS

In the current study, our objective was to evaluate the effectiveness of different proteomic workflows in plasma sample analysis, with a focus on biomarker discovery. The analysis was conducted on samples from a cohort of 20 patients, employing three distinct methodologies: unfractionated, fractionated-pooled, and fractionated-separated (figure 1). The intention behind these workflows was to explore the potential for increased proteome coverage and the enhanced detection of low-abundance proteins. The unfractionated approach provided a baseline by analyzing the plasma samples in their entirety, without any pre-processing steps. Conversely, the fractionated approaches aimed to deepen our insights into the plasma proteome by segregating the samples into fractions, which were then analyzed either collectively (pooled) or individually (separated). The primary goal was to identify a workflow that not only maximizes proteome coverage but also remains practical for routine applications in the context of infectious disease biomarker identification. All results presented below have been collected through DIA analysis, unless stated otherwise.

Enhanced Protein Detection with Fractionation

Mean number of proteins detected and quantified in human plasma are found to be significantly higher, with an increase of around 50% for fractionated-pooled samples as compared to unfractionated samples, with an average of 1,321 and 894 proteins per patients for fractionated-pooled and unfractionated samples respectively (right-tailed, paired, t-test, p-value = 1.17e-06). A similar trend is seen for total unique quantified proteins, with 2,031 total unique proteins found in fractionated-pooled samples and 1,765 in unfractionated samples. The numbers of common proteins detected in all patients was also significantly increased in fractionated-pooled samples, with 570 common proteins (around 43% of proteins on average) compared to 303 in unfractionated samples (around 34% of proteins on average) (two sample proportion test, p-value = 1.38e-63).

Alongside the enhanced detection of proteins within fractionated-pooled samples, fractionation also appears to improve protein detection consistency between samples. This is visualised in figure 2A, which shows a higher consistency of protein identification across patient samples with fractionation-pooled as opposed to unfractionated samples.

Not only are more unique proteins found within fractionated-pooled samples, but a higher proportion of these proteins are found within a higher number of samples. Looking at figure 2B, we can also see the majority of information (in terms of detected proteins) is almost completely found within the fractionated-pooled samples, with unfractionated samples providing only a small number of unique proteins. Indeed, out of 2,061 unique proteins in both fractionated-pooled and unfractionated samples, 296 are uniquely found in fractionated-pooled samples, 1,735 are found in both, and only 30 are found uniquely in unfractionated samples.

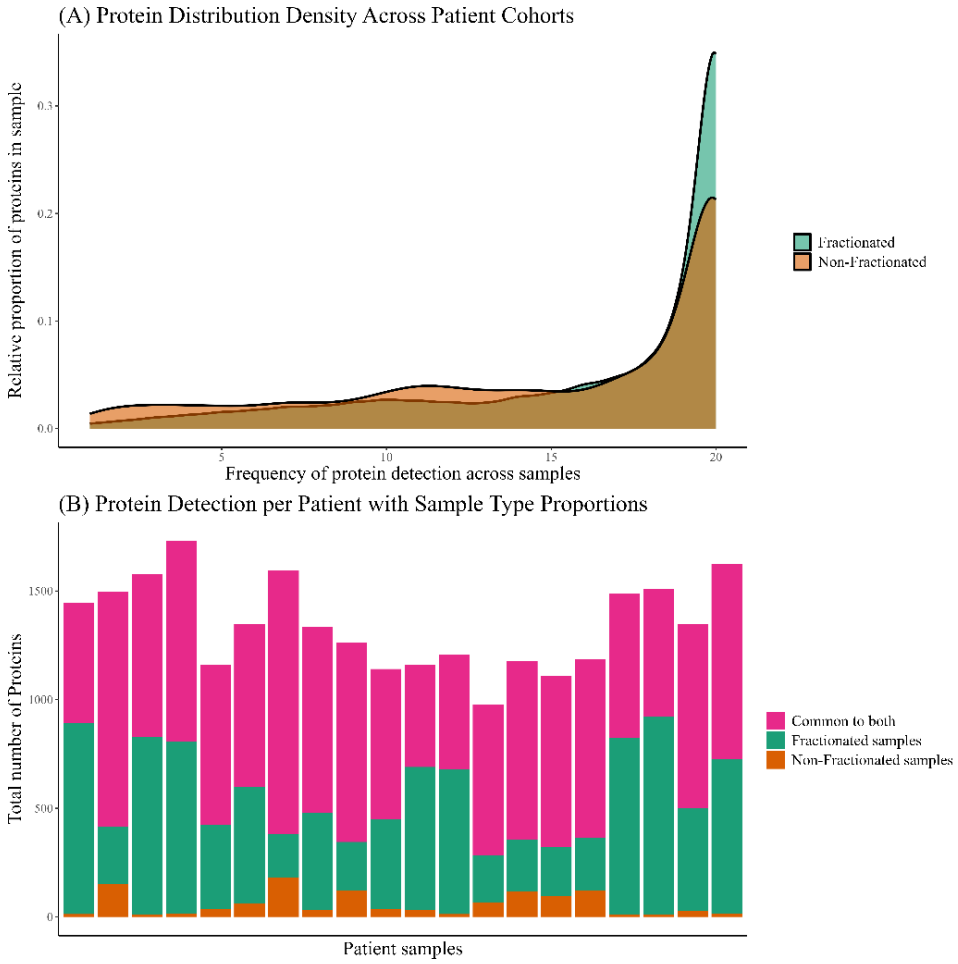


Figure 2. Protein distribution density across patient cohorts: Density plot. Illustrates the proportion to which proteins are found in each sample within the cohort (20 patients) for each group. A higher peak toward the right of the graph suggests proteins are found more consistently in a higher proportion of the patient cohort. Protein detection per patient with sample type proportions: Bar plot. Number of proteins detected per patient; color grouping within each bar shows which proportion of the proteins are found in both fractionated-pooled and unfractionated samples (common to both) (pink) and which are unique to fractionated-pooled (green) or unfractionated samples (orange).

Looking at how protein intensities were aggregated, fractionated-pooled samples generally aggregate proteins using more unique precursors (83% of proteins aggregated with two or more unique precursors), whilst a major fraction of unfractionated proteins, 42%, are aggregated from just one unique precursor (Supplementary figure 2). The mean number of unique precursors used for protein aggregation was 12 vs 5 for fractionated-pooled and unfractionated samples respectively, whilst the median was 3 and 2 respectively, a significant difference (Mann-Whitney-Wilcoxon test, p-value < 2.2e-16).

In figure 3, most of the commonly identified proteins tend to be present at higher concentrations than the uniquely identified proteins, which are all almost always identified uniquely in the fractionated samples and present at lower concentrations. Fractionation of samples results in a slight enhanced detection of proteins found at lower biological concentrations (log10 concentration (mg/mL) of -4.8 vs -4.6 for fractionated-pooled and unfractionated samples respectively, left-tailed t-test, p-value = 0.0007). Although both methodologies are able to detect similarly low abundant proteins, fractionated-pooled samples are able to detect these proteins more commonly across a cohort, with denser data allowing for far superior downstream data analysis.

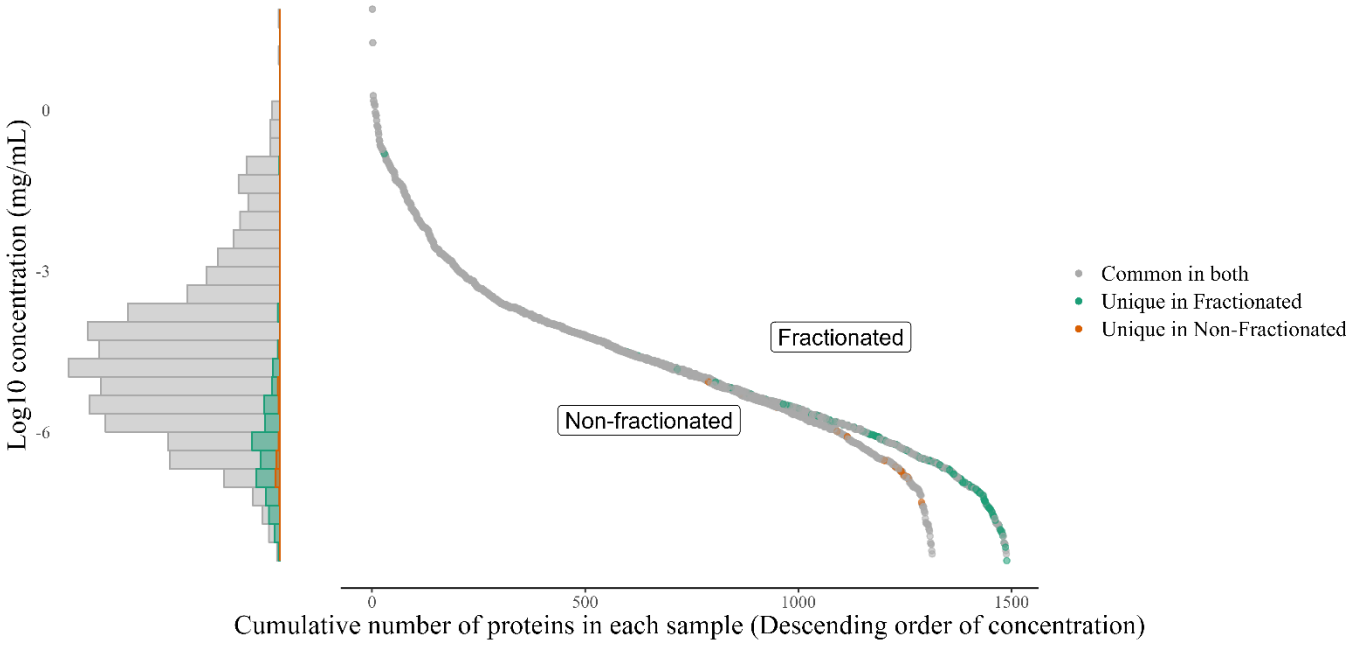


Figure 3. Plasmatic concentration of identified proteins. The left-hand side represents the data in histogram format, while the right-hand side shows the data as a point graph, with each point representing a protein and ranked and ordered along the *x*-axis by descending concentration. Proteins found in both fractionated-pooled and unfractionated samples are marked in gray, those unique to fractionated-pooled samples are marked in green, and those unique to unfractionated samples are marked in orange. Proteins that did not have a concentration listed in the human protein atlas database36,37 were not shown (542 fractionated proteins and 451 nonfractionated proteins).

Comparative Advantages of DIA over Traditional DDA Approaches

As far as how these additional precursors relate to protein identification, figure 4 shows data from the same samples processed with the 3 different fractionation methods and acquired in the LC-MS/MS system in either DDA or DIA modes, in order to make a comparison between fractionation methods as well as acquisition methods. Figure 4 shows a large increase in protein identification in both fractionation strategies compared to the unfractionated strategy. This increased protein identification tends to be predominantly for lower abundant proteins. In terms of how the pooling process affects protein identification, we can see a 16% drop (232 proteins) from the fractionated-separated to fractionated-pooled. For DDA data, this drop is more pronounced, with a 24% drop in protein identification between fractionated-pooled and fractionated-separated (121 proteins). As expected, these proteins tend to be towards the lower end of the concentration range for each method, although both fractionation workflows are able to identify proteins in equally low concentrations. Figure 4 shows a significant increase in the number of identified proteins using DIA as compared to DDA. Using DIA boosts the number of unique, detected proteins 249% for unfractionated samples (+744 proteins), 211% for fractionated-pooled (+826 proteins), and 183% for fractionated-separated (+937 proteins). Additionally, the proteins uniquely identified in samples ran in DIA mode all tend to be low-abundant proteins, and although there is some overlap between the abundances of proteins identified in DDA and DIA modes, DIA mode has a much greater abundance range of acquisition. 90% of the identified DDA proteins have a concentration between 92.5μg/ml and 0.082μg/ml, where as 90% of DIA proteins have an abundance between 10.1μg/ml and 0.0014μg/ml. Median concentration was 2.1μg/ml and 0.055μg/ml for DDA and DIA proteins respectively.

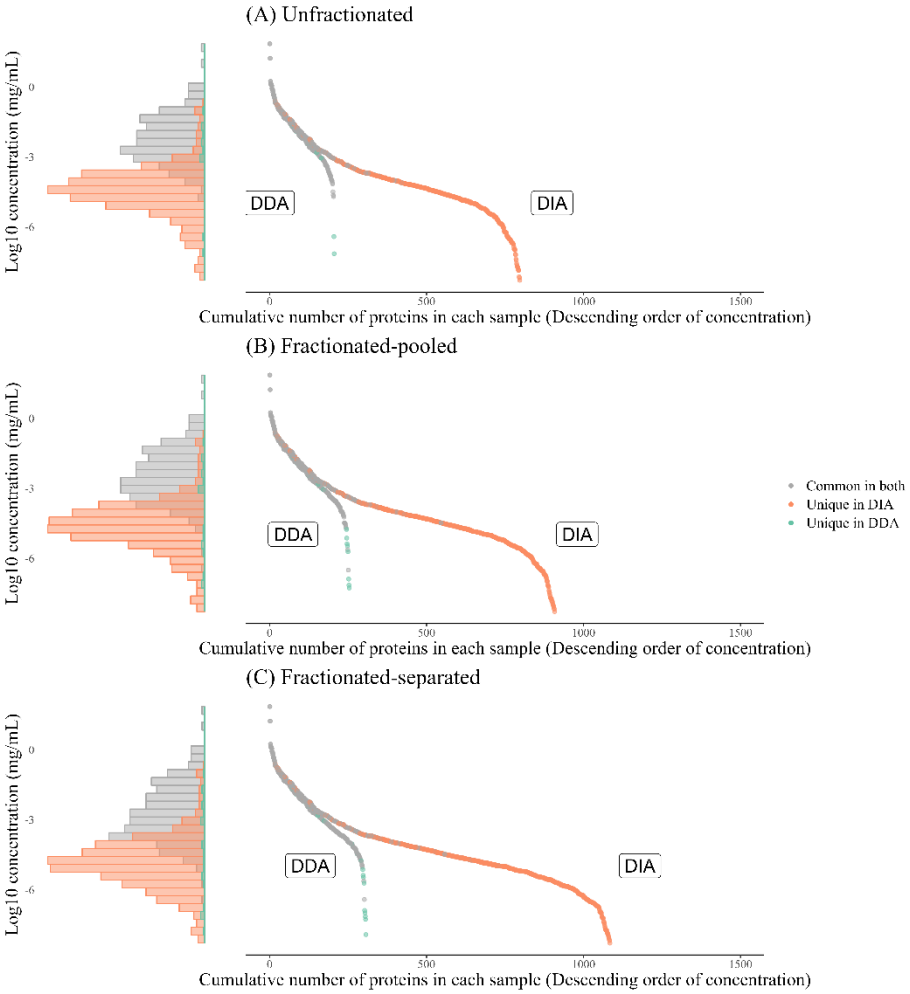


Figure 4. Left-hand side represents data as a histogram, while the right-hand side is a point graph in which each point represents a unique protein, as identified in either DDA or DIA workflows, arranged along the *x*-axis in descending order of plasmatic concentration (*y*-axis). Graphs are separated into data related to unfractionated, fractionated-pooled, or fractionated-separated. Proteins common to both DDA and DIA are identified in gray. Proteins unique to DIA workflows are identified in orange, and proteins unique to DDA workflows are identified in green. Proteins with no listed concentration in the human protein atlas database,36,37 excluded (unfractionated: DDA = 23, DIA = 157; fractionated-pooled: DDA = 27, DIA = 208; fractionated-separated: DDA = 43, DIA = 252).

Using the entire 20 patient cohort, figure 5 shows a direct comparison between DDA and DIA analytical modes for unfractionated samples. More than triple the average number of proteins per sample are found in DIA samples as compared to DDA samples, 838 vs 236 respectively, and a similar magnitude of increase is seen for the total unique proteins between DIA and DDA, 1,765 vs 563 respectively. Further, DIA is also seen to have slightly better coverage in terms of identification of each protein within samples, with each protein appearing in an average of 9.49 samples vs an average of 8.39 samples for DDA proteins (out of 20 samples total) (right-tail t-test, p-value = 0.0015). When considering proteins found in both DIA and DDA, the difference is further exacerbated, with these proteins being found in 17.1 DIA samples vs 9.77 DDA samples (right-tail t-test, p-value < 2.2e-16). Finally, in terms of core proteins (those proteins found within all 20 samples), DIA has more than double the number of core proteins at 303, as compared to 116 core proteins found with DDA (DIA vs DDA, unfractionated samples).

Taken together, these data would suggest that not only does DIA allow for a great increase in the number of proteins detected per sample and at lower abundances, but that it also allows for a much greater identification rate of those proteins between samples.

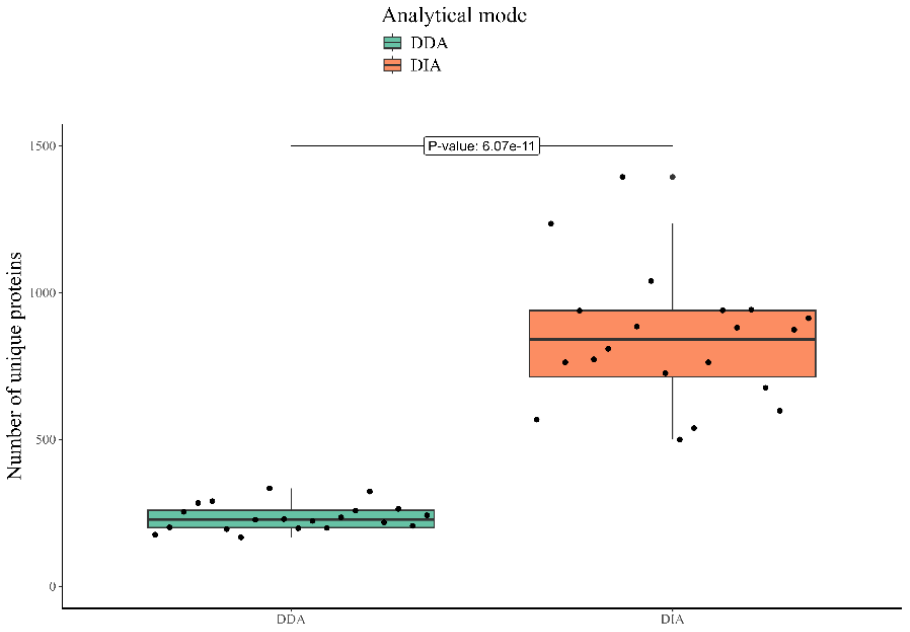


Figure 5. Boxplot of the number of unique proteins detected per patient in DDA and DIA modes using identical unfractionated samples. Points represent individual patients. Statistical test used: right-tailed, paired, *t* test, $t = 12.55$, p-value = $6.07 \times 10–11$.

Biomarker Discovery in COVID-19: Insights from a Preliminary Cohort

As the cohort used here was part of the larger HYGIEIA cohort for a study into COVID-19, we provide here some preliminary biostatistical analyses to investigate how the fractionated-pooled samples compare to unfractionated samples when investigating biological differences. Figure 6 shows that both methodologies can separate healthy controls and moderate COVID-19 from the respiratory failure group and severe COVID-19 which required hospitalisation, when analysed by Principal component analysis (PCA, principal components 1 and 2, only core proteins retained for analysis). The unfractionated samples separate these four groups along PC1 and PC2, whilst the fractionated samples separate the four groups along PC1 only. Including PC3 for fractionated-pooled samples can help to further separate overlapping healthy controls and moderate COVID-19 patients to some extent. Unfractionated samples are able to capture around 65% of the data variation in PC1 and PC2, whilst fractionated-pooled samples are only able to capture around 40% in these two components.

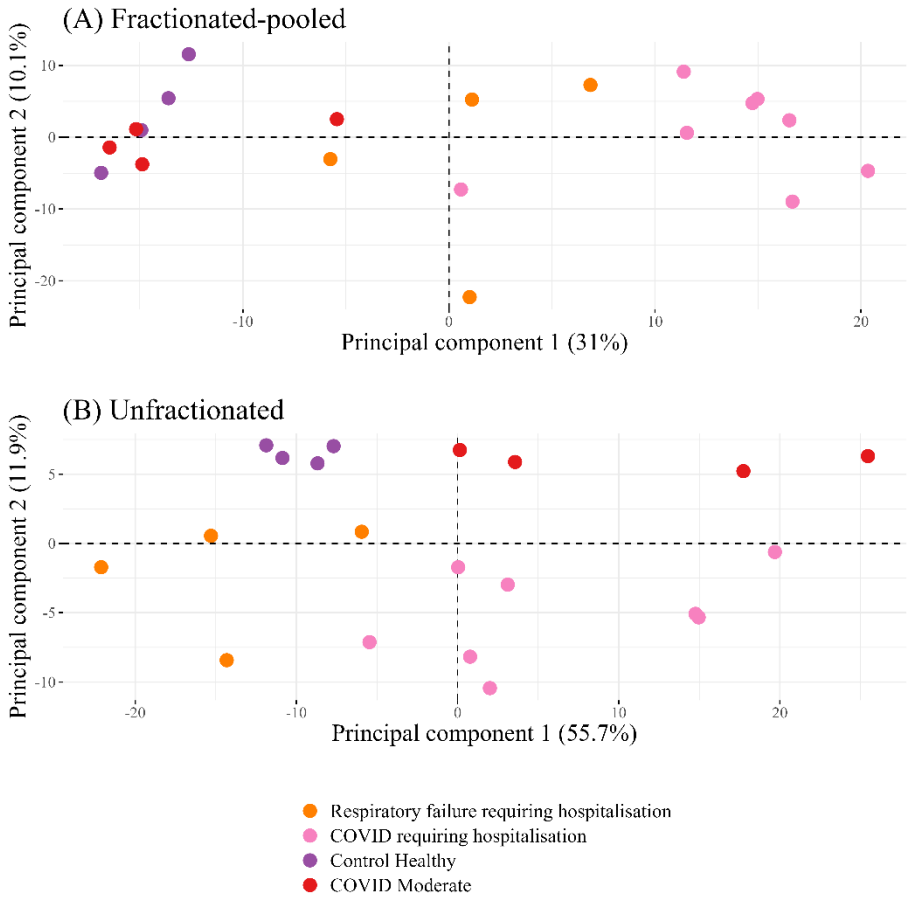


Figure 6. PCA of fractionated-pooled samples (A) and unfractionated samples (B). Patients are grouped into four categories: two controls, a healthy control (purple) and a severe respiratory failure control (orange), and two COVID-19 groups, moderate COVID-19 (red), which did not require hospitalization, and severe/critical COVID-19 (pink), which did require hospitalization. PCA was conducted on proteins present in all samples (no missing values), fractionated-pooled = 570 total proteins, and unfractionated = 303 total proteins.

When looking at a differential abundance analysis (moderate COVID-19 patients vs hospitalised (severe and critical) COVID-19 patients), we see the fractionated-pooled samples (figure 7A and 8B) significantly outperform the unfractionated samples (figure 7C and 8D) at identifying differentially abundant proteins, 264 vs 23 (two sample proportion test, p-value = 4.73e-35). Of these differentially abundant proteins (full list found in Supporting Material S3), the number of COVID-19 biomarkers (OncoMX COVID-19 biomarker database [38]) is also greater in fractionated-pooled samples (9 vs 5), although not at a significantly different proportion (two sample proportion test, p-value = 0.086). Identified biomarkers were C-reactive protein, serum amyloid A1, cystatin C, albumin, colony stimulating factor 1, von Willebrand factor, selectin P, galactin 3, and S100 calcium binding protein 9 for fractionated-pooled samples, and C-reactive protein, serum amyloid A1, cystatin C, von Willebrand factor, and S100 calcium binding protein 9 for unfractionated samples. Finally, we are also able to detect a significantly higher number of COVID-19 associated proteins in fractionated-pooled samples (80) than in unfractionated samples (13) (two sample proportion test, p-value = 1.67e-10).

Some of the most significantly abundant proteins in fractionated samples were tyrosine 3-monooxygenase, reticulon 4, pleckstrin, profilin 1, and haptoglobin.

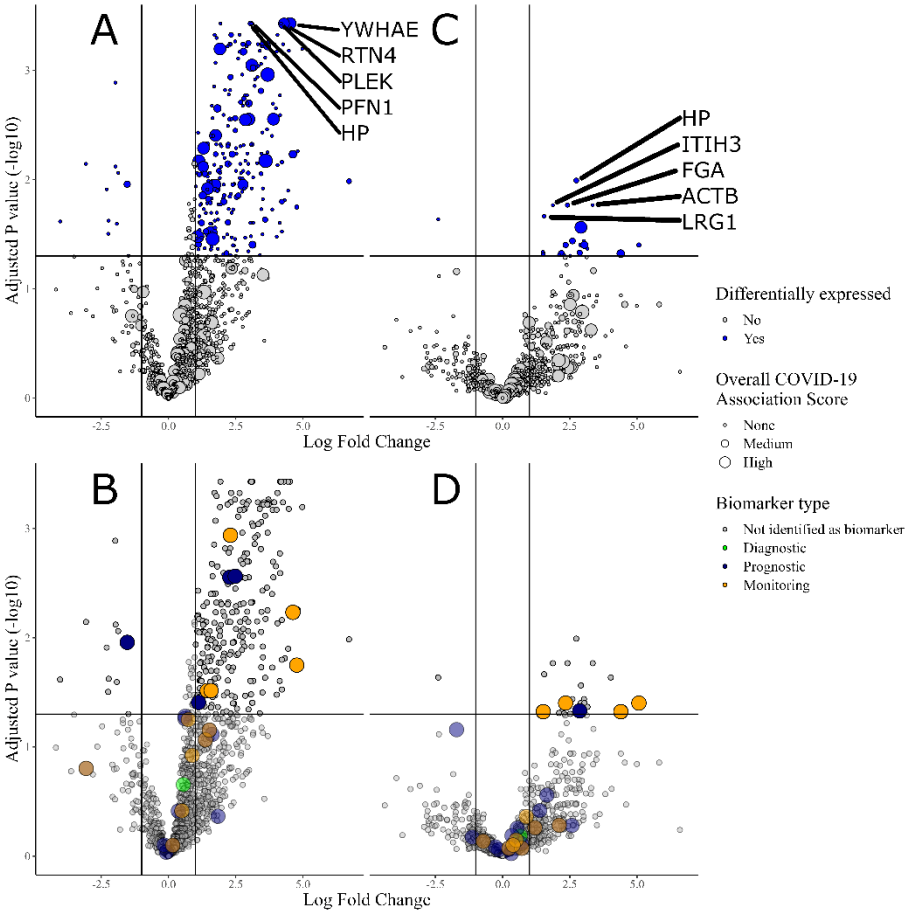


Figure 7. Volcano plot of differentially abundant proteins between nonhospitalized COVID-19 patients and hospitalized COVID-19 patients. Panels (A, B) show differentially abundant proteins in fractionated-pooled samples, while panels (C, D) show differentially abundant proteins in unfractionated samples. Panels (A, C) show differentially abundant proteins (absolute log fold change >1 and adjusted p-value ≤0.05) colored in blue, and point size represents overall COVID-19 association score as calculated via the OpenTargets platform.39 Panels (B, D) highlight points that have been identified as either diagnostic, prognostic, or monitoring biomarkers (point size is irrelevant and is used to better highlight the biomarkers). OncoMX COVID-19 biomarker database was used for biomarker identification.38

DISCUSSION

Our data robustly demonstrate that fractionation of samples leads to improved results in terms of the number of precursors and proteins identified, the reliability of their detection across samples, and downstream differential analysis between groups. The benefits of plasma prefractionation methods have been long established using DDA methodologies Extensive fractionation techniques have often been employed in deep plasma proteome studies to overcome the limitations of DDA techniques. In our data, we identified an average of around 236 proteins identified per patient with DDA (unfractionated), which aligns with what has been reported in other studies [41]. In contrast, our DIA samples detected an average of 838 unique proteins per patient, reaching nearly 1,500 in some patients (figure 5). Additionally, we observed clear improvements in the number of core proteins and reliability of protein identification between samples, as highlighted in figure 2A, which shows an increased proportion of identified proteins present in all patients.

The comparison seen in figure 4 shows that DIA identifies and quantifies significantly more proteins than DDA, with an average improvement of over 200% additional unique proteins within our study. This improvement may vary in other studies depending on methodological conditions, sample preparation, system sensitivity, bioinformatics employed, and the analytical cohort.

Several factors may explain this performance improvement. Firstly, DIA collects more detailed and comprehensive data than DDA. Unlike DDA, which excludes many precursors from MS2 analysis, DIA independently selects, groups, and fragments precursors across multiple predefined m/z windows (5-25 m/z). This prevents small changes having snowballing effects on data acquisition, improving reproducibility and reliability, allowing for the fragmentation of both low and high abundant precursors [41]. Secondly, tools such as DIA-NN excel at interpreting complex DIA spectra by explicitly tolerating co-fragmentation.

Logically, this gives DIA much higher data density as it identifies more precursors per spectra than DDA, which is only able to identify one precursor per spectrum unless using tools which specifically allow for chimeric spectra [42].

The fractionation-pooled method used in this study increases the average number of identified proteins to 1,321, and just over 1,700 proteins for certain patients. We also observe better inter-patient data uniformity in fractionated-pooled samples compared to unfractionated samples, with the number of core proteins increasing by 88%, from 303 to 570. Practically, the proteins identified in fractionated-pooled samples include almost all proteins identified by unfractionated samples (only 30 out of 2,061 proteins were unique to unfractionated samples), indicating minimal gain in running unfractionated samples alongside fractionated-pooled samples for improving detection. This allows for a reduction to three injections per subject.

The additional proteins identified in fractionated-pooled samples are mostly towards the lower end of the abundance range. There are two main reasons for this, firstly fractionation strategies result in less complex samples with improved peptide separation, and secondly, splitting a sample into multiple fractions that are then injected separately increases the total amount of sample being run. This increase in protein identification at lower abundances is due to increased sensitivity of precursor identification. Fractionation of the sample allows for less interference of competing peptides for fragmentation and produces clearer and more sensitive MS2 spectra for bioinformatic analysis. This leads not only to the identification of lower abundant proteins but also to the identification of multiple precursors derived from single proteins. Consequently, proteins identified in fractionated-pooled samples are aggregated less from single unique precursors and more from multiple unique precursors (Supplementary figure 2). This redundancy means that missing a single precursor in a run will not necessarily

prevent protein identification, contributing to an increase in the number of core proteins and more representative quantitation.

Looking at more traditional DDA fractionation studies, polyacrylamide gel electrophoresis (PAGE) and C18 peptide fractionation approaches can identify between 3,254 and 4,219 proteins by analysing either 24 gel bands for PAGE or 84 fractions concatenated into 24 for the C18 approach[43]. One of the most in-depth plasma proteome studies identified an average of 4,641 proteins per patient using a two-step depletion of the top 50-100 most abundant proteins, followed by reverse-phase peptide fractionation totalling 86 fractions pooled into 30 [44]. It should be noted that studies such as Geyer *et al.* (2016) have shown that robust plasma proteomics can be performed using non-fractionated DDA methods, but deep proteome analysis may be limited by the low number of identified proteins (437 average proteins identified per sample) [45]. Other studies have employed fraction sizes of 72 [46], 60 pooled into 18 [47], 6 [48], or 18 [49], and have identified a total of 1,917, 1,069, 567, and 169 proteins across patients/samples, respectively.

However, the methodologies for these extensive fractionation studies, are complex, expensive, time-consuming, and impractical for many clinical applications and settings, restricting their utility outside well-funded research environments. The MS run times, in these studies range between 468 and 3,600 minutes per patients/sample. Viode *et al.* (2023) demonstrated a high-throughput method capable of processing 60 samples per day, and detecting more than 1,300 proteins per run, although the lowest abundant proteins are around 900ng/L [50]. Like goldilocks in her search for the right bed, we have presented above a stream-lined, time- and cost- sensitive protocol capable of identifying proteins as lowly abundant as 6.2ng/L, suitable for both exploratory research and clinical applications. This protocol uses easily sourced reagents and kits, shorter experimental times compared to other such studies, and

produces only 7 fractions concatenated into 3 pooled fractions, with an MS runtime of just 360 minutes per sample, identifying over 1300 proteins per patient on average. Reducing the cost and time investment of proteomic experiments allows lower-funded projects and laboratories to introduce large-scale MS proteomics into their research and enables current MS proteomic labs to increase their sample and cohort sizes.

Pooling 7 fractions into 3 fractions reduced unique precursor and protein identification by around 15%, but improved the efficiency of each fraction in terms of total and unique precursors per fraction (Supplementary figure 4). The dropped precursors and proteins were from the lower abundance range, though both techniques detected proteins/precursors at equally low abundances. Total MS run time by pooling fractions was reduced by almost 60%, from 840 minutes to 360 minutes. Running un-pooled fractions results in superior protein identification, yet depending on the goals, funding, and time constraints, the slight drop in capability may be worthwhile in exchange for the massive reduction in running time and costs, especially as extensive fractionation results in diminishing returns in terms of unique precursors per subsequent fraction.

Previously, extensive fractionation was required in DDA experiments due to higher missing values, lower reproducibility, lower quantitative accuracy, and lower protein identification [21,51,52]. Now, DIA can greatly improve results when either paired with the same protocol, or, as shown here, simpler, faster, and more cost-effective protocols using DIA proteomic methods can yield similarly large and deep proteome coverage as more complex DDA approaches. However, the work here also demonstrates limits to how simple the protocol may become, even with the vast improvements offered by a DIA approach, the use of fractionation is a must for studies looking to investigate differentially abundant proteins, which may act as pathophysiological signals or biomarkers.

For the COVID-19 preliminary cohort used here, figure 6 shows superior separation of all 4 groups in the unfractionated PCA that is better than in the fractionated PCA, which only clearly separate moderate COVID-19/healthy controls from severe COVID-19 and respiratory failure. However, figure 7 shows that further investigations into unfractionated samples yields sub-par results compared to fractionated-pooled samples. This performance difference highlights the trade-off between capturing broad patterns of variability and enhancing detection sensitivity and specificity. Unfractionated samples may outperform fractionated samples during PCA due to their higher complexity and dynamic range, providing a richer variance structure that PCA can exploit for better separation as the dominant patterns and differences between samples are more visible. In contrast, fractionation reduces complexity, enhances the detection of low-abundance proteins, and improves the signal-to-noise ratio. The resulting data are denser, with more accurate quantification of low-abundant proteins, leading to more robust and significant differential abundance results.

In terms of differentially abundant proteins between moderate and severe/critical COVID-19, both fractionated-pooled and unfractionated samples were able to identify 264 and 23 proteins respectively. Notably, potential biomarkers such as C-reactive protein, serum amyloid A1, cystatin C, von Willebrand factor, and S100 calcium binding protein 9 were significantly upregulated in both samples [53–57]. Albumin was significantly downregulated in fractionated-pooled samples, consistent with other studies identifying hypoalbuminemia as an independent prognostic biomarker [58,59]. Additionally, fractionated-pooled samples identified significantly increased abundance of previously identified biomarkers such as macrophage colony-stimulating factor 1, P-selectin, and Galectin-3 in hospitalized COVID-19 patients compared to non-hospitalized patients [54,57,60,61]. Three biomarkers—surfactant protein D, aspartate aminotransferase, and myoglobin—had a positive log fold change over 1, aligning

with other studies associating them with severe disease [54,62–64]. However, they lacked significance, possibly due to the small cohort size.

In fractionated-pooled samples, the most significant proteins were 14-3-3 protein epsilon, reticulon-4, pleckstrin, profilin-1, and haptoglobin; haptoglobin and profilin-1 were differentially abundant in unfractionated samples, albeit at lower significance. Haptoglobin and 14-3-3 protein epsilon have been associated with COVID-19 through the OpenTargets aggregated association score [39]. Pleckstrin, while not associated with COVID-19 in this scoring system, was significantly differentially abundant in a study investigating SARS-CoV-2 infection [65].

In unfractionated samples, Type 2 lactosamine alpha-2,3-sialyltransferase was the only differentially abundant protein that was not differentially abundant in fractionated-pooled samples (Unfractionated: logFC –2.39, adjusted p-value 0.023. Fractionated-pooled: logFC -0.23, adjusted p-value 0.73.). This protein is not a known COVID-19 biomarker and has not been associated with COVID-19 in the OpenTargets Platform or general literature.

Some of the lowest abundant differentially abundant proteins in fractionated samples include polypeptide N-acetylgalactosaminyltransferase 12, tetratricopeptide repeat domain 36, and G protein subunit alpha 13, with concentrations of 47ng/L, 100ng/L, and 320ng/L, respectively. For unfractionated samples, the top three lowest abundant proteins were ST3 beta-galactoside alpha-2,3-sialyltransferase 6, tryptophanyl-tRNA synthetase 1, and integrin subunit alpha 2b, with concentrations of 5.8μg/L, 49μg/L and 90μg/L respectively. The median concentration of differentially abundant proteins in fractionated-pooled samples was around 1/70th of that in unfractionated samples, at 58.5μg/L vs 4.1mg/L respectively. Fractionation enhances the detection of low-abundance proteins across a cohort.

Low abundant proteins identified in fractionated samples relevant to COVID-19 include fibroblast growth factor receptor 4 (7.4 μg/L), a drug target in phase III trials (National Library of Medicine [NLM], NCT04541680) and alpha-1,3-mannosyl-glycoprotein 2-beta-N-acetylglucosaminyltransferase (12 μg/L), involved in SARS-CoV-2 spike protein maturation [67].

While our study highlights the significant advantages of fractionation and DIA methods, including enhanced proteome coverage and improved detection of low-abundance proteins, these approaches also have notable drawbacks. The increased LC-MS/MS run time, extending to 360 minutes per sample, limits throughput, making it less suitable for very high-volume studies. Additionally, the complexity of sample preparation, involving multiple handling and processing steps, raises the risk of sample loss and variability, and requires greater technical expertise. The depletion of high-abundance proteins can introduce biases in relative quantification, particularly for proteins carried by these depleted proteins, potentially distorting their proportionality between samples. Furthermore, the specialized reagents and extended instrument time increase overall costs, which may be prohibitive in some research settings. Researchers must weigh these factors when considering the application of these methods in large-scale studies.

CONCLUSIONS

In conclusion, we have presented an exploratory proteomic protocol with a simplified fractionation procedure and boosted by the utilisation of DIA methodologies. This pilot study illustrates the potential clinical applicability of this protocol when used in conjunction with a DIA bioinformatics pipeline. Using this protocol, hundreds of extremely low abundant proteins usually present at concentrations as low as 47ng/L have been identified as significantly differentially abundant. In addition to this, we show how the use of fractionation methods in addition to DIA technologies can significantly boost unique protein identification within samples and greatly improve identification of the same proteins between samples. The method discussed in this study was able to identify an average of 1,321 proteins per patient using plasma samples collected as part of a 20-patient COVID-19 cohort. Across the entire cohort, 2,031 total unique proteins were identified. The protocol employs the use of readily-available kits and materials for protein depletion, digestion, and pooled fractionation for a relatively simple sample preparation.

Utilising such a protocol significantly reduces the cost, time, and complexity required in performing exploratory proteomic studies on human plasma and is currently being applied in our setting to a large, 200 +, multi-timepoint patient cohort in a multi-omics context [30].

■ ASSOCIATED CONTENT

Data Availability Statement

Data are available via ProteomeXchange with identifier PXD047901.

Supporting Information

The Supporting Information is available free of charge at https://pubs.acs.org/doi/10.1021/acs.jproteome.4c00104.

Supporting Material S1: R script detailing data processing, figure generation, and statistical analysis (R File) (TXT)

Supporting Material S2: Results. Analysis of data after filtering precursors present in less than 25% of patients, information on protein and precursor abundances, information on precursor distribution across fractions, and a PCA done using precursor abundances. Figures S1 – S5 included (PDF)

Supporting Material S3: Differential abundance results. Table includes UniProtKB accession numbers (Protein), log fold change (log FC), average log abundance (AveExpr), *t* statistic (t), *p*-value (*P*.Value), adjusted *p*value (adj.P.Val), b statistic (B), if protein meets differential expression criteria of adjusted *p*-value 1 (differentially_expressed), Entrez ID (ENTREZID), gene symbol (SYMBOL), and the fractionation method of the sample (Experimental_method) (XLSX)

Supporting Material S4: Linking the protein names (protein name) used in this paper to the corresponding UniprotKB accession number (UniprotKB accession number) (CSV File) (XLSX)

Author Contributions

† B.W., S.P.d.R., D.V. and L.E contributed equally to this work. Conceptualization, J.C.Y., J.-L.B., L.G., J.d.G., L.B., and L.E.; methodology, B.W., S.P.d.R., M.L., D.V., and L.E.; investigation, B.W., J.C.Y., J.d.G., J.-L.B., P.DC., J.-F.C., J.P.D., L.G., V.H., S.J., B.K., S.P.d.R., D.V., L.E., and L.B.; resources, J.C.Y., J.-L.B., L.G., J.d.G., V.H., B.K., J.-F.C., L.B., and L.E.; writing-original draft preparation, B.W., S.P.d.R., and L.E.; writing-review and editing, J.C.Y., J.d.G., J.-L.B., P.DC., J.-F.C., J.P.D., L.G., V.H., S.J., B.K., L.B., and D.V.; supervision, J.C.Y., J.-L.B., L.G., J.d.G., L.B., and L.E.; project administration, J.-L.B. and J.C.Y.; funding acquisition, J.C.Y., J.-L.B., L.G., J.d.G., L.B., and L.E. All authors have read and agreed to the published version of the manuscript. The manuscript was written through the contributions of all authors. All authors have given approval to the final version of the manuscript.

Funding

This research was financially supported by the Sofina COVID Solidarity Fund, administered by the King Baudouin Foundation, initiated by the Fondation Saint-Luc

(grant number 2021-I4201010 – 221801), and the FNRS Urgent Research Credit (CUR: HC01020F). P.D.C., J.-F.C., and J.-L.B. are recipients of FNRS grants (Projet de Recherche FRFSWELBIO: WELBIO-CR-2022 A-02; WELBIO-CR-2022 A-01). B.W. is the recipient of an FRC starting grant (Promotor Leil¨ a Belkhir) and FSR grant (Promotor Laure Elens).

Notes

Informed consent was obtained from all subjects involved in the study. The study was conducted in accordance with the Declaration of Helsinki and approved by the Institutional Review Board (or Ethics Committee) of Cliniques Universitaires Saint-Luc (comite´ e´thique hospital-facultaire) (protocol code 2021/30DEC/543, date of approval: 30 December 2021). The authors declare the following competing financial interest(s): P.D.C. is inventor on patent applications dealing with the use of specific bacteria and components in the treatment of different diseases. P.D.C. was co-founder of The Akkermansia Company SA and Enterosys.

■ Acknowledgments

The investigators extend their heartfelt thanks to all of the patients actively engaged or intending to participate in this clinical study. Special appreciation is also extended to the clinical medical research coordinators at Cliniques Universitaires Saint-Luc for their invaluable support in patient recruitment and the collection of biological samples.

■ Abbreviations

DDA, data-dependent acquisition; DIA, data-independent acquisition; LC-MS/MS, liquid chromatography tandem mass spectrometry; COVID-19, novel coronavirus disease 2019; LC, liquid chromatography; MS, mass spectrometry; LC-MS, liquid chromatography mass spectrometry; RT, room temperature; RPM, rotations per minute; TEAB, triethylammonium bicarbonate; ACN, acetonitrile; TFA, trifluoroacetic acid; APD, advanced peak detection; HPLC, high-performance liquid chromatography; fwhm, full width at half-maximum resolution; HCD, higher energy collisional dissociation; AGC, automatic gain control; FDR, false discovery rate; HYGIEIA, hypothesizing the genesis of infectious diseases and epidemics through an integrated systems biology approach; AUC, area under the curve; PCA, principal component analysis; PC, principal component; QC, quality control; PAGE, polyacrylamide gel electrophoresis; logFC, log fold change; NLM, national library of medicine

REFERENCES

(1) Williams, S. A.; Kivimaki, M.; Langenberg, C.; Hingorani, A. D.; Casas, J. P.; Bouchard, C.; Jonasson, C.; Sarzynski, M. A.; Shipley, M. J.; Alexander, L.; Ash, J.; Bauer, T.; Chadwick, J.; Datta, G.; DeLisle, R. K.; Hagar, Y.; Hinterberg, M.; Ostroff, R.; Weiss, S.; Ganz, P.; Wareham, N. J. Plasma Protein Patterns as Comprehensive Indicators of Health. *Nat Med* **2019**, *25* (12), 1851–1857. https://doi.org/10.1038/s41591-019-0665-2.

(2) Zahn-Zabal, M.; Michel, P. A.; Gateau, A.; Nikitin, F.; Schaeffer, M.; Audot, E.; Gaudet, P.; Duek, P. D.; Teixeira, D.; De Laval, V. R.; Samarasinghe, K.; Bairoch, A.; Lane, L. The NeXtProt Knowledgebase in 2020: Data, Tools and Usability Improvements. *Nucleic Acids Res* **2020**, *48* (D1), D328–D334. https://doi.org/10.1093/nar/gkz995.

(3) Deutsch, E. W.; Omenn, G. S.; Sun, Z.; Maes, M.; Pernemalm, M.; Palaniappan, K. K.; Letunica, N.; Vandenbrouck, Y.; Brun, V.; Tao, S. C.; Yu, X.; Geyer, P. E.; Ignjatovic, V.; Moritz, R. L.; Schwenk, J. M. Advances and Utility of the Human Plasma Proteome. *Journal of Proteome Research*. American Chemical Society December 3, 2021, pp 5241–5263. https://doi.org/10.1021/acs.jproteome.1c00657.

(4) Chen, L.; Long, X.; Xu, Q.; Tan, J.; Wang, G.; Cao, Y.; Wei, J.; Luo, H.; Zhu, H.; Huang, L.; Meng, F.; Huang, L.; Wang, N.; Zhou, X.; Zhao, L.; Chen, X.; Mao, Z.; Chen, C.; Li, Z.; Sun, Z.; Zhao, J.; Wang, D.; Huang, G.; Wang, W.; Zhou, J. Elevated Serum Levels of S100A8/A9 and HMGB1 at Hospital Admission Are Correlated with Inferior Clinical Outcomes in COVID-19 Patients. *Cellular and Molecular Immunology*. Springer Nature September 1, 2020, pp 992–994. https://doi.org/10.1038/s41423-020-0492-x.

(5) Abers, M. S.; Delmonte, O. M.; Ricotta, E. E.; Fintzi, J.; Fink, D. L.; Almeida de Jesus, A. A.; Zarember, K. A.; Alehashemi, S.; Oikonomou, V.; Desai, J. V.; Canna, S. W.; Shakoory, B.; Dobbs, K.; Imberti, L.; Sottini, A.; Quiros-Roldan, E.; Castelli, F.; Rossi, C.; Brugnoni, D.; Biondi, A.; Bettini, L. R.; D'Angio', M.; Bonfanti, P.; Castagnoli, R.; Montagna, D.; Licari, A.; Marseglia, G. L.; Gliniewicz, E. F.; Shaw, E.; Kahle, D. E.; Rastegar, A. T.; Stack, M.; Myint-Hpu, K.; Levinson, S. L.; DiNubile, M. J.; Chertow, D. W.; Burbelo, P. D.; Cohen, J. I.; Calvo, K. R.; Tsang, J. S.; Su, H. C.; Gallin, J. I.; Kuhns, D. B.; Goldbach-Mansky, R.; Lionakis, M. S.; Notarangelo, L. D. An Immune-Based Biomarker Signature Is Associated with Mortality in COVID-19 Patients. *JCI Insight* **2021**, *6* (1). https://doi.org/10.1172/jci.insight.144455.

(6) Sahin, A. T.; Yurtseven, A.; Dadmand, S.; Ozcan, G.; Akarlar, B. A.; Kucuk, N. E. O.; Senturk, A.; Ergonul, O.; Can, F.; Tuncbag, N.; Ozlu, N. Plasma Proteomics Identify Potential Severity Biomarkers from COVID-19 Associated Network. *Proteomics Clin Appl* **2023**, *17* (2), 2200070. https://doi.org/10.1002/prca.202200070.

(7) Zoodsma, M.; de Nooijer, A. H.; Grondman, I.; Gupta, M. K.; Bonifacius, A.; Koeken, V. A. C. M.; Kooistra, E.; Kilic, G.; Bulut, O.; Gödecke, N.; Janssen, N.; Kox, M.; Domínguez-Andrés, J.; van Gammeren, A. J.; Ermens, A. A. M.; van der Ven, A. J. A. M.; Pickkers, P.; Blasczyk, R.; Behrens, G. M. N.; van de Veerdonk, F. L.; Joosten, L. A. B.; Xu, C.-J.; Eiz-Vesper, B.; Netea, M. G.; Li, Y. Targeted Proteomics Identifies Circulating Biomarkers Associated with Active COVID-19 and Post-COVID-19. *Front Immunol* **2022**, *13*, 1027122. https://doi.org/10.3389/fimmu.2022.1027122.

(8) Qin, C.; Zhou, L.; Hu, Z.; Zhang, S.; Yang, S.; Tao, Y.; Xie, C.; Ma, K.; Shang, K.; Wang, W.; Tian, D. S. Dysregulation of Immune Response in Patients with Coronavirus 2019 (COVID-19) in Wuhan, China. *Clinical Infectious Diseases* **2020**, *71* (15), 762–768. https://doi.org/10.1093/cid/ciaa248.

(9) Anderson, N. L.; Anderson, N. G. The Human Plasma Proteome: History, Character, and Diagnostic Prospects. *Molecular & cellular proteomics : MCP*. Elsevier November 1, 2002, pp 845–867. https://doi.org/10.1074/mcp.R200007-MCP200.

(10) Zhao, Y.; Xue, Q.; Wang, M.; Meng, B.; Jiang, Y.; Zhai, R.; Zhang, Y.; Dai, X.; Fang, X. Evolution of Mass Spectrometry Instruments and Techniques for Blood Proteomics. *Journal of Proteome Research*. American Chemical Society April 7, 2023, pp 1009–1023. https://doi.org/10.1021/acs.jproteome.3c00102.

(11) Kou, Q.; Zhu, B.; Wu, S.; Ansong, C.; Tolić, N.; Paša-Tolić, L.; Liu, X. Characterization of Proteoforms with Unknown Post-Translational Modifications Using the MIScore. *J Proteome Res* **2016**, *15* (8), 2422–2432. https://doi.org/10.1021/acs.jproteome.5b01098.

(12) Manfredi, M.; Brandi, J.; Di Carlo, C.; Vita Vanella, V.; Barberis, E.; Marengo, E.; Patrone, M.; Cecconi, D. Mining Cancer Biology through Bioinformatic Analysis of Proteomic Data. *Expert Review of Proteomics*. Taylor and Francis Ltd 2019, pp 733–747. https://doi.org/10.1080/14789450.2019.1654862.

(13) Liotta, L. A.; Ferrari, M.; Petricoin, E. Written in Blood. *Nature*. Nature Publishing Group October 30, 2003, p 905. https://doi.org/10.1038/425905a.

(14) Granger, J.; Siddiqui, J.; Copeland, S.; Remick, D. Albumin Depletion of Human Plasma Also Removes Low Abundance Proteins Including the Cytokines. *Proteomics* **2005**, *5* (18), 4713–4718. https://doi.org/10.1002/pmic.200401331.

(15) Z, C.; HY, T.; H, W.; Q, L.; DW, S. Systematic Comparison of Fractionation Methods for In-Depth Analysis of Plasma Proteomes. *J Proteome Res* **2012**, *11* (6). https://doi.org/10.1021/PR201068B.

(16) Gillet, L. C.; Navarro, P.; Tate, S.; Röst, H.; Selevsek, N.; Reiter, L.; Bonner, R.; Aebersold, R. Targeted Data Extraction of the MS/MS Spectra Generated by Data-Independent Acquisition: A New Concept for Consistent and Accurate Proteome Analysis. *Molecular and Cellular Proteomics* **2012**, *11* (6). https://doi.org/10.1074/mcp.O111.016717.

(17) Carvalho, P. C.; Han, X.; Xu, T.; Cociorva, D.; da Gloria Carvalho, M.; Barbosa, V. C.; Yates, J. R. XDIA: Improving on the Label-Free Data-Independent Analysis. *Bioinformatics* **2010**, *26* (6), 847–848. https://doi.org/10.1093/bioinformatics/btq031.

(18) Plumb, R. S.; Johnson, K. A.; Rainville, P.; Smith, B. W.; Wilson, I. D.; Castro-Perez, J. M.; Nicholson, J. K. UPLC/MSE; a New Approach for Generating Molecular Fragment Information for Biomarker Structure Elucidation. *Rapid Communications in Mass Spectrometry* **2006**, *20* (13), 1989–1994. https://doi.org/10.1002/rcm.2550.

(19) Panchaud, A.; Scherl, A.; Shaffer, S. A.; Von Haller, P. D.; Kulasekara, H. D.; Miller, S. I.; Goodlett, D. R. Precursor Acquisition Independent from Ion Count: How to Dive Deeper into the Proteomics Ocean. *Anal Chem* **2009**, *81* (15), 6481–6488. https://doi.org/10.1021/ac900888s.

(20) Geiger, T.; Cox, J.; Mann, M. Proteomics on an Orbitrap Benchtop Mass Spectrometer Using All-Ion Fragmentation. *Molecular and Cellular Proteomics* **2010**, *9* (10), 2252–2261. https://doi.org/10.1074/mcp.M110.001537.

(21) Fernández-Costa, C.; Martínez-Bartolomé, S.; McClatchy, D. B.; Saviola, A. J.; Yu, N. K.; Yates, J. R. Impact of the Identification Strategy on the Reproducibility of the DDA and DIA Results. *J Proteome Res* **2020**, *19* (8), 3153–3161. https://doi.org/10.1021/acs.jproteome.0c00153.

(22) MacLean, B.; Tomazela, D. M.; Shulman, N.; Chambers, M.; Finney, G. L.; Frewen, B.; Kern, R.; Tabb, D. L.; Liebler, D. C.; MacCoss, M. J. Skyline: An Open Source Document Editor for Creating and Analyzing Targeted Proteomics Experiments. *Bioinformatics* **2010**, *26* (7), 966–968. https://doi.org/10.1093/bioinformatics/btq054.

(23) Röst, H. L.; Aebersold, R.; Schubert, O. T. Automated Swath Data Analysis Using Targeted Extraction of Ion Chromatograms. In *Methods in Molecular Biology*; Humana Press Inc., 2017; Vol. 1550, pp 289–307. https://doi.org/10.1007/978-1-4939-6747-6_20.

(24) Searle, B. C.; Swearingen, K. E.; Barnes, C. A.; Schmidt, T.; Gessulat, S.; Küster, B.; Wilhelm, M. Generating High Quality Libraries for DIA MS with Empirically Corrected Peptide Predictions. *Nat Commun* **2020**, *11* (1), 1–10. https://doi.org/10.1038/s41467-020-15346-1.

(25) Bernhardt, O.; Selevsek, N.; Gillet, L.; Rinner, O.; Picotti, P.; Aebersold, R.; Reiter, L. Spectronaut: A Fast and Efficient Algorithm for MRM-like Processing of Data Independent Acquisition (SWATH-MS) Data; Conference: 60th American Society for Mass Spectometry Conference, 2014.

(26) Tsou, C. C.; Avtonomov, D.; Larsen, B.; Tucholska, M.; Choi, H.; Gingras, A. C.; Nesvizhskii, A. I. DIA-Umpire: Comprehensive Computational Framework for Data-Independent Acquisition Proteomics. *Nat Methods* **2015**, *12* (3), 258–264. https://doi.org/10.1038/nmeth.3255.

(27) Demichev, V.; Messner, C. B.; Vernardis, S. I.; Lilley, K. S.; Ralser, M. DIA-NN: Neural Networks and Interference Correction Enable Deep Proteome Coverage in High Throughput. *Nat Methods* **2020**, *17* (1), 41–44. https://doi.org/10.1038/s41592-019-0638-x.

(28) Kistner, F.; Grossmann, J. L.; Sinn, L. R.; Demichev, V. QuantUMS: Uncertainty Minimisation Enables Confident Quantification in Proteomics. *bioRxiv* **2023**, 2023.06.20.545604. https://doi.org/10.1101/2023.06.20.545604.

(29) Fröhlich, K.; Brombacher, E.; Fahrner, M.; Vogele, D.; Kook, L.; Pinter, N.; Bronsert, P.; Timme-Bronsert, S.; Schmidt, A.; Bärenfaller, K.; Kreutz, C.; Schilling, O. Benchmarking of Analysis Strategies for Data-Independent Acquisition Proteomics Using a Large-Scale Dataset Comprising Inter-Patient Heterogeneity. *Nat Commun* **2022**, *13* (1), 1–13. https://doi.org/10.1038/s41467-022-30094-0.

(30) Ward, B.; Yombi, J. C.; Balligand, J. L.; Cani, P. D.; Collet, J. F.; Greef, J. de; Dewulf, J. P.; Gatto, L.; Haufroid, V.; Jodogne, S.; Kabamba, B.; Ruys, S. P. D.; Vertommen, D.; Elens, L.; Belkhir, L. HYGIEIA: HYpothesizing the Genesis of Infectious Diseases and Epidemics through an Integrated Systems Biology Approach. *Viruses* **2022**, *14* (7), 1373. https://doi.org/10.3390/v14071373.

(31) Marshall, J. C.; Murthy, S.; Diaz, J.; Adhikari, N.; Angus, D. C.; Arabi, Y. M.; Baillie, K.; Bauer, M.; Berry, S.; Blackwood, B.; Bonten, M.; Bozza, F.; Brunkhorst, F.; Cheng, A.; Clarke, M.; Dat, V. Q.; de Jong, M.; Denholm, J.; Derde, L.; Dunning, J.; Feng, X.; Fletcher, T.; Foster, N.; Fowler, R.; Gobat, N.; Gomersall, C.; Gordon, A.; Glueck, T.; Harhay, M.; Hodgson, C.; Horby, P.; Kim, Y. J.; Kojan, R.; Kumar, B.; Laffey, J.; Malvey, D.; Martin-Loeches, I.; McArthur, C.; McAuley, D.; McBride, S.; McGuinness, S.; Merson, L.; Morpeth, S.; Needham, D.; Netea, M.; Oh, M. D.; Phyu, S.; Piva, S.; Qiu, R.; Salisu-Kabara, H.; Shi, L.; Shimizu, N.; Sinclair, J.; Tong, S.; Turgeon, A.; Uyeki, T.; van de Veerdonk, F.; Webb, S.; Williamson, P.; Wolf, T.; Zhang, J. A Minimal Common Outcome Measure Set for COVID-19 Clinical Research. *The Lancet Infectious Diseases*. Lancet Publishing Group August 1, 2020, pp e192–e197. https://doi.org/10.1016/S1473-3099(20)30483-7.

(32) Bateman, A.; Martin, M. J.; Orchard, S.; Magrane, M.; Ahmad, S.; Alpi, E.; Bowler-Barnett, E. H.; Britto, R.; Bye-A-Jee, H.; Cukura, A.; Denny, P.; Dogan, T.; Ebenezer, T. G.; Fan, J.; Garmiri, P.; da Costa Gonzales, L. J.; Hatton-Ellis, E.; Hussein, A.; Ignatchenko, A.; Insana, G.; Ishtiaq, R.; Joshi, V.; Jyothi, D.; Kandasaamy, S.; Lock, A.; Luciani, A.; Lugaric, M.; Luo, J.; Lussi, Y.; MacDougall, A.; Madeira, F.; Mahmoudy, M.; Mishra, A.; Moulang, K.; Nightingale, A.; Pundir, S.; Qi, G.; Raj, S.; Raposo, P.; Rice, D. L.; Saidi, R.; Santos, R.; Speretta, E.; Stephenson, J.; Totoo, P.; Turner, E.; Tyagi, N.; Vasudev, P.; Warner, K.; Watkins, X.; Zaru, R.; Zellner, H.; Bridge, A. J.; Aimo, L.; Argoud-Puy, G.; Auchincloss, A. H.; Axelsen, K. B.; Bansal, P.; Baratin, D.; Batista Neto, T. M.; Blatter, M. C.; Bolleman, J. T.; Boutet, E.; Breuza, L.; Gil, B. C.; Casals-Casas, C.; Echioukh, K. C.; Coudert, E.; Cuche, B.; de Castro, E.; Estreicher, A.; Famiglietti, M. L.; Feuermann, M.; Gasteiger, E.; Gaudet, P.; Gehant, S.; Gerritsen, V.; Gos, A.; Gruaz, N.; Hulo, C.; Hyka-Nouspikel, N.; Jungo, F.; Kerhornou, A.; Le Mercier, P.; Lieberherr, D.; Masson, P.; Morgat, A.; Muthukrishnan, V.; Paesano, S.; Pedruzzi, I.; Pilbout, S.; Pourcel, L.; Poux, S.; Pozzato, M.; Pruess, M.; Redaschi, N.; Rivoire, C.; Sigrist, C. J. A.; Sonesson, K.; Sundaram, S.; Wu, C. H.; Arighi, C. N.; Arminski, L.; Chen, C.; Chen, Y.; Huang, H.; Laiho, K.; McGarvey, P.; Natale, D. A.; Ross, K.; Vinayaka, C. R.; Wang, Q.; Wang, Y.; Zhang, J. UniProt: The Universal Protein Knowledgebase in 2023. *Nucleic Acids Res* **2023**, *51* (D1), D523–D531. https://doi.org/10.1093/nar/gkac1052.

(33) *R: The R Project for Statistical Computing*. https://www.r-project.org/ (accessed 2023-09-05).

(34) *Bioconductor - QFeatures*. https://bioconductor.org/packages/release/bioc/html/QFeatures.html (accessed 2023-09-05).

(35) Sticker, A.; Goeminne, L.; Martens, L.; Clement, L. Robust Summarization and Inference in Proteome-Wide Label-Free Quantification. *bioRxiv* **2019**, 668863. https://doi.org/10.1101/668863.

(36) Uhlen, M.; Oksvold, P.; Fagerberg, L.; Lundberg, E.; Jonasson, K.; Forsberg, M.; Zwahlen, M.; Kampf, C.; Wester, K.; Hober, S.; Wernerus, H.; Björling, L.; Ponten, F. Towards a knowledge-based Human Protein Atlas. Nature biotechnology 2010, 28 (12), 1248–1250. https://doi.org/10.1038/nbt1210-1248.

(37) Data available from v23.0.proteinatlas.org

(38) Gogate, N.; Lyman, D.; Bell, A.; Cauley, E.; Crandall, K. A.; Joseph, A.; Kahsay, R.; Natale, D. A.; Schriml, L. M.; Sen, S.; Mazumder, R. COVID-19 Biomarkers and Their Overlap with Comorbidities in a Disease Biomarker Data Model. *Brief Bioinform* **2021**, *22* (6). https://doi.org/10.1093/bib/bbab191.

(39) Ochoa, D.; Hercules, A.; Carmona, M.; Suveges, D.; Baker, J.; Malangone, C.; Lopez, I.; Miranda, A.; Cruz-Castillo, C.; Fumis, L.; Bernal-Llinares, M.; Tsukanov, K.; Cornu, H.; Tsirigos, K.; Razuvayevskaya, O.; Buniello, A.; Schwartzentruber, J.; Karim, M.; Ariano, B.; Martinez Osorio, R. E.; Ferrer, J.; Ge, X.; Machlitt-Northen, S.; Gonzalez-Uriarte, A.; Saha, S.; Tirunagari, S.; Mehta, C.; Roldán-Romero, J. M.; Horswell, S.; Young, S.; Ghoussaini, M.; Hulcoop, D. G.; Dunham, I.; Mcdonagh, E. M. The Next-Generation Open Targets Platform: Reimagined, Redesigned, Rebuilt. *Nucleic Acids Res* **2023**, *51* (D1), D1353–D1359. https://doi.org/10.1093/nar/gkac1046.

(40) Perez-Riverol, Y.; Bai, J.; Bandla, C.; García-Seisdedos, D.; Hewapathirana, S.; Kamatchinathan, S.; Kundu, D. J.; Prakash, A.; Frericks-Zipper, A.; Eisenacher, M.; Walzer, M.; Wang, S.; Brazma, A.; Vizcaíno, J. A. The PRIDE Database Resources in 2022: A Hub for Mass Spectrometry-Based Proteomics Evidences. *Nucleic Acids Res* **2022**, *50* (D1), D543–D552. https://doi.org/10.1093/nar/gkab1038.

(41) Palstrøm, N. B.; Rasmussen, L. M.; Beck, H. C. Affinity Capture Enrichment versus Affinity Depletion: A Comparison of Strategies for Increasing Coverage of Low-Abundant Human Plasma Proteins. *Int J Mol Sci* **2020**, *21* (16), 5903. https://doi.org/10.3390/ijms21165903.

(42) Frejno, M.; Berger, M. T.; Tüshaus, J.; Hogrebe, A.; Seefried, F.; Graber, M.; Samaras, P.; Fredj, S. Ben; Sukumar, V.; Eljagh, L.; Brohnshtein, I.; Mamisashvili, L.; Schneider, M.; Gessulat, S.; Schmidt, T.; Kuster, B.; Zolg, D. P.; Wilhelm, M. Unifying the Analysis of Bottom-up Proteomics Data with CHIMERYS. *bioRxiv* **2024**, 2024.05.27.596040. https://doi.org/10.1101/2024.05.27.596040.

(43) Kaur, G.; Poljak, A.; Ali, S. A.; Zhong, L.; Raftery, M. J.; Sachdev, P. Extending the Depth of Human Plasma Proteome Coverage Using Simple Fractionation Techniques. *J Proteome Res* **2021**, *20* (2), 1261–1279. https://doi.org/10.1021/acs.jproteome.0c00670.

(44) Keshishian, H.; Burgess, M. W.; Gillette, M. A.; Mertins, P.; Clauser, K. R.; Mani, D. R.; Kuhn, E. W.; Farrell, L. A.; Gerszten, R. E.; Carr, S. A. Multiplexed, Quantitative Workflow for Sensitive Biomarker Discovery in Plasma Yields Novel Candidates for Early Myocardial Injury. *Molecular and Cellular Proteomics* **2015**, *14* (9), 2375–2393. https://doi.org/10.1074/mcp.M114.046813.

(45) Geyer, P. E.; Wewer Albrechtsen, N. J.; Tyanova, S.; Grassl, N.; Iepsen, E. W.; Lundgren, J.; Madsbad, S.; Holst, J. J.; Torekov, S. S.; Mann, M. Proteomics Reveals the Effects of Sustained Weight Loss on the Human Plasma Proteome. *Mol Syst Biol* **2016**, *12* (12). https://doi.org/10.15252/msb.20167357.

(46) Babačić, H.; Lehtiö, J.; Pico De Coaña, Y.; Pernemalm, M.; Eriksson, H. In-Depth Plasma Proteomics Reveals Increase in Circulating PD-1 during Anti-PD-1 Immunotherapy in Patients with Metastatic Cutaneous Melanoma. *J Immunother Cancer* **2020**, *8* (1), e000204. https://doi.org/10.1136/jitc-2019-000204.

(47) Xu, R.; Gong, C. X.; Duan, C. M.; Huang, J. C.; Yang, G. Q.; Yuan, J. J.; Zhang, Q.; Xiong, X.; Yang, Q. Age-Dependent Changes in the Plasma Proteome of Healthy Adults. *Journal of Nutrition, Health and Aging* **2020**, *24* (8), 846–856. https://doi.org/10.1007/s12603-020-1392-6.

(48) Zhang, Y.; Mao, Y.; Zhao, W.; Su, T.; Zhong, Y.; Fu, L.; Zhu, J.; Cheng, J.; Yang, H. Glyco-CPLL: An Integrated Method for In-Depth and Comprehensive N-Glycoproteome Profiling of Human Plasma. *J Proteome Res* **2020**, *19* (2), 655–666. https://doi.org/10.1021/acs.jproteome.9b00557.

(49) Henriksson, A.; Lindqvist, M.; Sihlbom, C.; Bergström, J.; Bylund, D. Identification of Potential Plasma Biomarkers for Abdominal Aortic Aneurysm Using Tandem Mass Tag Quantitative Proteomics. *Proteomes* **2018**, *6* (4), 43. https://doi.org/10.3390/proteomes6040043.

(50) Viode, A.; van Zalm, P.; Smolen, K. K.; Fatou, B.; Stevenson, D.; Jha, M.; Levy, O.; Steen, J.; Steen, H. A Simple, Time- and Cost-Effective, High-Throughput Depletion Strategy for Deep Plasma Proteomics. *Sci Adv* **2023**, *9* (13). https://doi.org/10.1126/sciadv.adf9717.

(51) Muntel, J.; Xuan, Y.; Berger, S. T.; Reiter, L.; Bachur, R.; Kentsis, A.; Steen, H. Advancing Urinary Protein Biomarker Discovery by Data-Independent Acquisition on a Quadrupole-Orbitrap Mass Spectrometer. *J Proteome Res* **2015**, *14* (11), 4752–4762. https://doi.org/10.1021/acs.jproteome.5b00826.

(52) Barkovits, K.; Pacharra, S.; Pfeiffer, K.; Steinbach, S.; Eisenacher, M.; Marcus, K.; Uszkoreit, J. Reproducibility, Specificity and Accuracy of Relative Quantification Using Spectral Librarybased Data-Independent Acquisition. *Molecular and Cellular Proteomics* **2020**, *19* (1), 181–197. https://doi.org/10.1074/mcp.RA119.001714.

(53) Shi, H.; Zuo, Y.; Yalavarthi, S.; Gockman, K.; Zuo, M.; Madison, J. A.; Blair, C.; Woodward, W.; Lezak, S. P.; Lugogo, N. L.; Woods, R. J.; Lood, C.; Knight, J. S.; Kanthi, Y. Neutrophil Calprotectin Identifies Severe Pulmonary Disease in COVID-19. *J Leukoc Biol* **2021**, *109* (1), 67–72. https://doi.org/10.1002/JLB.3COVCRA0720-359R.

(54) Goshua, G.; Pine, A. B.; Meizlish, M. L.; Chang, C. H.; Zhang, H.; Bahel, P.; Baluha, A.; Bar, N.; Bona, R. D.; Burns, A. J.; Dela Cruz, C. S.; Dumont, A.; Halene, S.; Hwa, J.; Koff, J.; Menninger, H.; Neparidze, N.; Price, C.; Siner, J. M.; Tormey, C.; Rinder, H. M.; Chun, H. J.; Lee, A. I. Endotheliopathy in COVID-19-Associated Coagulopathy: Evidence from a Single-Centre, Cross-Sectional Study. *Lancet Haematol* **2020**, *7* (8), e575–e582. https://doi.org/10.1016/S2352-3026(20)30216-7.

(55) Kermali, M.; Khalsa, R. K.; Pillai, K.; Ismail, Z.; Harky, A. The Role of Biomarkers in Diagnosis of COVID-19 – A Systematic Review. *Life Sciences*. Elsevier Inc. August 1, 2020. https://doi.org/10.1016/j.lfs.2020.117788.

(56) Li, H.; Xiang, X.; Ren, H.; Xu, L.; Zhao, L.; Chen, X.; Long, H.; Wang, Q.; Wu, Q. Serum Amyloid A Is a Biomarker of Severe Coronavirus Disease and Poor Prognosis. *Journal of Infection* **2020**, *80* (6), 646–655. https://doi.org/10.1016/j.jinf.2020.03.035.

(57) Xiang, J.; Wen, J.; Yuan, X.; Xiong, S.; Zhou, X.; Liu, C.; Min, X. Potential Biochemical Markers to Identify Severe Cases among COVID-19 Patients. *medRxiv* **2020**, 2020.03.19.20034447. https://doi.org/10.1101/2020.03.19.20034447.

(58) Li, J.; Li, M.; Zheng, S.; Li, M.; Zhang, M.; Sun, M.; Li, X.; Deng, A.; Cai, Y.; Zhang, H. Plasma Albumin Levels Predict Risk for Nonsurvivors in Critically Ill Patients with COVID-19. *Biomark Med* **2020**, *14* (10), 827–837. https://doi.org/10.2217/bmm-2020-0254.

(59) Liu, Y.; Yang, Y.; Zhang, C.; Huang, F.; Wang, F.; Yuan, J.; Wang, Z.; Li, J.; Li, J.; Feng, C.; Zhang, Z.; Wang, L.; Peng, L.; Chen, L.; Qin, Y.; Zhao, D.; Tan, S.; Yin, L.; Xu, J.; Zhou, C.; Jiang, C.; Liu, L. Clinical and Biochemical Indexes from 2019-NCoV Infected Patients Linked to Viral Loads and Lung Injury. *Sci China Life Sci* **2020**, *63* (3), 364–374. https://doi.org/10.1007/s11427-020-1643-8.

(60) Deng, H.-J.; Long, Q.-X.; Liu, B.-Z.; Ren, J.-H.; Liao, P.; Qiu, J.-F.; Tang, X.-J.; Zhang, Y.; Tang, N.; Xu, Y.-Y.; Mo, Z.; Chen, J.; Hu, J.-L.; Huang, A.-L. Cytokine Biomarkers of COVID-19. *medRxiv* **2020**, 2020.05.31.20118315. https://doi.org/10.1101/2020.05.31.20118315.

(61) Garcia-Revilla, J.; Deierborg, T.; Venero, J. L.; Boza-Serrano, A. Hyperinflammation and Fibrosis in Severe COVID-19 Patients: Galectin-3, a Target Molecule to Consider. *Front Immunol* **2020**, *11*. https://doi.org/10.3389/fimmu.2020.02069.

(62) Qiu, H.; Wu, J.; Hong, L.; Luo, Y.; Song, Q.; Chen, D. Clinical and Epidemiological Features of 36 Children with Coronavirus Disease 2019 (COVID-19) in Zhejiang, China: An Observational Cohort Study. *Lancet Infect Dis* **2020**, *20* (6), 689–696. https://doi.org/10.1016/S1473-3099(20)30198-5.

(63) Shen, B.; Yi, X.; Sun, Y.; Bi, X.; Du, J.; Zhang, C.; Quan, S.; Zhang, F.; Sun, R.; Qian, L.; Ge, W.; Liu, W.; Liang, S.; Chen, H.; Zhang, Y.; Li, J.; Xu, J.; He, Z.; Chen, B.; Wang, J.; Yan, H.; Zheng, Y.; Wang, D.; Zhu, J.; Kong, Z.; Kang, Z.; Liang, X.; Ding, X.; Ruan, G.; Xiang, N.; Cai, X.; Gao, H.; Li, L.; Li, S.; Xiao, Q.; Lu, T.; Zhu, Y.; Liu, H.; Chen, H.; Guo, T. Proteomic and Metabolomic Characterization of COVID-19 Patient Sera. *Cell* **2020**, *182* (1), 59-72.e15. https://doi.org/10.1016/j.cell.2020.05.032.

(64) Saito, A.; Moniwa, K.; Takahashi, S.; Takahashi, H.; Chiba, H. Serum Surfactant Protein A and D May Be Novel Biomarkers of COVID-19 Pneumonia Severity. **2020**. https://doi.org/10.21203/rs.3.rs-29567/v1.

(65) Vastrad, B.; Vastrad, C.; Tengli, A. Bioinformatics Analyses of Significant Genes, Related Pathways, and Candidate Diagnostic Biomarkers and Molecular Targets in SARS-CoV-2/COVID-19. *Gene Rep* **2020**, *21*, 100956. https://doi.org/10.1016/j.genrep.2020.100956.

(66) Ingelheim, B. *National Library of Medicine (U.S.)*. Nintedanib for the Treatment of SARS-Cov-2 Induced Pulmonary Fibrosis (NINTECOR). https://clinicaltrials.gov/study/NCT04541680 (accessed 2023-07-31).

(67) Watanabe, Y.; Allen, J. D.; Wrapp, D.; McLellan, J. S.; Crispin, M. Site-Specific Glycan Analysis of the SARS-CoV-2 Spike. *Science (1979)* **2020**, *369* (6501), 330–333. https://doi.org/10.1126/science.abb9983.

Section V Longitudinal multi-omics network analysis reveals complement–coagulation rewiring in Long COVID

Bradley Ward[1,2,†], Jean Cyr Yombi[3,†], Jean-Luc Balligand[4], Patrice D. Cani[5], Jean-François Collet[6], Julien de Greef[2,3], Joseph P. Dewulf[2,7,8], Laurent Gatto[9], Vincent Haufroid[2,7], Sébastien Jodogne[10], Benoît Kabamba[7,11], Sébastien Pyr dit Ruys[1], Didier Vertommen[12], Leïla Belkhir[2,3,*,‡] and Laure Elens[1,2,*,‡]

Corresponding Author

* Laure Elens: Laure.Elens@UCLouvain.be
* Leïla Belkhir: Leila.Belkhir@SaintLuc.UCLouvain.be

Present Addresses

1. Integrated Pharmacometrics, Pharmacogenomics and Pharmacokinetics Group (PMGK), Louvain Drug Research Institute (LDRI), UCLouvain, Université Catholique de Louvain, Brussels, 1200, Belgium; bradley.ward@uclouvain.be (B.W.); sebastien.pyrditruys@uclouvain.be (S.P.d.R.)
2. Louvain Center for Toxicology and Applied Pharmacology (LTAP), Institut de Recherche Expérimentale et Clinique (IREC), UCLouvain, Université Catholique de Louvain, Brussels, 1200, Belgium; julien.degreef@saintluc.uclouvain.be (J.d.G.); joseph.dewulf@saintluc.uclouvain.be (J.P.D.); vincent.haufroid@saintluc.uclouvain.be (V.H.)
3. Department of Internal Medicine, Cliniques Universitaires Saint-Luc, UCLouvain, Université Catholique de Louvain, Brussels, 1200, Belgium; jean.yombi@uclouvain.be
4. WELBIO (Walloon Excellence in Life Sciences and Biotechnology), Pole of Pharmacology and Therapeutics (FATH), Institut de Recherche Experimentale et Clinique (IREC), Cliniques Universitaires Saint-Luc, UCLouvain, Université Catholique de Louvain, Brussels, 1200, Belgium; jean-luc.balligand@uclouvain.be
5. WELBIO (Walloon Excellence in Life Sciences and Biotechnology), Metabolism and Nutrition Research Group, Louvain Drug Research Institute (LDRI), UCLouvain, Université Catholique de Louvain, Brussels, 1200, Belgium; patrice.cani@uclouvain.be
6. WELBIO (Walloon Excellence in Life Sciences and Biotechnology), de Duve Institute, UCLouvain, Université Catholique de Louvain, Brussels, 1200, Belgium; jean-francois.collet@uclouvain.be
7. Department of Laboratory Medicine, Cliniques Universitaires Saint-Luc, UCLouvain, Université Catholique de Louvain, Brussels, 1200, Belgium; benoit.kabamba@saintluc.uclouvain.be
8. Department of Biochemistry, de Duve Institute, UCLouvain, Université Catholique de Louvain, Brussels, 1200, Belgium
9. Computational Biology and Bioinformatics Unit (CBIO), de Duve Institute, UCLouvain, Université Catholique de Louvain, Brussels, 1200, Belgium; laurent.gatto@uclouvain.be
10. Computer Science and Engineering Department (INGI), Institute of Information and Communication Technologies, Electronics and Applied Mathematics (ICTEAM), UCLouvain, Université Catholique de Louvain, Louvain-la-Neuve, 1348, Belgium; sebastien.jodogne@uclouvain.be
11. Pôle de Microbiologie, Institut de Recherche Expérimentale et Clinique, UCLouvain, Université Catholique de Louvain, Brussels, 1200, Belgium
12. de Duve Institute, and MASSPROT Platform, UCLouvain, Université Catholique de Louvain, Brussels, 1200, Belgium; didier.vertommen@uclouvain.be

†‡ These authors contributed equally to this work.

Abstract

Post-acute sequelae of COVID-19 (PASC) is heterogeneous and mechanistically unresolved. We profiled matched plasma proteomics, metabolomics and whole-blood transcriptomics at acute infection and convalescence (~3-month later) in a Belgian cohort. Late-stage integrative multi-omic analysis via linear mixed models and multi-omic GSEA revealed sustained enrichment of complement cascade pathways from acute illness to follow-up in PASC compared with recovered patients.

Correlation networks integrated with prior-knowledge databases were explored using a novel differential-correlation rewiring approach to highlight dysregulated components. Two main modules were resolved, a complement/coagulation cluster and an immunoglobulin V-gene transcript cluster. PASC correlation networks re-centred on a C3 amplification bottleneck and lost immunoglobulin co-expression seen in recovery. Among the top rewired nodes, coagulation regulators heparin cofactor II (SERPIND1) and alpha-1 antitrypsin (SERPINA1) and complement regulator complement factor H-related 5 (CFHR5) appear of particular interest due to their high network dysregulation and their overall importance to the regulation of the complement and coagulation pathways. Additionally, multiple minor hints appear to implicate prothrombin/thrombin (F2) with PASC, indicating altered thrombin context rather than large abundance changes. It is noteworthy that these insights only became obvious through an integrative network analysis as single-omic tests (limited by heterogeneity and small effects) yielded few FDR-significant hits.

Together, these trajectory-aware, cross-omic networks nominate a thrombo-inflammatory axis in which complement, and coagulation amplification remain pathologically dysregulated in PASC. These findings provide a systems framework for mechanistic validation and for exploring targeted interventions at the complement–coagulation–platelet interface in long COVID.

Introduction

COVID-19 overview

Coronavirus disease 2019 (COVID-19) is caused by severe acute respiratory syndrome coronavirus 2 (SARS-CoV-2), an RNA virus belonging to the Coronaviridae family. COVID-19 was first identified in Wuhan, China, in December 2019 and declared a global pandemic by the World Health Organization in March 2020. SARS-CoV-2 is structurally characterized by spike proteins that facilitate host cell entry through interactions with angiotensin-converting enzyme 2 (ACE2) receptors [1]. The virus is highly transmissible, primarily spreading through respiratory droplets and, to a lesser extent, via contact with contaminated surfaces. Epidemiological studies have revealed significant variability in transmission dynamics, with asymptomatic carriers playing a critical role in its spread [2].

Following infection, SARS-CoV-2 rapidly replicates in respiratory epithelial cells, triggering innate immune activation and inflammatory responses. Clinically, COVID-19 presents with a broad spectrum of symptoms, ranging from mild flu-like illness to severe pneumonia and multi-system organ failure [3]. Common clinical presentations include respiratory, gastrointestinal, and neurological involvement, whilst severe cases are associated with cytokine storms, acute respiratory distress syndrome (ARDS), and cardiovascular complications [4].

Furthermore, a significant proportion of patients go on to develop post-acute sequelae of COVID-19 (PASC), commonly referred to as "long COVID," which manifests itself as persistent fatigue, cognitive impairment, and organ-specific dysfunction months after recovery [5]. PASC affects up to 40% of COVID-19 survivors, placing substantial health and economic burdens on individuals and societies worldwide [6,7]. For instance, in Switzerland, over 2% of new disability insurance claims have been attributed to PASC, whereas in the United States, the combined direct and indirect annual costs related to PASC are estimated to reach up to US$600 billion [8,9].

The broad spectrum and complexity of COVID-19, particularly the substantial impacts of PASC, underscore the ongoing need for intensive research and sustained public health interventions to mitigate long-term consequences.

Post-acute sequelae of COVID-19 (PASC)

PASC refers to the persistence or emergence of symptoms following acute COVID-19 infection, which cannot be explained by alternative diagnoses. Definitions of PASC vary by study or organization; for instance, the World Health Organization defines PASC symptoms as those persisting or appearing at least three months after infection, whereas the UK National Institute for Health and Care Excellence recognizes symptoms occurring as early as four weeks post-infection [10,11].

Risk factors for the development of PASC include severe acute COVID-19 illness, female sex, older age, and pre-existing comorbidities such as diabetes and cardiovascular disease [12]. Clinical manifestations of PASC are diverse and can involve multiple organ systems simultaneously in a relapsing-remitting pattern, reflecting its complexity. Commonly reported symptoms include profound fatigue, post-exertional malaise, respiratory symptoms (e.g., shortness of breath, persistent cough, chest pain), and cognitive impairments such as memory deficits and difficulty concentrating ("brain fog") [11,13]. Neurological symptoms frequently observed in these patients include headaches, sleep disturbances, anosmia, and dysgeusia. Additionally, musculoskeletal pain and generalized weakness are common. Cardiovascular manifestations indicative of dysautonomia, such as palpitations, tachycardia, and postural hypotension (characteristic of postural orthostatic tachycardia syndrome, POTS), are well documented [14]. Gastrointestinal complaints, including persistent nausea and diarrhoea, as well as psychological effects such as anxiety and depression, also occur in subsets of patients [13].

Multiple mechanisms underlying the pathogenesis of PASC have been proposed. A prominent hypothesis is the persistence of SARS-CoV-2 RNA and viral proteins in tissues or immune-privileged sites (e.g., gut, brain, and lymphoid tissues), leading to ongoing antigenic stimulation and chronic inflammation [15]. Another central mechanism involves aberrant or delayed innate immune responses, characterized by persistent activation of

inflammatory cytokines ("cytokine storm"), resulting in chronic inflammation and immune-cell reprogramming, including alterations in neutrophils, monocytes, and tissue-resident macrophages [16]. Another theory is that SARS-CoV-2 infection may induce autoantibody production either de novo or by activating pre-existing autoreactive immune responses; it has been observed that such autoantibodies have been implicated with long-term symptoms [17]. Other proposed mechanisms include: injury to endothelial cells leading to the formation of microthrombi and abnormal organ function [18]; autonomic nervous system dysfunction [19]; reactivation of latent viruses (notably Epstein–Barr Virus) [20]; altered cellular metabolism and impaired mitochondrial function [21]; alterations in the gut microbiome and disruption of the intestinal barrier (“leaky gut”) [22].

Among the proposed mechanisms, persistent immune dysregulation and chronic inflammation receive substantial support from clinical studies and extensive reviews, including those by initiatives such as RECOVER. Patients with PASC frequently exhibit altered innate and adaptive immune responses, sustained elevations of inflammatory cytokines, and aberrant immune-cell profiles long after resolution of acute infection.

Given the multiplicity and complexity of these pathophysiological mechanisms, which are likely not mutually exclusive and may interact dynamically within individuals, PASC is increasingly recognized as a multifactorial disorder. This complexity underscores the necessity for integrative research approaches, such as multi-omics and network medicine, to comprehensively elucidate the underlying biology and inform effective therapeutic strategies.

Multi-omic studies of PASC

Although single-omic investigations have been pivotal in COVID-19 research, each modality in isolation provides only a piece of the puzzle. PASC is a complex syndrome likely arising from the interplay of viral, immunological, metabolic, and genetic factors, relationships often overlooked by single-layer studies. For example, a proteomic study might detect inflammatory cytokines, while a separate metabolomic analysis might independently detect abnormal metabolites; however, without integrating these datasets, the relationship between inflammation and metabolic dysregulation remains unclear. To

address this limitation, multi-omic approaches that simultaneously integrate various molecular data types from the same patients are essential. Such integration allows identification of convergent pathways and causal networks underlying PASC, facilitating a more comprehensive understanding than achievable through single-omic analyses alone.

One of the first comprehensive multi-omic studies of PASC was by Su *et al*. (2022), who identified four independent risk factors (high viral load in blood, EBV reactivation, certain autoantibodies, and type 2 diabetes), that robustly stratify patients according to their likelihood of developing PASC [23]. In addition, immune profile analysis revealed four immunological endotypes associated with different symptom clustering and PASC outcomes. Subsequent studies have built on these insights: Thompson et al. used whole-blood transcriptomics and serology to distinguish two post-COVID clusters differentiated by immunoglobulin gene expression, suggesting distinct immunological etiologies for PASC [24]. Wang *et al*. further demonstrated a persistent inflammatory and hypercoagulable state in PASC patients (elevated cytokines, signs of platelet activation) accompanied by significant metabolic disturbances affecting arginine and energy metabolism, and gut dysbiosis [25]. Complementary work by Wei *et al*., integrating plasma proteomics and metabolomics, revealed that PASC patients exhibit marked disturbances in coagulation, complement cascade, and lipid metabolism compared to fully recovered individuals [26]. In a similar vein, Saito *et al.* (2024) focused on patients with chronic fatigue-like symptoms and found persistent pro-inflammatory cytokines alongside energy depletion and specific metabolic deficits, potentially underpinning cognitive and mood disturbances [27]. Lastly, Yang *et al*. provided a longitudinal perspective over three years, uncovering enduring alterations in proteomic and metabolomic signatures that correlated with pulmonary dysfunction, and identified a combined protein-metabolite predictor for long-term respiratory impairment [28].

Together, these multi-omic studies underscore the heterogeneity of PASC and illustrate how integrating diverse molecular data can uncover distinct biological pathways driving its pathogenesis. Nonetheless, each study has certain limitations. Many had only limited

multi-omic integration, lacked longitudinal data, had relatively small sample sizes, or underrepresented mild or non-hospitalised cases.

In contrast, our study leverages a comprehensive, integrative approach by simultaneously profiling shotgun proteomics, metabolomics, and RNA sequencing from the same plasma samples, coupled with whole exome sequencing and extensive clinical data, in a cohort balanced between mild and severe COVID-19 cases. By collecting samples both during the acute infection phase and approximately 70 days later, our longitudinal design enables robust investigation of molecular changes over time. This integrative approach is specifically designed to yield deeper insights into the molecular drivers of PASC, enhance patient stratification, facilitate biomarker discovery, and ultimately inform targeted therapeutic strategies. The inclusion of multiple rich omic datasets from matched patient samples uniquely positions this study to uncover causal pathways and construct predictive models that surpass previous efforts.

Methods

Below is a summarisation of the methodology employed in the study, for a full methodological description, please see the Supplementary information 4 for the wet and dry lab protocols, and Supplementary information 2 for the full bioinformatic scripts.

Patient cohort composition, sample collection, and storage

Participants for this analysis were selected from the HYGIEIA cohort [29]. The cohort comprised 25 healthy individuals, 24 influenza patients, 50 moderate COVID-19 cases (defined as non-hospitalised, WHO clinical Progression Scale score <4), and 57 severe COVID-19 patients (hospitalized, WHO Clinical Progression Scale score >4) recruited from Belgium hospitals between August 2020 and March 2024. Biological samples and medical data were first at inclusion and again follow-up during convalescence (81 days on average following inclusion).

Wet-lab methodology

DNA extraction and whole exome sequencing

DNA was extracted from EDTA blood using QIAamp DNA Blood Mini Kit (Qiagen, Germany) in random batches of 16. Library preparation and sequencing for WES were outsourced to Macrogen (Republic of Korea) who used the Twist Human Core Exome (+RefSeq) system (Twist Bioscience, USA), following the manufacturer's recommended protocols. Following library quality control via Picogreen (Thermo Fisher Scientific, USA) and Tapestation D1000 screen tape (Agilent, USA), sequencing was carried out on a Novaseq 6000 platform to a target depth of 5Gb, 50x mappable, 151 paired end reads.

Whole Transcriptomic Shotgun RNAseq

Total RNA was isolated from whole-blood samples collected in Tempus RNA tubes using the Tempus™ Spin RNA Isolation Kit (cat.# 4380204, Thermo Fisher Scientific, USA) in random batches of 20. Extracted RNA samples underwent further purification using the RNA Clean & Concentrator-5 Kit (cat.# R1013, Zymo Research, USA). Library preparation and sequencing for RNA-seq from whole blood was outsourced to Macrogen who used a combination of the Illumina Globin-Zero Gold Kit (Illumina, USA) for rRNA/globin mRNA depletion, followed by the TruSeq Stranded mRNA protocol (Illumina, USA) for library construction. Libraries were quality controlled using Picogreen (Thermo Fisher Scientific, USA) and Tapestation D1000 screen tape (Agilent, USA), and normalized pooled libraries were sequenced on a Novaseq 6000 (Illumina, USA) to a target depth of 30M 151 paired end reads.

DIA Shotgun Proteomics

Plasma samples were processed according to our published protocol in randomized batches of 16 [30]. Briefly, High Select Top14 Abundant Protein Depletion Resin (Thermo Fisher Scientific, USA) was used to collect depleted protein flow-through which was subsequently, denatured, reduced, and alkylated. Proteins were then precipitated, washed, resuspended, and digested overnight with sequencing grade modified trypsin (V5117, Promega, United States). Following digestion, peptides were acidified and

immediately loaded onto a Pierce High pH Reversed-Phase Peptide Fractionation column (Thermo Fisher Scientific, USA). Peptides were sequentially eluted into seven fractions using solutions of increasing acetonitrile concentration (7.5%, 10%, 12.5%, 15%, 17.5%, 20%, and 50%), each containing 0.1% triethylamine. Fractions were strategically combined into three pools, dried, and resuspended in 20 µL MS resuspension buffer (3.5% acetonitrile, 0.1% trifluoroacetic acid). 1 µg of peptides was injected into a reversed-phase pre-column (Acclaim PepMap 100, Thermo Fisher Scientific, USA) and separated using an EasySpray analytical column (Acclaim PepMap RSLC C18, 0.075 × 250 mm, Thermo Fisher Scientific, USA) over a 120-minute gradient at 300 nL/min. Separation employed a 120-minute gradient at 300 nL/min on an Ultimate 3000 RSLC nanoHPLC system (Thermo Fisher Scientific, United States). A data-independent acquisition (DIA) approach was employed to scan precursor ions across an m/z range of 500–740 with a 4 m/z isolation window at a resolution of 60,000 (FWHM).

Shotgun Metabolomics

Plasma samples were processed in random batches of 18 samples. Plasma proteins were precipitated with acetone followed by extraction of the upper phase into a clean tube, aliquots of which were dried down on a heating block at 30°C with nitrogen flush system. Two sample aliquots were then resuspended in 50% acetonitrile/0.1% formic acid, and another two aliquots were resuspended in 95% acetonitrile/0.1% formic acid/10 mM ammonium formate. Sample were then analysed via UPLC-MS in three batches of 100, 97, and 55 using a Synapt-XS quadrupole time-of-flight (Q-ToF) mass spectrometer (Waters, USA), operated in resolution mode, coupled to an Acquity Premier UPLC system (Waters, USA). Chromatographic separations were conducted using an Acquity Premier HSS T3 column (186009468, Waters, USA) for reverse-phase analyses and an Acquity Premier BEH Amide column (186009505, Waters, USA) for HILIC-based separations. Each chromatographic method employed one aliquot analysed in positive electrospray ionization mode and a second aliquot in negative ionization mode.

Bioinformatic preprocessing pipelines

Proteomics

Raw mass spectrometry data (.mzML files) were initially processed using DIA-NN (v1.8.1) [31], with an in-silico predicted spectral library generated from the UniProtKB human reference proteome (accession UP000005640, Swiss-Prot filtered) [32]. Following this, high-missingness precursors were then removed and remaining missing precursors were marked missing not at random (MNAR) or missing at random (MAR) and imputed using Quantile Regression Imputation of Left-Censored data (QRILC) or random forest respective. Data were then normalized via variance stabilization normalization (VSN) and aggregated to protein level via the robust summary method (robust M-estimation) from MsCoreUtils using QFeatures [33,34].

Metabolomics

Raw data was imported into Progenesis QI (V4.2, Nonlinear Dynamics, UK) for lock mass correction and raw spectra were converted to a 2D ion intensity map. Feature detection was carried out via peak picking, identifying ion features based on accurate mass, and retention time (RT). A reference run from a pool representative of all the samples was selected to guide alignment. Following alignment, raw abundance values were filtered for missingness and imputed based on MNAR/MAR as previously described for proteomics; imputed data were then normalized using VSN, and batch corrected. Finally, metabolite identifications from Progenesis QI were used to annotate features (if known), and known metabolites were aggregated using the same robust summary method as previously mentioned.

Transcriptomics

Raw fastq files were first trimmed to remove low-quality bases using Trimmomatic (v0.39) and reads were aligned to the GRCh38 human genome using HISAT2 (v2.2.1) [35,36]. Gene-level expression was then quantified with featureCounts from Subread (v2.0.3) using the GRCh38.105 genome assembly [37]. Normalized count matrices were generated using DESeq2 variance stabilization transformation (VST) [38].

Genomics

Genomic reads were aligned to the human reference genome GRCh38 using BWA-mem (v0.7.17) [39]. Resulting BAM files then underwent duplicate removal with SAMTools (v1.12) and base quality recalibration using GATK BaseRecalibrator (v4.2.1) [40,41]. Germline single nucleotide variants (SNVs) and short INDELs were called sample-by-sample using GATK HaplotypeCaller [41]. Structural variations were detected by combining "read depth" (ExomeDepth) with "split read" (GRIDSS-Purple-Linx) [42,43]. The resulting VCF files were normalized, filtered according to GATK best practices, and annotated with snpEff (v5.0e) [41,44]. Variants were then fully annotated by in-house algorithms using Highlander [45].

Analytical methodologies

Long-COVID multi-omics modelling

Proteomic and metabolomic abundance abundances (VSN-normalized) and RNA-seq counts were used as dependent variables for linear mixed modelling with dream (variancePartition v1.36.3) [46]. For the longitudinal analysis, we tested the PASC status(PASC/recovered) x Visit (1/2) interaction (difference-in-differences: [PASC V2 − PASC V1] − [Recovered V2 − Recovered V1]) in a linear mixed model (dream, variancePartition), with a random intercept for patient ID and covariates (COVID severity (moderate/severe), vaccine status (full vaccination yes/no), sex (male/female), and age (years)) [47]. RNA-seq counts were processed with voomWithDreamWeights prior to modelling; proteomics and metabolomics were modelled directly. Features with near-zero variance were removed. The pipeline was then re-run for cross-sectional analysis of PASC status at visit 1 and visit 2 independently (not longitudinally) using linear models with empirical-Bayes moderation (limma), adjusting for covariates (Visit 1 analysis: COVID severity (moderate/severe), vaccine status (full vaccination yes/no), sex (male/female), and age (years); Visit 2 analysis: vaccination, sex, and age) [48]. Multi-omics pathway enrichment used multiGSEA across KEGG and Reactome: each omic was pre-ranked, per-omic GSEA was computed, and pathway p-values were combined across omics and FDR-adjusted [49].

Genomic GWAS and SKAT-O/burden analysis

Annotated SNP data was filtered according to strict QC metrics, per-sample and SNP call rates, and predictive damaging scores (as calculated within Highlander); remaining missing genotypes were mean-imputed per SNP. PCA was computed on LD-pruned, position-sorted genotypes. PC1 accounted for the most captured variation (2.4%), including ethnicity. For the final GWAS model, we tested the association between SNP dosage (0-2, additive) and PASC status (PASC vs recovered) using logistic regression, adjusting for age (years), sex (male/female), and ancestry (PC1).

Following, we tested per-gene burden/variance effects using a gene-level aggregation analysis (SKAT-O from SKAT package), requiring a minimum two SNPs per gene [50]. A logistic SKAT null model was built using the same GWAS covariates (Age, Sex, PC1) and case status coded 0/1 (recovered/PASC). SKAT-O was then run using predictive damaging scores (as calculated within Highlander), coinciding with the estimated damage of the SNP.

Network Construction and Multi-Omic Integration

Here, a specific pathway (Reactome "Complement Cascade" pathway, which also contains the sub-pathway "Regulation of Complement Cascade") was selected for targeted network analysis following multiGSEA results. All proteins, transcripts, and metabolites for this network were selected as seed nodes. The network was then expanded to included first-neighbours of seed nodes from a curated "prior knowledge" network. This network included protein-metabolite interactions (Recon3D, KEGG), protein–protein interactions (STRING), transcription-factor gene regulations (TRRUST v2), miRNA-mediated post-transcriptional interactions (DIANA-TarBase v8), drug-target information (OpenTargets), and finally, a layer incorporating central biology dogma was included, whereby each protein-coding transcript was additionally linked to its translation product and gene where relevant [52–57].

Following the creation of this expanded complement cascade network, proteomic, metabolomic, and transcriptomic abundance data of the relevant features were analysed separately in the following pipeline. For each omic, differential abundance correlation testing between recovered and PASC was performed using Differential Gene Correlation Analysis (DGCA) (ddcorALL) [51]. Edges (node connections) with weak correlation or insignificant in both groups were removed (absolute correlation > 0.3 and fdr adjusted p-value < 0.01). The resulting z-score difference is used as edge weights to represent the strength of association change (DGCA z-score, scaled to 0–1 within each omic). These separate differential correlation networks for each omic were then combined, and edges pertaining to prior knowledge (protein-protein interaction edge, miRNA target edge, drug interactions, etc) were incorporated for data visualisation and exploration purposes.

For each node (*i*) (protein, transcript, etc), we then summarised how much their edges changed between the PASC and recovered networks. For each node, its edge weights were combined using the Euclidean (L2) norm (root-sum-of-squares). To make scores comparable across nodes and omics, a degree-matched z-score (DMZ) was then computed for each node within bins/groups of similar degree (number of edges connected to node) (subtract bin mean, divide by bin SD). In this way, nodes rewiring is compared against similar peers, preventing large regulatory nodes from overpowering the analysis through sheer number of connections. The score was then scaled 0-1 for ease of interpretation. Higher scores mean that a node's interaction pattern changed more strongly between the two groups. This metric differs from DyNet's Dn-score (which uses a different approach to measure variability across many states): here we measure the magnitude of change between two states, directly using the differential-correlation statistics, which is better aligned with our study aims.

Results

Differential expression and GSEA analysis

Using single-omic models adjusted for age, sex, vaccination, and acute severity, no individual features reached FDR < 0.05 across acute (visit 1), convalescent (visit 2), or longitudinal contrasts. Ranked multi-omic GSEA detected coordinated pathway shifts: 569 pathways were identified as being significantly altered in their activity trajectory from the acute to convalescent phase in patients developing PASC, 711 pathways were identified as being significantly enriched/depleted at visit 1 in patients who would develop PASC compared to those who would recover, and 44 pathways were significantly enriched/depleted at visit 2 in patients with PASC vs recovered patients. Twenty-six pathways were significant in all three analyses, including RNA-processing/translation modules. Four pathways were significant at both visit 1 and visit 2 but not longitudinally, suggesting sustained elevation or depletion in PASC patients vs recovered patients: Complement cascade, Regulation of complement cascade, Intraflagellar transport, and Regulation of tubulin folding by CCT/TriC. Of these pathways, the complement cascade was selected for deeper investigation due to its previously suggested involvement in PASC pathogenesis. In the two complement pathways (Fig. 1), proteomic signal drove the enrichment at both timepoints, whereas transcriptomic signal was weak and metabolomics did not contribute (no complement-mapped metabolites). Among metabolic pathways, G-alpha signalling and bile-acid synthesis via 27-hydroxycholesterol showed upward trajectories but no FDR-significant metabolic pathway remained after correction.

Genome-wide analyses of WES did not reveal any significant SNPs at conventional thresholds, likely due to the small cohort size (relative to other GWAS studies) and lack of genomic involvement toward PASC development. The top PASC associated SNPs were rs767558704 (*ZNF233*), rs17283 (*TRBV13*), and rs1730409324 (*MUC4*), with p-values of 0.0029, 0.0037, and 0.0038 respectively, far above the typical $5x10^{-8}$ GWAS threshold. To raise investigational power, a combined burden and SKAT test (SKAT-O) was employed to investigate aggregate effects of multiple variants at the gene level. Here, *ITPR2*, *GANC*,

and *AC011005.1* were identified as the most significantly associated genes, but FDR values remained above significance for all genes (0.26, 0.57, and 0.67 respectively).

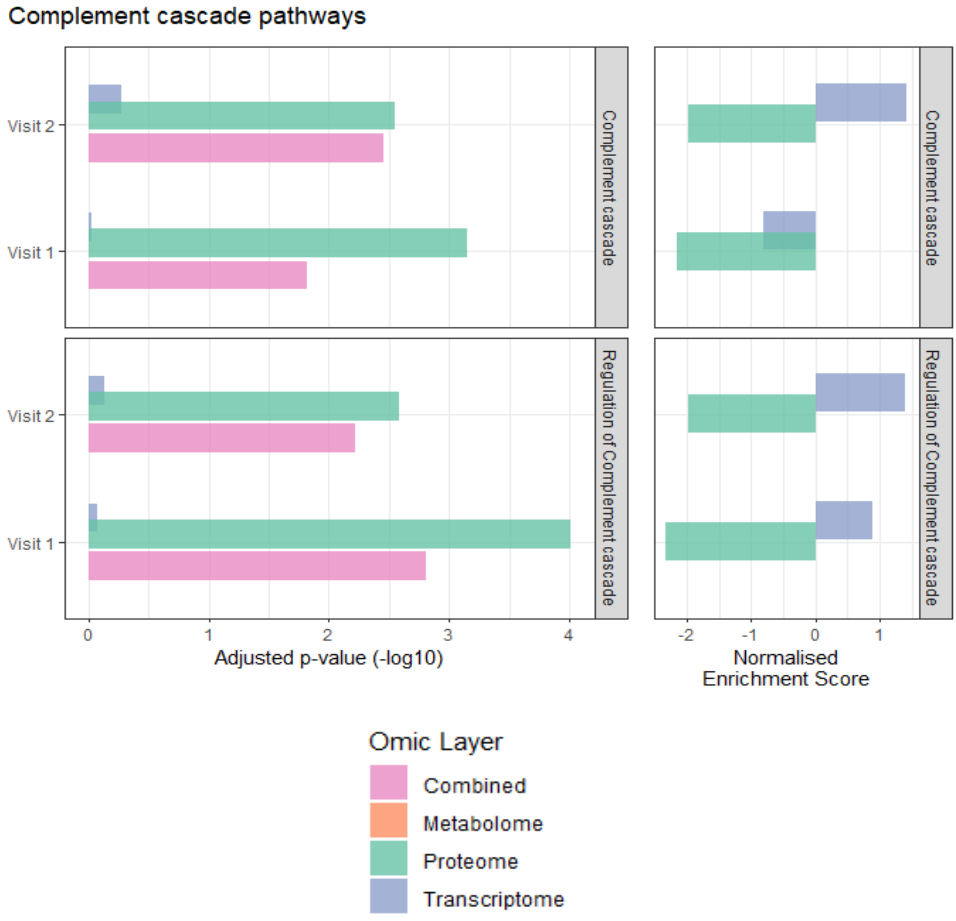


Figure 1: multiGSEA of selected Reactome pathways **Complement Cascade** and **Regulation of Complement Cascade**.

Multi-omic network construction and topology

We integrated cross-omic interactions pertaining to transcription, translation, transcription factor-gene targets, miRNA-mRNA targets, curated protein-protein and protein-metabolite interactions, and significant within-omic correlations to build visit 2 networks for PASC and recovered groups (Fig. 2A–B respectively). In the recovered patient network (Fig. 2A, representing a healthy network structure), nodes appeared to partition into two modules: a complement/coagulation module (lower network segment) and an immunoglobulin V-gene transcript module (upper network segment). This network structure was used to position nodes in figures 2B and 3 to allow for easier visual network comparisons. In recovered patients (Fig. 2A), MASP1 and CFH, complement cascade regulators, represent the prominent hubs within the network, alongside C1QA, which appears to act as a significant bridge between the immunoglobulin transcript module and the complement module. Contrastingly, in PASC (Fig. 2B), C3 is the dominant bottleneck, with a large portion of traffic funnelling between C3 and C5, and a relatively lesser amount to regulator proteins like MASP1 and SERPING1. This concentrates shortest paths at the level of C3 amplification/terminal activation and potentially indicates a shift towards a C3-centric amplification bottleneck in PASC, away from a more regulatory control centred network in recovery patients. Additionally, recovered patients show a prominently more densely connected immunoglobulin transcript module as compared to PASC, dominated by strong positive correlations and several hubs including IGKV3-15, IGLV3-1, and IGLV3-19, which all strongly bridge towards the C1QA transcript, which acts as one of the central hubs of this network alongside MASP1. In PASC however, the majority of these transcript correlations are lost, resulting in a much sparser network and a shift towards IGKV3-20 acting as the central hub. This shift results in the loss of the C1QA-GZMM-CD46 association pathway which acted as a major source of network connectivity in recovered patients.

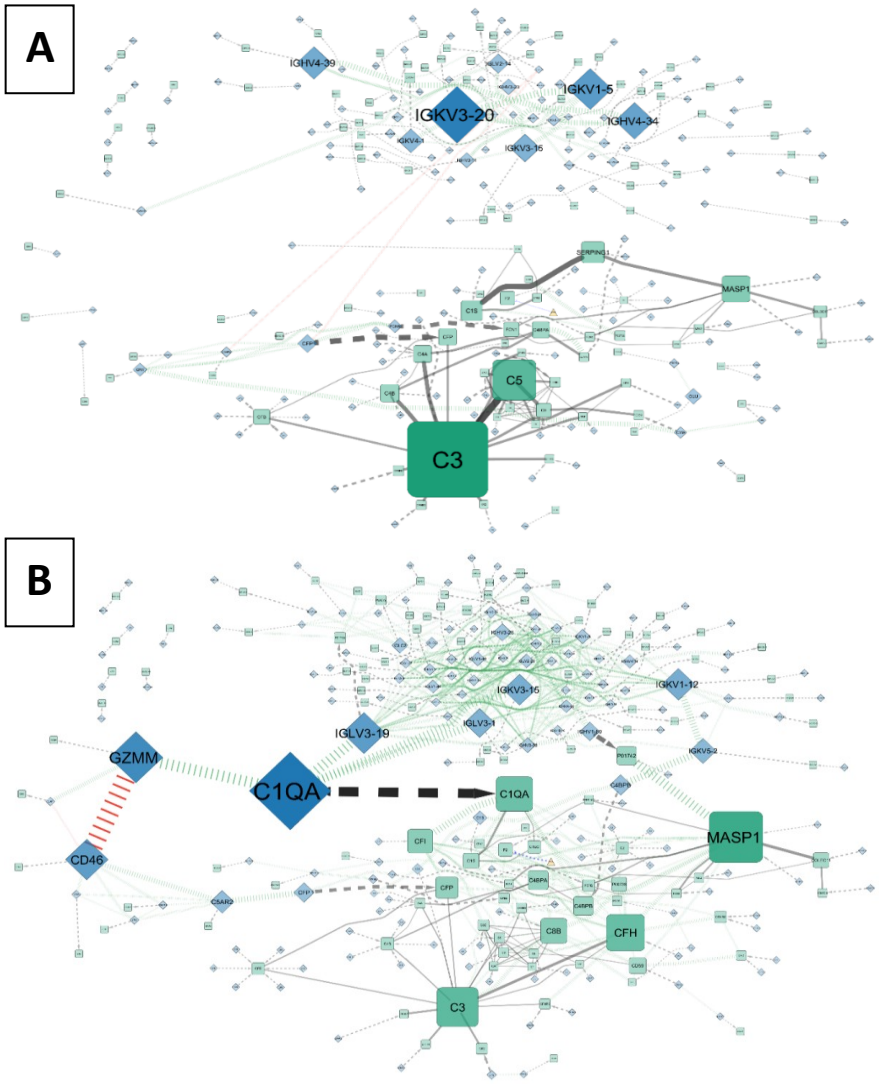


Figure 2: Complement cascade network in PASC patients (A) and recovered patients (B) during convalescent phase of COVID-19. Nodes: Green squares = proteins, blue diamonds = RNA, orange triangles = metabolites. Edges: dashed black edge = transcription, solid black edge = protein-protein interaction, green vertical dashed edge = significant positive correlation, red vertical dashed edge = significant negative correlation, blue dotted edge = protein-metabolite interaction. Larger node size and edge thickness correspond to a higher betweenness score of the node/edge. Node positions were calculated based on prefuse force directed layout algorithm on the recovered network, and then mapped to the PASC network. Network A contains 165 RNA, 113 proteins, and 1 metabolite. Network B contains 165 RNA, 114 proteins, and 1 metabolite.

Differential wiring (PASC vs recovered)

Combining the networks and analysing nodes through the rewiring score previously discussed showed that immunoglobulin transcripts account for most rewiring, with IGLV3-21 the top rewired node in PASC (normalised rewiring score (NRS) = 1), alongside IGHV4-39 as a secondary hub (NRS = 0.62) (Fig. 3). IGLV3-21 displays 4 gained negative correlations (green vertical dashed edge), 9 lost positive correlations (red vertical dashed edge), 17 inversed correlations (solid purple edge, all positive to negative), and 1 strengthened-negative correlation (red zigzag edge); the more general message here is that the node switches from loosely positive embedded within the IgV cluster in recovered to becoming a negatively correlated hub in PASC. The only positive correlation within PASC is a new gained positive connection with the CD19 transcript (PASC cor = 0.73, z-score = -3.27, adj. p-value = 0.024). Other notable partners include the transcripts C1QA, C5AR2, FCN1, and GZMM whose associations flipped positive to negative, and CFD, CFH, and CFP, who gained a negative correlation; the remaining partners are other immunoglobulin chain transcripts. In addition to this topological dominance, IGLV3-21 shows relatively large abundance change, as compared to the rest of the network, although far from significant (LogFC = 0.51, non-adjusted p-value = 0.14). Additional nodes that surface via many small edge changes rather than a few large ones include P01742 (IGHV1-69 product), CFHR5 (C3 regulator in the alternative pathway), and COLEC10 (lectin pathway).

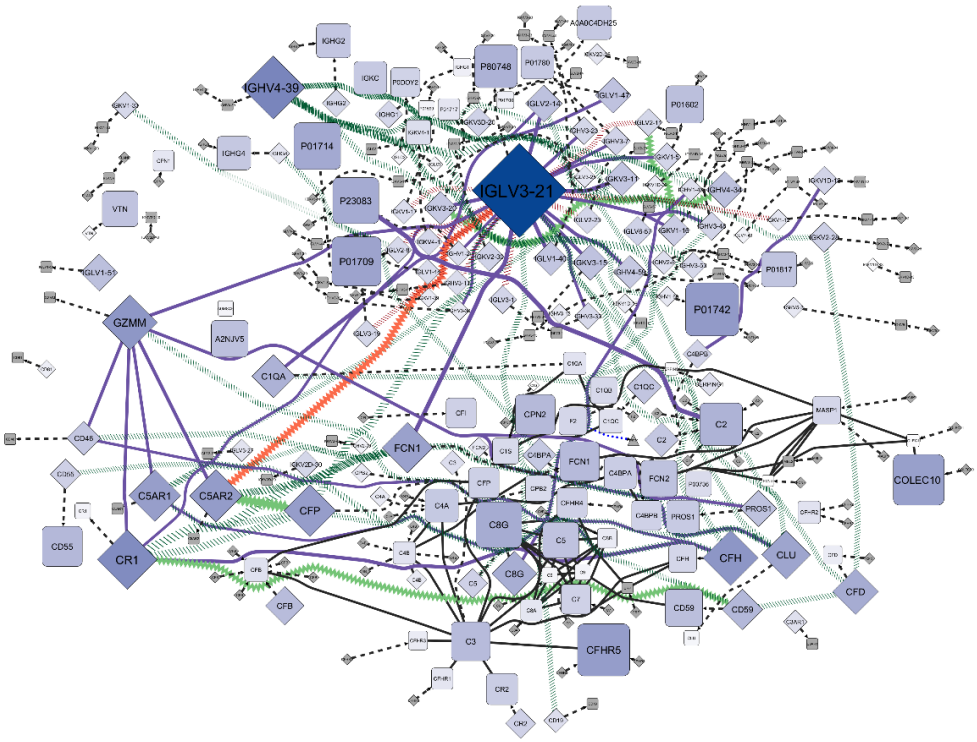


Figure 3: Differential network analysis of the complement cascade network, PASC vs recovered. Nodes: squares = proteins, diamonds = RNA, triangles = metabolites. Edges: dashed black edge = transcription, solid black edge = protein-protein interaction, green vertical dashed edge = correlation gained in PASC, red vertical dashed edge = correlation lost in PASC, green zigzag edge = strengthened positive correlation in PASC, red zigzag edge = strengthened negative correlation in PASC, red sinewave edge = weakened negative correlation in PASC, green sinewave edge = weakened positive correlation in PASC, purple solid edge = correlation sign flip in PASC, blue dotted edge = protein-metabolite interaction. Larger node size and deeper color corresponds to normalized rewiring score, edge thickness corresponds to z-score of correlation difference PASC vs recovered. Node positions were calculated based on prefuse force directed layout algorithm on the recovered network (Fig. 2B). Edges were pruned to only show significant, strong changes (adjusted p-value < 0.05). Network contains 165 RNA, 116 proteins, and 1 metabolite.

Regulation within the complement control layer

Activation of the complement system is tightly regulated by complement control proteins which generally prevent activation; the most well studied of these are CD46 (Membrane Cofactor Protein (MCP)), CD55 (Decay Accelerating Factor (DAF)), CD59 (Protectin), CD35 (Complement C3b/C4b Receptor 1 (CR1)), CRIg (Complement Regulator of the Immunoglobulin Superfamily), CFH (complement factor H), and C4bp (C4-Binding Protein).

Of these, complement factor H (CFH) appears of particular interest as it is both one of the most rewired control proteins (NRS = 0.53) and appears as a first neighbour to the IGLV3-21 transcript, the most rewired node in our network. Whilst the CFH transcript changes little in abundance in PASC, the protein product trends downwards, but not significantly (LogFC ≈ −0.34, non-adjusted p-value = 0.09). The CFH transcript gains a significant negative correlation in PASC patients with IGLV3-21 (PASC cor = -0.64, z-score = 3.24, adjusted p-value = 0.025) and appears to flip negative correlations to positive with CD46 (PASC cor = 0.60, z-score = -3.17, adjusted p-value = 0.026), CR1 (PASC cor = 0.64, z-score = -4.13, adjusted p-value = 0.003), and C5AR1 (PASC cor = 0.49, z-score = -3.0, adjusted p-value = 0.041); a new positive correlation was also gained with C5AR2 (PASC cor = 0.72, z-score = -3.76, adjusted p-value = 0.008). Most interestingly, figure 3 reveals a related protein, the previously mentioned CFHR5, presenting as one of the most rewired nodes in the network (NRS = 0.49), representing potential dysregulation in PASC patients. Although CFHR5 does not show any large significant changes in correlation associations with other proteins (except P01780, a protein transcript of IGHV3-7), it appears its high rewiring score is the result of smaller, but numerous correlation changes. It is linked to the CFH protein in our network through shared protein-protein interactions with C3.

Importantly, the CR1 transcript is the most rewired node within this group of regulators (NRS = 0.58) and seems to act as one of the main nodes within the complement/coagulation module. CR1 gains many strong significant correlations in PASC with other regulatory members (CD59, CFH), but also with GZMM, CFP, FCN1, and IGLV2-14. However, when expanding the network to include first neighbours related to the

complement cascade (Fig. 4), CFH regains this top spot and appears to be a major source of new positive correlations in PASC.

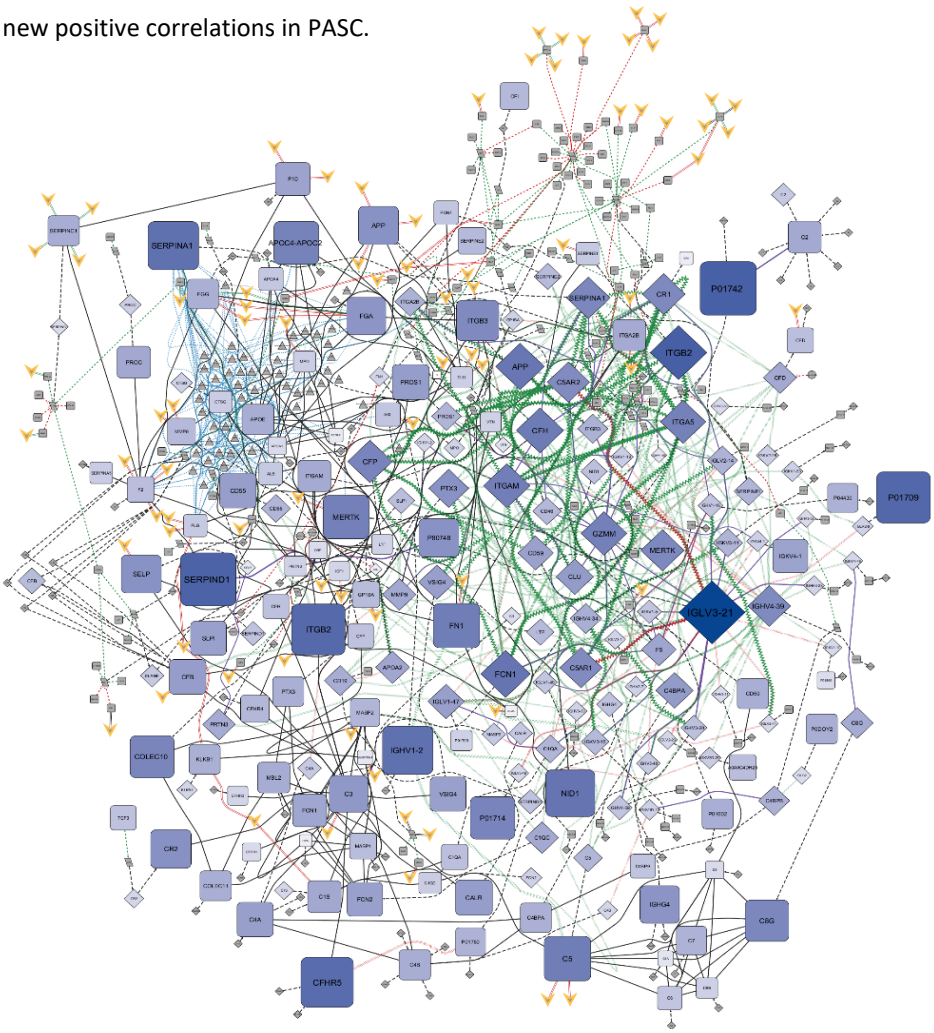


Figure 4: Differential network analysis of the complement cascade network, PASC vs recovered, with non-correlation edge first neighbors. Nodes: squares = proteins, diamonds = RNA, triangles = metabolites, ellipse = miRNA, parallelogram = gene, yellow V = drug. Edges: dashed black edge = transcription, solid black edge = protein-protein interaction, green vertical dashed edge = correlation gained in PASC, red vertical dashed edge = correlation lost in PASC, green zigzag edge = strengthened positive correlation in PASC, red zigzag edge = strengthened negative correlation in PASC, red sinewave edge = weakened negative correlation in PASC, green sinewave edge = weakened positive correlation in PASC, purple solid edge = correlation sign flip in PASC, blue dotted edge = protein-metabolite interaction, green dashed edge = activation, red dashed edge = repression, green parallel edge = drug activation/agonist, red parallel edge = drug repression/antagonist. Larger node size and deeper color corresponds to normalized rewiring score, edge thickness corresponds to z-score of correlation difference PASC vs recovered. Node positions were calculated based on prefuse force directed layout algorithm on the recovered network (Fig. 2B). Edges were pruned to only show significant, strong changes (adjusted p-value < 0.05). Network contain 175 RNA, 5 miRNA, 205 proteins, 49 metabolites, 32 genes, and 77 drugs.

Broader coagulation and anticoagulant neighbourhoods

Zooming out to investigate the broader regulatory landscape around the complement cascade (Fig.4), IGLV3-21 still remains the largest rewired node. IGLV3-21 is the most rewired node despite no significant abundance change (LogFC ≈ 0.8, non-adjusted p-value = 0.12), indicating topology, and not expression, is the dominant signal. Its edge set shows 14 gains (13 negative, 1 positive, green vertical dashed edges), 10 losses (all positive, red vertical dashed edges), 16 sign-flips (all positive to negative, purple solid edges), and 2 strengthened-negative links (red zigzag edges). The gains are predominantly *de-novo* negative correlations in PASC (typical PASC r around −0.6 to −0.9), including some of the strongest changes in the network. Losses mostly reflect positive partners in recovered that fade in PASC (typical recovered around 0.5 to 0.8). The sign-flips are striking: many partners move from moderate/strong positive in recovered (r around 0.6 to 0.8) to negative in PASC (r around −0.4 to −0.8). Most partners in this list are other immunoglobulin V genes, so the net effect is that IGLV3-21 switches from being loosely/positively embedded within the IgV cluster in recovered to acting as a negatively correlated hub in PASC, including several very strong de-novo negatives. Together, these patterns appear to point to a reorganization of IgV co-expression structure around IGLV3-21 rather than a simple up- or downregulation of the transcript itself.

Prothrombin (F2) shows a small but significant decrease (LogFC = −0.32, non-adjusted p-value = 0.05) with a non-significant transcript increase (LogFC = 0.6, non-adjusted p-value = 0.36), alongside a moderate normalised rewiring score of 0.32, consistent with altered interaction context. Upstream F10 is also moderately rewired, whilst F5 shows little rewiring. FGA/FGG (protein chains of fibrinogen) and GP1BA (enhancing platelet adhesion) remain near-static in abundance and moderately rewired. Among anticoagulants, SERPINC1 (antithrombin) trends lower (RNA and protein, both non-adjusted insignificant) and PROC (Protein C (anticoagulant)) shows mild downregulation at RNA and protein (both non-adjusted insignificant) in PASC. SERPIND1 (heparin cofactor II (thrombin inhibitor)) is one of the most dysregulated proteins by rewiring (NRS = 0.78), gaining a

strong negative correlation with P80748 (IGLV3-21 protein) despite stable abundance (z-score = 3.72, PASC cor -0.55 vs recovered cor = 0.53).

SERPINE2 (PN-1) protein trends downwards in PASC (LogFC = -0.36, non-adjusted insignificant) with stable RNA (LogFC -0.06, non-adjusted insignificant). SERPINA1, FN1, and NID1 are highly rewired in PASC: FN1 trends lower at protein (LogFC = -0.44, non-adjusted p-value = 0.06) and RNA (LogFC = -0.45, non-adjusted insignificant) with a complex TF/miRNA regulator set (e.g., NF-κB, RELA, EGR1 activation; SOX17/KLF8 repression; hsa-miR-429/-206 inhibition). NID1 protein is slightly reduced (LogFC = -0.26, non-adjusted insignificant) and gains a positive correlation with MASP2 (PASC cor = 0.80, z-score = 3.58, adj. p-value = 0.038), while NID1 RNA gains positive correlations with PTX3 (PASC cor = 0.63, z-score = -2.15, adj. p-value = 0.049), MERTK (PASC cor = 0.85, z-score = -3.08, adj. p-value = 0.009), and IGHV3-33 (PASC cor = 0.71, z-score = -2.17, adj. p-value = 0.048). Together, these edges hint towards ECM/vascular remodelling, lectin-pathway components, efferocytosis, and humoral features.

In PASC, ITGB2 (CD18) is among the most rewired nodes at both protein (NRS = 0.78) and RNA (NRS = 0.84) levels. At the protein level, ITGB2 gains strong, significant positive correlations with SERPINA1 and CFB. At the transcript level, ITGB2 acquires multiple significant positive correlations with ITGAM, ITGA5, ITGB3, C5AR1, C5AR2, CR1, CD46, CFP, CLU, F5, and APP. These additions cluster into two modules: complement receptors/regulators (CR1, C5AR1/2, CD46, CFP, CLU) and integrin/platelet–coagulation genes (ITGAM/ITGA5/ITGB3, F5, APP), indicating, relative to recovered patients, that ITGB2 co-varies more tightly with complement and coagulation/platelet modules in PASC, despite only modest changes in mean abundance.

CRP shows a trend to higher protein (logFC = 0.98, non-adjusted p-value = 0.13) but very low rewiring (NRS = 0.17), and the transcript is likewise stable and only linked to its protein. Within the multi-omic network, CRP forms only three physical edges without any significant or strong correlations present in either PASC or recovered networks, indicating that the manner in which CRP interacts with the wider complement and coagulation network is essentially unchanged in PASC patients.

Discussion

This exploratory multi-omic analysis nominates complement as a candidate pathway for targeted follow-up in PASC investigations, with three convergent signals: pathway-level enrichment at both acute and convalescent phases; topological re-centring on C3 in the PASC multi-omic network; and broad rewiring across regulatory components of the complement and coagulation pathways, despite limited differential abundance at the single-feature level.

As shown by our network analysis (Fig. 4), key coagulation and complement components exhibit extensive rewiring in PASC. Figure 5 has been created in an effort to summarise and explain the main findings of our investigations, showing how some of the nodes we have identified as most rewired or interesting (SERPIND1, SERPINA1, MERTK, CD18, CR2, COLEC10, CFHR5, Protein C, and FN1 (highlighted in yellow/orange)) fit into the complex, interconnected, and oftentimes confusing, coagulation and complement pathways.

Our work has highlighted changes to thrombin (F2) and its regulatory partners. In PASC patients, prothrombin protein levels were slightly decreased (LogFC = ~0.3) despite an upward transcript trend, suggesting consumption of F2 into active thrombin. Upstream prothrombinase factors Factor X (F10) and cofactor V (F5) showed moderate and minimal network rewiring respectively, indicating the prothrombin activation mechanism remains engaged. Downstream, fibrinogen chains (FGA, FGG) and the platelet adhesion receptor (GP1b) remained quantitatively stable but displayed altered correlations, consistent with clotting function being retained yet embedded in a different interaction context in PASC. Notably, multiple natural anticoagulants were downregulated or dysregulated: antithrombin (SERPINC1) and protein C (PROC) trended lower at both RNA and protein levels, and heparin cofactor II (SERPIND1) emerged as one of the most rewired proteins in the entire network. SERPIND1's role is to neutralize thrombin on glycosaminoglycan-rich surfaces (e.g. dermatan sulphate on the endothelium), thus applying a negative regulation to coagulation activity. Dysregulation within this breaking pathway could theoretically lead to increased thrombin on healthy surfaces, resulting in abhorrent clot formation, whilst the excessive active thrombin could further activate the complement cascade through C5

and C3 cleavage. C3 and C5 fragments then lead to activation of monocytes, neutrophils, endothelial cells, and platelets, which further activates complement and coagulation pathways as seen in figure 5. PROC should curb this thrombin generation through inactivation of Va, which prevents thrombin activation directly, and through inactivation of VIIIa, which shuts down the amplification/intrinsic pathway of thrombin generation. On the other hand, CFHR5 upregulates complement activity inhibiting factor H, an inhibitor of the alternative complement pathway. C3 fragments also go on to bind to CR2 on B cells, lowering their threshold for activation and increasing antibody production, yet a large number of antibody components also showed significant rewiring.

Indeed, IGLV3-21 was the most rewired/dysregulated node in the PASC network (despite no significant abundance change), switching from a loosely co-expressed immunoglobulin cluster in recovered patients to a negatively correlated hub linked with coagulation regulators. This implies dysregulation, compared to recovered patients, in the B-cell/antibody activity and the thrombin-coagulation axis in PASC. Consistently, we observed that integrin β2 (ITGB2, CD18), a leukocyte adhesion molecule and component of complement receptor 3, became highly rewired in PASC, acquiring new correlations with both complement receptors (CR1, C5AR1/2, CD46) and coagulation/platelet genes (e.g. ITGAM, ITGB3, F5). CD18 is involved in allowing leukocytes to dock onto thrombi or inflamed endothelium. Its new network orientation indicates enhanced crosstalk between leukocyte integrin signalling, complement, and coagulation pathways, potentially facilitating platelet-leukocyte aggregate formation and immune-thrombotic feedback loops unique to PASC when compared to recovered patients. Furthermore, markers of endothelial and matrix integrity reflected ongoing vascular perturbation: fibronectin (FN1), a high-molecular-weight glycoprotein that stabilises fibrin clots, and nidogen-1 (NID1), a basement membrane protein, were modestly downregulated and rewired in PASC.

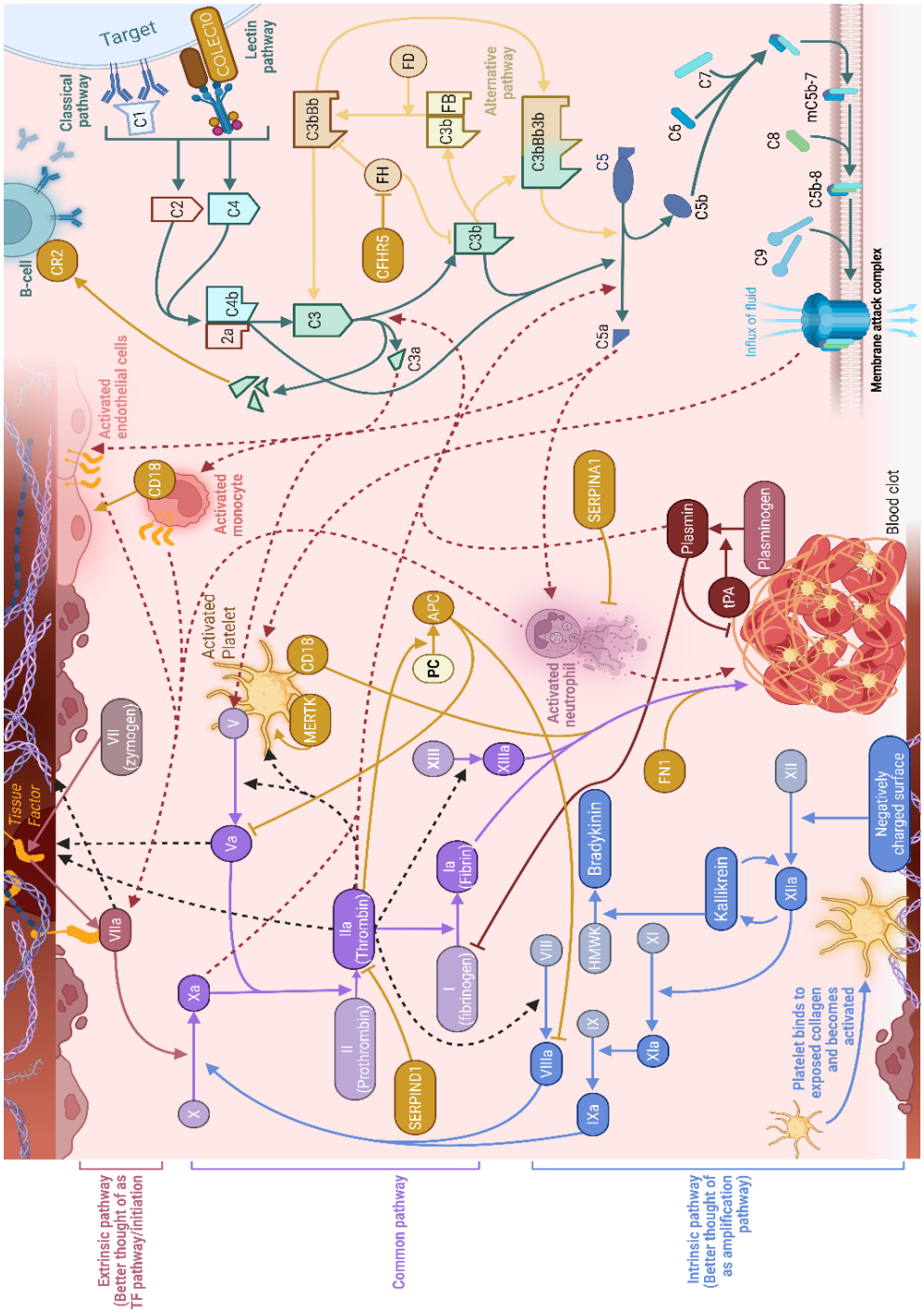

Target
Classical pathway
Lectin pathway
C1
COLEC10
B-cell
CR2
C2
C4
C4b
2a
C3
C3a
C3bBb
FD
FH
CFHR5
C3b
FB
Alternative pathway
C3bBb3b
C5
C5a
C5b
C6
C7
C8
mC5b-7
C5b-8
C9
Influx of fluid
Membrane attack complex
Activated endothelial cells
CD18
Activated monocyte
Activated Platelet
MERTK
APC
PC
Activated neutrophil
SERPINA1
Plasmin
tPA
Plasminogen
Blood clot
Tissue Factor
VII (zymogen)
V
Va
VIIa
X
Xa
II (Prothrombin)
IIa (Thrombin)
SERPIND1
XIII
XIIIa
I (fibrinogen)
Ia (Fibrin)
FN1
VIII
VIIIa
IX
IXa
XI
XIa
HMWK
Bradykinin
Kallikrein
XII
XIIa
Negatively charged surface
Platelet binds to exposed collagen and becomes activated
Extrinsic pathway (Better thought of as TF pathway/initiation
Common pathway
Intrinsic pathway (Better thought of as amplification pathway)

Figure 5: Complement coagulation pathways with interactions and proteins of interest (this figure of the complement and coagulation pathways is adapted from figure 1 of Section I of this thesis which discusses these pathways in full, here, we will only discuss the ways in which the specific proteins of interest (highlights in orange/yellow) interact with these pathways).

APC: When thrombin binds to thrombomodulin on intact endothelium, it activates protein C (APC) which inactivates Va and VIIIa, shutting down thrombin generation. Losing this pathway tilts you towards a procoagulant environment.
SERPIND1. Heparin cofactor II (SERPIND1) inhibits thrombin (IIa). Loss of this inhibition increases thrombin activity.
SERPINA1: α1-antitrypsin (SERPINA1) inhibits neutrophil elastase (released during NETosis), limiting neutrophil-mediated tissue damage.
MerTK: Platelets express TAM (Tyro3, Axl, and Mer) receptors like MerTK. MerTK amplifies platelet activation upon binding with GAS6 (released by endothelial cells and macrophages after stimulation by factors such as thrombin, collagen, etc).
FN1: Plasma fibronectin (FN1) gets crosslinked into fibrin clots by factor XIIIa which improves clot stability, platelet adhesion to the fibrin network, and supports wound repair.
CD18/ITGB2: CD18/Integrin β2 (ITGB2) pairs with α subunits (like ITGAM/CD11b) to form Mac-1, which on activated neutrophils/monocytes binds fibrinogen/fibrin and iC3b (C3b breakdown product),and also binds ICAM-1 on activated endothelium. This lets leukocytes dock onto thrombi and onto inflamed endothelium.
CFHR5: Complement Factor H-Related protein 5 (CFHR5) regulates the complement system by modulating factor H's inhibitory activity against C3b and other binding targets, attenuating its effect on complement activation. Dysregulation here could increase or decrease the amplification step of complement activation.
CR2: Complement receptor 2/CD21 (CR2) on B cells binds C3 breakdown products (C3d/iC3b/C3dg) which lowers the threshold for B cell activation and helps retain immune complexes, feeding antibody production, which then feeds the classical pathway via C1q binding IgG/IgM. Dysregulation here could affect antibody production and classical complement activation.
COLEC10: Collectin-10 (COLEC10), also called collectin liver-1 or CL-L1, is a soluble pattern-recognition lectin in the lectin pathway that forms complexes with MASPs. It binds mainly with mannose, fucose, and galactose. Dysregulation here could result in abhorrent lectin pathway activation.

Created in BioRender. Elens, L. (2025) https://BioRender.com/w1ylbg9

Taken together, these findings suggest that PASC is a state of persistent thrombo-inflammatory disequilibrium: the dysregulated nodes highlighted within our network are linked to humoral immunity, complement pathways, extracellular matrix dynamics, and thrombin-mediated coagulation. This network-level reorganisation aligns with clinical reports of a pro-coagulant, inflammatory milieu in PASC patients and underscores that ongoing endothelial injury with lectin complement engagement and aberrant clotting factor regulation may be a core feature of PASC [16,58,59].

Mechanistically, thrombin's central role in this process warrants detailed consideration. Thrombin is the pivotal effector of coagulation, converting fibrinogen to fibrin and activating platelets, and it also propagates inflammation by signalling through protease-activated receptors on endothelium and immune cells [60]. It acts as the main effector protease of coagulation and, under normal conditions, its thrombin generation is tightly controlled [60]. Classically, thrombin is generated when vascular integrity is disrupted, allowing extravascular tissue factor (TF) to kickstart the coagulation cascade, resulting in the formation of the FXa-FVa prothrombinase complex which greatly accelerates prothrombin cleavage. Such a process is already seen during COVID-19, whereby the cytokine storm upregulates TF expression on endothelial cells and monocytes, while concurrently suppressing anticoagulant pathways (antithrombin, heparin cofactor II, protein C, etc), triggering the coagulation cascade, thrombin and fibrin generation, and perpetuating the coagulopathy observed in severe patients [61].

In COVID-19, this coagulopathy is caused by a mixture of dysregulated immune responses and SARS-CoV-2 direct interaction, and it has been suggested that impaired regulation of complement clearance mechanisms may contribute to autoinflammatory responses involved in the pathogenesis of PASC [62,63]. Converging evidence has shown persistent complement activation in PASC [63–65]. Elevations have been observed in markers of the classical, alternative, and terminal pathways, signs of increased attack complex formation have been observed, and multiple studies have identified large insoluble amyloid microclots in PASC patient plasma [58,63,64,66–69]. These findings are accompanied by biochemical features of haemolysis (low hemopexin, increased heme), consistent with

ongoing endothelial damage and reduced oxygen-carrying capacity [63]. Exposure of endothelial cells to complement fragments, viral antigens, and cytokines upregulates adhesion molecules (ICAM-1, VCAM-1, selectins) and procoagulant factors while downregulating anticoagulant pathways, priming microthrombosis [70].

Clinically, vWF antigen and propeptide are elevated in PASC and inversely correlate with 6-minute walk distance (reflective of functional exercise capacity), while vWF and platelet activation markers normalize in those who recover, underscoring persistent thromboinflammation and microvascular injury in PASC [63,71]. Additional vascular biomarkers—ANG-1, soluble P-selectin, and VE-cadherin—are increased, with soluble P-selectin particularly associated with PASC [72–74]. Two meta-analyses confirm endothelial dysfunction lasting up to a year and tracking with symptom severity [75,76]; mechanistically, endothelial barrier failure, glycocalyx shedding, and phosphatidylserine-rich filopodia formation propagate permeability, inflammation, and thrombosis [77,78]. Beyond lingering vascular damage, residual SARS-CoV-2 fragments may also contribute to PASC coagulation. Insoluble amyloid microclots found in PASC patient plasma may be directly induced by SARS-CoV-2 spike protein, whilst the virus also binds platelets via ACE2/TMPRSS2, driving activation, adhesion, and aggregation [66,79]. The result of such a coagulatory environment in PASC patients is microvascular occlusion leading to tissue hypoxia and organ dysfunction, forming the basis of the most common PASC symptoms such as brain fog, shortness of breath, and fatigue.

Our multi-omic data support this hypothesis and suggest a tilt toward a prothrombotic state in PASC. The link between thrombin and platelet activation may arises through glycoprotein Ib-alpha (GPIbα (GP1BA)), which is capable of binding thrombin to activate platelets at the site of vascular injury [80]. These activated platelets then expose P-selectin (SELP) and a phosphatidylserine-rich surface that supports assembly of classical/lectin and alternative pathway C3 convertases, leading to C3 cleavage and iC3b deposition. Leukocyte CR3 (ITGAM/ITGB2) then binds iC3b, stabilizing platelet–leukocyte aggregates and amplifying thrombo-inflammation. This would support a model in which platelet

activation is linked to complement amplification at leukocyte–platelet–endothelial interfaces.

In essence, our data suggest PASC appears to be characterized by a pathological coupling of coagulation and complement systems, with thrombin appearing to play an integral role in this intersection: endothelial damage and ECM exposure trigger lectin-pathway complement activation, which in turn interfaces with platelets and neutrophils (via integrins and complement receptors) to sustain thrombin generation and fibrin formation. The resulting blockages within the microcirculation then result in decreased blood flow, oxygenation, and impaired exchange of nutrition and cellular waste [81]. This model can help explain the concurrent mild coagulopathy and inflammation observed in convalescent COVID-19 survivors, even when individual coagulation factors or cytokines are only subtly perturbed.

It is noteworthy that these insights only became apparent through an integrative, network-based approach. In our single-omic analyses, very few features reached significance after multiple-testing correction, reflecting the heterogeneity and moderate effect sizes in PASC. Yet, coherent signals emerged at the pathway level: multi-omic gene set enrichment pointed to coagulation and complement dysregulation across data layers (even when no single analyte was decisively altered). Similarly, our genome-wide genetic analyses (GWAS and exome-based SKAT-O) did not identify any genome-wide significant variants predisposing to PASC, likely due to limited sample size and phenotype complexity. Likewise, the top gene-level associations highlighted some candidates such as *ITPR2*, but at nominal significance. Overall, the lack of clear single-gene/protein/metabolite signals reinforces that PASC is driven by multifactorial perturbations in immune–coagulative homeostasis, rather than a single catastrophic molecular change.

Importantly, if these mechanisms are confirmed, this would open the door to targeted interventions. Therapies aiming to rebalance coagulation and complement, for example, low-dose anticoagulation, antiplatelet agents, or complement pathway inhibitors, could be explored to mitigate the chronic coagulation–inflammation feedback cycle in long COVID. Looking at the network in Fig. 4, thrombin has three FDA-approved drugs which

have completed phase 4 clinical trials, of which, two have already been, or suggested to be, employed against COVID-19. DABIGATRAN has already been recommended for use in the context of COVID-19 to reduce the thrombotic complications in AF recovering patients [82]. ARGATROBAN meanwhile has shown success in anticoagulation management of severe COVID-19 undergoing ECMO and has further been suggested to exhibit direct virucidal action against SARS-CoV-2 [59,83,84]. Downstream of this pathway, ANFIBATIDE acts as a platelet GPIbα antagonist, which could potentially block thrombin-mediated GPIbα signalling, preventing aberrant platelet activation; it was previously suggested as a potential therapeutic against the thrombo-cardiovascular disorders associated with acute COVID-19 [85]. Further downstream, PEGCETACOPLAN acts as a direct complement C3 inhibitor and is currently prescribed in the treatment of paroxysmal nocturnal hemoglobinuria, a disease characterised by red blood cell destruction and blood clotting [86]. Finally, upstream targets could include F10 inhibition through RIVAROXABAN, which has already been assessed in an open-label, multicentre, randomized, controlled trial to improve clinical outcomes following discharge after COVID-19 related hospitalisation [87]. Our results suggest not only repurposing these drugs for severe COVID, but also to avoid PASC may warrant investigation.

In summary, our multi-omic study not only reveals a novel interconnected network of coagulation, complement, and matrix-remodelling disturbances in PASC, with thrombin as a focal point, but also provides a roadmap for future research to translate these insights into mechanistic understanding and potential treatments for the millions suffering from long COVID.

References

1. Turner, A. J., Hiscox, J. A. & Hooper, N. M. ACE2: from vasopeptidase to SARS virus receptor. *Trends Pharmacol. Sci.* **25**, 291–294 (2004).
2. Huang, K. *et al.* A retrospective analysis of the epidemiology, clinical manifestations, and imaging characteristics of familial cluster- onset COVID-19. *Ann. Transl. Med.* **8**, 747–747 (2020).
3. Mehta, O. P., Bhandari, P., Raut, A., Kacimi, S. E. O. & Huy, N. T. Coronavirus Disease (COVID-19): Comprehensive Review of Clinical Presentation. *Front. Public Health* **8**, 582932 (2021).
4. Sattar, Y. *et al.* COVID-19 cardiovascular epidemiology, cellular pathogenesis, clinical manifestations and management. *IJC Heart Vasc.* **29**, 100589 (2020).
5. Abdel-Gawad, M. *et al.* Post-COVID-19 Syndrome Clinical Manifestations: A Systematic Review. *Anti-Inflamm. Anti-Allergy Agents Med. Chem.* **21**, 115–120 (2021).
6. Nehme, M. *et al.* The chronification of post-COVID condition associated with neurocognitive symptoms, functional impairment and increased healthcare utilization. *Sci. Rep.* **12**, 14505 (2022).
7. Whitaker, M. *et al.* Persistent COVID-19 symptoms in a community study of 606,434 people in England. *Nat. Commun.* **13**, 1957 (2022).
8. Mirin, A. A. A preliminary estimate of the economic impact of long COVID in the United States. *Fatigue Biomed. Health Behav.* **10**, 190–199 (2022).
9. Voruz, P., Assal, F. & Péron, J. A. The economic burden of the post-COVID-19 condition: Underestimated long-term consequences of neuropsychological deficits. *J. Glob. Health* **13**, 03019 (2023).
10. Venkatesan, P. NICE guideline on long COVID. *Lancet Respir. Med.* **9**, 129 (2021).
11. Soriano, J. B. *et al.* A clinical case definition of post-COVID-19 condition by a Delphi consensus. *Lancet Infect. Dis.* **22**, e102–e107 (2022).
12. Hill, E. L. *et al.* Risk factors associated with post-acute sequelae of SARS-CoV-2: an N3C and NIH RECOVER study. *BMC Public Health* **23**, 2103 (2023).
13. Kenny, G., Townsend, L., Savinelli, S. & Mallon, P. W. G. Long COVID: Clinical characteristics, proposed pathogenesis and potential therapeutic targets. *Front. Mol. Biosci.* **10**, 1157651 (2023).
14. Raj, S. R. *et al.* Long-COVID postural tachycardia syndrome: an American Autonomic Society statement. *Clin. Auton. Res.* **31**, 365–368 (2021).
15. Sherif, Z. A. *et al.* Pathogenic mechanisms of post-acute sequelae of SARS-CoV-2 infection (PASC). *eLife* **12**, e86002 (2023).
16. Mohandas, S. *et al.* Immune mechanisms underlying COVID-19 pathology and post-acute sequelae of SARS-CoV-2 infection (PASC). *eLife* **12**, e86014 (2023).
17. Wang, E. Y. *et al.* Diverse functional autoantibodies in patients with COVID-19. *Nature* **595**, 283–288 (2021).
18. Wu, X. *et al.* Damage to endothelial barriers and its contribution to long COVID. *Angiogenesis* **27**, 5–22 (2024).
19. Chadda, K. R., Blakey, E. E., Huang, C. L.-H. & Jeevaratnam, K. Long COVID-19 and Postural Orthostatic Tachycardia Syndrome- Is Dysautonomia to Be Blamed? *Front. Cardiovasc. Med.* **9**, 860198 (2022).
20. Gold, J. E., Okyay, R. A., Licht, W. E. & Hurley, D. J. Investigation of Long COVID Prevalence and Its Relationship to Epstein-Barr Virus Reactivation. *Pathogens* **10**, 763 (2021).
21. Scherer, P. E., Kirwan, J. P. & Rosen, C. J. Post-acute sequelae of COVID-19: A metabolic perspective. *eLife* **11**, e78200 (2022).
22. Su, Q. *et al.* The gut microbiome associates with phenotypic manifestations of post-acute COVID-19 syndrome. *Cell Host Microbe* **32**, 651-660.e4 (2024).
23. Su, Y. *et al.* Multiple early factors anticipate post-acute COVID-19 sequelae. *Cell* **185**, 881-895.e20 (2022).
24. Thompson, R. C. *et al.* Molecular states during acute COVID-19 reveal distinct etiologies of long-term sequelae. *Nat. Med.* **29**, 236–246 (2023).
25. Wang, K. *et al.* Sequential multi-omics analysis identifies clinical phenotypes and predictive biomarkers for long COVID. *Cell Rep. Med.* **4**, 101254 (2023).
26. Wei, Y. *et al.* Proteomic and metabolomic profiling of plasma uncovers immune responses in patients with Long COVID-19. *Front. Microbiol.* **15**, 1470193 (2024).
27. Saito, S. *et al.* Metabolomic and immune alterations in long COVID patients with chronic fatigue syndrome. *Front. Immunol.* **15**, 1341843 (2024).

28. Yang, H. *et al.* Longitudinal multi-omics analysis of convalescent individuals with respiratory sequelae 6-36 months after COVID-19. *BMC Med.* **23**, 134 (2025).
29. Ward, B. *et al.* HYGIEIA: HYpothesizing the Genesis of Infectious Diseases and Epidemics through an Integrated Systems Biology Approach. *Viruses* **14**, 1373 (2022).
30. Ward, B. *et al.* Deep Plasma Proteomics with Data-Independent Acquisition: Clinical Study Protocol Optimization with a COVID-19 Cohort. *J. Proteome Res.* **23**, 3806–3822 (2024).
31. Demichev, V., Messner, C. B., Vernardis, S. I., Lilley, K. S. & Ralser, M. DIA-NN: neural networks and interference correction enable deep proteome coverage in high throughput. *Nat. Methods* **17**, 41–44 (2020).
32. The UniProt Consortium *et al.* UniProt: the Universal Protein Knowledgebase in 2023. *Nucleic Acids Res.* **51**, D523–D531 (2023).
33. RforMassSpectrometry Package Maintainer, Laurent Gatto, Johannes Rainer, Sebastian Gibb, Adriaan Sticker, Sigurdur Smarason, Thomas Naake. MsCoreUtils. Bioconductor https://doi.org/10.18129/B9.BIOC.MSCOREUTILS.
34. Laurent Gatto, Christophe Vanderaa. QFeatures. Bioconductor https://doi.org/10.18129/B9.BIOC.QFEATURES.
35. Bolger, A. M., Lohse, M. & Usadel, B. Trimmomatic: a flexible trimmer for Illumina sequence data. *Bioinformatics* **30**, 2114–2120 (2014).
36. Kim, D., Langmead, B. & Salzberg, S. L. HISAT: a fast spliced aligner with low memory requirements. *Nat. Methods* **12**, 357–360 (2015).
37. Liao, Y., Smyth, G. K. & Shi, W. featureCounts: an efficient general purpose program for assigning sequence reads to genomic features. *Bioinforma. Oxf. Engl.* **30**, 923–930 (2014).
38. Michael Love, S. A. DESeq2. Bioconductor https://doi.org/10.18129/B9.BIOC.DESEQ2 (2017).
39. Li, H. Aligning sequence reads, clone sequences and assembly contigs with BWA-MEM. Preprint at https://doi.org/10.48550/ARXIV.1303.3997 (2013).
40. Li, H. *et al.* The Sequence Alignment/Map format and SAMtools. *Bioinformatics* **25**, 2078–2079 (2009).
41. DePristo, M. A. *et al.* A framework for variation discovery and genotyping using next-generation DNA sequencing data. *Nat. Genet.* **43**, 491–498 (2011).
42. Plagnol, V. *et al.* A robust model for read count data in exome sequencing experiments and implications for copy number variant calling. *Bioinformatics* **28**, 2747–2754 (2012).
43. Cameron, D. L. *et al.* GRIDSS, PURPLE, LINX: Unscrambling the tumor genome via integrated analysis of structural variation and copy number. Preprint at https://doi.org/10.1101/781013 (2019).
44. Cingolani, P. *et al.* A program for annotating and predicting the effects of single nucleotide polymorphisms, SnpEff: SNPs in the genome of Drosophila melanogaster strain w1118; iso-2; iso-3. *Fly (Austin)* **6**, 80–92 (2012).
45. Helaers, R. & Vikkula, M. Highlander: variant filtering made easy. Preprint at https://doi.org/10.7490/F1000RESEARCH.1116108.1 (2018).
46. Hoffman, G. E. variancePartition. Bioconductor https://doi.org/10.18129/B9.BIOC.VARIANCEPARTITION (2017).
47. Hoffman, G. E. & Schadt, E. E. variancePartition: interpreting drivers of variation in complex gene expression studies. *BMC Bioinformatics* **17**, 483 (2016).
48. Gordon Smyth [Cre, A. limma. Bioconductor https://doi.org/10.18129/B9.BIOC.LIMMA (2017).
49. Sebastian Canzler, Jörg Hackermüller. multiGSEA. Bioconductor https://doi.org/10.18129/B9.BIOC.MULTIGSEA.
50. Wu, M. C. *et al.* Rare-variant association testing for sequencing data with the sequence kernel association test. *Am. J. Hum. Genet.* **89**, 82–93 (2011).
51. McKenzie, A. T., Katsyv, I., Song, W.-M., Wang, M. & Zhang, B. DGCA: A comprehensive R package for Differential Gene Correlation Analysis. *BMC Syst. Biol.* **10**, 106 (2016).
52. Brunk, E. *et al.* Recon3D enables a three-dimensional view of gene variation in human metabolism. *Nat. Biotechnol.* **36**, 272–281 (2018).
53. Kanehisa, M. KEGG: Kyoto Encyclopedia of Genes and Genomes. *Nucleic Acids Res.* **28**, 27–30 (2000).
54. Szklarczyk, D. *et al.* STRING v11: protein-protein association networks with increased coverage, supporting functional discovery in genome-wide experimental datasets. *Nucleic Acids Res.* **47**, D607–D613 (2019).
55. Han, H. *et al.* TRRUST v2: an expanded reference database of human and mouse transcriptional regulatory interactions. *Nucleic Acids Res.* **46**, D380–D386 (2018).

56. Buniello, A. *et al.* Open Targets Platform: facilitating therapeutic hypotheses building in drug discovery. *Nucleic Acids Res.* **53**, D1467–D1475 (2025).
57. Karagkouni, D. *et al.* DIANA-TarBase v8: a decade-long collection of experimentally supported miRNA–gene interactions. *Nucleic Acids Res.* **46**, D239–D245 (2018).
58. Kell, D. B., Laubscher, G. J. & Pretorius, E. A central role for amyloid fibrin microclots in long COVID/PASC: origins and therapeutic implications. *Biochem. J.* **479**, 537–559 (2022).
59. Schiavoni, L. *et al.* Anticoagulation Management for Veno-Venous ECMO in COVID-19 Patients: Argatroban as Rescue Therapy in Heparin-Associated Thrombocytopenia. *J. Clin. Med.* **13**, 6984 (2024).
60. Coughlin, S. R. Thrombin signalling and protease-activated receptors. *Nature* **407**, 258–264 (2000).
61. Subramaniam, S., Kothari, H. & Bosmann, M. Tissue factor in COVID-19-associated coagulopathy. *Thromb. Res.* **220**, 35–47 (2022).
62. Baillie, K. *et al.* Complement dysregulation is a predictive and therapeutically amenable feature of long COVID. Preprint at https://doi.org/10.1101/2023.10.26.23297597 (2023).
63. Cervia-Hasler, C. *et al.* Persistent complement dysregulation with signs of thromboinflammation in active Long Covid. *Science* **383**, eadg7942 (2024).
64. Baillie, K. *et al.* Complement dysregulation is a prevalent and therapeutically amenable feature of long COVID. *Med* **5**, 239-253.e5 (2024).
65. Bayarri-Olmos, R., Bain, W. & Iwasaki, A. The role of complement in long COVID pathogenesis. *JCI Insight* **10**, e194314 (2025).
66. Grobbelaar, L. M. *et al.* SARS-CoV-2 spike protein S1 induces fibrin(ogen) resistant to fibrinolysis: implications for microclot formation in COVID-19. *Biosci. Rep.* **41**, BSR20210611 (2021).
67. Pretorius, E. *et al.* Persistent clotting protein pathology in Long COVID/Post-Acute Sequelae of COVID-19 (PASC) is accompanied by increased levels of antiplasmin. *Cardiovasc. Diabetol.* **20**, 172 (2021).
68. Pretorius, E. *et al.* Prevalence of symptoms, comorbidities, fibrin amyloid microclots and platelet pathology in individuals with Long COVID/Post-Acute Sequelae of COVID-19 (PASC). *Cardiovasc. Diabetol.* **21**, 148 (2022).
69. Kruger, A. *et al.* Proteomics of fibrin amyloid microclots in long COVID/post-acute sequelae of COVID-19 (PASC) shows many entrapped pro-inflammatory molecules that may also contribute to a failed fibrinolytic system. *Cardiovasc. Diabetol.* **21**, 190 (2022).
70. Ahamed, J. & Laurence, J. Long COVID endotheliopathy: hypothesized mechanisms and potential therapeutic approaches. *J. Clin. Invest.* **132**, e161167 (2022).
71. Fogarty, H. *et al.* Persistent endotheliopathy in the pathogenesis of long COVID syndrome. *J. Thromb. Haemost.* **19**, 2546–2553 (2021).
72. Patel, M. A. *et al.* Elevated vascular transformation blood biomarkers in Long-COVID indicate angiogenesis as a key pathophysiological mechanism. *Mol. Med.* **28**, 122 (2022).
73. Espín, E. *et al.* Cellular and molecular biomarkers of long COVID: a scoping review. *eBioMedicine* **91**, 104552 (2023).
74. Di Ciaula, A. *et al.* Neutrophil degranulation, endothelial and metabolic dysfunction in unvaccinated long COVID patients. *Eur. J. Clin. Invest.* **54**, e14155 (2024).
75. Ambrosino, P. *et al.* Clinical assessment of endothelial function in convalescent COVID-19 patients: a meta-analysis with meta-regressions. *Ann. Med.* **54**, 3233–3248 (2022).
76. Theofilis, P. *et al.* Endothelial dysfunction in convalescent COVID-19 patients: Systematic review and meta-analysis. *Arch. Cardiovasc. Dis.* **115**, 675–677 (2022).
77. Wettschureck, N., Strilic, B. & Offermanns, S. Passing the Vascular Barrier: Endothelial Signaling Processes Controlling Extravasation. *Physiol. Rev.* **99**, 1467–1525 (2019).
78. Xu, S., Ilyas, I. & Weng, J. Endothelial dysfunction in COVID-19: an overview of evidence, biomarkers, mechanisms and potential therapies. *Acta Pharmacol. Sin.* **44**, 695–709 (2023).
79. Zhang, S. *et al.* SARS-CoV-2 binds platelet ACE2 to enhance thrombosis in COVID-19. *J. Hematol. Oncol.J Hematol Oncol* **13**, 120 (2020).
80. De Candia, E. Mechanisms of platelet activation by thrombin: A short history. *Thromb. Res.* **129**, 250–256 (2012).
81. Pretorius, E. *et al.* Persistent clotting protein pathology in Long COVID/Post-Acute Sequelae of COVID-19 (PASC) is accompanied by increased levels of antiplasmin. *Cardiovasc. Diabetol.* **20**, 172 (2021).
82. Cerezo-Manchado, J. J. *et al.* Dabigatran in patients with atrial fibrillation after COVID-19 hospitalization: an update of the ANIBAL protocol. *Drugs Context* **11**, 2021-9–4 (2022).

83. Arachchillage, D. J. *et al.* Anticoagulation with argatroban in patients with acute antithrombin deficiency in severe COVID-19. *Br. J. Haematol.* **190**, e286–e288 (2020).
84. El Sobky, S. A. *et al.* Drug repurposing of argatroban, glimepiride and ranolazine shows anti-SARS-CoV-2 activity via diverse mechanisms. *Heliyon* **11**, e41894 (2025).
85. Chérifi, F. & Laraba-Djebari, F. Bioactive Molecules Derived from Snake Venoms with Therapeutic Potential for the Treatment of Thrombo-Cardiovascular Disorders Associated with COVID-19. *Protein J.* **40**, 799–841 (2021).
86. Griffin, M. *et al.* Real-world experience of pegcetacoplan in paroxysmal nocturnal hemoglobinuria. *Am. J. Hematol.* **99**, 816–823 (2024).
87. Ramacciotti, E. *et al.* Rivaroxaban versus no anticoagulation for post-discharge thromboprophylaxis after hospitalisation for COVID-19 (MICHELLE): an open-label, multicentre, randomised, controlled trial. *The Lancet* **399**, 50–59 (2022).

Section VI Overall conclusions and holistic discussion of Long COVID mechanisms

This thesis had two main ambitions. First, **the creation of wet-lab and dry-lab pipelines**, integrated alongside healthcare partnerships (Cliniques universitaires Saint-Luc, and Grand Hôpital de Charleroi) that enable the **multi-omic analysis of rare and complex diseases**. Second, the **exploratory analysis of COVID-19**, and **specifically PASC**, through these pipelines, allowing for a multi-omic analysis of a complex, multi-organ disease with a heterogenous cause and clinical presentation. The combination of clinical characterisation with longitudinal sampling and broad molecular profiling allowed our analysis to follow the biology rather than any single biomarker, turning subtle molecular shifts into clear mechanistic leads.

Taken as a whole, the data seem to converge on a microvascular story. In our cohort of PASC patients, complement, coagulation, platelets, and endothelium appear to remain tightly coupled and dysregulated following acute illness. Importantly, our results promote a pathology **less about dramatic changes** in single proteins and **more about "rewiring" within modules**: coagulation context consistent with heightened thrombin generation/consumption (with prothrombin/F2 sitting in a telling position); adhesion and activation at the platelet–leukocyte–endothelial interface (e.g., P-SEL, ITGB2/ITGAM); and shifts in immunoglobulin architecture that plausibly tune complement and Fc-mediated effector functions. The phenotype this creates is one of low-grade, spatially heterogeneous microthrombosis with endothelial activation; enough to degrade function, often without flagrant abnormalities on routine tests.

How PASC risk is planted during the acute phase of COVID-19

The initial injury matters. Our respiratory shotgun metagenomics, which addressed a key gap in the literature, suggests a hypothesis that upper-airway commensals can buffer lung damage at the critical moment. ***Dolosigranulum pigrum*** **and several** ***Corynebacterium*** **species** were associated with milder courses and **lower subsequent PASC risk**, while antibiotic exposure was associated with both PASC development and with reduced

abundance of these taxa. Although overall diversity shifts were modest, the association structure was quite informative: potentially protective taxa (*D. pigrum* and some *Corynebacterium* species) negatively correlated with pathobionts and positively correlated with host-compatible communities. These potential protective taxa had further been shown to reduces pathogenic bacterial overgrowth, reduce epithelial and endothelial stress through immunomodulation, and help maintain mucosal homeostasis. To hypothesis on our associative data, they seem to suggest that the airway ecosystem shapes the magnitude of the initial hit by modulating interferon/inflammatory tone and limiting secondary injury, and that disruption of this ecosystem, whether by antibiotics or severe inflammation, removes a layer of protection precisely when it is needed during acute COVID-19. While directionality cannot be proven from association alone, the pattern aligns with our broader observational findings that individuals with certain bacterial species during acute disease are less likely to develop PASC.

Parallel evidence from Section I, chapter 3.2.4 and the wider literature reinforces this "seeded in the acute phase" view by showing that persistent symptoms often mirror residual organ damage after severe COVID-19. Mechanistically, SARS-CoV-2 can injure tissues through direct cellular invasion, endothelial inflammation with secondary damage, microthrombosis leading to ischemia–hypoxia, and toxin-like cytokine surges; unsurprisingly, hospitalized and ICU patients can have more than double the risk of PASC, plausibly due to unresolved injury and is exacerbated by ongoing inflammation and endothelial dysfunction. The extent of this organ damage during the initial phase of disease is further explored in the Supplementary information 1, which discusses how SARS-CoV-2 propagates and sustains damage to multiple organ systems including neurological, cardiovascular, gastrointestinal, hepatic, and importantly to our findings, the pulmonary and endothelial systems.

Severe COVID-19 often begins in the lungs as an acute viral pneumonia that often progresses into ARDS with diffuse alveolar damage. The immune response, if not properly dampened, leads to distinctive COVID-19 features versus typical ARDS such as abundant alveolar-capillary microthrombi and pulmonary endothelialitis, with survivors showing

persistent lung damage (fibrotic changes/reduced DLCO) up to six months post infection. Systemically, the endothelium, which is normally a homeostatic, semi-permeable layer regulating coagulation and leukocyte traffic, becomes a central disease target in our hypothetical pathophysiological model. SARS-CoV-2 infects endothelial cells via ACE2, and ACE2 loss skews RAAS toward excess angiotensin II, increasing vasoconstriction and permeability. Clinically, vWF and factor VIII elevations mark diffuse endothelial activation and thrombo-inflammation, while cytokines (IL-6, IL-1β, TNF-α, IFN-γ) upregulate adhesion molecules and disrupt junctions (e.g., VE-cadherin, ZO-1); complement deposition and NETs amplify injury and microthrombosis.

This reaction within the circulatory system can be evidenced within our own data as detailed in Supplementary information 3, figure 2 and 3, whereby the unsupervised clustering and analysis of fused patient multi-omic networks revealed two naturally occurring clusters within the data, one cluster composed of primarily severe COVID-19 patients, and the other primarily of mild/moderate COVID-19 patients. Feature ranking and subsequent multi-omic pathway analysis of these clusters identified enriched pathways in severe COVID-19 patients based around the complement cascade, activity of complement activators, antibody-mediated complement activation, regulation of complement cascade, and formation of fibrin clots (clotting cascade), as among the most significantly enriched pathways.

This framework also explains the long, shallow decline in PASC prevalence over years as organ function slowly recovers. Even in low-risk cohorts without severe disease, 70% showed damage to at least one organ, with one-year follow-up still finding 59% with single-organ injury; for multi-organ injuries, the percentages are 29% and 27% respective.

In this context, these observations argue that the location and magnitude of acute organ damage set the initial conditions for PASC: chronic hypoxia from lung fibrosis, persistent endothelial and inflammatory activation in the microvasculature, and metabolic dysregulation from cardiac, renal, or pancreatic injury create a physiological backdrop in which multisystem symptoms can persist, even while routine labs normalize, gradually abating only as true tissue repair proceeds.

Factors propagating PASC during the convalescent phase of COVID-19

The post-acute phase is where our multi-omic integration is most informative. The significance with which the complement and coagulation systems are first activated during severe COVID-19 disease has already been observed; this is evidenced from our own analysis as well as in the literature. Our further analysis into PASC now suggests both that the complement-coagulation system still appears to be significantly over activated in those patients presenting with symptoms following COVID-19, as well as potential components within this system that are dysregulated within these patients, as compared to recovered individuals. Signals from Section V, as summarised within figure 5 of this section, support four interacting layers.

1. **Complement control on a hair-trigger.** Regulatory nodes (e.g., CFHR5, CR1) were prominently rewired in PASC networks. In conjunction with signs of ongoing complement activation, this re-positioning of the regulatory network may result in favouring ongoing, low-grade activation rather than a clean shutdown, theoretically resulting in residual debris, incomplete clearance, or persistent local triggers.
2. **Thrombin amplification rather than a single "clotting spike."** Network patterns around F2 and anticoagulant trends suggest easier thrombin generation on activated platelets and endothelial surfaces, even if mean factor levels look unremarkable.
3. **A stickier blood–vessel interface.** Rewiring of P-SEL and ITGB2/ITGAM within our PASC networks supports platelet–leukocyte adhesion and surface-bound thrombin generation, providing a physical platform for complement deposition and further activation.
4. **Humoral architecture shifts.** Immunoglobulin modules are strongly dysregulated within PASC networks, however, the way in which this rewiring may promote PASC is yet not fully understood. As discussed in Section I, chapter 3.2.2, immunoglobulin signatures have previously been linked to PASC predictability. Here, it appears this change in their internal balance may plausibly be

involved/implicated in altering complement engagement and downstream inflammatory tone.

In combination, these layers suggest a self-reinforcing loop: endothelial disturbance, thrombin generation, platelet activation and leukocyte adhesion, complement deposition, thrombin amplification, more endothelial stress, etc. Symptoms then follow from microvascular inefficiency, not necessarily from large, organ-level lesions.

A unifying model

It could be proposed that acute organ injury plants the seed for PASC development, and in some individuals the system never fully returns to baseline. Loss or depletion of certain bacterial species within the NP microbiome may worsen the initial damage of the respiratory system in certain individuals, thus increasing their risk of PASC (we provide associations in this thesis between these species and PASC development, but this predisposition to PASC could also involve an overactive immune system that does not return to baseline, a persistent stimulus, or another, yet unknown, dysregulating mechanism). During recovery, due to whichever mechanism, the complement and coagulation systems appear to have sustained activation, and throughout recovery into convalescence, complement–coagulation–platelet–endothelium remain dysregulated, sustaining a low-grade pro-thrombo-inflammatory state. What may keep the loop running, such as lack of sufficient regulation, imperfect healing, antigen persistence, or another latent driver, remains unresolved and is precisely what the next phase of research should test. This is discussed more in depth in Section I, chapter 3.2.

The implication of this proposed model is twofold. **First**, primary prevention seems to reduce PASC and so limiting the initial injury via vaccination and early/enhanced therapeutics in high PASC risk individuals should lower risk by preserving both tissue integrity and airway commensals. **Secondly**, measuring mechanisms, not just molecules, is integral to PASC pathogenesis research. For exploratory work, this means pathways should be investigated ideally in a multi-omic methodology. For interventional work, this means understanding the multi-omic biological pathways involved in order to identify important molecular interactions, predict their responses to appropriate intervention, and test the

response to intervention on the entire pathway. Such composite endpoints better match the biology observed throughout this thesis (subtle, system level changes) and offer higher sensitivity than single markers and single-omic analyses.

Future steps: from exploration to testable hypotheses

Our priority is to substantiate the respiratory microbiome signal because it provides a concrete route from the acute illness to downstream risk. The central hypothesis is that the presence of *Dolosigranulum pigrum* and certain *Corynebacterium* species in the NP microbiome dampens early epithelial and endothelial injury by modulating host interferon and inflammatory tone; by buffering the initial hit, it reduces the probability of later PASC. This hypothesis arises directly from our metagenomic findings: overall diversity shifts were modest, yet differential abundance and co-association structure associated these taxa to milder acute disease and lower PASC risk, while antibiotic exposure was associated with depletion of the same species. Validation should first confirm the correlations between the species observed in the analysis, this can be done most simply in a pairwise spent media analysis to investigate competition for nutrients and reaction to metabolic products, or through cocultures to investigate interactions. Secondly, bacterial response to host cells can be investigated through human lung model systems. Such systems would need to include immune cells such as AMs and challenges from SARS-CoV-2 viruses. The goal of the investigations would initially be to assess if and how *D. pigrum* or *Corynebacterium* modulate the immune response, and next to see if immunomodulatory features can be extracted (i.e. a potentially therapeutic metabolite).

The second line of work tests the complement–coagulation–platelet model that emerged from our integrative multi-omic network. Here the hypothesis is that, in PASC, complement deposition on activated platelets lower the threshold for thrombin generation on perturbed endothelium, increasing microthrombosis despite near-normal single markers. Section V showed convergent rewiring around regulators such as CFHR5 and CR1, activity surrounding F2 consistent with greater consumption and easier thrombin amplification, tighter coupling of P-SEL and ITGB2/ITGAM with complement receptors and coagulation genes, and endothelial activation signatures. Because the disturbance resides

in the wiring (correlations) rather than large abundance shifts, evaluation should focus on functional dynamics and coupled markers (thrombin generation profiles alongside split products of complement and measures of platelet activation) rather than isolated abundance readouts. A number of the proteins involved in the complement cascade exist in activate and inactive states, and so whilst abundance changes can be minimal, ratios of activate to inactive proteins can be drastically different and may explain the dysregulation, function testing is therefore of the upmost priority.

Third, we should investigate whether targeted specific components of the identified pathways can change network interactions in predicted directions. Interventions such as short-course antithrombotic or antiplatelet strategies may blunt thrombin amplification and platelet–endothelium activation, whilst multi-omic patient stratification could predict who benefits. This follows naturally from what is observed in our findings: single markers were noisy, while pathway-level composites were coherent. If these studies move the modules as predicted, they would both strengthen causal inference and provide a practical blueprint for targeted care.

Limitations

The present work is constrained first by its vantage point. **Our measurements are predominantly blood-based**, which biases detection toward circulating processes and inevitably blurs tissue-level phenomena; upper-airway sampling cannot fully represent distal lung biology, and we did not directly profile other likely contributors such as the gut, liver, or brain in their local compartments. This limits our ability to apportion risk between compartments or to say whether a systemic signature reflects truly global activation or the echo of a regional nidus (pulmonary microvasculature being the chief suspect), whose molecular footprint propagates through plasma. The obvious remedy is to add tissue-adjacent sampling where feasible (induced sputum, nasal or bronchial brushings, stool and bile-adjacent surrogates) and to link molecular modules to organ-specific physiological tests so that localization and mechanism can be inferred with greater confidence.

Causality is a second, deeper limitation. Correlation-based networks, even when cross-validated and consistent across omics, cannot reveal whether the complement–

coagulation–platelet coupling we observe is a driver of symptoms or a downstream consequence of another persistent stimulus such as unresolved tissue injury or antigenic debris. The respiratory metagenomics suffers a parallel ambiguity: the depletion of *Dolosigranulum*/*Corynebacterium* may increase susceptibility to severe acute disease and later PASC, or it may simply mark severe disease and aggressive early immunity, which themselves set the stage for persistent dysfunction. Disentangling these directions requires richer longitudinal sampling to establish temporal precedence, targeted perturbations that affect the predicted mechanism, and replication in independent cohorts.

Cohort size and structure also impose limits. Although the study is large by multi-omic standards, power remains limited, particularly for conducting GWAS, and missingness across modalities reduces the strength of integrative inference and may distort network edges. Recruitment was unavoidably shaped by the evolving clinical landscape: widespread vaccination and better therapeutics reduced the pool of severe cases relative to the original target, potentially shifting case-mix. Selection bias toward individuals willing and able to return for follow-up may further constrain generalisability. These issues can be addressed by targeted expansion of recruitment, pre-registration of analysis plans to minimise researcher degrees of freedom, and external validation in geographically and clinically diverse cohorts.

Temporal resolution is another constraint. With two primary timepoints, we cannot establish the ordering of events with the precision needed to claim mechanism; small shifts that define propagation may peak and recede between visits. Denser sampling early after infection and during symptom fluctuation, even in a subset, would allow us to model onset, persistence, and decay, and to distinguish sustained drivers from transient noise. Alongside this, finer alignment of clinical phenotypes with sampling, especially around exertional intolerance and autonomic symptoms, would reduce misclassification and sharpen associations with microvascular modules.

Pre-analytical and analytical factors deserve explicit mention. Even with standard operating procedures, variations in processing time, storage, and freeze–thaw can imprint

subtle structure on omic layers. DIA proteomics carries its own sensitivities, including spectral library composition and alignment across runs; metagenomics in low-biomass airway samples is vulnerable to contamination and requires careful background control. Batch correction, normalization choices, multiple-testing penalties, and network construction parameters can all nudge edge weights and community structure. We mitigated these risks through harmonised pipelines and sensitivity analyses, but the only durable solution is replication across different methodologies, stability testing across alternative pipelines, and, where possible, using functional assays that do not share the same biases.

Proteomic bias in multi-omic analysis. During the multi-omic analysis of Section V, the proteome appears as the driving force in the analysis. Despite integration of transcriptomic and metabolomics, the selection of the complement cascade as the main pathway of interest was primarily due to the overwhelming significance of this pathway at the proteomic layer, and indeed, figure 1 within Section V shows a lack of transcriptomic or metabolomic involvement. Additionally, during multi-omic network analysis, the majority of the top rewired nodes are proteins. Further, no metabolites were found to be significantly rewired due to difficulties in confidently identifying the relevant metabolites in our exploratory study. The takeaway is that our results are heavily influenced by the proteomic layer, rather than equal involvement of all -omic layers. This can be explained partly by the differential abundance/expression results which show proteomic features to the most differential in terms of significance and magnitude, followed by transcripts and metabolites, indicating that dysregulation in PASC (at least when investigating feature abundance/expression) is mainly at the proteomic level. Investigation of other disorders may reveal a more balanced dysregulation. Additionally, future investigations could be aided by first moving forward with other multi-omic analyses to identify the pathways of interest, then conducting targeted metabolomics on metabolites within the proposed pathways, preventing metabolite identification from becoming an issue downstream.

Finally, **heterogeneity and confounding remain inescapable** in real-world cohorts. Vaccination status, prior infections, concurrent medications (notably antibiotics and

anticoagulants), and comorbidities are imperfectly measured and can interact with the very pathways under study. While modelling can adjust for known factors, residual confounding is likely. Future designs should incorporate stratification by these variables from the outset, prospectively record exposures that shape the microbiome and haemostatic systems, and consider adaptive sampling schemes that balance key strata. Together, these steps will allow the next phase of work to overcome the current study's constraints and to convert its strongest signals into decisive tests of mechanism.

Closing note

Science advances not only through new findings but through the infrastructures that make discovery repeatable, rapid, and trustworthy. This thesis set out to do both: to extract insights from a post-infectious condition shrouded in complexity, and to assemble the laboratory and analytical scaffolding that allows such insights to be rapidly generated. The result is more than an investigation into PASC. It is a playbook for how to study complexity when the signal is distributed, subtle, and dynamic; exactly the situation one faces in rare diseases and during the first chaotic months of a new outbreak.

The hypotheses we derive here are deliberately practical. By defining biology as connected and coordinated networks rather than static molecules, we can explore pathways and hypothesis mechanistic targets in a holistic manner: if a pathway is truly causal, perturbing it should move it in a predicted direction. This provide a rapid route from systems data to hypothesis generation, and it is agnostic to the disease at study. The same discipline applies to other heterogeneous syndromes where no single biomarker suffices such as complex or rare disorders that fragment into molecular subtypes. Network-defined endpoints offer sensitivity, interpretability, and a way to match interventions to the biology of the system.

Preparedness benefits directly from this approach. The pipelines built here composed of standardised pre-analytics, deep multi-omic, transparent computation, and modular analysis plans, reduce the time from sample to inference. They are designed to be broadly applicable and to survive context shifts: a new respiratory pathogen, a neurotropic virus, or an unexpected post-infectious phenotype. As pipeline components are modular,

reusable, and adjustable, establishing a new cohort largely becomes a matter of configuration rather than rebuilding pipelines. As network biology is able to leverage complementary information, early proof-of-mechanism studies can be designed with smaller sample sizes. Finally, explicit provenance of data origins and analytical histories enables more direct comparison of results across sites by reducing variability introduced by site-specific analytical workflows. In short, advances in scientific questions are inseparable from advances in the infrastructure that allows those questions to be asked at speed and scale.

Network biology is central to this approach and is used as the primary analytical framework rather than a descriptive addition. Complex disease rarely announces itself through large shifts in single nodes; it hides in the patterning of many modest signals that, together, define the state of a pathway or interface. By prioritising the wiring of the network (who moves with whom, and under what conditions), we gain the ability to detect disease when abundance is quiet, to separate adaptive responses from pathological dysregulation, and to identify candidate points for intervention that may be missed by univariate analyses. As tools mature, moving from multi-omic factor models to robust, cross-batch network inference, the field will continue to move away from lists of differentially expressed features to network-level analyses that are interpretable and suitable for both discovery and mechanistic trials.

To add some poetic flair to this final chapter, a useful analogy is to view single-omic analyses as individual instruments: each can carry a clear signal, but each is also limited in range and context. Multi-omic integration, by contrast, brings these instruments into an ensemble orchestra, where transcriptomic, proteomic, metabolomic, and microbial layers can be interpreted in relation to one another rather than in isolation. In this setting, the role of the investigator is to act as a conductor by imposing structure through study design, defining tempo through quality control, and ensuring that the resulting model remains coherent through ensuring reproducibility and remaining biologically grounded, so that the overall pattern can be heard more clearly than any one component alone.

The value of these analyses is strengthened by the infrastructure that supports them. In this thesis, standard operating procedures, reusable code, and transparent analysis workflows were used to improve consistency in sample handling and computation. Governance and biobanking procedures were aligned with downstream analytical aims to support comparability across cohorts. Lastly, structured metadata facilitates reuse to make it possible to federate evidence rather than hoard it. Together, these practical measures reduce site-specific analytical variability and will make it easier to evaluate whether findings replicate in independent data and settings.

Finally, there is the matter of direction. The picture that emerges from this work, one of a microvascular coupling problem seeded by acute injury and sustained by incomplete resolution, does not claim to be the whole story of PASC. Rather, it proposes a coherent and testable component of the syndrome and specifies hypotheses that can be evaluated in independent cohorts and in targeted mechanistic studies. The lasting contribution is not just a set of results, but a way of working that converts complexity into tractable questions, and questions into experiments whose answers shift practice. When the next complex disease or pandemic arrives, what will matter is not that we once studied PASC, but that we learned how to listen for biology in places where it is quiet, to measure it with tools that generalise, and to turn those measurements into timely decisions.

Appendix

Supplementary information 1: Multi-Organ Involvement of COVID-19

1.1 Pulmonary Pathology and ARDS Development

Severe COVID-19 primarily manifests as an acute viral pneumonia that progresses to ARDS, a potentially life-threatening condition whereby the alveolar damage causes fluid leakage which perturbs gas exchange. Most often, patients also develop diffuse alveolar damage (DAD) during the early stages of ARDS, an acute lung condition in which hyaline membranes (composed of dead cells, surfactant, and proteins) are deposited along the alveolar walls, impeding gas exchange. In autopsy series, the majority of patients (>80%) that succumb to COVID-19 show DAD in mixed phases (exudative, organizing, and fibrotic), and is frequently accompanied by microthrombosis and vascular injury [1–3]. In the acute stage, the lungs typically exhibit oedematous and thickened alveolar septa, intra-alveolar oedema, hyaline membrane formation [4]. This stage is also marked by dense infiltration of immune cells, primarily macrophages and neutrophils, which are responsible for initiating and sustaining the inflammatory response (discussed in more detail in Section I, chapter 2.2). These pathological changes contribute to the severe hypoxemia observed clinically in COVID-19-related ARDS patients. Type II pneumocyte hyperplasia and squamous metaplasia are also evident as the lungs attempt to regenerate and repair the alveolar epithelium [5]. Less frequently, and generally in cases of prolonged illness, an organizing phase follows, characterized by fibroblast proliferation, interstitial expansion, and formation of Masson bodies [6]. Some patients then progress to interstitial fibrosis, particularly those with extended or severe disease, which raises concerns for long-term pulmonary function.

There are notably several distinctive features which set COVID-19 lung pathology apart from typical ARDS. Firstly, the amount of new vessel growth through intussusceptive angiogenesis was 2.7 higher in the lungs of COVID-19 associated ARDS patients as compared to influenza associated ARDS patient lungs [7]. The lungs of COVID-19 patients

also frequently exhibit widespread microvascular thrombosis, with alveolar capillary microthrombi found in the majority of fatal cases, occurring nine times more frequently than in severe influenza [7]. Another hallmark is pulmonary endothelialitis, an inflammation of the capillary endothelium, in which the endothelial cells exhibit disruption of intercellular junctions, cell swelling, and detachment from the basement membrane [8]. Together, endothelialitis and intra-alveolar fibrin deposits generate severe airflow/blood flow (V/Q) mismatch, explaining the early "silent hypoxemia" that progresses to classic ARDS. These vascular injuries promote inflammatory cell infiltration into alveolar septa and contribute to capillary leak and oedema.

As one of the primary points of SARS-CoV-2 infection and replication, viral infection of the respiratory parenchyma is direct and diffuse. Following nasopharyngeal infection, SARS-CoV-2 colonises downwards towards the airway epithelial cells in bronchioles, and bronchiolitis/tracheobronchitis with ciliated cell loss is commonly observed, even in patients not subjected to mechanical ventilation [9]. Ciliated cell loss in COVID-19 impairs mucociliary clearance, allowing mucus, viral particles, and environmental pathogens to accumulate in the airways [10,11]. This weakens epithelial barrier defences and facilitates deeper viral invasion into the distal lung. The destruction of these cells not only prolongs viral presence but also initiates a pro-inflammatory cascade which further damages the airway epithelium and promotes a cycle of inflammation and tissue injury [10,12]. As SARS-CoV-2 migrates deeper in the lungs, AT2 cells represent early infection targets, presenting classic cytopathic changes such as, cell rounding, detachment, and syncytia formation [13]. These cells are critical for proper alveolar function by releasing surfactant. Surfactant is a complex lipoprotein that reduces surface tension at the air-liquid interface to support alveolar structure and the alveolar-capillary barrier [14]. The extensive death of AT2 cells due to SARS-CoV-2 results in loss of surfactant production. The loss of surfactant increases surface tension, promoting alveolar collapse and thus impaired gas exchange. Simultaneously, surfactant loss, alongside infection and inflammation, damages the alveolar-capillary barrier, increasing its permeability. This allows fluid, proteins, and immune cells to leak into the alveolar space, causing alveolar flooding and pulmonary oedema. The barrier dysfunction perpetuates alveolar collapse and gas exchange failure.

In addition, the influx of inflammatory cells, including neutrophils and macrophages, further amplifies tissue injury and cytokine release, leading to DAD, and in some cases, progression to fibrosis [13].

In parallel to direct viral injury, the host immune response as discussed in Section I, chapter 2 drives a large portion of the lung damage. In severe COVID-19 ARDS, alveolar spaces become filled with macrophages and neutrophils that release pro-inflammatory proteases, ROSs, and cytokines. Neutrophils infiltrate the airspaces and may release NETs that promote capillary thrombosis and direct epithelial injury 8 [15–17]. Macrophages meanwhile, can become hyperactivated and exhibit hemophagocytosis, which while classically described in the bone marrow, recent evidence suggests can also be exhibited in hilar lymph nodes and potentially alveolar spaces [18,19]. Whilst this amplifies pulmonary tissue inflammation, oedema, and destruction in conjunction with neutrophil activity, pulmonary hemophagocytic activity may also feed into a systemic HLH-like reaction, worsening multi-organ injury and mortality risk. These combined viral and immune processes culminate in ARDS, marked by diffuse infiltrates, decreased lung compliance, severe hypoxemia, and a need for prolonged mechanical ventilation. Early in the pandemic, some patients exhibited severe hypoxemia despite relatively preserved lung compliance; a presentation labelled “atypical ARDS.” This was hypothesized to result from alveolar shunting, microvascular occlusion, and impaired hypoxic vasoconstriction [7]. As the disease progresses, just under 30% of patients with early atypical ARDS go on to meet the Berlin criteria of typical ARDS within around 3 days, marked by worsening gas exchange and decreased lung compliance [20]. Progression to ARDS increase relevant patient mortality risk by around 60% compared to non-progressing patients [20].

Importantly, the pulmonary pathology extends beyond the lungs themselves. The overactive immune response in the respiratory tract during severe COVID-19 (see Section I, chapter 2.3) leads to high circulating levels of cytokines, which trigger widespread endothelial activation. This response amplifies proinflammatory and procoagulant signalling both locally in the pulmonary vasculature and systemically in distant organs [21,22].

In addition, emboli from distant clots, such as deep veins thromboses, may lodge in pulmonary arteries, compounding gas exchange issues [23]. Many COVID-19 patients also suffer secondary ventilator-associated pneumonia (54% of mechanically ventilated patients) or superinfection (26% of all patients), further complicating pathology [24,25]. Long-terms complications are also seen in survivors of severe COVID-19 ARDS, with up to 60 % showing ground-glass or fibrotic changes with reduced DLCO at 3–6 months [26]. This suggests that the acute diffuse lung injury can evolve into a fibrotic lung disease reminiscent of organizing pneumonia or even fibrotic interstitial lung disease in a subset of patients.

To conclude, COVID-19 provokes destructive pneumonia that unites direct viral cytopathic injury of the alveolar epithelium with an overwhelming immune-mediated damage to the lung's delicate gas-exchange apparatus. The cytokine storm and endothelialitis interweave with this process to produce an ARDS often accompanied by extensive microthrombosis and new vessel growth in the lungs. These unique pathological features (diffuse alveolar damage with microangiopathy and angiogenesis) distinguish COVID-19 from typical ARDS and underlie the severe, refractory respiratory failure seen in critical illness. Understanding this pulmonary pathophysiology has directly informed treatment, for example the use of corticosteroids and anti-cytokine therapies to mitigate inflammatory lung injury (see Section V).

1.2 Endothelial Dysfunction and Endothelialitis

The endothelium is the innermost cellular lining of all blood vessels, composed of a continuous monolayer of endothelial cells. This thin layer forms a semi-permeable barrier between the circulating blood and the surrounding tissues, regulating the exchange of fluids, solutes, and cells. Endothelial cells are connected by intercellular junctions (tight and adherens junctions) that control vascular permeability and maintain blood-tissue barriers such as the BBB and alveolar–capillary barrier. In addition to barrier function, the endothelium plays a pivotal homeostatic role: modulation of vascular tone through release of vasodilators and vasoconstrictors; regulation of blood fluidity and clotting through production of anticoagulant and fibrinolytic factors; and control of leukocyte

trafficking and inflammation [27,28]. By dynamically sensing and responding to hormonal and mechanical signals, the endothelial monolayer acts as an active paracrine, endocrine, and autocrine organ that preserves vascular homeostasis [27]. Notably, evidence identifies widespread endothelial dysfunction as a central mechanism in COVID-19, to the extent that severe COVID-19 is considered as much a vascular disease as a respiratory one [29]. Clinical investigations of severe COVID-19 have reported marked elevations of vWF (released from damaged endothelial cells) and Factor VIII, indicating diffuse endothelial activation and initiating a cascade of thrombosis [30]. Meta-analysis confirmed that elevations in these markers in COVID-19 patients correlate with disease severity and thus endothelial and thrombotic complications are hypothesized to be central drivers of COVID-19 [31].

SARS-CoV-2 can directly infect endothelial cells via ACE2, which is expressed on vascular endothelium in multiple organs (including the lungs, heart, kidneys, and intestines). A highly influential post-mortem study demonstrated viral particles within endothelial cells in diverse organs of COVID-19 patients [29]. Endothelial cells infected by SARS-CoV-2 undergo injury and apoptosis, leading to endothelial inflammation (endothelialitis) and necrosis, indicating that the virus's cytopathic effects can directly compromise the vascular lining [7,29,32]. The initial point of viral entry also has pathogenic sequelae: ACE2 is a key negative regulator of the renin–angiotensin system (degrading angiotensin II (Ang II)). SARS-CoV-2 binding causes ACE2 internalization and loss, tipping the balance toward excess Ang II signalling. Ang II plays a crucial role in regulating blood pressure and fluid balance, able to increase blood pressure through vasoconstriction, and causing the body to retain sodium and water through aldosterone and antidiuretic hormone (ADH) release. It also increases vascular permeability; ACE2 downregulation and resulting RAAS activation lead to leaky pulmonary vessels and neutrophil infiltration, the resulting neutrophil-mediated destruction of alveolar epithelium leads to atypical form of ARDS in COVID-19 [33].

Endothelial damage in COVID-19 is also driven by the host inflammatory response discussed in Section I, chapter 2. Cytokines such as IL-6, IL-1β, and TNF-α, can activate endothelial cells even if they are not infected, leading to the expression of adhesion

molecules like E-selectin, ICAM-1, VCAM-1, and pro-inflammatory mediators [34,35]. Consequently, leukocytes are attracted to, adhere to and transmigrate across the endothelium, contributing to endothelialitis. Adding to this, IFN-γ, TNF-α, and various ILs (1, 2, 4, 6, 8, 10, and 13) also disrupt endothelial junctions, degrading proteins like VE-cadherin, ZO-1, β-catenin and gap junction proteins, causing loss of barrier integrity [36,37]. The result is increased vascular permeability and microvascular leak, permitting plasma proteins and immune cells to flood into tissues. Beyond cytokines, complement activation is strongly implicated as COVID-19 autopsy studies have found deposition of complement complexes (C5b-9 and C4d) on endothelium, with associated microthromboses in the lungs and skin [38,39]. Endothelial damage and complement activation are closely linked and self-reinforcing; the previously mentioned studies evidence that SARS-CoV-2 triggers and perpetuates this cycle. NETs are another contributor, released in large amounts in severe COVID-19, these web-like DNA/protein complexes can directly injure the endothelium and propagate clot formation in small vessels [40]. In summary, SARS-CoV-2 instigates a multifaceted assault on the endothelium: direct viral infection and ACE2-related pathways operate in tandem with indirect mechanisms (cytokine-induced activation, immune cell infiltration, complement and NET-mediated damage) to cause diffuse endotheliopathy in COVID-19.

The widespread endothelial injury and endothelialitis in COVID-19 have dire downstream effects on the microvasculature and organ function. In the heart, injury to coronary micro vessels and endothelial activation can promote myocardial ischemia, microinfarcts, and contribute to the acute cardiac injury seen in COVID-19. In the kidneys, widespread endotheliopathy and microthrombi in glomerular capillaries can precipitate acute kidney injury [41]. Indeed, acute renal dysfunction is relatively common in severe COVID-19 and is thought to stem in part from renal microvascular clotting and inflammation of peritubular capillaries [39,41,42]. Systemic endothelial damage can also lead to a vascular leakage syndrome, aggravating shock and organ oedema [43–45]. A Nature Reviews analysis noted that in severe cases, massive endothelial dysfunction, widespread coagulopathy, and complement-induced thrombosis can converge into life-threatening complications and ultimately multi-organ failure in COVID-19 [46]. In summary, SARS-CoV-2 infection of the

endothelium and the ensuing endothelialitis set off a chain reaction of microvascular injury and thrombosis throughout the body. This endothelial pathology is a key link between the viral infection and COVID-19's most severe outcomes – from pulmonary failure to thromboembolic events – underscoring the endothelium's central role in the disease's pathogenesis.

1.3 Neurological Implications

Available data indicates COVID-19 is associated with numerous CNS and peripheral nervous system (PNS) complications. For the CNS, encephalopathy and neurodegenerative diseases are the most commonly reported symptoms, whilst olfactory deficits and skeletal muscle symptoms are the most commonly reported PNS symptoms [47]. Other patients may also experience stroke, delirium, brain fog, myasthenia gravis, and/or Guillain-Barré syndrome (GBS), among other complications. It is estimated that around 82% of hospitalized patients experience neurological complications, with a higher incidence among patients with severe disease than with mild disease [48]. The BBB and blood-cerebrospinal fluid (CSF) barrier are structured to prevent pathogen invasion into the brain, but are not totally impermeable, as evidenced by the presence of SARS-CoV-2 in the CSF fluid and brain tissue of deceased COVID-19 patients [49]. SARS-CoV-2 likely accesses the CNS through multiple, not mutually exclusive, pathways. The most direct route of entry for SARS-CoV-2 is via the hematogenous route, whereby viral sepsis is followed by BBB traversal. Mechanisms include: using "Trojan horses", where viral particles hitchhike across the BBB using lipoproteins or exosomes; direct infection of BBB cells like endothelial cells and astrocytes, which express high levels of ACE2; or the exploitation of "holes in the wall", circumventricular organ regions which lack a complete BBB and are rich in ACE2 [50–55].

Another notable mechanism, neuronal retrograde transmission along the olfactory system, appears particularly interesting due to its potential involvement in anosmia. This entry route, through olfactory nerves traversing the cribriform plate, is supported by the presence of viral RNA and proteins detected in olfactory mucosa, bulbs, and connected cortical regions [56]. Although olfactory sensory neurons themselves lack significant ACE2

and TMPRSS2 expression, the primary cellular entry receptors for SARS-CoV-2, the virus efficiently infects sustentacular and perivascular supporting cells that richly express these entry factors [57]. Infection of these supporting cells results in a few compounding issues. First, the excessive loss (80-90%) of support cells are believed to energetically starve the neuronal cilia, and thus impede their signalling abilities, due to a lack of mitochondria within sensory cilia [58]. Secondly, viral infection results in myeloid cell infiltration and inflammation of the olfactory epithelium, followed by the deciliation and disruption of epithelium integrity [59]. Thirdly, infection and dysfunction of these olfactory epithelial supporting cells leads to 3D changes in the chromatin structure of adjacent sensory neurons, disrupting long-range enhancer-promoter interactions and thus inhibiting expression of odorant receptor-related genes [60,61]. Clinically, these molecular events culminate in observed transient anosmia, as neuronal cells are disrupted but not infected/damaged, allowing for restoration of cell function over weeks as supporting cells are restored. Intriguingly, dysfunction of the olfactory transduction pathway itself, resulting in the loss-of-smell phenotype, correlates paradoxically with -faster disease recovery [62,63]. This observation may reflect an ultra-rapid antiviral response intrinsic to olfactory receptor neurons [64]. This mechanism might partly explain why elderly individuals exhibit increased COVID-19 severity, as they typically have fewer olfactory neurons, potentially delaying their antiviral response.

Once SARS-CoV-2 breaches the nervous system, the bulk of evidence suggests that widespread, productive neuronal infection and tans-synaptic spread are rare, particularly in immunocompetent humans [65–68]. It has been observed that SARS-CoV-2 may infect certain supporting cells, as evidenced from autopsy studies detecting viral RNA and/or protein in astrocytes, pericytes, and choroid-plexus cells in a subset of brains [69,70]. However, this occurs far less frequently than the massive infection of sustentacular or perivascular cells in the olfactory epithelium. The overall CNS infection burden appears to be low, sporadic, and typically subclinical [71,72]. The neurological complications described above, ranging from encephalopathy and delirium to stroke and neurodegenerative issues, are likely to arise predominantly from indirect mechanisms such as the systemic cytokine storms, endothelial injury, micro-thrombi, and hypoxia. Direct cytopathic damage

within the CNS is extremely rare, and while infection of supporting cells may contribute to neuronal dysfunction, it likely represents a secondary and comparatively infrequent insult.

Endothelial injury is a critical pathway contributing to neurological sequelae. COVID-19 associated endothelial damage (discussed in Supplementary information 1.2) leads to a leaky BBB, allowing entry of inflammatory mediators into the brain parenchyma. The infiltrating viral particles, or more commonly, high systemic levels of cytokines and complement, activate astrocytes and microglial, leading to the further additional proinflammatory cytokine production and contributing to brain damage [73,74]. Activated astrocytes produced CXCL10, CCL1, and CXCL13 chemokines, which have roles in the migration of leukocytes into CNS tissues, further activating microglia, and also promoting pro-inflammatory and neuron modulating factors (IL-6, BDNF) [75–77]. Activation of microglia leads to NLRP3-inflammasome activation, resulting in the release of potent pro-inflammatory cytokines IL-1β and IL-18, which work together to increases BBB permeability, recruit leukocytes, induce the encephalitogenic phenotype of Th17 cells, and generally perpetuate inflammation [78–80]. Specifically, amoeboid CD68-positive (activated and phagocytic) microglial were significantly enriched in the brainstem and hippocampus of SARS-CoV-2-infected patients with delirium, hinting that COVID-19 encephalopathic syndrome appears to be a specific topographical phenomenon [81].

In addition to cytokine-associated damage, endothelial dysfunction by itself can result in cerebral injury via nitric oxide synthase depletion and a subsequent deficiency of nitric oxide (NO) through various pathways [82]. NO is a potent vasodilator, inhibiting platelet and leukocyte adhesion. In addition, direct SARS-CoV-2-ACE2 binding on endothelial cells can lead to a reduction of ACE2 on the cell surface, resulting in accumulation of Ang II. Ang II is a powerful vasoconstrictor and its accumulation can lead to increased fluid retention, hypertension, blood coagulation [83]. The reduction of NO and the accumulation of Ang II, taken together, greatly contribute to the hypercoagulation state observed in COVID-19, and in conjunction with the cytokine CNS effect, significantly increase the risk of thrombosis and stroke. Other contributing factors towards this risk include the significant increase in neutrophil-to-lymphocyte ratios observed in COVID-19 patients who

experienced ischemic stroke [84,85]. The neutrophilia observed in these patients can result in the overproduction of NETs, which are known to increase thrombi formation [85].

In parallel to these endothelial and cerebral implications, ARDS hypoxia can occur as a consequence of respiratory implications, which can have deleterious effects on the brain, including oedema, congestion, and neuronal degeneration [86,87].

Autopsy studies provide an in-depth picture of severe COVID-19 associated brain injury. The most commonly reported findings include microglial activation (35.6%), perivascular infiltrates (34.2%), arteriosclerosis (29.5%), global hypoxic-ischemic injury (28.1%), diffuse brain oedema (17.1%), recent microscopic cortical infarcts (16.4%), and acute microscopic/punctate haemorrhages (10.3%) [88]. These findings corroborate the mechanisms discussed above and depict a brain exposed to vascular insufficiency (arteriosclerosis, microinfarcts), inflammatory injury (microglial activation, perivascular infiltrates), global metabolic crisis (hypoxic-ischemic damage, oedema) and microvascular fragility (microbleeds). The combined effect is widespread neuronal network disintegration and loss of cognitive reserve, encephalopathy and stroke are common outcomes.

Cardiovascular disease occurs in approximately 1.4% of COVID-19 patients, representing a 7.6-fold increased risk compared to influenza patients [89]. The most common manifestation of this cardiovascular involvement was acute ischemic stroke (87.4%), while intracerebral haemorrhage was less common (11.6%) [89]. The suspected cause of these strokes relates generally to the COVID-19 linked endothelial damage and hypercoagulation state as discussed. Endothelial dysfunction leads to elevated vasoconstriction, increased BBB permeability, and increased blood pressure; the hyperinflammatory and hypercoagulation state promotes atherosclerosis, plaque rupture, thrombosis, and venous thromboembolism; all these factors come together to greatly increase the possibility of stroke. Notably, COVID-19 related strokes, when compared to non-COVID-19 strokes, affected patients who were on average six years younger, presented with a higher stroke severity (NIH stroke scale (NIHSS) 15 vs 10), had a higher frequency of large vessel occlusion (OR = 2.73), and were more likely to lead to fatal outcomes (OR = 5.21) [89].

Beyond focal events like stroke, diffuse encephalopathy or delirium is common. Meta-analysis found that delirium has been reported to present in 24.3% of COVID-19 patients on average, with this figure rising dramatically to 84.3% in certain ICU patient cohorts [90,91]. One meta-analysis placed the incidence of encephalopathy at 0.215% of all COVID-19 patients [92], while another reported a figure of 23.5% [93]. Among patients who underwent neuro-imaging, 13% were found to have encephalopathy [94]. It is important to note that encephalopathy refers to the underlying brain dysfunction or damage, whilst delirium is the clinical manifestation of encephalopathy; delirium usually implies an underlying acute encephalopathy, and the two diagnoses are often used interchangeably. The differences in prevalence between delirium and encephalopathy metanalyses may be due to COVID-19 encephalopathy being overlooked and simply diagnosed as delirium. Regardless, these symptoms are likely a multifactorial response to systemic inflammation, hypoxemia, or metabolic imbalances, and as previously mentioned, autopsy studies of COVID-19 brains show results indicative of widespread these processes.

There is also growing concern that SARS-CoV-2 infection may exacerbate or even trigger neurodegenerative-like processes. In a Parkinson's disease model, inflammasome activation induces caspase-1 cleavage of α-synuclein, generating a truncated protein highly prone to aggregation and able to provoke neuronal cell death [95]. Furthermore, in the context of West Nile virus infection, activated microglia, dependent on complement activation, mediate presynaptic terminal loss in the hippocampi, a potential mechanism of virus-mediated spatial memory impairment [96]. Similar processes could occur in COVID-19 pathogenesis. Memory impairment has commonly been observed in COVID-19, with an increasing deficient as disease severity increases [97]. The previously described mechanism may be responsible for this association, with increased memory impairment due to increased cytokine-mediated activation of microglial cells, in conjunction with hyperinflammatory coagulation state.

Focusing on COVID-19 again, growing evidence suggests that COVID-19 may increase the risk of AD, and autopsy studies have found that post-COVID brains can show Alzheimer-like changes [98]. It has been suggested that NLRP3 inflammasome activation could lead to

downstream tau aggregation and neurodegeneration [99]. Supporting these concerns, elevated levels of amyloid beta peptide (Aβ), neurofilament light chain, neurogranin, glial fibrillary acidic protein, and tau were reported in CSF from patients 1–3 months after recovery from COVID-19, showing correlation with neurological symptoms [100,101]. These markers are all associated with dementia and neurodegeneration and suggest increased amyloid plaque deposition, synaptic stress, tauopathy, neuronal degeneration, and neuro-inflammation.

Other specific neurologic syndromes have also been associated with COVID-19. GBS, an immune-mediated demyelinating polyneuropathy, and skeletal-muscle injury represent the most robustly documented peripheral neurological sequelae of acute COVID-19 [102]. GBS typically emerges two to three weeks after COVID-19 onset, as patients develop generalized limb weakness and areflexia. Generally, GBS development in the context of COVID-19 is attributed to the systemic cytokine storm. More specifically, autoimmunity has been hypothesized as a mechanism; however, anti-ganglioside antibodies were only identified in around 1.5% of GBS COVID-19 patients, compared to around 60% of non-COVID-19 GBS cases [102,103]. This significant difference in autoantibody prevalence suggests that other mechanisms of action are likely present in COVID-19 induced GBS, such as inflammatory mediated motor neuropathy seen in autonomic imbalances of PASC (as will be discussed in Section I, chapter 3.2.4).

1.4 Cardiovascular Implications

SARS-CoV-2 infection profoundly affects the cardiovascular system. It was quickly discovered that many COVID-19 patients had elevated troponin levels, ranging from 4.8% in patients with mild disease to 54% in patients with critical disease [104]. Elevations in troponin levels usually indicate myocardial injury and is associated with markedly higher mortality. Mortality is around 60% in patients with troponin >10 times the upper normal limit compared to 9%-23% among patients within the normal limit, however, even mild increases above this normal limit are associated with worsening outcomes [105–107]. Importantly, increased mortality in COVID-19 is primarily associated with new myocardial injury acquired during infection, as patients without prior cardiovascular disease but with

myocardial injury had worse outcomes than those with pre-existing cardiac conditions but no injury [105,108]

The mechanisms by which this myocardial injury arises are multifactorial. Initially, it was suspected that direct viral injury was the culprit due to ACE2 expression on cardiomyocytes. Supporting this, early autopsy studies of COVID-19 patients revealed viral RNA and particles within cardiomyocytes and other cardiac cells alongside myocarditis, inflammation of the heart muscle [109–111]. *In vitro* studies followed, identifying that host gene expression of infected cardiomyocytes shifts towards glycolytic metabolism and down-regulation of contractile and sarcomeric proteins [112]. However, this mode of direct viral damage was updated in subsequent studies which identified pericytes, supporting cells within the cardio vasculature, to be the primary targets of infection within the heart [113]. Direct invasion of vascular cells reduces ACE2, leading to excessive build-up of Ang II and dysregulation of the RAAS pathway, as in other tissues and organs, which may lead to apoptosis within the heart [83,114]. As previously mentioned, this imbalance promotes vasoconstriction, oxidative stress, and inflammatory cell recruitment in the vasculature. The end result is impairment of both their electrophysiological and contractile function alongside widespread inflammation and cell death. Moreover, exposure to SARS-CoV-2 spike protein (due to local infection or released into the bloodstream from a leaking pulmonary epithelial-endothelial barrier) can bind to CD147 on cardiac pericyte, initiating signalling that alters its function, impacting endothelial cell support and promoting inflammation and endothelial cell death, which might underlie acute myocarditis [115].

However, a growing body of evidence suggests that while direct viral infection of cardiac cells can occur, it tends to be focal. Unlike viruses such as Coxsackie B, which are known to cause fulminant myocarditis, this severe form of heart muscle inflammation is an uncommon presentation in COVID-19, with reported cases being exceptional [116]. Instead, the profound cardiovascular impact of SARS-CoV-2 infection appears to be largely driven by indirect mechanisms, particularly endothelial damage, widespread systemic inflammation, and hypoxia. As understanding evolved, it was increasingly speculated that

for many patients, troponin elevations and myocardial injury are secondary to these systemic effects, rather than solely direct viral invasion of cardiac tissue [105].

The systemic effects of SARS-CoV-2, including the cytokine storm, hypoxic stress stemming from pulmonary damage, and a pronounced state of hypercoagulation, are significant contributors to cardiac damage [117]. Myocardial injury during systemic inflammatory responses and cytokine storms is a well-documented phenomenon, notably in conditions like sepsis [118]. In COVID-19, this aggressive inflammatory response, characterized by surges in IL-6 and other cytokines, can induce myocardial depression and trigger apoptosis of cardiomyocytes [116]. These cytokines have direct and indirect toxic effects on the heart. They can accelerate atherogenesis, destabilize atherosclerotic plaques, activate platelets and endothelium, and promote further coronary vasoconstriction [118,119]. Further to this, during severe COVID, systemically high cytokines in conjunction with systemic hypoxia, stimulates excessive catecholamine (adrenaline, dopamine, etc) release from the sympathetic nervous system, the “fight or flight” response. Excessive catecholamine signalling can inflict cardiovascular harm through several mechanisms. Increased myocardial oxygen demand due to heightened heart rate and contractility, frequently in a setting of already compromised oxygen supply, can starve the heart of oxygen and increase cellular stress [120]. Next, sustained high levels of catecholamines can exert direct toxic effects on cardiomyocytes, inducing injury and necrosis via pathways such as Ca2+ overload and oxidative stress, promoting necrosis, inflammation, and subsequent fibrosis [121]. This hyperadrenergic state can also alter cardiomyocyte ion channel function and electrical stability, modulating contractile efficiency. Additionally, catecholamines can contribute to microvascular dysfunction and exacerbate endothelial injury, further impairing cardiac perfusion and function, which are processes linked to acute cardiac events [122]. These mechanisms all work together to cause acute coronary syndromes by inducing local inflammation in coronary arteries. The systemic inflammation in cardiac cells can lead to a breakdown of myocardial cellular structure due to necrosis and/or apoptosis. Holistically throughout the body, this process contributes to the release of complement components into circulation, alongside a rise in inflammatory markers such as CRP and ferritin, which are associated with poorer outcomes [104].

Autopsy studies have provided further insight into these mechanisms. Cardiomyocyte necrosis, predominantly in the left ventricle, was found in 35% of COVID-19 patients [123]. The most common cause of this necrosis however was not myocarditis, but was instead microthrombi, presenting in 64% of hearts that exhibited such damage. In addition, there was no significant difference of viral RNA within cardiac tissues between individuals with or without myocardial necrosis, further evidencing that direct viral infection plays a relatively non-significant role in cardiac injury. Crucially, this systemic inflammation in SARS-CoV-2 infection is frequently associated with significant endothelial dysfunction and coagulation. Briefly, endothelial activation causes the release of pro-thrombotic factors which enhance platelet adhesion and aggregation, promoting an environment ripe for microthrombosis within the cardiac microcirculation and other organs. Corroborating these findings, a large multi-national study of over 16 thousand hospitalised patients and autopsy meta analyses of almost 300 post-mortem examinations put the prevalence of myocarditis at between 0.2% and 1.4%, respective [124,125]. Additionally, while biochemical evidence of myocardial injury (elevated troponin) is common, clinical features of myocarditis, including specific electrocardiographic and echocardiographic abnormalities, are relatively rare [104,126].

Rather, thromboembolic effects were more commonly observed, with 3.5% of hospitalised patients presenting with pulmonary embolism and 0.7% presenting with venous thrombosis [125]. These complications were all higher in patients who died during admission. In autopsy investigations, acute cardiovascular histopathologic findings, such as macro or microvascular thrombi, inflammation, or intraluminal megakaryocytes, were present in nearly half (47.8%) of autopsies [124]. Investigations of these cardiac microthrombi found that they were unusually rich in fibrin and terminal complement, suggesting they formed *in situ* as a result of severe inflammation rather than the rupture of classic atherosclerotic plaques [123]. Taken together, the evidence suggests that cardiac injury is a result of the hypercoagulable environment induced indirectly due to SARS-CoV-2 infection.

Early meta-analysis found that the most common cardiovascular manifestations of these systems are acute cardiac injury (21%), cardiac insufficiency (17.4%), and arrhythmias

(10.4%) [127]. Later large-scale cohorts and meta-analyses showed a reduction in some of the most serious complications: myocardial infarction (0.6%), *de novo* heart failure (1.2%), cardiac insufficiency (6.8%-14%), arrhythmias (9.3%-18%) [104,125,128,129]. This is likely due to improvements in patient care along with cohort difference such as vaccination status. However rates of thrombotic complications was still relatively high in these cohorts, ranging from 7.4% to 16.5% mean incidence [104,130]. Comparisons to other pneumonias or influenza found rates of embolism/thrombosis are two to three times higher in COVID-19, indicating unique prothrombotic tendencies of SARS-CoV-2 infection [131].

Arrhythmias are a common manifestation and are likely precipitated by the systemic immunoinflammatory response. The most common type was atrial tachycardia (81.8%), whilst ventricular tachycardia and bradyarrhythmia presented relatively less commonly at 20.7% and 22.6% respective [128]. Generally patient presenting with arrhythmia were had worse outcomes, with 43% of arrhythmia-developing patients having mechanical ventilation and 49% having fatal outcomes. Atrioventricular block, whereby electrical signals between the upper and lower chambers are disturbed, may account for up to 12% of arrhythmias seen in patients with COVID-19 [132]. Pro-inflammatory cytokines can directly disrupt the electrical stability of cardiomyocytes and have been shown to prolong cardiac action potentials and QT intervals, predisposing individuals to ventricular arrhythmias [133,134]. These cytokines can also induce delayed afterdepolarizations (DAds), increasing the potential for premature heart contractions and subsequent atrial arrhythmias [135]. Especially in severe disease, hypoxemia, electrolyte disturbances, and excessive catecholamine release collectively drive tachycardia and augment cardiac workload. Concurrently, these conditions impair ATP generation, fostering a “perfect storm” highly conducive to arrhythmogenesis.

The profound hypoxemia and metabolic stress that frequently observed in severe COVID-19, also play a crucial role in precipitating other forms of myocardial injury, including stress-induced cardiomyopathies. One such condition is Takotsubo cardiomyopathy (TCM), colloquially known as “broken heart syndrome”, a transient state characterized by distinctive left ventricular apical ballooning [136]. The development of TCM in COVID-19 is

often attributed to a significant supply-demand mismatch at the myocardial level, where systemic inflammation increases metabolic demand and can reduce cardiac perfusion [120]. Hypoxemia from severe pneumonia or ARDS exacerbate this imbalance, alongside high fever and tachycardia, augmenting cardiac workload while oxygen delivery is compromised. Superimposed on this metabolically stressed environment, the pronounced catecholamine surge is thought to further induce microvascular injury and directly trigger TCM [122]. Such conditions can lead to TCM, particularly in susceptible individuals, and notably, reports have emerged of this stress-induced cardiomyopathy developing in COVID-19 patients without pre-existing coronary disease [137]. Although TCM is considered a relatively rare complication of COVID-19, it carries a substantial risk, with a meta-analysis reporting a mortality rate of 36.3% among affected patients, a figure that underscores its potential severity even in vaccinated populations [137].

1.5 Gastrointestinal and Hepatic Effects

Whilst SARS-CoV-2 is primarily a respiratory pathogen, the GI tract is a significant site for viral activity. The viral entry receptor, ACE2, is expressed within the GI tract to an even higher degree than the pulmonary system, particularly in the stratified epithelial cells of the upper oesophagus and the enterocytes of the ileum and colon [138]. This is substantiated by the detection of SARS-CoV-2 in endoscopic biopsy specimens from GI tissues of some severely ill patients [139]. Further to this, a meta-analysis of 4,805 patients found that 41% had detectable viral RNA in faecal samples and some laboratories have reported isolating live virus from similar samples [140–142]. Together, these findings support the GI tract as a target for viral infection and replication, and open up the possibility of faecal-oral transmission routes alongside respiratory droplet transmission.

Clinically, GI symptoms are a frequent feature of COVID-19, occurring in between 12% and 61% of patients, and at a rate almost twice as high as other similarly severe diseases [140,143–146]. The most consistently reported symptoms include loss of appetite (up to 35%), diarrhoea (up to 34%), nausea (up to 27%), vomiting (up to 16%), and abdominal pain (up to 11%) [140,144–146]. Additionally, GI symptoms are associated with a three-fold higher incidence of acute renal insufficiency (9.3% vs. 3.1%) [147].

Hepatic involvement is notably significant in severe COVID-19 cases, with incidences of liver injury ranging from 58% to 78% among fatal outcomes [148–151]. These liver injuries may results from COVID-19 systemic effects, GI dysfunction, or perhaps even direct viral invasion, as both liver cells and bile duct cells express ACE2 [152]. This is supported by autopsy studies which detected SARS-CoV-2 in 68% of biopsy samples [153]. In-depth proteomic assessments found enriched signatures consistent with profibrotic pathways, immune activation, and dysregulated fatty acid oxidation and oxidative phosphorylation [154]. However, in the same analysis, there was little evidence of active viral replication, and these signatures were instead associated with the presence of multi-organ dysfunction, hepatic steatosis and coagulative hepatocyte necrosis. Additional autopsies revealed the majority of COVID-19 patients with hepatic involvement present with widespread vascular abnormalities such as hepatic vascular thrombosis, micro and macro vesicular steatosis, and portal inflammation and fibrosis [153,155,156]. These findings indicate that liver injury sustained during COVID-19 likely results from systemic thrombotic implications rather than direct SARS-CoV-2-mediated damage.

Other mechanisms of injury are revealed by abnormal liver biomarkers, which are frequently observed, with 14% to 53% of patients exhibiting elevated alanine aminotransferase and aspartate aminotransferase (ALT and AST), enzymes in hepatocytes which leak into the blood during liver damage or inflammation [157]. Generally, viral hepatitis manifests with ALT predominance, indicating a more specific liver origin as it is more concentrated within liver cells. However, hepatocellular injury in COVID-19 patients appears to be AST predominant; this enzymes is more broadly found in various tissues like the heart, skeletal muscle, and the brain, indicating more systemic issues [158]. The mechanisms of AST-predominance could relate to COVID-19-related mitochondrial dysfunction, SARS-CoV-2-induced hepatic steatosis, or decreased blood flow to the liver. Decreased blood flow to and within the liver logically follows the thrombotic complications observed within liver biopsies discussed previously. Further supporting COVID-19 induced systemic thrombosis/hypoxia as the cause, AST elevations have previously been reported with other viral pneumonias where levels increased in parallel with diminishing peripheral oxygen saturations [159]. Hypoxia leads to the production of

ROS, which combined with lipid peroxidation products, induce redox-sensitive transcription factors and release various liver-damaging pro-inflammatory factors which exaggerate the ischemia of hepatocytes, influence the excretion of toxic metabolites and eventually stimulate liver injury [160].

Drug-induced liver damage in severe patients is also another important mechanism to not overlook and likely works in parallel to the hypoxia these same patients also greatly exhibit. Antibiotics, antivirals, and steroids, widely used for the treatment of COVID-19, are all potential causes of liver injury through various mechanisms (direct toxicity, homeostatic disruption, etc). The prescription of lopinavir–ritonavir, an inhibitor of the SARS-CoV main protease, early on in the COVID-19 pandemic was associated with an increased signal for drug-induced liver injury [161]. The mechanism of this injury is likely due to its metabolism by the cytochrome P450 (CYP) system in the liver. There have also been associations between tocilizumab or remdesivir and liver damage in COVID-19 patients [162,163].

Liver diseases can disrupt the gut-liver axis by altering immune responses, bile acid secretion and composition, and gut barrier integrity, leading to the overgrowth of harmful bacteria and a reduction in beneficial taxa [164].

Shotgun metagenomic analysis of hospitalized COVID-19 patients revealed substantial dysbiosis, marked by a depletion of beneficial commensals such as *Faecalibacterium prausnitzii*, a known anti-inflammatory bacterium, and an enrichment of opportunistic pathogens including *Coprobacillus*, *Clostridium ramosum*, and *Clostridium hathewayi* [165]. Notably, these microbial alterations persisted even after recovery from SARS-CoV-2 infection, indicating long-term disruption of gut homeostasis (discussed in Section I, chapter 3.2.1). Further analysis has shown an increased abundance and expression of virulence factors and antimicrobial resistance genes in COVID-19 gut microbiomes [166]. Beyond bacteria, gut fungal populations were also disrupted, with increased proportions of opportunistic fungal pathogens such as *Candida albicans*, *Candida auris*, and *Aspergillus flavus* reported in faecal samples [165]. The gut virome has also been implicated and showed distinct alterations in COVID-19 patients, compared to non-COVID controls. These

alterations also persisted after disease resolution, with functional shifts indicating increased stress and inflammatory responses, including upregulation of virulence-associated gene functions such as arginine repressor and hemolysin channel protein [167]. The gut virome plays an important immunomodulatory role, with animal viruses influencing intestinal and systemic immunity [168]. CrAss-like and microviridae bacteriophages are the most stable colonizers of the human gut and are highly connected to bacterial taxa such as *Bacteroides*, *Prevotella*, and *Faecalibacterium*, implicating the bacterial microbiome as an intermediary through which COVID-19 affects the gut virome [169].

Changes in microbiomes lead to changes in microbiota metabolites, small molecules originating either from bacterial degradation of dietary substrates or from intrinsic bacterial processes. These metabolites have essential roles in maintaining immune homeostasis and may influence host responses to respiratory viruses via the gut–lung axis. For example, evidence suggests that microbiota-derived components are essential to condition DCs in a steady-state, enabling them to initiate immune responses effectively when challenged [170].

SCFAs, such as acetate, propionate, and butyrate, are among the most studied microbial metabolites and can modulate immune responses through several mechanisms. Butyrate, for instance, supports M2 macrophage polarization by upregulating Arg-1, leading to decreased expression of inflammatory mediators like TNF, Nos2, IL-6, and IL-12b [171]. However, patients with COVID-19 have been shown to exhibit reduced SCFA biosynthesis capacity, a deficit that can persist even after viral clearance [172]. This reduction in SCFA production may compromise intestinal and systemic immune regulation, potentially contributing to sustained inflammation or impaired recovery. Further, several bacterial species such as *Bifidobacterium animalis*, *Bacteroides thetaiotaomicron*, *Lactobacillus casei*, and *Enterobacter cloacae*, produce riboflavin derivatives that activate mucosal-associated invariant T (MAIT) cells which can then migrate and exert antiviral effects in the lungs, particularly during the early stages of SARS-CoV-2 infection [173,174]. Another immunomodulatory microbial metabolite, deaminotyrosine (DAT), is derived from the

degradation of dietary flavonoids by *Clostridium orbiscindens*. It was demonstrated that DAT protects the host from influenza infection by amplifying type I IFN signalling and enhancing the host's antiviral defence mechanisms, reducing mortality, lowering viral gene expression, and decreasing cell damage in the airways [175]. Though not yet directly studied in COVID-19, similar mechanisms may contribute to SARS-CoV-2 outcomes via modulation of the host's immune response.

In addition to hepatic involvement on the gut microbiome, SARS-CoV-2 also directly contributes to the aforementioned dysbiosis through its binding to ACE2, which also acts as a chaperone for the sodium-dependent neutral amino acid transporter B0AT1 (SLC6A19). B0AT1 facilitates the uptake of key neutral amino acids, including tryptophan and glutamine, across the luminal surface of intestinal epithelial cells [176]. These substrates are critical for maintaining gut barrier integrity through promotion of TJ formation, downregulation of proinflammatory cytokines, and induction of antimicrobial peptides through regulation of mTOR signalling [176,177]. However, during SARS-CoV-2 infection, the co-internalization of ACE2 and B0AT1 leads to a significant reduction in B0AT1 surface expression, impairing amino acid uptake and compromising these protective functions [178]. These physical barriers prevent opportunistic pathogen invasion, and in the case of "leaky gut", pathogens may enter circulation and cause systemic inflammation and infection (this is discussed further in Section I, chapter 3.2.1 in regards to PASC). This is evidenced by markers of intestinal leakage (LPS and CCL25) being significantly increased in COVID-19 patients [179]. In particular, CCL25, is involved in the inflammatory response and is expressed in the small intestinal epithelium to recruit CCR9+ CD4+ T cells, impairing gut immune balance and disrupting microbiota stability [180,181]. This, in turn, promotes Th17 cell polarization in the intestines which produce large amounts of IL-17A, recruiting more neutrophils to the site and culminating in intestinal inflammation, diarrhoea, and broader GI symptoms [182].

Furthermore, the tryptophan deficiency impairs niacin synthesis, and its chronic insufficiency can lead to pellagra, a condition in which over 90% of patients develop colitis [183,184]. This pathway is supported by the significant elevation (> 50µg/g) of faecal

calprotectin, a reliable faecal biomarker for IBD and infectious colitis, in COVID-19 patients with GI symptoms [185–187]. Diarrhoea can result from this inflammation alone but is further exacerbated by gut flora dysbiosis due to disrupted antimicrobial peptide production and antibacterials provided in severe COVID-19. Furthermore, this dysbiosis, in turn, facilitates the overgrowth of opportunistic pathogens and increases the risk of systemic inflammation and cytokine storm, worsening symptoms.

The presence of SARS-CoV-2 in the GI tract may also have implications with other organs such as through the brain–gut axis, a bidirectional communication system linking the CNS and the enteric nervous system. Once in the GI tract, SARS-CoV-2 may reach the CNS through neuronal retrograde transmission along the vagus nerve, in a similar manner to invasion of the olfactory bulb in Supplementary information 1.3 [188]. The vagus nerve is a major communication pathway between the brain, heart, and digestive system, and may be infected through its supporting cells, allowing for an additional CNS invasion route through the GI system. SARS-CoV-2 can also disrupt the gut microbiota (discussed below), which plays a role in modulating neurotransmitter levels through their metabolic products, such as SCFA, bile acids, choline metabolites, lactic acids, and vitamins [189]. These disruptions can potentially contribute to neurological symptoms discussed in the neurological implications chapter, and may exacerbate or trigger neurodegenerative conditions [188,189].

In conclusion, the GI and hepatic impacts of SARS-CoV-2 infection highlight the virus's systemic nature beyond respiratory involvement. High ACE2 receptor expression in the GI tract facilitates significant viral replication, leading to common GI symptoms and potential faecal-oral transmission. COVID-19 liver damage is predominantly driven by systemic inflammatory and thrombotic processes, exacerbated by drug-induced injury. Persistent gut dysbiosis further contributes to immune dysregulation and barrier dysfunction.

References

1. Henkel M, Weikert T, Marston K, et al. Lethal COVID-19: Radiologic-Pathologic Correlation of the Lungs. Radiol Cardiothorac Imaging. 2020;2(6):e200406. doi:10.1148/ryct.2020200406
2. Ramos-Rincon JM, Alenda C, García-Sevila R, et al. Histopathological and virological features of lung, heart and liver percutaneous tissue core biopsy in patients with COVID-19: A clinicopathological case series. Malays J Pathol. 2022;44(1):83-92.
3. Medhi P, Dowerah S, Barman N, Singh M. Histopathological changes in lungs of patients with fatal COVID 19 infection: A series of 15 cases. Indian J Pathol Microbiol. 2023;66(4):834-838. doi:10.4103/ijpm.ijpm_866_21
4. Angeles Montero-Fernandez M, Pardo-Garcia R. Histopathology features of the lung in COVID-19 patients. Diagn Histopathol. 2021;27(3):123-127. doi:10.1016/j.mpdhp.2020.11.009
5. Tian S, Xiong Y, Liu H, et al. Pathological study of the 2019 novel coronavirus disease (COVID-19) through postmortem core biopsies. Mod Pathol. 2020;33(6):1007-1014. doi:10.1038/s41379-020-0536-x
6. Deacu M, Enciu M, Nicolau AA, et al. Morphopathological features induced by SARS-CoV-2 infection - a series of 57 autopsies. Histol Histopathol. 2022;38(05):513-524. doi:10.14670/HH-18-561
7. Ackermann M, Verleden SE, Kuehnel M, et al. Pulmonary Vascular Endothelialitis, Thrombosis, and Angiogenesis in Covid-19. N Engl J Med. 2020;383(2):120-128. doi:10.1056/NEJMoa2015432
8. Rodríguez C, Luque N, Blanco I, et al. Pulmonary Endothelial Dysfunction and Thrombotic Complications in Patients with COVID-19. Am J Respir Cell Mol Biol. 2021;64(4):407-415. doi:10.1165/rcmb.2020-0359PS
9. Bradley BT, Maioli H, Johnston R, et al. Histopathology and ultrastructural findings of fatal COVID-19 infections in Washington State: a case series. The Lancet. 2020;396(10247):320-332. doi:10.1016/S0140-6736(20)31305-2
10. Robinot R, Hubert M, De Melo GD, et al. SARS-CoV-2 infection induces the dedifferentiation of multiciliated cells and impairs mucociliary clearance. Nat Commun. 2021;12(1):4354. doi:10.1038/s41467-021-24521-x
11. Li Q, Vijaykumar K, Phillips SE, et al. Mucociliary transport deficiency and disease progression in Syrian hamsters with SARS-CoV-2 infection. JCI Insight. 2023;8(1):e163962. doi:10.1172/jci.insight.163962
12. Chen H, Liu W, Wang Y, Liu D, Zhao L, Yu J. SARS-CoV-2 activates lung epithelial cell proinflammatory signaling and leads to immune dysregulation in COVID-19 patients. EBioMedicine. 2021;70:103500. doi:10.1016/j.ebiom.2021.103500
13. Santana MF, Pinto RADA, Marcon BH, et al. Pathological findings and morphologic correlation of the lungs of autopsied patients with SARS-CoV-2 infection in the Brazilian Amazon using transmission electron microscopy. Rev Soc Bras Med Trop. 2021;54:e0850-2020. doi:10.1590/0037-8682-0850-2020
14. Mirastschijski U, Dembinski R, Maedler K. Lung Surfactant for Pulmonary Barrier Restoration in Patients With COVID-19 Pneumonia. Front Med. 2020;7:254. doi:10.3389/fmed.2020.00254
15. Castanheira FVS, Kubes P. Neutrophils and NETs in modulating acute and chronic inflammation. Blood. 2019;133(20):2178-2185. doi:10.1182/blood-2018-11-844530
16. Peñaloza HF, Lee JS, Ray P. Neutrophils and lymphopenia, an unknown axis in severe COVID-19 disease. Morrison TE, ed. PLOS Pathog. 2021;17(9):e1009850. doi:10.1371/journal.ppat.1009850
17. Yang SC, Tsai YF, Pan YL, Hwang TL. Understanding the role of neutrophils in acute respiratory distress syndrome. Biomed J. 2021;44(4):439-446. doi:10.1016/j.bj.2020.09.001
18. Prilutskiy A, Kritselis M, Shevtsov A, et al. SARS-CoV-2 Infection–Associated Hemophagocytic Lymphohistiocytosis. Am J Clin Pathol. 2020;154(4):466-474. doi:10.1093/ajcp/aqaa124
19. Jusovic-Stocanin A, Kaemmerer E, Ihle H, et al. Hemophagocytosis of the Hilar Pulmonary Lymph Nodes Is a More Sensitive Indicator of the Severity of COVID-19 Disease than Bone Marrow Hemophagocytosis. Diseases. 2024;12(10):241. doi:10.3390/diseases12100241
20. Isha S, Olaizola G, Carboni Bisso I, et al. Evaluating the Newly Proposed ARDS Definition in Hospitalized Patients With COVID-19 Treated With High-Flow Nasal Oxygen. Respir Care. 2025;70(2):119-125. doi:10.4187/respcare.11933
21. Zhang J, Tecson KM, McCullough PA. Endothelial dysfunction contributes to COVID-19-associated vascular inflammation and coagulopathy. Rev Cardiovasc Med. 2020;21(3):315. doi:10.31083/j.rcm.2020.03.126
22. Osburn WO, Smith K, Yanek L, et al. Markers of endothelial cell activation are associated with the severity of pulmonary disease in COVID-19. Pon Velayutham AB, ed. PLOS ONE. 2022;17(5):e0268296. doi:10.1371/journal.pone.0268296
23. Smadja DM, Mentzer SJ, Fontenay M, et al. COVID-19 is a systemic vascular hemopathy: insight for mechanistic and clinical aspects. Angiogenesis. 2021;24(4):755-788. doi:10.1007/s10456-021-09805-6
24. Wicky PH, d'Humières C, Timsit JF. How common is ventilator-associated pneumonia after coronavirus disease 2019? Curr Opin Infect Dis. 2022;35(2):170-175. doi:10.1097/QCO.0000000000000817
25. Suleiman AS, Islam MdA, Akter MS, Amin MR, Werkneh AA, Bhattacharya P. A meta-meta-analysis of co-infection, secondary infections, and antimicrobial resistance in COVID-19 patients. J Infect Public Health. 2023;16(10):1562-1590. doi:10.1016/j.jiph.2023.07.005
26. Cabo-Gambin R, Benítez ID, Carmona P, et al. Three to Six Months Evolution of Pulmonary Function and Radiological Features in Critical COVID-19 Patients: A Prospective Cohort. Arch Bronconeumol. 2022;58:59-62. doi:10.1016/j.arbres.2021.07.005
27. Flammer AJ, Anderson T, Celermajer DS, et al. The Assessment of Endothelial Function: From Research Into Clinical Practice. Circulation. 2012;126(6):753-767. doi:10.1161/CIRCULATIONAHA.112.093245

28. Xu S wen, Ilyas I, Weng J ping. Endothelial dysfunction in COVID-19: an overview of evidence, biomarkers, mechanisms and potential therapies. Acta Pharmacol Sin. 2023;44(4):695-709. doi:10.1038/s41401-022-00998-0
29. Varga Z, Flammer AJ, Steiger P, et al. Endothelial cell infection and endotheliitis in COVID-19. The Lancet. 2020;395(10234):1417-1418. doi:10.1016/S0140-6736(20)30937-5
30. Helms J, Tacquard C, Severac F, et al. High risk of thrombosis in patients with severe SARS-CoV-2 infection: a multicenter prospective cohort study. Intensive Care Med. 2020;46(6):1089-1098. doi:10.1007/s00134-020-06062-x
31. Rostami M, Mansouritorghabeh H, Parsa-Kondelaji M. High levels of Von Willebrand factor markers in COVID-19: a systematic review and meta-analysis. Clin Exp Med. 2022;22(3):347-357. doi:10.1007/s10238-021-00769-x
32. Colmenero I, Santonja C, Alonso-Riaño M, et al. SARS-CoV-2 endothelial infection causes COVID-19 chilblains: histopathological, immunohistochemical and ultrastructural study of seven paediatric cases. Br J Dermatol. 2020;183(4):729-737. doi:10.1111/bjd.19327
33. Diamond B. The renin–angiotensin system: An integrated view of lung disease and coagulopathy in COVID-19 and therapeutic implications. J Exp Med. 2020;217(8):e20201000. doi:10.1084/jem.20201000
34. Meager A. Cytokine regulation of cellular adhesion molecule expression in inflammation. Cytokine Growth Factor Rev. 1999;10(1):27-39. doi:10.1016/S1359-6101(98)00024-0
35. Singh V, Kaur R, Kumari P, Pasricha C, Singh R. ICAM-1 and VCAM-1: Gatekeepers in various inflammatory and cardiovascular disorders. Clin Chim Acta. 2023;548:117487. doi:10.1016/j.cca.2023.117487
36. Al-Sadi R, Boivin M, Ma T. Mechanism of cytokine modulation of epithelial tight junction barrier. Front Biosci Landmark Ed. 2009;14(7):2765-2778. doi:10.2741/3413
37. Capaldo CT, Nusrat A. Cytokine regulation of tight junctions. Biochim Biophys Acta BBA - Biomembr. 2009;1788(4):864-871. doi:10.1016/j.bbamem.2008.08.027
38. Magro C, Mulvey JJ, Berlin D, et al. Complement associated microvascular injury and thrombosis in the pathogenesis of severe COVID-19 infection: A report of five cases. Transl Res. 2020;220:1-13. doi:10.1016/j.trsl.2020.04.007
39. Macor P, Durigutto P, Mangogna A, et al. Multiple-Organ Complement Deposition on Vascular Endothelium in COVID-19 Patients. Biomedicines. 2021;9(8):1003. doi:10.3390/biomedicines9081003
40. Zuo Y, Yalavarthi S, Shi H, et al. Neutrophil extracellular traps in COVID-19. JCI Insight. Published online April 24, 2020. doi:10.1172/jci.insight.138999
41. Pfister F, Vonbrunn E, Ries T, et al. Complement Activation in Kidneys of Patients With COVID-19. Front Immunol. 2021;11:594849. doi:10.3389/fimmu.2020.594849
42. Bouquegneau A, Erpicum P, Grosch S, et al. COVID-19–associated Nephropathy Includes Tubular Necrosis and Capillary Congestion, with Evidence of SARS-CoV-2 in the Nephron. Kidney360. 2021;2(4):639-652. doi:10.34067/KID.0006992020
43. Duan CY, Zhang J, Wu HL, Li T, Liu LM. Regulatory mechanisms, prophylaxis and treatment of vascular leakage following severe trauma and shock. Mil Med Res. 2017;4(1):11. doi:10.1186/s40779-017-0117-6
44. Case R, Ramaniuk A, Martin P, Simpson PJ, Harden C, Ataya A. Systemic Capillary Leak Syndrome Secondary to Coronavirus Disease 2019. Chest. 2020;158(6):e267-e268. doi:10.1016/j.chest.2020.06.049
45. Kosaka A, Goto T, Washino T, Sakamoto N, Iwabuchi S, Nakamura-Uchiyama F. Two cases of systemic capillary leak syndrome associated with COVID-19 in Japan. J Infect Chemother. 2024;30(3):250-254. doi:10.1016/j.jiac.2023.10.005
46. Perico L, Benigni A, Casiraghi F, Ng LFP, Renia L, Remuzzi G. Immunity, endothelial injury and complement-induced coagulopathy in COVID-19. Nat Rev Nephrol. 2021;17(1):46-64. doi:10.1038/s41581-020-00357-4
47. Pang Z, Tang A, He Y, et al. Neurological complications caused by SARS-CoV-2. Forrest GN, ed. Clin Microbiol Rev. 2024;37(4):e00131-24. doi:10.1128/cmr.00131-24
48. Liotta EM, Batra A, Clark JR, et al. Frequent neurologic manifestations and encephalopathy-associated morbidity in Covid-19 patients. Ann Clin Transl Neurol. 2020;7(11):2221-2230. doi:10.1002/acn3.51210
49. Paniz-Mondolfi A, Bryce C, Grimes Z, et al. Central nervous system involvement by severe acute respiratory syndrome coronavirus-2 (SARS-CoV-2). J Med Virol. 2020;92(7):699-702. doi:10.1002/jmv.25915
50. Zubair AS, McAlpine LS, Gardin T, Farhadian S, Kuruvilla DE, Spudich S. Neuropathogenesis and Neurologic Manifestations of the Coronaviruses in the Age of Coronavirus Disease 2019: A Review. JAMA Neurol. 2020;77(8):1018. doi:10.1001/jamaneurol.2020.2065
51. Erickson MA, Rhea EM, Knopp RC, Banks WA. Interactions of SARS-CoV-2 with the Blood–Brain Barrier. Int J Mol Sci. 2021;22(5):2681. doi:10.3390/ijms22052681
52. Ribeiro DE, Oliveira-Giacomelli Á, Glaser T, et al. Hyperactivation of P2X7 receptors as a culprit of COVID-19 neuropathology. Mol Psychiatry. 2021;26(4):1044-1059. doi:10.1038/s41380-020-00965-3
53. Lam SM, Huang X, Shui G. Neurological aspects of SARS-CoV-2 infection: lipoproteins and exosomes as Trojan horses. Trends Endocrinol Metab. 2022;33(8):554-568. doi:10.1016/j.tem.2022.04.011
54. Ong WY, Satish RL, Herr DR. ACE2, Circumventricular Organs and the Hypothalamus, and COVID-19. NeuroMolecular Med. 2022;24(4):363-373. doi:10.1007/s12017-022-08706-1
55. Wei ZYD, Liang K, Shetty AK. Complications of COVID-19 on the Central Nervous System: Mechanisms and Potential Treatment for Easing Long COVID. Aging Dis. 2023;14(5):1492. doi:10.14336/AD.2023.0312
56. Meinhardt J, Radke J, Dittmayer C, et al. Olfactory transmucosal SARS-CoV-2 invasion as a port of central nervous system entry in individuals with COVID-19. Nat Neurosci. 2021;24(2):168-175. doi:10.1038/s41593-020-00758-5

57. Bilinska K, Jakubowska P, Von Bartheld CS, Butowt R. Expression of the SARS-CoV-2 Entry Proteins, ACE2 and TMPRSS2, in Cells of the Olfactory Epithelium: Identification of Cell Types and Trends with Age. ACS Chem Neurosci. 2020;11(11):1555-1562. doi:10.1021/acschemneuro.0c00210
58. Butowt R, Von Bartheld CS. Timing and cause of olfactory deciliation in COVID-19. Physiol Rev. 2024;104(2):589-590. doi:10.1152/physrev.00035.2023
59. Verma AK, Zheng J, Meyerholz DK, Perlman S. SARS-CoV-2 infection of sustentacular cells disrupts olfactory signaling pathways. JCI Insight. 2022;7(24):e160277. doi:10.1172/jci.insight.160277
60. Zazhytska M, Kodra A, Hoagland DA, et al. Non-cell-autonomous disruption of nuclear architecture as a potential cause of COVID-19-induced anosmia. Cell. 2022;185(6):1052-1064.e12. doi:10.1016/j.cell.2022.01.024
61. Anastassopoulou C, Davaris N, Ferous S, et al. The Molecular Basis of Olfactory Dysfunction in COVID-19 and Long COVID. Lifestyle Genomics. Published online May 15, 2024. doi:10.1159/000539292
62. Yan CH, Faraji F, Prajapati DP, Ostrander BT, DeConde AS. Self-reported olfactory loss associates with outpatient clinical course in COVID-19. Int Forum Allergy Rhinol. 2020;10(7):821-831. doi:10.1002/alr.22592
63. Lechien JR, Chiesa-Estomba CM, De Siati DR, et al. Olfactory and gustatory dysfunctions as a clinical presentation of mild-to-moderate forms of the coronavirus disease (COVID-19): a multicenter European study. Eur Arch Otorhinolaryngol. 2020;277(8):2251-2261. doi:10.1007/s00405-020-05965-1
64. Sepahi A, Kraus A, Casadei E, et al. Olfactory sensory neurons mediate ultrarapid antiviral immune responses in a TrkA-dependent manner. Proc Natl Acad Sci. 2019;116(25):12428-12436. doi:10.1073/pnas.1900083116
65. Monje MHG. Severe Acute Respiratory Syndrome Coronavirus 2, Olfactory Mucosa, and the Entrance in the Central Nervous System: Expanding the Evidence? Mov Disord Clin Pract. 2021;8(3):350-351. doi:10.1002/mdc3.13157
66. Basak I, Harfoot R, Palmer JE, et al. Neuroproteomic Analysis after SARS-CoV-2 Infection Reveals Overrepresented Neurodegeneration Pathways and Disrupted Metabolic Pathways. Biomolecules. 2023;13(11):1597. doi:10.3390/biom13111597
67. Kettunen P, Lesnikova A, Räsänen N, et al. SARS-CoV-2 Infection of Human Neurons Is TMPRSS2 Independent, Requires Endosomal Cell Entry, and Can Be Blocked by Inhibitors of Host Phosphoinositol-5 Kinase. Gallagher T, ed. J Virol. 2023;97(4):e00144-23. doi:10.1128/jvi.00144-23
68. Luczo JM, Edwards SJ, Ardipradja K, et al. SARS-CoV and SARS-CoV-2 display limited neuronal infection and lack the ability to transmit within synaptically connected axons in stem cell–derived human neurons. J Neurovirol. 2024;30(1):39-51. doi:10.1007/s13365-023-01187-3
69. Malik JR, Acharya A, Avedissian SN, et al. ACE-2, TMPRSS2, and Neuropilin-1 Receptor Expression on Human Brain Astrocytes and Pericytes and SARS-CoV-2 Infection Kinetics. Int J Mol Sci. 2023;24(10):8622. doi:10.3390/ijms24108622
70. Haverty R, McCormack J, Evans C, et al. SARS-CoV-2 infects neurons, astrocytes, choroid plexus epithelial cells and pericytes of the human central nervous system in vitro. J Gen Virol. 2024;105(7). doi:10.1099/jgv.0.002009
71. Matschke J, Lütgehetmann M, Hagel C, et al. Neuropathology of patients with COVID-19 in Germany: a post-mortem case series. Lancet Neurol. 2020;19(11):919-929. doi:10.1016/S1474-4422(20)30308-2
72. Stein SR, Ramelli SC, Grazioli A, et al. SARS-CoV-2 infection and persistence in the human body and brain at autopsy. Nature. 2022;612(7941):758-763. doi:10.1038/s41586-022-05542-y
73. Li Y, Fu L, Gonzales DM, Lavi E. Coronavirus Neurovirulence Correlates with the Ability of the Virus To Induce Proinflammatory Cytokine Signals from Astrocytes and Microglia. J Virol. 2004;78(7):3398-3406. doi:10.1128/JVI.78.7.3398-3406.2004
74. Albornoz EA, Amarilla AA, Modhiran N, et al. SARS-CoV-2 drives NLRP3 inflammasome activation in human microglia through spike protein. Mol Psychiatry. 2023;28(7):2878-2893. doi:10.1038/s41380-022-01831-0
75. Akimoto N, Ifuku M, Mori Y, Noda M. Effects of chemokine (C–C motif) ligand 1 on microglial function. Biochem Biophys Res Commun. 2013;436(3):455-461. doi:10.1016/j.bbrc.2013.05.126
76. McKimmie C, Michlmayr D. Role of CXCL10 in central nervous system inflammation. Int J Interferon Cytokine Mediat Res. Published online February 2014:1. doi:10.2147/IJICMR.S35953
77. Price BR, Johnson LA, Norris CM. Reactive astrocytes: The nexus of pathological and clinical hallmarks of Alzheimer's disease. Ageing Res Rev. 2021;68:101335. doi:10.1016/j.arr.2021.101335
78. Bossu P, Ciaramella A, Salani F, et al. Interleukin-18, From Neuroinflammation to Alzheimers Disease. Curr Pharm Des. 2010;16(38):4213-4224. doi:10.2174/138161210794519147
79. Lukens JR, Barr MJ, Chaplin DD, Chi H, Kanneganti TD. Inflammasome-Derived IL-1β Regulates the Production of GM-CSF by CD4+ T Cells and γδ T Cells. J Immunol. 2012;188(7):3107-3115. doi:10.4049/jimmunol.1103308
80. Lin CC, Edelson BT. New Insights into the Role of IL-1β in Experimental Autoimmune Encephalomyelitis and Multiple Sclerosis. J Immunol. 2017;198(12):4553-4560. doi:10.4049/jimmunol.1700263
81. Poloni TE, Medici V, Moretti M, et al. COVID-19-related neuropathology and microglial activation in elderly with and without dementia. Brain Pathol. 2021;31(5):e12997. doi:10.1111/bpa.12997
82. Ismael S, Umar M, Bix GJ. Endothelial nitric oxide synthase deficiency exacerbates SARS-CoV-2 induced neuropathology in a mouse model of vascular dementia. Alzheimers Dement. 2024;20(S1):e092618. doi:10.1002/alz.092618
83. Gironacci MM, Cerniello FM, Longo Carbajosa NA, Goldstein J, Cerrato BD. Protective axis of the renin–angiotensin system in the brain. Clin Sci. 2014;127(5):295-306. doi:10.1042/CS20130450
84. Liu Y, Du X, Chen J, et al. Neutrophil-to-lymphocyte ratio as an independent risk factor for mortality in hospitalized patients with COVID-19. J Infect. 2020;81(1):e6-e12. doi:10.1016/j.jinf.2020.04.002

85. Wijeratne T, Gillard Crewther S, Sales C, Karimi L. COVID-19 Pathophysiology Predicts That Ischemic Stroke Occurrence Is an Expectation, Not an Exception—A Systematic Review. Front Neurol. 2021;11:607221. doi:10.3389/fneur.2020.607221
86. Gu J, Gong E, Zhang B, et al. Multiple organ infection and the pathogenesis of SARS. J Exp Med. 2005;202(3):415-424. doi:10.1084/jem.20050828
87. Politi LS, Salsano E, Grimaldi M. Magnetic Resonance Imaging Alteration of the Brain in a Patient With Coronavirus Disease 2019 (COVID-19) and Anosmia. JAMA Neurol. 2020;77(8):1028. doi:10.1001/jamaneurol.2020.2125
88. Pajo AT, Espiritu AI, Apor ADAO, Jamora RDG. Neuropathologic findings of patients with COVID-19: a systematic review. Neurol Sci Off J Ital Neurol Soc Ital Soc Clin Neurophysiol. 2021;42(4):1255-1266. doi:10.1007/s10072-021-05068-7
89. Nannoni S, De Groot R, Bell S, Markus HS. Stroke in COVID-19: A systematic review and meta-analysis. Int J Stroke. 2021;16(2):137-149. doi:10.1177/1747493020972922
90. Helms J, Kremer S, Merdji H, et al. Delirium and encephalopathy in severe COVID-19: a cohort analysis of ICU patients. Crit Care. 2020;24(1):491. doi:10.1186/s13054-020-03200-1
91. Shao SC, Lai CC, Chen YH, Chen YC, Hung MJ, Liao SC. Prevalence, incidence and mortality of delirium in patients with COVID-19: a systematic review and meta-analysis. Age Ageing. 2021;50(5):1445-1453. doi:10.1093/ageing/afab103
92. Siow I, Lee KS, Zhang JJY, Saffari SE, Ng A. Encephalitis as a neurological complication of COVID-19: A systematic review and meta-analysis of incidence, outcomes, and predictors. Eur J Neurol. 2021;28(10):3491-3502. doi:10.1111/ene.14913
93. Vitalakumar D, Sharma A, Kumar A, Flora SJS. Neurological Manifestations in COVID-19 Patients: A Meta-Analysis. ACS Chem Neurosci. 2021;12(15):2776-2797. doi:10.1021/acschemneuro.1c00353
94. Kim PH, Kim M, Suh CH, et al. Neuroimaging Findings in Patients with COVID-19: A Systematic Review and Meta-Analysis. Korean J Radiol. 2021;22(11):1875. doi:10.3348/kjr.2021.0127
95. Wang W, Nguyen LTT, Burlak C, et al. Caspase-1 causes truncation and aggregation of the Parkinson's disease-associated protein α-synuclein. Proc Natl Acad Sci. 2016;113(34):9587-9592. doi:10.1073/pnas.1610099113
96. Vasek MJ, Garber C, Dorsey D, et al. A complement–microglial axis drives synapse loss during virus-induced memory impairment. Nature. 2016;534(7608):538-543. doi:10.1038/nature18283
97. Hampshire A, Azor A, Atchison C, et al. Cognition and Memory after Covid-19 in a Large Community Sample. N Engl J Med. 2024;390(9):806-818. doi:10.1056/NEJMoa2311330
98. Golzari-Sorkheh M, Weaver DF, Reed MA. COVID-19 as a Risk Factor for Alzheimer's Disease. J Alzheimers Dis. 2023;91(1):1-23. doi:10.3233/JAD-220800
99. Reiken S, Sittenfeld L, Dridi H, Liu Y, Liu X, Marks AR. Alzheimer's-like signaling in brains of COVID-19 patients. Alzheimers Dement. 2022;18(5):955-965. doi:10.1002/alz.12558
100. Ciaccio M, Lo Sasso B, Scazzone C, et al. COVID-19 and Alzheimer's Disease. Brain Sci. 2021;11(3):305. doi:10.3390/brainsci11030305
101. Sun B, Tang N, Peluso MJ, et al. Characterization and Biomarker Analyses of Post-COVID-19 Complications and Neurological Manifestations. Cells. 2021;10(2):386. doi:10.3390/cells10020386
102. Pimentel V, Luchsinger VW, Carvalho GL, et al. Guillain-Barré syndrome associated with COVID-19: A systematic review. Brain Behav Immun - Health. 2023;28:100578. doi:10.1016/j.bbih.2022.100578
103. Hughes RA, Cornblath DR. Guillain-Barré syndrome. The Lancet. 2005;366(9497):1653-1666. doi:10.1016/S0140-6736(05)67665-9
104. Pellicori P, Doolub G, Wong CM, et al. COVID-19 and its cardiovascular effects: a systematic review of prevalence studies. Cochrane Heart Group, ed. Cochrane Database Syst Rev. 2021;2022(4). doi:10.1002/14651858.CD013879
105. Lala A, Johnson KW, Januzzi JL, et al. Prevalence and Impact of Myocardial Injury in Patients Hospitalized With COVID-19 Infection. J Am Coll Cardiol. 2020;76(5):533-546. doi:10.1016/j.jacc.2020.06.007
106. Metkus TS, Sokoll LJ, Barth AS, et al. Myocardial Injury in Severe COVID-19 Compared With Non–COVID-19 Acute Respiratory Distress Syndrome. Circulation. 2021;143(6):553-565. doi:10.1161/CIRCULATIONAHA.120.050543
107. Sanz-Sánchez J, Vrachatis DA, Reimers B, et al. Impact of myocardial injury on mortality in patients with COVID-19: a meta-analysis. Hellenic J Cardiol. 2021;62(3):253-255. doi:10.1016/j.hjc.2020.07.004
108. Guo T, Fan Y, Chen M, et al. Cardiovascular Implications of Fatal Outcomes of Patients With Coronavirus Disease 2019 (COVID-19). JAMA Cardiol. 2020;5(7):811. doi:10.1001/jamacardio.2020.1017
109. Dolhnikoff M, Ferreira Ferranti J, De Almeida Monteiro RA, et al. SARS-CoV-2 in cardiac tissue of a child with COVID-19-related multisystem inflammatory syndrome. Lancet Child Adolesc Health. 2020;4(10):790-794. doi:10.1016/S2352-4642(20)30257-1
110. Lindner D, Fitzek A, Bräuninger H, et al. Association of Cardiac Infection With SARS-CoV-2 in Confirmed COVID-19 Autopsy Cases. JAMA Cardiol. 2020;5(11):1281. doi:10.1001/jamacardio.2020.3551
111. Tavazzi G, Pellegrini C, Maurelli M, et al. Myocardial localization of coronavirus in COVID-19 cardiogenic shock. Eur J Heart Fail. 2020;22(5):911-915. doi:10.1002/ejhf.1828
112. Marchiano S, Hsiang TY, Khanna A, et al. SARS-CoV-2 Infects Human Pluripotent Stem Cell-Derived Cardiomyocytes, Impairing Electrical and Mechanical Function. Stem Cell Rep. 2021;16(3):478-492. doi:10.1016/j.stemcr.2021.02.008
113. Chen L, Li X, Chen M, Feng Y, Xiong C. Corrigendum to: The ACE2 expression in human heart indicates new potential mechanism of heart injury among patients infected with SARS-CoV-2. Cardiovasc Res. 2020;116(12):1994-1994. doi:10.1093/cvr/cvaa157

114. Yang Y, Wei Z, Xiong C, Qian H. Direct mechanisms of SARS-CoV-2-induced cardiomyocyte damage: an update. Virol J. 2022;19(1):108. doi:10.1186/s12985-022-01833-y
115. Avolio E, Carrabba M, Kavanagh Williamson M, et al. The SARS-CoV-2 Spike protein alters human cardiac pericyte function and interaction with endothelial cells through a non-infective mechanism involving activation of CD147 receptor signalling. Eur Heart J. 2021;42(Supplement_1):ehab724.3383. doi:10.1093/eurheartj/ehab724.3383
116. Nair A, Deswal A. COVID-19–Associated Fulminant Myocarditis. J Am Coll Cardiol. 2022;80(4):313-315. doi:10.1016/j.jacc.2022.06.003
117. Mehta P, McAuley DF, Brown M, Sanchez E, Tattersall RS, Manson JJ. COVID-19: consider cytokine storm syndromes and immunosuppression. The Lancet. 2020;395(10229):1033-1034. doi:10.1016/S0140-6736(20)30628-0
118. Imazio M, Klingel K, Kindermann I, et al. COVID-19 pandemic and troponin: indirect myocardial injury, myocardial inflammation or myocarditis? Heart. 2020;106(15):1127-1131. doi:10.1136/heartjnl-2020-317186
119. Spagnoli LG, Bonanno E, Sangiorgi G, Mauriello A. Role of Inflammation in Atherosclerosis. J Nucl Med. 2007;48(11):1800-1815. doi:10.2967/jnumed.107.038661
120. Giustino G, Pinney SP, Lala A, et al. Coronavirus and Cardiovascular Disease, Myocardial Injury, and Arrhythmia. J Am Coll Cardiol. 2020;76(17):2011-2023. doi:10.1016/j.jacc.2020.08.059
121. Sethi P, Peiris CD. A Review of Catecholamine Associated Cardiomyopathies and Channelopathies. Cureus. 2020;12(2):e6957. doi:10.7759/cureus.6957
122. Gubbi S, Nazari MA, Taieb D, Klubo-Gwiezdzinska J, Pacak K. Catecholamine physiology and its implications in patients with COVID-19. Lancet Diabetes Endocrinol. 2020;8(12):978-986. doi:10.1016/S2213-8587(20)30342-9
123. Pellegrini D, Kawakami R, Guagliumi G, et al. Microthrombi as a Major Cause of Cardiac Injury in COVID-19: A Pathologic Study. Circulation. 2021;143(10):1031-1042. doi:10.1161/CIRCULATIONAHA.120.051828
124. Halushka MK, Vander Heide RS. Myocarditis is rare in COVID-19 autopsies: cardiovascular findings across 277 postmortem examinations. Cardiovasc Pathol. 2021;50:107300. doi:10.1016/j.carpath.2020.107300
125. Linschoten M, Uijl A, Schut A, et al. Clinical presentation, disease course, and outcome of COVID-19 in hospitalized patients with and without pre-existing cardiac disease: a cohort study across 18 countries. Eur Heart J. 2022;43(11):1104-1120. doi:10.1093/eurheartj/ehab656
126. Deng Q, Hu B, Zhang Y, et al. Suspected myocardial injury in patients with COVID-19: Evidence from front-line clinical observation in Wuhan, China. Int J Cardiol. 2020;311:116-121. doi:10.1016/j.ijcard.2020.03.087
127. Kunutsor SK, Laukkanen JA. Cardiovascular complications in COVID-19: A systematic review and meta-analysis. J Infect. 2020;81(2):e139-e141. doi:10.1016/j.jinf.2020.05.068
128. Coromilas EJ, Kochav S, Goldenthal I, et al. Worldwide Survey of COVID-19–Associated Arrhythmias. Circ Arrhythm Electrophysiol. 2021;14(3):e009458. doi:10.1161/CIRCEP.120.009458
129. Zhao YH, Zhao L, Yang XC, Wang P. Cardiovascular complications of SARS-CoV-2 infection (COVID-19): a systematic review and meta-analysis. Rev Cardiovasc Med. 2021;22(1):159. doi:10.31083/j.rcm.2021.01.238
130. Suh YJ, Hong H, Ohana M, et al. Pulmonary Embolism and Deep Vein Thrombosis in COVID-19: A Systematic Review and Meta-Analysis. Radiology. 2021;298(2):E70-E80. doi:10.1148/radiol.2020203557
131. Piroth L, Cottenet J, Mariet AS, et al. Comparison of the characteristics, morbidity, and mortality of COVID-19 and seasonal influenza: a nationwide, population-based retrospective cohort study. Lancet Respir Med. 2021;9(3):251-259. doi:10.1016/S2213-2600(20)30527-0
132. Wang Y, Wang Z, Tse G, et al. Cardiac arrhythmias in patients with COVID-19. J Arrhythmia. 2020;36(5):827-836. doi:10.1002/joa3.12405
133. Lazzerini PE, Capecchi PL, Laghi-Pasini F. Systemic inflammation and arrhythmic risk: lessons from rheumatoid arthritis. Eur Heart J. Published online June 1, 2016:ehw208. doi:10.1093/eurheartj/ehw208
134. Lazzerini PE, Laghi-Pasini F, Acampa M, et al. Systemic Inflammation Rapidly Induces Reversible Atrial Electrical Remodeling: The Role of Interleukin-6–Mediated Changes in Connexin Expression. J Am Heart Assoc. 2019;8(16):e011006. doi:10.1161/JAHA.118.011006
135. Aviles RJ, Martin DO, Apperson-Hansen C, et al. Inflammation as a Risk Factor for Atrial Fibrillation. Circulation. 2003;108(24):3006-3010. doi:10.1161/01.CIR.0000103131.70301.4F
136. Brenner ZR, Powers J. Takotsubo cardiomyopathy. Heart Lung J Crit Care. 2008;37(1):1-7. doi:10.1016/j.hrtlng.2006.12.003
137. Ghasemi H, Kazemian S, Nejadghaderi SA, Shafie M. Takotsubo syndrome and COVID-19: A systematic review. Health Sci Rep. 2023;6(1):e972. doi:10.1002/hsr2.972
138. Bertram S, Heurich A, Lavender H, et al. Influenza and SARS-Coronavirus Activating Proteases TMPRSS2 and HAT Are Expressed at Multiple Sites in Human Respiratory and Gastrointestinal Tracts. Thiel V, ed. PLoS ONE. 2012;7(4):e35876. doi:10.1371/journal.pone.0035876
139. Lin L, Jiang X, Zhang Z, et al. Gastrointestinal symptoms of 95 cases with SARS-CoV-2 infection. Gut. 2020;69(6):997-1001. doi:10.1136/gutjnl-2020-321013
140. Parasa S, Desai M, Thoguluva Chandrasekar V, et al. Prevalence of Gastrointestinal Symptoms and Fecal Viral Shedding in Patients With Coronavirus Disease 2019: A Systematic Review and Meta-analysis. JAMA Netw Open. 2020;3(6):e2011335. doi:10.1001/jamanetworkopen.2020.11335
141. Wang W, Xu Y, Gao R, et al. Detection of SARS-CoV-2 in Different Types of Clinical Specimens. JAMA. Published online March 11, 2020. doi:10.1001/jama.2020.3786
142. Xiao F, Sun J, Xu Y, et al. Infectious SARS-CoV-2 in Feces of Patient with Severe COVID-19. Emerg Infect Dis. 2020;26(8):1920-1922. doi:10.3201/eid2608.200681

143. El Moheb M, Naar L, Christensen MA, et al. Gastrointestinal Complications in Critically Ill Patients With and Without COVID-19. JAMA. 2020;324(18):1899. doi:10.1001/jama.2020.19400
144. Hajifathalian K, Krisko T, Mehta A, et al. Gastrointestinal and Hepatic Manifestations of 2019 Novel Coronavirus Disease in a Large Cohort of Infected Patients From New York: Clinical Implications. Gastroenterology. 2020;159(3):1137-1140.e2. doi:10.1053/j.gastro.2020.05.010
145. Luo S, Zhang X, Xu H. Don't Overlook Digestive Symptoms in Patients With 2019 Novel Coronavirus Disease (COVID-19). Clin Gastroenterol Hepatol. 2020;18(7):1636-1637. doi:10.1016/j.cgh.2020.03.043
146. Redd WD, Zhou JC, Hathorn KE, et al. Prevalence and Characteristics of Gastrointestinal Symptoms in Patients With Severe Acute Respiratory Syndrome Coronavirus 2 Infection in the United States: A Multicenter Cohort Study. Gastroenterology. 2020;159(2):765-767.e2. doi:10.1053/j.gastro.2020.04.045
147. Al-Shammari M, Naffouj S, Salgia R. S2140 Treatment of Colonic Varices With Superior Mesenteric Venous Stent: A Case Report Describing a Unique Approach. Am J Gastroenterol. 2020;115(1):S1129-S1130. doi:10.14309/01.ajg.0000710608.33489.a6
148. Zhang B, Zhou X, Qiu Y, et al. Clinical characteristics of 82 death cases with COVID-19. Published online February 27, 2020. doi:10.1101/2020.02.26.20028191
149. Cai Q, Huang D, Ou P, et al. COVID-19 in a Designated Infectious Diseases HospitalOutside Hubei Province,China. Published online February 19, 2020. doi:10.1101/2020.02.17.20024018
150. Huang C, Wang Y, Li X, et al. Clinical features of patients infected with 2019 novel coronavirus in Wuhan, China. The Lancet. 2020;395(10223):497-506. doi:10.1016/S0140-6736(20)30183-5
151. Huang Y, Yang R, Xu Y, Gong P. Clinical characteristics of 36 non-survivors with COVID-19 in Wuhan, China. Published online February 29, 2020. doi:10.1101/2020.02.27.20029009
152. Chai X, Hu L, Zhang Y, et al. Specific ACE2 Expression in Cholangiocytes May Cause Liver Damage After 2019-nCoV Infection. Published online February 4, 2020. doi:10.1101/2020.02.03.931766
153. Sonzogni A, Previtali G, Seghezzi M, et al. Liver histopathology in severe COVID 19 respiratory failure is suggestive of vascular alterations. Liver Int. 2020;40(9):2110-2116. doi:10.1111/liv.14601
154. Nie X, Qian L, Sun R, et al. Multi-organ proteomic landscape of COVID-19 autopsies. Cell. 2021;184(3):775-791.e14. doi:10.1016/j.cell.2021.01.004
155. Díaz LA, Idalsoaga F, Cannistra M, et al. High prevalence of hepatic steatosis and vascular thrombosis in COVID-19: A systematic review and meta-analysis of autopsy data. World J Gastroenterol. 2020;26(48):7693-7706. doi:10.3748/wjg.v26.i48.7693
156. Xu Z, Shi L, Wang Y, et al. Pathological findings of COVID-19 associated with acute respiratory distress syndrome. Lancet Respir Med. 2020;8(4):420-422. doi:10.1016/S2213-2600(20)30076-X
157. Xu L, Liu J, Lu M, Yang D, Zheng X. Liver injury during highly pathogenic human coronavirus infections. Liver Int Off J Int Assoc Study Liver. 2020;40(5):998-1004. doi:10.1111/liv.14435
158. Bloom PP, Meyerowitz EA, Reinus Z, et al. Liver Biochemistries in Hospitalized Patients With COVID-19. Hepatology. 2021;73(3):890-900. doi:10.1002/hep.31326
159. Papic N, Pangercic A, Vargovic M, Barsic B, Vince A, Kuzman I. Liver involvement during influenza infection: perspective on the 2009 influenza pandemic. Influenza Other Respir Viruses. 2012;6(3):e2-5. doi:10.1111/j.1750-2659.2011.00287.x
160. Tian D, Ye Q. Hepatic complications of COVID-19 and its treatment. J Med Virol. 2020;92(10):1818-1824. doi:10.1002/jmv.26036
161. Tang H, Zhou L, Li X, et al. Drug-induced liver injury associated with lopinavir-ritonavir in patients with COVID-19: a disproportionality analysis of U.S. food and drug administration adverse event reporting system (FAERS) data. Int J Clin Pharm. 2021;43(4):1116-1122. doi:10.1007/s11096-021-01311-5
162. Aleem A, Mahadevaiah G, Shariff N, Kothadia JP. Hepatic manifestations of COVID-19 and effect of remdesivir on liver function in patients with COVID-19 illness. Proc Bayl Univ Med Cent. 2021;34(4):473-477. doi:10.1080/08998280.2021.1885289
163. Gao Q, Yin X, Tan B, et al. Drug-induced liver injury following the use of tocilizumab or sarilumab in patients with coronavirus disease 2019. BMC Infect Dis. 2022;22(1):929. doi:10.1186/s12879-022-07896-0
164. Niu MW, Chen P. Gut microbiota and drug-induced liver injury: an update. Chin Med J (Engl). 2020;133(4):494-495. doi:10.1097/CM9.0000000000000651
165. Zuo T, Zhang F, Lui GCY, et al. Alterations in Gut Microbiota of Patients With COVID-19 During Time of Hospitalization. Gastroenterology. 2020;159(3):944-955.e8. doi:10.1053/j.gastro.2020.05.048
166. de Nies L, Galata V, Martin-Gallausiaux C, et al. Altered infective competence of the human gut microbiome in COVID-19. Microbiome. 2023;11(1):46. doi:10.1186/s40168-023-01472-7
167. Zuo T, Liu Q, Zhang F, et al. Temporal landscape of human gut RNA and DNA virome in SARS-CoV-2 infection and severity. Microbiome. 2021;9(1):91. doi:10.1186/s40168-021-01008-x
168. Neil JA, Cadwell K. The Intestinal Virome and Immunity. J Immunol. 2018;201(6):1615-1624. doi:10.4049/jimmunol.1800631
169. Shkoporov AN, Clooney AG, Sutton TDS, et al. The Human Gut Virome Is Highly Diverse, Stable, and Individual Specific. Cell Host Microbe. 2019;26(4):527-541.e5. doi:10.1016/j.chom.2019.09.009
170. Schaupp L, Muth S, Rogell L, et al. Microbiota-Induced Type I Interferons Instruct a Poised Basal State of Dendritic Cells. Cell. 2020;181(5):1080-1096.e19. doi:10.1016/j.cell.2020.04.022

171. Scott NA, Andrusaite A, Andersen P, et al. Antibiotics induce sustained dysregulation of intestinal T cell immunity by perturbing macrophage homeostasis. Sci Transl Med. 2018;10(464):eaao4755. doi:10.1126/scitranslmed.aao4755
172. Zhang F, Wan Y, Zuo T, et al. Prolonged Impairment of Short-Chain Fatty Acid and L-Isoleucine Biosynthesis in Gut Microbiome in Patients With COVID-19. Gastroenterology. 2022;162(2):548-561.e4. doi:10.1053/j.gastro.2021.10.013
173. Kjer-Nielsen L, Patel O, Corbett AJ, et al. MR1 presents microbial vitamin B metabolites to MAIT cells. Nature. 2012;491(7426):717-723. doi:10.1038/nature11605
174. Legoux F, Salou M, Lantz O. MAIT Cell Development and Functions: the Microbial Connection. Immunity. 2020;53(4):710-723. doi:10.1016/j.immuni.2020.09.009
175. Steed AL, Christophi GP, Kaiko GE, et al. The microbial metabolite desaminotyrosine protects from influenza through type I interferon. Science. 2017;357(6350):498-502. doi:10.1126/science.aam5336
176. Verrey F, Ristic Z, Romeo E, et al. NOVEL RENAL AMINO ACID TRANSPORTERS. Annu Rev Physiol. 2005;67(1):557-572. doi:10.1146/annurev.physiol.67.031103.153949
177. Perlot T, Penninger JM. ACE2 – From the renin–angiotensin system to gut microbiota and malnutrition. Microbes Infect. 2013;15(13):866-873. doi:10.1016/j.micinf.2013.08.003
178. Yan R, Zhang Y, Li Y, Xia L, Guo Y, Zhou Q. Structural basis for the recognition of SARS-CoV-2 by full-length human ACE2. Science. 2020;367(6485):1444-1448. doi:10.1126/science.abb2762
179. Hoel H, Heggelund L, Reikvam DH, et al. Elevated markers of gut leakage and inflammasome activation in COVID-19 patients with cardiac involvement. J Intern Med. 2021;289(4):523-531. doi:10.1111/joim.13178
180. Papadakis KA, Prehn J, Nelson V, et al. The Role of Thymus-Expressed Chemokine and Its Receptor CCR9 on Lymphocytes in the Regional Specialization of the Mucosal Immune System. J Immunol. 2000;165(9):5069-5076. doi:10.4049/jimmunol.165.9.5069
181. Stenstad H, Ericsson A, Johansson-Lindbom B, et al. Gut-associated lymphoid tissue–primed CD4+ T cells display CCR9-dependent and -independent homing to the small intestine. Blood. 2006;107(9):3447-3454. doi:10.1182/blood-2005-07-2860
182. Crowe CR, Chen K, Pociask DA, et al. Critical Role of IL-17RA in Immunopathology of Influenza Infection. J Immunol. 2009;183(8):5301-5310. doi:10.4049/jimmunol.0900995
183. Segal I, Tim Lou, Demetriou A, Paterson A, Hale M, Lerios M. Rectal manifestations of pellagra. Int J Colorectal Dis. 1986;1(4):238-243. doi:10.1007/BF01648345
184. Darby WJ, McNutt KW, Todhunter EN. Niacin. Nutr Rev. 2009;33(10):289-297. doi:10.1111/j.1753-4887.1975.tb05075.x
185. Magro F, Lopes J, Borralho P, et al. Comparison of different histological indexes in the assessment of UC activity and their accuracy regarding endoscopic outcomes and faecal calprotectin levels. Gut. 2019;68(4):594-603. doi:10.1136/gutjnl-2017-315545
186. Effenberger M, Grabherr F, Mayr L, et al. Faecal calprotectin indicates intestinal inflammation in COVID-19. Gut. 2020;69(8):1543-1544. doi:10.1136/gutjnl-2020-321388
187. Ojetti V, Saviano A, Covino M, et al. COVID-19 and intestinal inflammation: Role of fecal calprotectin. Dig Liver Dis. 2020;52(11):1231-1233. doi:10.1016/j.dld.2020.09.015
188. Bostancıklıoğlu M. Temporal Correlation Between Neurological and Gastrointestinal Symptoms of SARS-CoV-2. Inflamm Bowel Dis. 2020;26(8):e89-e91. doi:10.1093/ibd/izaa131
189. Shinu P, Morsy MA, Deb PK, et al. SARS CoV-2 Organotropism Associated Pathogenic Relationship of Gut-Brain Axis and Illness. Front Mol Biosci. 2020;7:606779. doi:10.3389/fmolb.2020.606779

Supplementary information 2: Data management plan

The full analysis for this thesis can be found only accessible through this link:
https://gist.github.com/captianward/665723adb0d12732cd34f73d76abdd33



Supplementary information 3: Additional multi-omic analytical methodologies.

One of the first methods used to analyse our multi-omic data was similarity network fusion (SNF) [1]. SNF is a method through which multi-omic data can be integrated through constructing networks of samples for each available data type, whereby nodes are patients, and edges between them represent the similarity of these patients based on the feature data provided. The following step is then efficiently fusing these into one network that represents the full spectrum of underlying data, creating a multi-omic network which clusters similar patients together. The method is mainly used in the identification of subtypes within data, for example, the identification of molecular subtypes of brain samples in relation to cognitive decline and neuropathology [2], the identification of phenotypes of small-for-gestational-age foetuses [3], and clustering of microbiome samples [4]. To this end, it was hoped that SNF would potentially be able to identify, in an unsupervised manner, the presence of PASC subtypes within our data set, with further analyses identifying the features through which these subtypes differ.

The methodology through which SNF works is as follows:

- A pair-wise Euclidean distance matrix is constructed from a single-omic data matrix.
- An affinity matrix is then constructed based on this distance matrix, in which rather than each element representing a distance. Each element is transformed into a similarity weight using a locally adaptive rule: for each pair of samples, the raw distance is compared with how far each sample typically is from its K nearest neighbours. Relatively close pairs have strong affinity whilst relatively distant pairs have weak affinity.
- Following this, the affinity matrices are then fused together in an iterative process which strengthens mutually recognised edges and weakens unrecognised edges. This network fusion step is a non-linear process whereby networks are iteratively updated using the averaged similarity values from other networks that align with its own nearest-neighbour structure. An edge between nodes gets boosted if

other networks like it and it's consistent with the local neighbourhoods in that network. With each step, networks resemble each other more, and after a set number of iterations the fused network is created.

- Following this, networks can then be examined in an unsupervised manner by first calculating the number of clusters present within the network. Here, two methods were utilised: Eigen-gap and rotation cost methods. The Eigen-gap method works as a "find the elbow" type rule on the Laplacian's eigenvalues by creating a graph Laplacian and listing eigenvalues from smallest upwards. If the data naturally form K groups, the first K eigenvalues sit close together and then there's a big gap to the next one; the K with the biggest gap is picked. The other method embeds samples using the first K eigenvectors on a k-dimensional space and "rotating" this space until all eigenvectors are aligned. Rotation cost measures how well alignment along a single axis can be achieved, the lower this cost (better alignment), the better the clustering.
- Once an estimate of the number of clusters is calculated, spectral clustering is then used to assign patients/samples/nodes to each cluster. This algorithm works by building a normalised graph Laplacian and taking the K smallest eigenvectors to get a low-dimensional embedding of the samples. The embedded vectors are then normalized according to the eigenvector and k-means is then run on the embedded points to get cluster labels.
- The use of this clustering information can then be used to identify features of interest between these clusters. This can be done by creating another patient network using just a single feature, and running the same clustering algorithm as described above. The clusters of the two networks (single-feature and multi-omic fused network) can be compared using normalised mutual information, which quantifies how much information the two labelling's share on a 0–1 scale (1 = identical, 0 = independent). High ranking features are thus of interest as they result in similar patient clustering, whilst low ranking features are less useful.

Patient grouping according to disease severity were analysed initially due to two reasons. The biomolecular signatures associated with severe disease would be stronger, allowing

for more obvious designability of the predicted patient clusters. Secondly, predicted patient clusters could be more confidently confirmed due to the greater certainty around the applied patient groupings (severe/moderate COVID-19, respiratory failure, healthy) than compared to the certainty of a patient exhibiting PASC, which is much more difficult to diagnose and recognise.

When analysing the resulting networks (figure 1), two major observations can be seen. The first is that the single-omic networks, in this case our shotgun metabolomic, shotgun proteomic, bulk RNA-seq, and clinical biologics, produced worse patient clustering than our fused network (~0.3 NMI max for individual networks, to over 0.5 NMI for fused networks), which produced a reasonable accurately clustered patient network. The second observation is that reducing the complexity of clustering resulted in better clustering performance. Networks clustered into 2 groups (healthy/moderate disease and severe COVID/severe respiratory failure) scored more highly (NMI = 0.53) that clustering patients into three or four categories (NMI = 0.3/0.31). Clustering performance was assessed with reducing the number of features and focusing on the X% most variable features per -omic level, but reduced NMI score.

Focusing on COVID only patients from the network (figure 2, NMI = 0.49), several moderate patients were clustered within the severe category, but it is difficult to say definitively if these patients are really misclassified, or if these patients simply did not seek out medical attention as their symptoms worsened. For severe patients misclassified as moderate, patient 160 appears to be a borderline case, and whilst this patient does not appear to reach the full definition of severe COVID-19 (achieving a WHO score of 4), the case was assessed as a severe case by medical staff within the hospital, requiring hospitalisation. The other two patients, 001 and 239, both had a more severe disease, but were both much older (73 and 75 years of age) and had a number of complications during their hospitalization such as renal failure and cardiac problems that were present before COVID-19 onset, likely exacerbating disease symptoms.

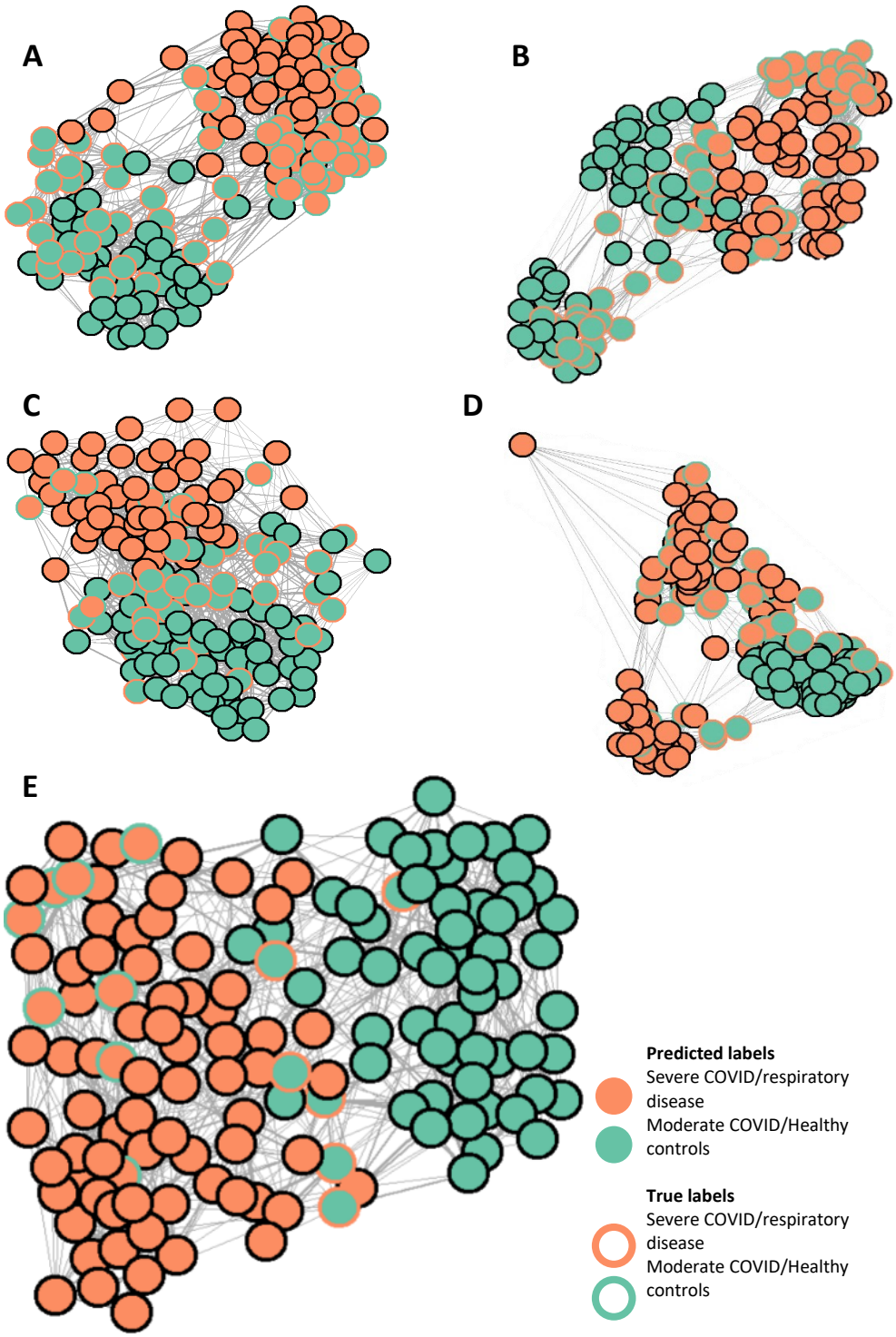

A
B
C
D
E
Predicted labels
Severe COVID/respiratory disease
Moderate COVID/Healthy controls
True labels
Severe COVID/respiratory disease
Moderate COVID/Healthy controls

Figure 1: Similarity network fusion of metabolomic data (A), proteomic data (B), transcriptomic data (C), and hospital laboratories (D), resulting in a final multi-omic fused patient network (E).

Node frame colour was only included if predicted label did not match true label, otherwise frame colour was left as black. Metabolomic, proteomic, transcriptomic, and hospital laboratory networks resulted in NMI scores of 0.03, 0.07, 0.22, and 0.26, respectively. The fused network achieved an NMI score of 0.53.

Networks were visualised from the affinity matrix using the force-directed Fruchterman-Reingold algorithm. Increasing edge width relates to increasing patient affinity between the connected nodes. Networks were sparsified by keeping only the top nearest neighbours based on edge weight/affinity (k = square root of the number of nodes in the network (k = 12 in networks A-E)). 142 patients were included in the final network fusion.

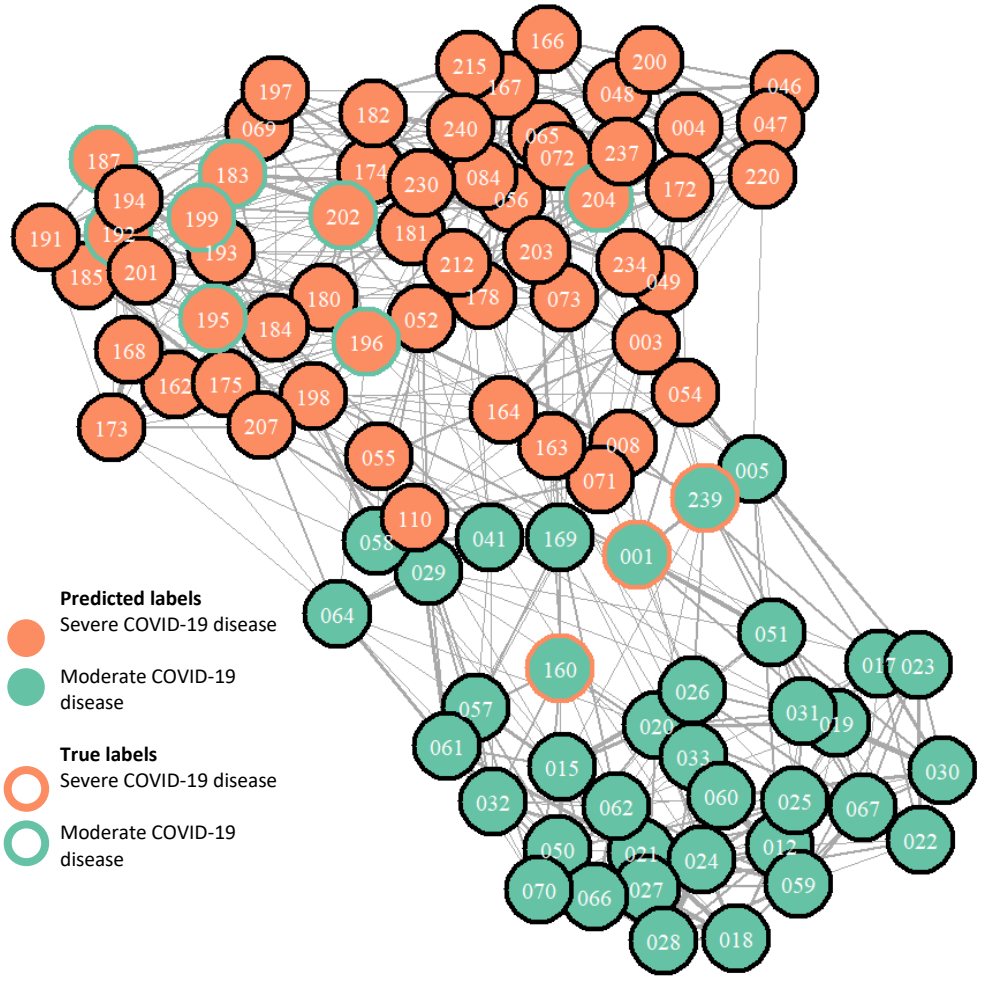

Predicted labels
Severe COVID-19 disease
Moderate COVID-19 disease
True labels
Severe COVID-19 disease
Moderate COVID-19 disease

Figure 2: COVID-19 only patient multi-omic fused network.
Node frame colour was only included if predicted label did not match true label, otherwise frame colour was left as black. The fused network achieved an NMI score of 0.49, 3 severe patients were misclassified as moderate patients, and 8 moderate patients were misclassified as severe patients.
The network was visualised from the affinity matrix using the force-directed Fruchterman-Reingold algorithm. Increasing edge width relates to increasing patient affinity between the connected nodes. The network was sparsified by keeping only the top nearest neighbours based on edge weight/affinity (k = square root of the number of nodes in the network (k = 10)). 95 patients were included in the final network fusion.

This classification performance is made more significant by the fact that biological samples at visit 1 were taken usually on the first day of hospital admission or patient recruitment. These biological samples are thus taken at the onset of disease, before the development of severe symptoms, and thus show the potential of this technique in terms of predicting patient disease progression and patient triaging. Clustering via a similarity network fusion - spectral clustering pipeline is efficient when data can be classified according to significantly different classes (no disease -> severe disease).

Following this, an analysis of the COVID-19 patient network can reveal a number of important factors (figure 3A) that can then be analysed to reveal a number of biological pathways (figure 3B) that are of importance between the severe COVID-19 cluster and the moderate COVID-19 cluster. Most of these pathways relate to the immune systems, complement activity, and coagulation pathways, all of which are known to be highly involved in acute COVID-19 disease (see Section I, chapter 2 for more details). The top features from the clinical laboratories is also confirmatory of the existing literature, with increased levels of neutrophils (neutrophilia), decreased or absent basophils (basopenia), and the presence of immature erythroblasts in the peripheral blood indicative of the body's severe, dysregulated response to COVID-19. INR, a measure of blood clotting, and total bilirubin, a marker of liver function, can also be elevated in severe cases.

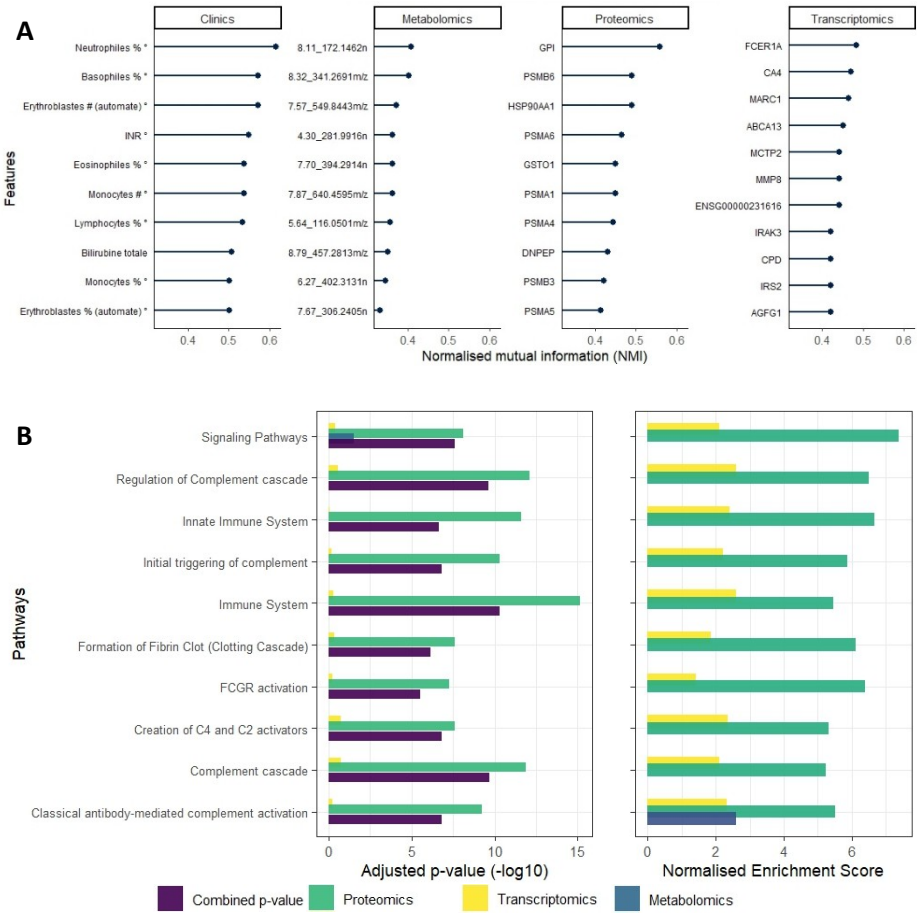


Figure 3: Top features (A) and pathways (B) between predicted cluster 1 (mostly moderate COVID-19) and cluster 2 (mostly severe COVID-19 patients).

Proteomic and transcriptomic features converted from Uniprot and ENSEMBL IDs to gene name where possible. Metabolomic features converted to HMDB IDs where possible (none of the top 10 features could be confidently converted to a HMDB ID). Pathway identification was conducted using multi-GSEA on Uniprot IDs for proteomic features, ENSEMBL IDs for transcriptomic features, and HMDB IDs for metabolomic features.

The same process could be applied to investigate PASC, by generating and clustering a patient network, and identifying features of importance to between those patient clusters (figure 4). However, this approach was decided against, and instead, the network biology approach outlined in Section V was put forth. The reasons for this were that as discussed earlier, SNF works best when patients/nodes can cluster in significantly distinct categories (i.e. severe COVID-19 vs moderate COVID-19), and as categories become less distinct and more subtle (i.e. severe flu vs severe COVID vs moderate COVID vs healthy controls), the technique losses its ability to distinguish and form correct clustering. This was assessed in figure 4A, whereby PASC and non-PASC patients as visit 2 were assessed and clustered in an unsupervised manner, but the clustering was unable to accurately separate these two groups (NMI = 0.04). This may be due to the molecular subtilty of PASC causing it difficult to separate patients based on these signals, or it may be due to the sample size of the cohort. Whilst it would be possible to create a PASC network and find patient clusters, as seen in figure 4B and 4C, the significance of the clustering and results is called into question based on the results from figure 4A, especially as inter-PASC clusters are likely to be less significantly differential than PASC vs non-PASC clusters, in addition to the small sample size resulting from such granularity.

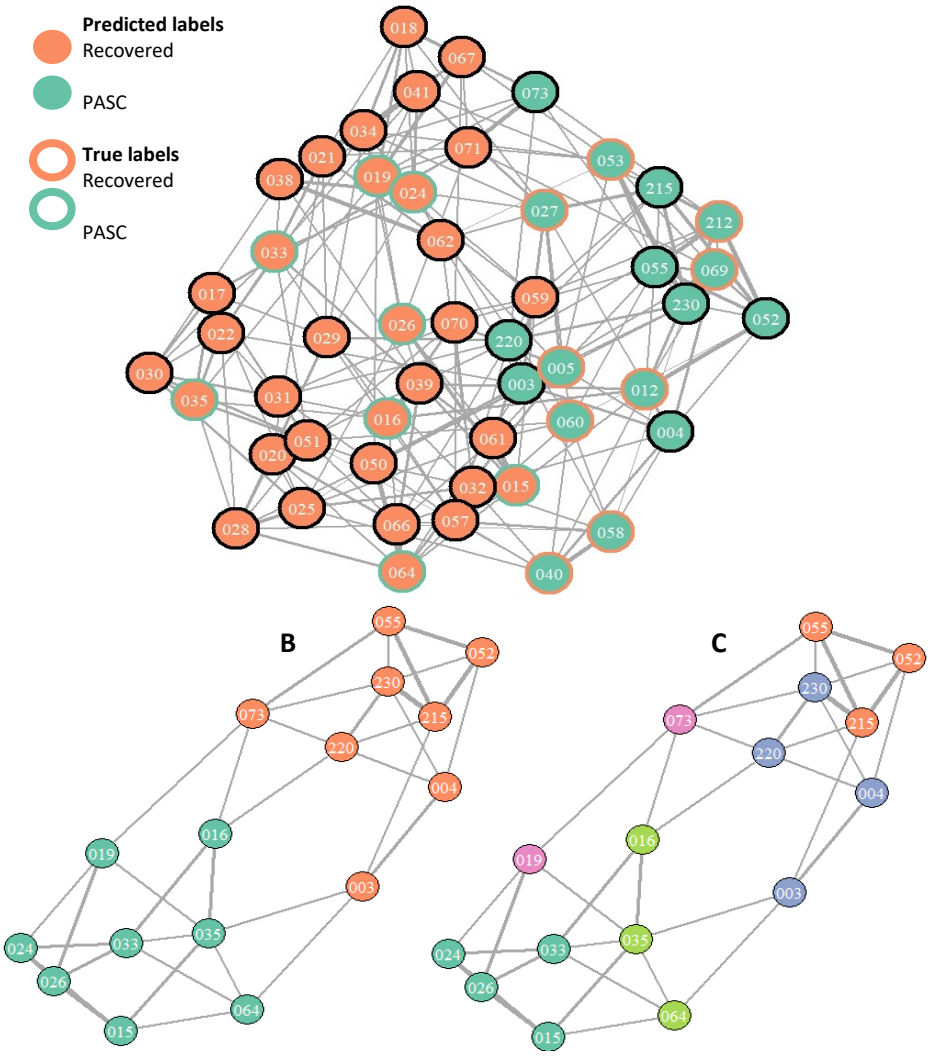


Figure 4: Similarity network fusion of COVID-19 patients at visit 2.
Clustering performance can be seen between recovered and PASC patients (A) and compared to the true labels (as assessed by medical professionals), achieving a very week score of 0.04 (close to random assignment). PASC-only networks can also be assessed in network B (2 clusters based on Eigen-gap cluster estimation) and network C (5 clusters based on rotation cost cluster estimation). Node colouring of networks B and C does not relate to any known medical values and is used only to distinguish one identified cluster from another.

The MOFA (Multi-Omics Factor Analysis) methodology[5] was also assessed in its ability to separate PASC and recovered patients in an unsupervised manner (figure 5A). MOFA can be thought of as an extension of PCA in that it relies on dimensional reduction. It is a Bayesian multi-view factor model that integrates multiple omics data sets in an unsupervised way to learn a small set of latent factors capturing the principal biological (and technical) sources of variation across views and samples. The methodology could be used to extract features of importance related to identified factors capable of separating patients based on PASC status (figure 5B). However, it was decided that supervised methods, like those used in Section V, would be superior for the investigation of PASC, when patient phenotypes (PASC vs recovered) had already been identified by competent medical professionals. However, in the case of novel disease, or when patient phenotypes are unknown, the methods described above (MOFA, SNF), could be viable techniques to integrate multi-omic data and rapidly identify patient subgroups that are not immediately obvious or understandable to the medical community. Indeed, if the study population of PASC patients here was larger, these techniques may have offered a glimpse at the molecular intricacies between PASC phenotypes as has been suggested in other studies.

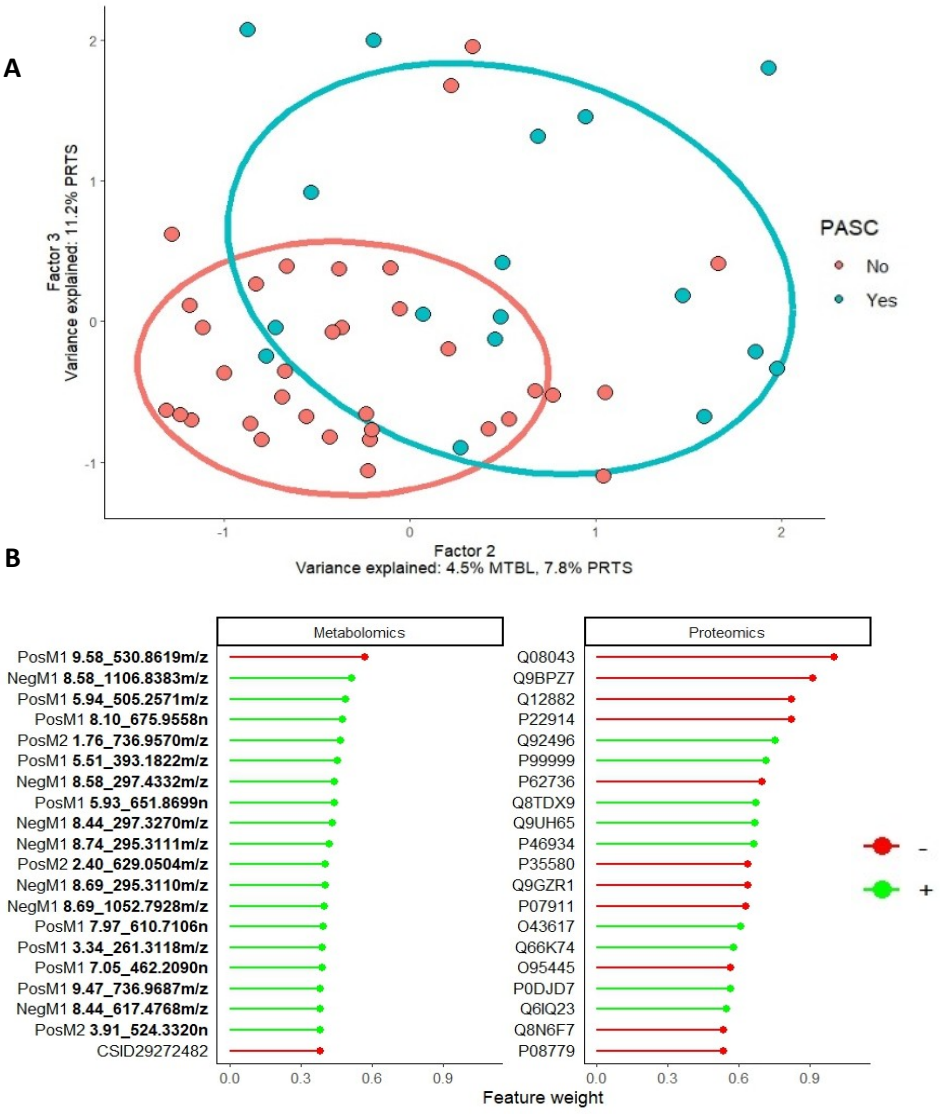


Figure 5: MOFA multi-omic analysis of proteomic, metabolomic, and transcriptomic data. Factors 2 and 3 were found to separate PASC and recovered patients at visit 2 most and thus were selected for PCA visualisation (A). Metabolomic and proteomic data features contributed the most to these factors, with the contribution of transcriptomic data variability being negligible. Factors 2 was selected for further analysis due to having the best PASC vs recovered separation, and top contributing features to this factor were visualised in plot B, showing either positive (green) or negative (red) contribution. Feature weight is scaled to 0-1.

References

1. Wang B, Mezlini AM, Demir F, et al. Similarity network fusion for aggregating data types on a genomic scale. *Nat Methods*. 2014;11(3):333-337. doi:10.1038/nmeth.2810
2. Yang M, Matan-Lithwick S, Wang Y, De Jager PL, Bennett DA, Felsky D. Multi-omic integration via similarity network fusion to detect molecular subtypes of ageing. *Brain Communications*. 2023;5(2):fcad110. doi:10.1093/braincomms/fcad110
3. Miranda J, Paules C, Noell G, et al. Similarity network fusion to identify phenotypes of small-for-gestational-age fetuses. *iScience*. 2023;26(9):107620. doi:10.1016/j.isci.2023.107620
4. Zhang Y, Hu X, Jiang X. Multi-View Clustering of Microbiome Samples by Robust Similarity Network Fusion and Spectral Clustering. *IEEE/ACM Trans Comput Biol and Bioinf*. 2017;14(2):264-271. doi:10.1109/TCBB.2015.2474387
5. Argelaguet R, Velten B, Arnol D, et al. Multi-Omics Factor Analysis—a framework for unsupervised integration of multi-omics data sets. *Molecular Systems Biology*. 2018;14(6):e8124. doi:10.15252/msb.20178124

Supplementary information 4: Supplementary methodology relating to section V

Patient cohort composition, sample collection, and storage

Participants for this analysis were selected from the HYGIEIA cohort [1]. The cohort comprised 25 healthy individuals, 24 influenza patients, 50 moderate COVID-19 cases (defined as non-hospitalised, WHO clinical Progression Scale score <4), and 57 severe COVID-19 patients (hospitalized, WHO Clinical Progression Scale score >4) recruited from Cliniques Universitaires Saint-Luc and Grand Hôpital de Charleroi [2]. Enrolment occurred from August 2020 to March 2024. Ethical approval was obtained from the local ethics committee (reference 2021/30DEC/543), and the study protocol is registered on ClinicalTrials.gov (identifier NCT05557539).

Participant samples and medical data were collected at two time points, first at participant inclusion (usually one day after admission for hospitalised patients, or during acute disease for non-hospitalised patients) and again at a second time point during convalescence. 80% of participants completed both visits, resulting in follow-up samples from 24 healthy controls, 16 influenza patients, 46 moderate COVID-19 patients, and 38 severe COVID-19 patients, with an average interval of 81 days between sampling events. At each time point, study nurses collected the following samples/data: one tube whole blood 4 mL EDTA K3E S-Monovette (Sarstedt, Germany); one tube whole blood 4 mL Lithium heparin gel prepared S-Monovette (Sarstedt, Germany); Tempus Blood RNA Tube (Thermo Fisher Scientific, USA); patient signs and symptoms recorded as part of a patient medical questionnaire. Additional information was also collected from medical data bases including full medical histories, pre-existing conditions and comorbidities, medications taken, treatment prescribed before/during hospitalisation, blood-based clinical laboratory data from hospitalisation, physiological vital parameters during hospitalisation/inclusion.

Immediately following sample collection, samples were transported in a cold box to a pre-analytical laboratory for processing. Tempus blood and EDTA blood were aliquoted, flash frozen (liquid nitrogen), and stored at -80°C. Plasma was separated from lithium heparin

blood via centrifugation (2600g for 10 minutes at 4°C) (Sigma 3-16KL, Sigma Laboratory Centrifuges, Osterode am Harz, Germany), then aliquoted, flash frozen (liquid nitrogen), and stored at -80°C. Time from sample collection to storage was kept under 2 hours for all sample types.

To avoid unintentional batch effects in the data generation phase, sample batches were randomly created programmatically, ensuring patient sex, cohort group (healthy, flu, mild COVID, severe COVID), sample collection date, and visit number of samples was consistent as regarding the cohort as a whole.

Clinical and medical parameters

Clinical data and biological parameters were collected systematically at each study visit by a registered nurse. Additionally, comprehensive clinical histories and patient medical records were obtained via detailed review of digital hospital documentation by clinical researchers. Collected data encompassed patient demographics, clinical severity classifications (WHO Clinical Progression Scale scores), hospitalization details (admission, discharge, ICU stays), medical history, symptomatology (including respiratory, neurological, gastrointestinal, cardiovascular, and general symptoms), comorbidities, medication use, vaccination status, and treatment interventions (oxygen therapy, ventilation support, ECMO, vasopressors, renal replacement, tracheostomy, and antibiotic treatments).

Further, all routine laboratory data from clinical blood and biochemical analyses when performed on the participants during hospitalisation and/or study visits were also recorded. The data encompass coagulation parameters (activated partial thromboplastin time [APTT], prothrombin time [PT], international normalized ratio [INR]), complete blood counts (haemoglobin, haematocrit, erythrocyte parameters, leukocyte differential, platelet counts), inflammatory biomarkers (CRP, procalcitonin, ferritin, fibrinogen, D-dimer), renal and hepatic function tests (urea, creatinine, glomerular filtration rate [eGFR], electrolytes, bilirubin, AST, ALT, alkaline phosphatase), metabolic parameters (glucose, albumin, lipids, lactate dehydrogenase [LDH], creatine kinase [CK]), hormonal assays (TSH,

free T4), and infection-specific parameters (SARS-CoV-2 viral load, anti-SARS-CoV-2 antibody levels). Blood gas measurements, including acid-base status and respiratory function (pH, bicarbonate, arterial oxygen and carbon dioxide tensions, oxygen saturation), and specialized hematological and biochemical markers (e.g., troponin-T, NT-proBNP, vitamin D, HbA1c, immunoglobulins, complement levels, and autoantibodies) were also documented.

Wet lab methodology

DNA extraction and whole exome sequencing

DNA was extracted from EDTA blood using QIAamp DNA Blood Mini Kit (Qiagen, Germany) in random batches of 16 as previously described. 400 µL EDTA blood and 40 µL QIAGEN protease was combined and homogenised via pipetting. 400 µL buffer AL was then added, pulse-vortexed for 20 seconds, briefly spun-down (3–5 seconds) in a benchtop mini-centrifuge, then incubated for 10 minutes as 56°C. Following, samples were spun down and 400 µL absolute ethanol was added. Samples were then pulse-vortexed for 20 seconds and spun down again briefly. Subsequently, 600 µL of mixture was transferred onto a QIAamp Mini spin column, then centrifuged at 6,000 × g for 1 minute and flow-through was discarded. This step was repeated twice for a total of 1200 µL sample mixture. Columns were then transferred to a new collection tube and 500 µL buffer AW1 was added to each column, followed by centrifugation at 6,000 × g for 1 minute. After discarding flow-through, columns were placed in new collection tubes and washed with 500 µL buffer AW2, followed by centrifugation at 20,000 × g for 3 minutes. Flow-through was discarded, and columns underwent an additional centrifugation at 20,000 × g for 1 minute to remove residual buffer. For DNA elution, columns were transferred to 1.5 mL DNase-free tubes and DNA was eluted by adding 100 µL AE buffer directly onto the membrane, incubating at room temperature (15–25°C) for 5 minutes, then centrifuging at 6,000 × g for 1 minute. Eluted DNA was reapplied to the column, incubated, and centrifuged again to maximize DNA recovery.

Library preparation and sequencing for WES were performed using the Twist Human Core Exome (+RefSeq) system (Twist Bioscience, USA), following the manufacturer's recommended protocols. Briefly, 50 ng total gDNA in 10 µL was added to 40 µL enzymatic fragmentation master mix and placed within a thermo cycler at 32°C for 22 minutes, followed by 65°C for 30 minutes. 5 µL Twist Universal Adapters was then added to each tube, followed by 45 µL of ligation master mix (prepared according to manufacturer) and gently mixed before incubation in thermal cycler at 20°C for 15 minutes. DNA was subsequently purified using 80 µL of the provided DNA magnetic purification beads in two cycles of 200 µL 80% ethanol wash, followed by 5 minutes air-drying. DNA was then eluted from beads using 17 µL buffer EB; 15 µL was then transferred to new tube. Adapter-ligated libraries were PCR amplified using 10 µL Twist Unique Dual Indexed (UDI) Primers and 25 µL Equinox Library Amp Mix, following recommended conditions (98°C for 45 sec; 7 cycles of 98°C for 15 sec, 60°C for 30 sec, and 72°C for 30 sec; final extension at 72°C for 1 min), then purified with 50 µL of purification beads and eluted in 22 µL Buffer EB as previously described, resulting in 20 µL Amplified Indexed Libraries transferred to a new tube.

Amplified and indexed libraries were quantified and pooled (8-plex) using 187.5ng indexed library (1500 ng total mass per pool). Pools were then vacuum-concentrated with no heat then resuspended in 5 µL blocker solution and 7 µL universal blocker. Hybridisation probe solution was prepared according to manufactures protocol using Core Exome and RefSeq panel. Both probe solution and library pool were then heated to 95°C for 2 minutes and 5 minutes respective, before equilibration to room temperature. Probe solution was then added to the library pool followed by 30 µL Hybridization Enhancer, samples were then hybridized at 70°C for 16 hours. Following hybridization, probe-target complexes were captured on pre-washed streptavidin-coated magnetic beads, gently mixed for 30 minutes at room temperature, then washed once with 200 µL wash buffer 1 and three times with 200 µL wash buffer 2 at 48°C, followed by resuspension in 45 µL water to form bead slurry.

Post-capture amplification was carried out using 22.5 µL Streptavidin Binding Bead Slurry, 25 µL Equinox Library Amplification Mix and 2.5 µL Twist Amplification Primers, with PCR

settings according to manufacturer recommendations (98°C for 45 sec; 8 cycles of 98°C for 15 sec, 60°C for 30 sec, 72°C for 30 sec; and a final extension at 72°C for 1 min). The final enriched libraries were purified using 50 µL DNA purification beads, two washes of 200 µL 80% ethanol, and elution in 32 µL buffer EB, of which 30 µL was transferred to a clean tube. Libraries were quality controlled using Picogreen (Thermo Fisher Scientific, USA) and Tapestation D1000 screen tape (Agilent, USA). Sequencing was subsequently carried out on a Novaseq 6000 platform to a target depth of 5Gb, 50x mappable, 151 paired-end reads.

Whole Transcriptomic Shotgun RNAseq

Total RNA was isolated from whole-blood samples collected in Tempus RNA tubes using the Tempus™ Spin RNA Isolation Kit (cat.# 4380204, Thermo Fisher Scientific, USA) in batches of 20. Approximately 3 mL of blood was transferred into sterile 15 mL Falcon tubes along with 1 mL of PBS (Ca^2+/Mg^2+-free). The tubes were vortexed for 30 seconds and subsequently centrifuged at 3,000 × g for 30 minutes at 4°C. Following, the supernatant was discarded and tubes inverted 2 minutes to drain residual liquid, after which residual fluid at the rim was gently removed. RNA pellets were resuspended with 400 µL RNA purification resuspension solution, then solution was transferred onto a pre-wetted RNA purification filter column. Samples were incubated on filters for 2 minutes, then centrifuged at 16,000 × g for 30 seconds. The flow-through was discarded, and filters were washed once with 500 µL RNA purification wash solution 1, followed by two washes with 500 µL RNA purification wash solution 2, centrifuging each time at 16,000 × g for 30 seconds. After a final drying centrifugation step at 16,000 × g for 30 seconds, each column was transferred to a new collection tube. RNA was eluted by adding 100 µL Nucleic Acid Purification Elution Solution, incubating for 2 minutes at 70°C, and centrifuging at 16,000 × g for 30 seconds. The elution was repeated by adding the same eluate back onto the filter and centrifuging again at 18,000 × g for 2 minutes. Finally, 90 µL of the eluted RNA was carefully transferred to new RNase-free tubes without disturbing any residual pellet.

Extracted RNA samples underwent further purification using the RNA Clean & Concentrator-5 Kit (cat.# R1013, Zymo Research, USA). Briefly, each sample was treated

with 11.25 µL DNA Digestion Buffer and 11.25 µL reconstituted DNase I enzyme, vortexed briefly, and incubated at room temperature for 15 minutes. Post-treatment clean-up involved the addition of 225 µL RNA binding buffer and 450 µL absolute ethanol, followed by loading onto Zymo-spin IC columns in two steps. For each step, 450 µL of the sample was added to the column, centrifuged at 16,000 × g for 30 seconds, and flow-through discarded. Filters were then washed sequentially using 400 µL RNA prep buffer, followed by washes with 700 µL and 400 µL RNA wash buffer, each centrifuged at 16,000 × g for 30 seconds to 1 minute. RNA was finally eluted by adding 25 µL 60°C DNase/RNase-free water to the filter, incubating for 5 minutes at room temperature, and centrifuging at 16,000 × g for 30 seconds each time. Elution step was repeated twice for a total of 50 µL elute.

Library preparation and sequencing for RNA-seq from whole blood were performed using a combination of the Illumina Globin-Zero Gold Kit (Illumina, USA) for rRNA/globin mRNA depletion, followed by the TruSeq Stranded mRNA protocol (Illumina, USA) for library construction. Briefly, 1 µg of DNA-free total RNA in 26 µL RNase-Free Water was combined with 4 µL Globin-Zero Gold Reaction Buffer, and 10 µL Globin-Zero Gold Removal Solution. After thorough mixing, each sample was heated at 68 °C for 10 minutes, briefly cooled to room temperature, then incubated for a further 5 minutes. Following probe hybridisation, 65 µL of thoroughly washed magnetic beads (room-temperature-equilibrated) were added to each reaction. The mixture was then pipette-mixed, rapidly vortexed for 10 seconds, and incubated for 5 minutes at room temperature and an additional 5 minutes at 50 °C. The tubes were then placed on a magnetic stand for 1 minutes, and the supernatant was carefully transferred to new tubes.

Depleted RNA was subsequently purified and concentrated via ethanol precipitation. Sample volumes were adjusted to 180 µL using RNase-Free Water. 18 µL of 3 M sodium acetate and 2 µl of glycogen (10 mg/ml) were then added and the tube gently vortexed, followed by 600 µl of ice-cold 100% ethanol. Tubes were again gently vortexed and placed at -20 °C for 1 hour, then centrifuged at 10,000 x g for 30 minutes, after which

supernatant was discarded. The resulting pellet was then washed twice with ice-cold 70% ethanol and then air dried at room temperature for 5 minutes.

For subsequent library preparation, the final pellet was thoroughly dissolved in 18 µL FPF (Fragment, Prime, Finish Mix), followed by fragmentation at 94 °C for 8 minutes in a thermal cycler, cooling on ice, then collection by quick centrifugation. After, add 8 µL of First Strand Synthesis Act D Mix (FSA) containing reverse transcriptase (SuperScript II) to the RNA/FPF mixture and place sample in thermo cycler under recommended conditions (25 °C for 10 minutes, 42 °C for 15 minutes, 70 °C for 15 minutes). After first-strand cDNA synthesis, add 20 µL of Second Strand Marking Master Mix (SMM) to each sample, mix slowly, then incubate at 16 °C for 60 minutes in a thermal cycler. Once the incubation is complete, add 90 µL of resuspend AMPure XP beads and mix thoroughly, then let the mixture incubate at room temperature for 10–15 minutes. After incubation, wash the pellet twice in 200 µL of freshly prepared 80% ethanol, using a magnetic stand and discarding the supernatant each time, then let beads air-dry for about 15 minutes on magnetic stand. Remove samples from the magnetic stand and elute cDNA using 17.5 µL of Resuspension Buffer (RSB), then carefully transfer 15 µL of the supernatant to a fresh tube. Blunt-ended cDNA fragments were adenylated by adding 2.5 µL diluted CTA (A-Tailing Control) and 12.5 µL ATL (A-Tailing Mix) to each sample. The samples were thoroughly mixed and incubated at 37°C for 30 minutes followed by 5 minutes at 70°C. Reactions were rapidly cooled on ice for 1-minute post-incubation. Indexed adapters were ligated to the adenylated cDNA fragments by adding 2.5 µL diluted CTL (Ligation Control), 2.5 µL LIG (Ligation Mix), and 2.5 µL RNA adapters to each sample. Samples were thoroughly mixed, then incubated at 30°C for 10 minutes, after which they were placed on ice and 5 µL STL (Stop Ligation Buffer) was added. Ligated fragments were cleaned using two rounds of AMPure XP bead purification (first with 42 µL, second with 50 µL), in which beads were added to samples, incubated for 15 minutes, washed twice with 200 µL 80% ethanol, and eluted into RSB (first with 52.5 µL, second with 22.5 µL). Finally, 20 µL of RSB was transferred to a fresh PCR plate. Adapter-ligated fragments were enriched using PCR by adding 5 µL PCR Primer Cocktail (PPC) and 25 µL PCR Master Mix (PMM) to each sample, followed by mixing, then thermal cycling with initial denaturation at 98°C for 30

seconds, 15 cycles of amplification (98°C for 10 seconds, 60°C for 30 seconds, 72°C for 30 seconds), and final extension at 72°C for 5 minutes. Post-PCR clean-up involved adding 47.5 µL AMPure XP beads, washing twice with 80% ethanol, and eluting in 32.5 µL RSB, followed by transferring 30 µL elute to a new target sample plate.

Libraries were quality controlled using Picogreen (Thermo Fisher Scientific, USA) and Tapestation D1000 screen tape (Agilent, USA). Final libraries were normalized to a concentration of 10 nM in 10 mM Tris-HCl, pH 8.5 with 0.1% Tween 20. Normalized libraries were subsequently pooled in equal volumes to create a final sequencing pool. Pooled libraries were finally sequenced on a Novaseq 6000 (Illumina, USA) to a target depth of 30M 151 paired-end reads.

DIA Shotgun Proteomics

Plasma samples were processed according to our published protocol in batches of 16 [3]. Briefly, 600 µL of High Select Top14 Abundant Protein Depletion Resin (Thermo Fisher Scientific, USA) was equilibrated at room temperature, mixed gently with 22 µL of plasma, and incubated on a rotational mixer (12 rpm) for 10 min at room temperature. The resin-sample mixture was then transferred onto Pierce™ Micro-Spin columns (Thermo Fisher Scientific, USA) and centrifuged at 1000 × g for 2 minutes, with the depleted protein collected as flow-through.

The flow-through then underwent thermal denaturation at 95°C for 5 minutes, then cooled at room temperature. Proteins were reduced by adding 33 µL 50 mM DL-dithiothreitol (5 mM final concentration) and incubating at 56°C for 1 hour with shaking at 1000 rpm. Alkylation followed by adding 37µl of 500mM chloroacetamide (50 mM final concentration) and incubating for 30 min at room temperature in the dark. Proteins were precipitated using 65.5µl 100% trichloroacetic acid (15% final concentration), incubated on ice for 30 minutes, pelleted at 4000 × g for 7.5 minutes, and the resulting pellet washed three times with 500 µL -20°C acetone. After air-drying for 10 mintues, pellets were resuspended in 75µL 50 mM triethylammonium bicarbonate, sonicated twice at 37kHz

pulsed for 2 minutes, and digested overnight with 2.5 µg sequencing grade modified trypsin (V5117, Promega, United States) at 37°C, 750 rpm.

Following digestion, peptides were acidified by adding 8.3 µL of 1% trifluoroacetic acid (final concentration 0.1%) and 80 µg total peptide immediately loaded onto a Pierce High pH Reversed-Phase Peptide Fractionation column (Thermo Fisher Scientific, USA). Columns were centrifuged at 3000 × g for 2 minutes, flow-through discarded, and columns washed once with 300 µL MS-grade water at 3000 × g for 2 minutes. Peptides were sequentially eluted into seven fractions using solutions of increasing acetonitrile concentration (7.5%, 10%, 12.5%, 15%, 17.5%, 20%, and 50%), each containing 0.1% triethylamine. Fractionation was performed by centrifugation at 3000 × g for 2 minutes for each elution step.

Fractions were strategically pooled: fractions 1, 2, and 5 (100 µL each) were combined as pooled fraction 1; fractions 3 and 6 (150 µL each) as pooled fraction 2; and fractions 4 and 7 (150 µL each) as pooled fraction 3. The pooled samples were briefly frozen on dry ice for 5 minutes, then fully evaporated at 4°C using a vacuum concentrator at 4°C. Each dried pooled fraction was resuspended in 20 µL MS resuspension buffer (3.5% acetonitrile, 0.1% trifluoroacetic acid), sonicated three times at 37 kHz pulsed for 2 minutes, briefly vortexed, and spun down prior to LC-MS/MS analysis.

Peptides (1 µg per injection) were loaded onto a reversed-phase pre-column (Acclaim PepMap 100, Thermo Fisher Scientific, USA) and separated using an EasySpray analytical column (Acclaim PepMap RSLC C18, 0.075 × 250 mm, Thermo Fisher Scientific, USA). Separation employed a 120-minute gradient at 300 nL/min on an Ultimate 3000 RSLC nanoHPLC system (Thermo Fisher Scientific, United States): solvent B (0.1% TFA in 80% ACN) was linearly increased from 4% to 32% over 100 minutes, then raised to 50% over 5 minutes, increased further to 90% in the next 5 minutes, and maintained at 95% for the final 9 minutes.

Peptides were detected in the Orbitrap at a resolution of 30,000 (FWHM). MS/MS spectra were acquired using stepped higher-energy collisional dissociation (HCD) at 22%, 26%, and

30% of maximum. A data-independent acquisition (DIA) approach was employed to scan precursor ions across an m/z range of 500–740 with a 4 m/z isolation window at a resolution of 60,000 (FWHM). MS1 spectra were recorded with an automatic gain control (AGC) target of 1.2 × 10^6 ions and a maximum injection time of 55 ms, while MS2 spectra were collected with an AGC target of 1.5 × 10^5 ions and an automatically set maximum injection time, covering an m/z range of 145 to 1450. Each injection had a run time of 120 minutes.

Shotgun Metabolomics

Plasma samples were processed in batches of 18. 200 µL plasma was combined with 600 µL -20°C acetone (with internal standards at 50 µM) and vortexed vigorously for 10 seconds. Samples were then sonicated at 37 kHz pulsed for 2 minutes, then centrifuged at 10,000 x g at 4°C for 10 minutes. Carefully, 560 µL of the upper-phase was transferred to a clean tube. For the tube containing the lower-phase and pellet, 600 µL (without internal standards) was added, vortexed vigorously, sonicated at 37 kHz pulsed for 2 minutes, then centrifuged at 10,000 x g for 10 minutes at 4°C. 560 µL of the resulting upper-phase was then combined with the previously extracted upper-phase and vortexed to combine. The upper-phase mixture was then aliquoted into 280 µL samples, and all aliquots were dried down on a heating block at 30°C with nitrogen flush system. Two sample aliquots were then resuspended in 50% acetonitrile/0.1% formic acid, specifically prepared for reverse-phase chromatography. Two additional aliquots were then resuspended in 95% acetonitrile containing 0.1% formic acid and 10 mM ammonium formate, designed for hydrophilic interaction chromatography (HILIC). Samples then underwent centrifugation at 10,000 × g for 5 min at 4°C, after which the supernatants were carefully transferred into analytical vials ready for UPLC-MS injection.

Prepared samples were then analysed in three batches of 100, 97, and 55 using a Synapt-XS quadrupole time-of-flight (Q-ToF) mass spectrometer (Waters, USA), operated in resolution mode, coupled to an Acquity Premier UPLC system (Waters, USA). Chromatographic separations were conducted using an Acquity Premier HSS T3 column (2.1 × 100 mm, 1.8 µm particle size; cat.# 186009468, Waters, USA) for reverse-phase

analyses and an Acquity Premier BEH Amide column (2.1 × 100 mm, 1.7 µm particle size; cat.# 186009505, Waters, USA) for HILIC-based separations. Each chromatographic method employed one aliquot analysed in positive electrospray ionization mode and a second aliquot in negative ionization mode.

Bioinformatic pipelines

Proteomics

Raw mass spectrometry data (.mzML files) were initially processed using DIA-NN (v1.8.1) [4]. All files related to the same pooled fraction were processed together, thus in three batches, in order to leverage the homogeneous nature of each fraction to optimize peak detection and noise removal for improved identification and quantification. For each fraction, the DIA-NN analysis was performed with an in-silico predicted spectral library generated from the UniProtKB human reference proteome (accession UP000005640) filtered to include only reviewed (Swiss-Prot) canonical proteins [5]. The analysis was configured for library-free search with FASTA digestion; deep learning–based prediction of spectra, retention times (RTs), and ion mobilities (IMs); and employed customized parameters including a precursor FDR cutoff of 1%, fixed mass ranges for fragment (200–1800 m/z) and precursor ions (300–1800 m/z), N-terminal methionine excision, tryptic digestion with cuts at K* and R*, a maximum of 1 missed cleavage, and variable oxidation of methionine (UniMod:35, +15.994915 Da). Additional parameters were set to enable double-search mode, reanalysis, relaxed protein inference, smart profiling and peak centering.

R (v4.3.1) was used to process the precursor quantification data generated by DIA-NN for the three pooled fractions. Zero values were recoded as missing (NA) and data cleaning was then performed. Here, a logistic regression model was applied to each feature using clinical covariates of interest (cohort disease group, PASC development, and visit) as predictors of feature presence; features with a significant association (adjusted p-value ≤0.01) and less than 75% missing values were classified as missing not at random (MNAR), while non-significant features with less than 30% missing values were classified as missing

at random (MAR); all other features were removed. The use of these missing value thresholds ensured that only features with sufficient data coverage were retained for downstream analysis. Next, missing values were imputed using a mixed strategy: random forest imputation for MAR values and quantile regression imputation of left-censored data (QRILC) for MNAR values, ensuring robust recovery of low-abundance signals. The resulting imputed data were merged into a single combined dataset, which was subsequently log-transformed and normalized via variance stabilization normalization (VSN) using QFeatures [6]. Finally, precursor-level intensities were aggregated to the protein level via robust summary method (robust M-estimation) from MsCoreUtils using QFeatures, based on protein group annotation, resulting in the final abundance matrix used for downstream statistical analyses [6,7].

Metabolomics

Raw data files generated by the Waters Synapt-XS mass spectrometer were imported into Progenesis QI (V4.2, Nonlinear Dynamics, UK) for pre-processing. Here upon, lock mass correction as performed (based on theoretical m/z of leucine enkephalin) and raw spectra were converted to a 2D ion intensity map. Feature detection was carried out via peak picking, identifying ion features based on accurate mass and retention time (RT). A reference run from a pool representative of all the samples was selected to guide alignment, compensating for RT shifts and ensuring consistent feature matching. Following alignment, the software deconvoluted adducts and grouped isotopes, resulting in a list of retention time–m/z features. This feature list was exported for downstream bioinformatics analyses.

Raw abundance values generated by Progenesis QI were imported into R (v4.3.1). Zero values were recoded as missing (NA), and features were assessed as MNAR or MAR as previously described for proteomics, with the caveat that features present in fewer than 10% of samples within any MS/MS batch were removed to minimise batch effects. Missing values were imputed using random forest imputation for MAR values and QRILC for MNAR values, and imputed data were then log-transformed and normalized using VSN in the same manner as for proteomics. Following this, MS/MS batch correction was performed

using the ComBat method from the sva package [8]. Finally, metabolite identifications from Progenesis QI were used to annotate features (if known), and known metabolites were aggregated using a robust summary method as previously described for proteomics, yielding the final abundance matrix for downstream statistical analyses.

Transcriptomics

Raw fastq files were initially processed using a standard RNA-seq pipeline, where low-quality bases were trimmed with Trimmomatic (v0.39) and reads were aligned to the GRCh38 human genome using HISAT2 (v2.2.1) [9,10]. Gene-level expression was quantified with featureCounts from Subread (v2.0.3) using the Homo_sapiens.GRCh38.105.chr.gtf annotation [11].

The resulting raw count matrices were loaded into R (v4.3.1), and transformed into a DESeq2 using sample metadata, consisting of biological variables of interest for various design formulas [12]. Variance stabilising transformation (VST) was applied to generate normalized count matrices, which were subsequently used for downstream transcriptomic analyses.

Genomics

Raw paired-end fastq files were processed using a complete NGS pipeline to generate variant annotations. Genomic reads were aligned to the human reference genome GRCh38 using BWA-mem (v0.7.17) [13]. Resulting BAM files underwent duplicate removal with SAMTools (v1.12) and base quality recalibration using GATK BaseRecalibrator (v4.2.1) [14,15]. Germline single nucleotide variants (SNVs) and short INDELs were called sample-by-sample using GATK HaplotypeCaller [14]. Structural variations were detected by combining "read depth" (ExomeDepth) with "split read" (GRIDSS-Purple-Linx) [16,17]. The resulting VCF files were normalized with BCFTools (v1.12), filtered according to GATK best practices, and annotated with snpEff (v5.0e) [14,18,19]. Quality control metrics were gathered using FastQC (v0.11.9) and Mosdepth (v0.3.1) [20,21]. Finally, the normalized and filtered VCF files were imported onto the UCLouvain Highlander database, where variants are fully annotated by in-house algorithms (minor allele frequencies, coding impact predictions, splicing effects,

conservation scores, and gene function, etc) and public databases (currently Ensembl 100, DBNSFP 4.1 and COSMIC 92) [22].

Long-COVID multi-omic modelling

All analyses were conducted in R. For each omic layer, features with near-zero variance were removed using caret::nearZeroVar (default settings) [23]. Proteomic and metabolomic data were analyzed as VSN-normalized intensities; RNA-seq data were analyzed from raw counts using voomWithDreamWeights to obtain observation-level precision weights [24].

For the primary longitudinal analysis, linear mixed models were fit per feature using dream (variancePartition v1.36.3) we tested the PASC status(PASC/recovered) x Visit (1/2) interaction (difference-in-differences: [PASC V2 − PASC V1] − [Recovered V2 − Recovered V1]), with a random intercept for patient ID and covariates (COVID severity (moderate/severe), vaccine status (full vaccination yes/no), sex (male/female), and age (years)) [24]. The pipeline was then re-run for cross-sectional analysis of PASC status at visit 1 and visit 2 independently (not longitudinally) using linear models with empirical-Bayes moderation (limma), adjusting for covariates (Visit 1 analysis: COVID severity (moderate/severe), vaccine status (full vaccination yes/no), sex (male/female), and age (years); Visit 2 analysis: vaccination, sex, and age) [25]. For each fit, per-feature statistics (effect size, standard error, moderated t-statistic, raw p-value) were extracted; multiple testing correction was done via FDR-adjusted p-values. The longitudinal analysis reported statistics for the PASC×Visit interaction contrast; the V1 and V2 analyses reported statistics for the PASC main-effect contrasts.

Multi-omic pathway enrichment was performed separately for V1 and V2 using multiGSEA [26]. Within each omic, features were pre-ranked using the analysis-specific ranking function based on p-values and effect directions. Gene-set collections were obtained for KEGG and Reactome with identifiers mapped per layer (transcripts: Ensembl; proteins: UniProt; metabolites: HMDB) [27,28]. Per-omic GSEA was computed, pathway-level p-values were combined across omics, and combined p-values were adjusted for multiple testing by FDR.

Genomic GWAS and SKAT-O/burden analysis

Annotated SNP data was exported from the Highlander server and data was filtered according to the following details: all QC metrics passed, only autosomes SNPS, read depth > 10, enforced allelic balance 0.20–0.80, only diploid alleles, and consensus prediction score >= 5 (potentially damaging SNP). Per-sample call rate was then filtered to >= 0.95 and per-SNP call rate was filtered to >= 0.95 (in retained samples). SNPs with maximum allele frequency < 0.05 were removed (cohort MAF) and retained SNPs with Hardy-Weinberg exact test p-value > 1×10^{-6}. Monomorphic SNPs were then dropped following filters. Missing genotypes were mean-imputed per SNP (minimal impact at call-rate > 95%). PCA was computed on LD-pruned, position-sorted genotypes (r^2 threshold 0.2; window 1000 SNPs; step 200). Two PC outlier were identified via mahalanobis distance but kept as results were stable with/without inclusion (high Spearman ρ of −log10 p). PC1 was found to account for most of the captured variation, including ethnicity. For the final GWAS model, we tested the association between SNP dosage (0-2, additive) and PASC status (PASC vs recovered) using logistic regression, adjusting for age (years), sex (male/female), and ancestry (PC1). Calibration was assessed with genomic inflation factor λGC and QQ plot.

Following, we tested per-gene burden/variance effects using a gene-level aggregation analysis (SKAT-O from SKAT package) [29]. SNPs were mapped to their associated gene symbols to form per-gene sets (minimum two SNPs per gene). A logistic SKAT null model was built using the same GWAS covariates (Age, Sex, PC1) and case status coded 0/1 (recovered/PASC). SKAT-O was then run using predictive damaging scores (as calculated within Highlander), coinciding with the estimated damage of the SNP (scores were winsorized at the 99th percentile, log1p-transformed, rescaled to [0,1], and floored at $1e^{-3}$).

Network Construction and Multi-Omic Integration

Proteomic, metabolomic, and transcriptomic abundance matrices were analysed separately in the following pipeline. For each omic, differential abundance correlation

testing between recovered and PASC was performed using Differential Gene Correlation Analysis (DGCA) (ddcorALL) [30]. Pearson correlation was used, permutation testing was not used for edge inference. A-priori filtered removed edges with weak correlation or insignificant in both groups (<0.3 absolute correlation, adjusted p-value > 0.01); multiple-testing correction (FDR) was then performed on this reduced set. The resulting z-score difference is used as edge weights to represent the strength of association change.

For each node, we then summarize the magnitude and confidence of its interaction changes between PASC and recovered by aggregating the edge weights of all incident edges within the current network. For each node *n* with incident edges *E*(n) and weights W_e, the raw rewiring score *R*(*n*) is the Euclidean norm:

$$R(n) = \sqrt{\sum_{e \in E(n)} w_e^2}$$

Because node degree differs markedly across omic layers (e.g., RNA >> protein), the raw rewiring score is degree dependent. To overcome this, a degree-matched z-score (DMZ) was then employed to normalise the raw rewiring score within specific degree-matched bins *B(i)* (defined through $\log_2$(degree +1)). Within each bin, raw rewiring scores were z-scored, reflecting how extreme a node's rewiring is relative to degree-matched peers.

$$Z_i = \frac{R(n) - \mu B(i)}{\delta B(i)}$$

Following the creation of the differential correlation networks for each omic, the separate networks were then combined, and prior knowledge networks were incorporated. Metabolite–enzyme edges were incorporated by merging highly predicted protein-metabolite interactions from Recon3D with manually curated KEGG pathway maps [28,31]. Protein–protein interactions were extracted from STRING using all detected proteins from our experiments (~1600) as seed nodes and expanding to all first neighbours (physical subnetworks only, very high confidence (> 900)) [32]. Experimentally validated transcription-factor gene regulations were sourced from the manually curated TRRUST v2 database [33]. miRNA-mediated post-transcriptional interactions were imported from DIANA-TarBase v8,

composed of experimentally supported miRNA targets on protein-coding transcripts with a microT score > 0.7 [34]. Drug-target information was included using the known drug database from OpenTargets, a database of any approved or clinical candidate drug, and its known targets [35]. Finally, a layer incorporating biology central dogma was included, whereby each protein-coding transcript was additionally linked to its translation product, allowing logical traversal between RNA and protein layers.

References

1. Ward B, Yombi JC, Balligand JL, et al. HYGIEIA: HYpothesizing the Genesis of Infectious Diseases and Epidemics through an Integrated Systems Biology Approach. *Viruses*. 2022;14(7):1373. doi:10.3390/v14071373
2. Soriano JB, Murthy S, Marshall JC, Relan P, Diaz JV, WHO Clinical Case Definition Working Group on Post-COVID-19 Condition. A clinical case definition of post-COVID-19 condition by a Delphi consensus. *Lancet Infect Dis*. 2022;22(4):e102-e107. doi:10.1016/S1473-3099(21)00703-9
3. Ward B, Pyr Dit Ruys S, Balligand JL, et al. Deep Plasma Proteomics with Data-Independent Acquisition: Clinical Study Protocol Optimization with a COVID-19 Cohort. *J Proteome Res*. 2024;23(9):3806-3822. doi:10.1021/acs.jproteome.4c00104
4. Demichev V, Messner CB, Vernardis SI, Lilley KS, Ralser M. DIA-NN: neural networks and interference correction enable deep proteome coverage in high throughput. *Nat Methods*. 2020;17(1):41-44. doi:10.1038/s41592-019-0638-x
5. The UniProt Consortium, Bateman A, Martin MJ, et al. UniProt: the Universal Protein Knowledgebase in 2023. *Nucleic Acids Research*. 2023;51(D1):D523-D531. doi:10.1093/nar/gkac1052
6. Laurent Gatto, Christophe Vanderaa. QFeatures. doi:10.18129/B9.BIOC.QFEATURES
7. RforMassSpectrometry Package Maintainer, Laurent Gatto, Johannes Rainer, Sebastian Gibb, Adriaan Sticker, Sigurdur Smarason, Thomas Naake. MsCoreUtils. doi:10.18129/B9.BIOC.MSCOREUTILS
8. Wang M, Huang J, Liu Y, Ma L, Potash JB, Han S. COMBAT: A Combined Association Test for Genes Using Summary Statistics. *Genetics*. 2017;207(3):883-891. doi:10.1534/genetics.117.300257
9. Bolger AM, Lohse M, Usadel B. Trimmomatic: a flexible trimmer for Illumina sequence data. *Bioinformatics*. 2014;30(15):2114-2120. doi:10.1093/bioinformatics/btu170
10. Kim D, Langmead B, Salzberg SL. HISAT: a fast spliced aligner with low memory requirements. *Nat Methods*. 2015;12(4):357-360. doi:10.1038/nmeth.3317
11. Liao Y, Smyth GK, Shi W. featureCounts: an efficient general purpose program for assigning sequence reads to genomic features. *Bioinformatics*. 2014;30(7):923-930. doi:10.1093/bioinformatics/btt656
12. Michael Love SA. DESeq2. Published online 2017. doi:10.18129/B9.BIOC.DESEQ2
13. Li H. Aligning sequence reads, clone sequences and assembly contigs with BWA-MEM. *arXiv*. Preprint posted online 2013. doi:10.48550/ARXIV.1303.3997
14. DePristo MA, Banks E, Poplin R, et al. A framework for variation discovery and genotyping using next-generation DNA sequencing data. *Nat Genet*. 2011;43(5):491-498. doi:10.1038/ng.806
15. Li H, Handsaker B, Wysoker A, et al. The Sequence Alignment/Map format and SAMtools. *Bioinformatics*. 2009;25(16):2078-2079. doi:10.1093/bioinformatics/btp352
16. Plagnol V, Curtis J, Epstein M, et al. A robust model for read count data in exome sequencing experiments and implications for copy number variant calling. *Bioinformatics*. 2012;28(21):2747-2754. doi:10.1093/bioinformatics/bts526
17. Cameron DL, Baber J, Shale C, et al. GRIDSS, PURPLE, LINX: Unscrambling the tumor genome via integrated analysis of structural variation and copy number. *Bioinformatics*. Preprint posted online September 25, 2019. doi:10.1101/781013
18. Cingolani P, Platts A, Wang LL, et al. A program for annotating and predicting the effects of single nucleotide polymorphisms, SnpEff: SNPs in the genome of Drosophila melanogaster strain w1118; iso-2; iso-3. *Fly (Austin)*. 2012;6(2):80-92. doi:10.4161/fly.19695
19. Li H. A statistical framework for SNP calling, mutation discovery, association mapping and population genetical parameter estimation from sequencing data. *Bioinformatics*. 2011;27(21):2987-2993. doi:10.1093/bioinformatics/btr509
20. Pedersen BS, Quinlan AR. Mosdepth: quick coverage calculation for genomes and exomes. Hancock J, ed. *Bioinformatics*. 2018;34(5):867-868. doi:10.1093/bioinformatics/btx699
21. FastQC. Published online June 2015. https://qubeshub.org/resources/fastqc
22. Helaers R, Vikkula M. Highlander: variant filtering made easy. *F1000 Research Limited*. Preprint posted online 2018. doi:10.7490/F1000RESEARCH.1116108.1
23. Kuhn M. Building Predictive Models in *R* Using the **caret** Package. *J Stat Soft*. 2008;28(5). doi:10.18637/jss.v028.i05
24. Hoffman GE, Schadt EE. variancePartition: interpreting drivers of variation in complex gene expression studies. *BMC Bioinformatics*. 2016;17(1):483. doi:10.1186/s12859-016-1323-z
25. Gordon Smyth [Cre A. limma. Published online 2017. doi:10.18129/B9.BIOC.LIMMA
26. Sebastian Canzler, Jörg Hackermüller. multiGSEA. doi:10.18129/B9.BIOC.MULTIGSEA
27. Milacic M, Beavers D, Conley P, et al. The Reactome Pathway Knowledgebase 2024. *Nucleic Acids Research*. 2024;52(D1):D672-D678. doi:10.1093/nar/gkad1025
28. Kanehisa M. KEGG: Kyoto Encyclopedia of Genes and Genomes. *Nucleic Acids Research*. 2000;28(1):27-30. doi:10.1093/nar/28.1.27
29. Wu MC, Lee S, Cai T, Li Y, Boehnke M, Lin X. Rare-variant association testing for sequencing data with the sequence kernel association test. *Am J Hum Genet*. 2011;89(1):82-93. doi:10.1016/j.ajhg.2011.05.029
30. McKenzie AT, Katsyv I, Song WM, Wang M, Zhang B. DGCA: A comprehensive R package for Differential Gene Correlation Analysis. *BMC Syst Biol*. 2016;10(1):106. doi:10.1186/s12918-016-0349-1

31. Brunk E, Sahoo S, Zielinski DC, et al. Recon3D enables a three-dimensional view of gene variation in human metabolism. *Nat Biotechnol*. 2018;36(3):272-281. doi:10.1038/nbt.4072
32. Szklarczyk D, Gable AL, Lyon D, et al. STRING v11: protein-protein association networks with increased coverage, supporting functional discovery in genome-wide experimental datasets. *Nucleic Acids Res*. 2019;47(D1):D607-D613. doi:10.1093/nar/gky1131
33. Han H, Cho JW, Lee S, et al. TRRUST v2: an expanded reference database of human and mouse transcriptional regulatory interactions. *Nucleic Acids Research*. 2018;46(D1):D380-D386. doi:10.1093/nar/gkx1013
34. Karagkouni D, Paraskevopoulou MD, Chatzopoulos S, et al. DIANA-TarBase v8: a decade-long collection of experimentally supported miRNA–gene interactions. *Nucleic Acids Research*. 2018;46(D1):D239-D245. doi:10.1093/nar/gkx1141
35. Buniello A, Suveges D, Cruz-Castillo C, et al. Open Targets Platform: facilitating therapeutic hypotheses building in drug discovery. *Nucleic Acids Research*. 2025;53(D1):D1467-D1475. doi:10.1093/nar/gkae1128

Supplementary information 5: Supplementary results relating to section V

This section details some supplementary results that were not included in the main manuscript. Figure 1 details the volcano plots of the three PASC vs recovered models that were used in the analysis: A shows longitudinally differentially expressing features, B shows differentially expressed features at visit 1, and C shows differentially expressed features at visit 2. Figure 2 then shows the top multiGSEA results relating to these three models. Figure 3 shows the genome-wide association Manhattan plot of snps related to the development of PASC.

Finally, in regards to the logistic regression model employed in the imputation strategy outlined in the bioinformatic pipeline chapter of Supplementary information 4, which "rescued" a number of peptides/metabolites with high missingness but which were significantly present/absent across cohort groups (healthy, flu, mild COVID, severe COVID), PASC status (recovered/PASC), or visit (Visit 1/Visit 2). Whilst affected metabolites were included in the statistical models and potentially labelled as differentially abundant, it is more accurate to label these features as present/absent. For proteomics, controlling for false discovery rate using the Benjamini–Hochberg procedure (q <= 0.01), 0/13,285 peptides were significantly associated with PASC, 2,738/13,285 with cohort group, and 35/13,285 with visit. For metabolites, controlling for false discovery rate using the Benjamini–Hochberg procedure (q <= 0.01), 0/50,789 spectra were significantly associated with PASC, 11,324/50,789 with cohort group, and 445/50,789 with visit.

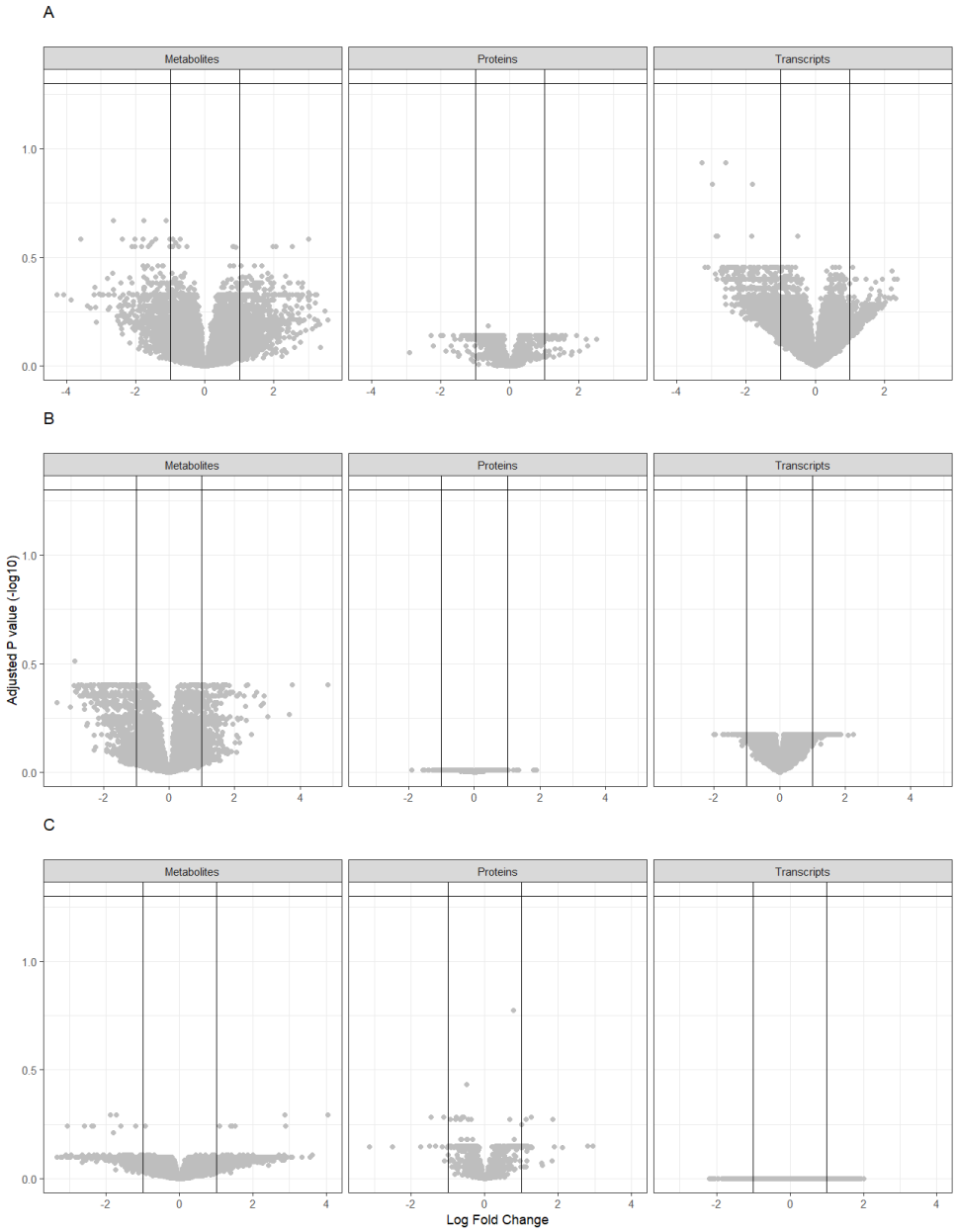


Figure 1: Differentially expressed features between COVID-19 patients developing PASC at visit 2 and COVID-19 patients who are recovered at visit 2. **A** Longitudinally differentially expressing features (Model design = ~ PASC status*Visit + COVID severity + Vaccination status + Sex + Age + (1|PatientID)). **B** Differentially expressed features at visit 1 (Model design = ~ PASC status + COVID Severity + Vaccination status + Sex + Age). **C** Differentially expressed features at visit 2 (Model design = ~ PASC status + Vaccination status + Sex + Age). No features reached significance after p-value adjustment.

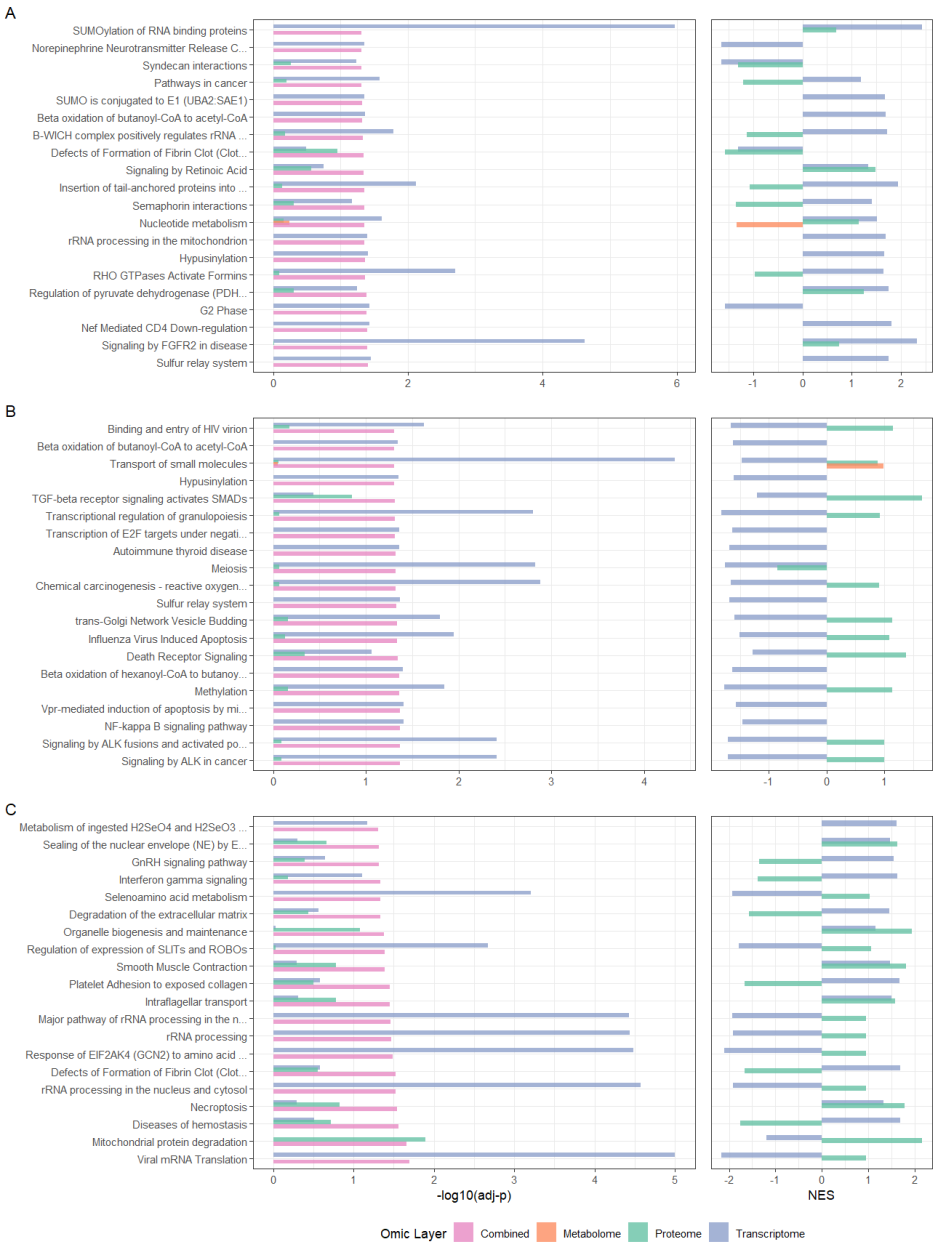


Figure 2: Reactome and Kegg pathways enriched/depleted as assessed via GSEA using features ranked according to differentially expressed features between COVID-19 patients developing PASC at visit 2 and COVID-19 patients who are recovered at visit 2. A Pathways with Differential Longitudinal Change (V2–V1) in PASC versus Recovered COVID-19 Patients. B Enriched/depleted pathways in PASC versus Recovered COVID-19 Patients at V1. C Enriched/depleted pathways in PASC versus Recovered COVID-19 Patients at V2.

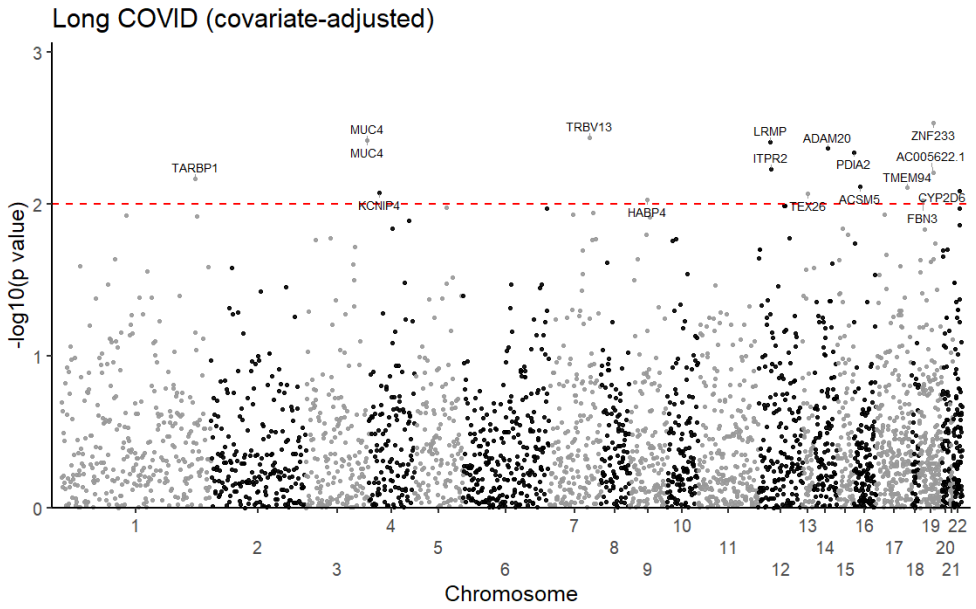


Figure 3: Genome-wide association of PASC at visit 2 (~3 months post-infection) versus full recovery, covariate-adjusted. Manhattan plot shows –log10(P) across chromosomes (black/grey alternating); dashed red line marks the suggestive threshold ($P=1\times10^{-2}$). Variants meeting this cutoff are gene-labeled; none reached genome-wide significance ($P<5\times10^{-8}$).